ABSTRACT

LI, LIANNA. The Cardiac Response to Reovirus Infection. (Under the direction of Dr. Barbara Sherry).

Viral myocarditis is a common disease in humans. Interferon-β (IFN-β) has been identified as critical for protection against viral myocarditis in mouse models, and IFN-α or -β treatment is beneficial in the treatment of human viral myocarditis. IFN-β expression and its antiviral effects are cell-type specific in murine cardiac myocytes and fibroblasts. However, expression and function of individual IFN-α subtypes in cardiac cells has not previously been investigated. Therefore, IFN-α subtype expression and antiviral effects were studied in reovirus-infected murine primary cardiac myocyte and cardiac fibroblast cultures. In order to quantify the thirteen highly conserved IFN-α subtypes, a quantitative Real-Time PCR assay was developed. Results demonstrated that IFN-α induction by reovirus T3D in cardiac cells is both subtype- and cell type-specific, and that some individual IFN-α subtypes are likely important in the antiviral cardiac response. In brief, reovirus T3D induced five IFN-α subtypes in primary cultures of cardiac myocytes and fibroblasts: IFN-α1, -α2, -α4, -α5, and -α8/6. The levels of IFN-α expression were both higher and spanned a greater range in cardiac myocytes than in fibroblasts. Viral induction of IFN-α1, -α2, -α5, and -α8/6 required IFN-α/β signaling in both cell types, while induction of IFN-β and -α4 was more dependent on IFN signaling in myocytes than fibroblasts. Murine IFN-α1, -α2, -α4, or -α5 treatment induced IRF7 and ISG56 in both cardiac cell types, however induction was always greater in cardiac fibroblasts than in cardiac myocytes. Finally, each IFN-α subtype inhibited reovirus T3D replication in both cell types, but protection was subtype-specific.

To discover novel proteins or protein post-translational modifications involved in the IFN pathway or displaying antiviral effects against viral myocarditis, a proteomics tool, two-dimensional difference gel electrophoresis (2D-DIGE) coupled with matrix absorption laser desorption ionization-time of flight-time of flight (MALDI-TOF-TOF) mass spectrometry, was used to investigate the reovirus-induced proteome changes in murine primary cardiac myocyte cultures. Results demonstrated that the 2D-DIGE technique is quantitative and reproducible. Whole proteome changes based on differentially expressed proteins were clustered according to viral pathogenic phenotypes and induction of IFN. One hundred and twenty-four differentially expressed proteins were identified, including those involved in calcium signaling, ERK/ MAPK signaling, protein ubiquitination, mitochondrial dysfunction, oxidative stress, amino acid metabolism, and other pathways. Interestingly, 2D-DIGE results and additional studies demonstrated that heat shock protein Hsp25 is modulated differentially by myocarditic and non-myocarditic reoviruses, and suggested that it may play a role in the cardiac antiviral response. This is the eighth virus family found to modulate Hsp25 or its human homolog, Hsp27, suggesting that Hsp25/27 participation in the antiviral response may be widespread. However, results here provide the first evidence for a virus-induced decrease in Hsp25/27, and suggest that viruses may have evolved a mechanism to subvert this protective response, as they have for IFN.

The Cardiac Response to Reovirus Infection

by
Lianna Li

A dissertation submitted to the Graduate Faculty of
North Carolina State University
in partial fulfillment of the
requirements for the degree of
Doctor of Philosophy

Functional Genomics

Raleigh, North Carolina

June 29, 2009

APPROVED BY:

Dr. Barbara Sherry Committee Chair	Dr. Jonathan M. Horowitz
Dr. Frank Scholle	Dr. James L. Stephenson, Jr.

DEDICATION

To my grandparents, who brought me up. To my parents, my husband, Hao Mei, my son, Leo Mei, and my unborn one, who support and encourage me always.

BIOGRAPHY

Lianna Li was born in China and was brought up by her grandparents in a small town. She obtained her MD from the China Medical University in 1997, and after working for several years in Shanghai, China, she came to the United States to pursue graduate education. She first studied at Kent State University from Aug. 2003 to May 2004, and then transferred to the Functional Genomics program at North Carolina State University for Ph.D. studies under the direction of Dr. Barbara Sherry. She will go to Tulane University for postdoctoral training.

ACKNOWLEDGMENTS

This is a great opportunity to express my appreciation and thanks to the following people, who trained, supported and encouraged me during my graduate studies:

First, I would like to thank Dr. Barbara Sherry for guiding, training and inspiring me in my studies and research. I want to say that it is my luckiest thing to study and work under her instruction. Appreciation is extended to all the Sherry lab members as well. I am also pleased to express gratitude to all my committee members, Dr. Jonathan M. Horowitz, Dr. Frank Scholle, and Dr. James L. Stephenson, Jr., who offered me valuable advice and suggestions for the projects. In addition, I want to thank Dr. Joel R. Sevinsky and Megan D. Rowland for necessary guidance and assistance for the proteomics project. Thanks to all the members in the Functional Genomics program, especially to Dr. David Bird and Juliebeth Briseno.

Finally, I would like to thank my husband, my son, my parents and all my friends for their endless support and encouragement.

TABLE OF CONTENTS

LIST OF TABLES……..……viii

LIST OF FIGURES……...……..x

CHAPTER 1: Background……...……...1

Orthoreovirus (reovirus)…….……1
Myocarditis…….……7
Interferon Regulatory Factors (IRFs)……...11
Interferon-alpha (IFN-α) …….……15
Proteomics…….……18
Two-dimensional gel-electrophoresis (2-DE) and shotgun proteomics…..……..20
Two-dimensional difference gel electrophoresis (2D-DIGE)…..…….…22
Heart Proteomics…….……..25
Heat shock proteins (HSPs)…….……28
Hsp25…….……29
Hsp70…….……31
HSPs and the heart…….……..33
Questions and approaches…….……36
References…….……..39

CHAPTER 2: IFN-α Expression and Antiviral Effects are Subtype- and Cell Type-Specific in the Cardiac Response to Viral Infection ……...……...74
Abstract……75
Introduction……..76
Materials and Methods……...……..79
Results……..……84
Discussion……..……..91
Acknowledgements…….……97
References…….……..98

CHAPTER 3: Proteomic Analysis Reveals Virus-Specific Hsp25 Modulation during the Cardiac Myocyte Antiviral Response ……...115
Abstract……...……116
Introduction……117
Results……119
Discussion……...…...127
Materials and Methods……..……130
Supplemental Materials and Methods……..138

Acknowledgements……140
References……141

APPENDIX 1: Over-Expression of IFN-α2, -α4 and –α5 in Primary Cardiac Myocyte and Fibroblast Cultures ……171
Introduction……171
Materials and Methods……172
Results……175
Discussion……178
References……179

APPENDIX 2: Proteomic Study of T3D-Infected Primary Cardiac Myocyte Cultures at Different Time Points by Two Dimensional Difference Gel Electrophoresis (2D-DIGE)……190
Introduction……190
Materials and Methods……191
Results……191
Discussion……195
References……196

APPENDIX 3: Proteomic Study of T3D-Infected Primary Cardiac Myocyte Cultures at 18 Hours Post-Infection by LC-MS/MS ……207
Introduction……207
Materials and Methods……207
Results……210
Discussion……210
References……212

APPENDIX 4: Ingenuity Pathway Analysis (IPA) of Differentially Expressed Proteins 12 Hours Post-Reovirus Infection of Primary Cardiac Myocyte Cultures……239
Introduction……239
Materials and Methods……239
Results……240
Discussion……241
References……242

APPENDIX 5: Over-Expression of Hsp27D and Hsp25 by Transfection of Primary Cardiac Fibroblast Cultures ……265
Introduction……265
Materials and Methods……266
Results……267
Discussion……268

References…….…….269

SUMMARY……..……..…..274

References..……281

LIST OF TABLES

Chapter 2: IFN-α Expression and Antiviral Effects are Subtype- and Cell Type-Specific in the Cardiac Response to Viral Infection

Table 2.1. Primers for subtype-specific detection of IFN-α……..……..……..106
Table 2.2. Reovirus T3D induction of IFN-α is subtype-specific in primary cardiac myocyte and cardiac fibroblast cultures…….……..108

Chapter 3: Proteomic analysis reveals virus-specific Hsp25 modulation during the cardiac myocyte antiviral response

Table 3.1. Reovirus selected for infection of primary cardiac myocyte cultures……..150
Supplemental Table 3.1. Gel set-up of the DIGE gels……...……152
Supplemental Table 3.2. Biological function of differentially expressed proteins in T3D- and 8B-infected primary cardiac myocyte cultures……..154
Supplemental Table 3.3. Swiss-Prot analysis of Spot #1 (most basic spot; putative unphosphorylated Hsp25)……..……160
Supplemental Table 3.4. Swiss-Prot analysis of Spot #2 (middle spot; putative mono-phosphorylated Hsp25)……..161
Supplemental Table 3.5. Swiss-Prot analysis of Spot #3 (most acidic spot; putative di-phosphorylated Hsp25)……..162

Appendix 1: Over-Expression of IFN-α2, -α4 and –α5 in Primary Cardiac Myocyte and Fibroblast Cultures

Table App.1.1. Reaction components for amplifying full length cDNA of IFN-α2 by PCR……..……..……180

Appendix 2: Proteomic Study of T3D-Infected Primary Cardiac Myocyte Cultures at Different Time Points by Two Dimensional Difference Gel Electrophoresis (2D-DIGE)

Table App.2.1 Gel set-up for T3D time-course comparison……197
Table App.2.2. Proteins identified from SwissProt database search of the T3D time-course comparison…….……202

Appendix 3: Proteomic Study of T3D-Infected Primary Cardiac Myocyte Cultures at 18 Hours Post-Infection by LC-MS/MS

Table App.3.1. Sample preparation for 1D gel electrophoresis (μl)……..213

Table App.3.2. Proteins differentially expressed between T3D-and mock-infected primary cardiac myocyte cultures……215
Table App.3.3. Proteins unique to T3D infection in primary cardiac myocyte cultures…...227
Table App.3.4. Proteins unique to Mock infection in primary cardiac myocyte cultures….230
Table App.3.5 Heat shock proteins identified by LC-MS/MS in T3D- and Mock-infected primary cardiac myocyte cultures…….…….237

Appendix 4: Ingenuity Pathway Analysis (IPA) of Differentially Expressed Proteins 12 Hours Post-Reovirus Infection of Primary Cardiac Myocyte Cultures

Table App.4.1. Comparison of differentially expressed proteins among the four different reovirus infections in primary cardiac myocyte cultures 12 hours post-infection…….……243
Table App.4.2. Differentially expressed proteins unique to T3D infection in primary cardiac myocyte cultures……244
Table App.4.3. Differentially expressed proteins unique to 8B infection in primary cardiac myocyte cultures……245
Table App.4.4. Comparison of differentially expressed proteins unique to both T3D and 8B infections in primary cardiac myocyte cultures…….248
Table App.4.5. Canonical pathway analysis for differentially expressed proteins in T3D- and 8B-infected primary cardiac myocyte cultures……..249
Table App.4.6 Network analysis comparing differentially expressed proteins from T3D- and 8B-infected primary cardiac myocyte cultures……...254
Table App.4.7. Differentially expressed proteins with putative PTMs…….264

Appendix 5: Over-Expression of Hsp27D and Hsp25 by Transfection of Primary Cardiac Fibroblast Cultures

Table App.5.1. Primers for amplifying wild type and mutated Hsp25……..…271

LIST OF FIGURES

Chapter 1: Background

Figure 1.1. Comparison of proteomics coupled with traditional two-dimensional gel electrophoresis and shot gun proteomics……72
Figure 1.2. Schematic steps for Two-dimensional difference gel electrophoresis (2D-DIGE)……...73

Chapter 2: IFN-α Expression and Antiviral Effects are Subtype- and Cell Type-Specific in the Cardiac Response to Viral Infection

Figure 2.1. Pyrosequencing confirmation of IFN-α products……107
Figure 2.2. Basal and reovirus T3D-induced expression of IFN-α is subtype- and cell type-specific in cardiac cells……..109
Figure 2.3. Peak time of IFN-α induction by reovirus T3D is cell type- and subtype-specific……...……110
Figure 2.4. Reovirus T3D induction of secreted IFN-α is cell type-specific……111
Figure 2.5. The role of IFN-mediated amplification in T3D induction of Type I IFN is cell type-specific……..……..112
Figure 2.6. IFN-α induction of ISG mRNA is subtype- and cell type-specific……113
Figure 2.7. Reovirus T3D sensitivity to IFN-α is subtype-specific in cardiac cells……..114

Chapter 3: Proteomic analysis reveals virus-specific Hsp25 modulation during the cardiac myocyte antiviral response

Figure 3.1. Representative 2D-DIGE gel image and 3D-view……..……151
Figure 3.2. Principle Component Analysis (PCA)……153
Supplemental Figure 3.1. Hsp25 2D-DIGE gel spots……...……....159
Figure 3.3. Quantification of Hsp25 by 2D-DIGE……163
Supplemental Figure 3.2. Reovirus modulation of Hsp25 is post-transcriptional……....164
Figure 3.4. Confirmation of Hsp25 expression and phosphorylation by Western blot…....165
Fig 3.5. Reovirus-induced phosphorylation and degradation of Hsp25 is virus strain-specific……..166
Fig 3.6. Reovirus-induced phosphorylation of Hsp25 is p38-MAPK-dependent and IFN-independent……167
Fig 3.7. Reovirus does not induce nuclear translocation of Hsp25……...168
Fig 3.8. Expression of Hsp25 is cell type-specific in the heart……169
Fig 3.9. Inhibition of p38-MAPK increases T3D- and 8B-induced CPE in cardiac myocytes……...……170

Appendix 1: Over-Expression of IFN-α2, -α4 and –α5 in Primary Cardiac Myocyte and Fibroblast Cultures

Figure App.1.1. Multiple sequence alignment results for pORF-IFNα4 (IFN-α4) against the RefSeq from NCBI (NM_010504.1)…….181
Figure App.1.2. Multiple sequence alignment results for pORF-IFNα (IFN-α5) against the RefSeq (NM_010505.1) from NCBI……...……..182
Figure App.1.3. Fold change of IFN-α mRNA expression in transfected primary cultures of cardiac myocytes and cardiac fibroblasts……..……183
Figure App.1.4. Over-expression and secretion of IFN-α in transfected primary cultures of cardiac myocytes and cardiac fibroblasts……..184
Figure App.1.5. Induction of heterologous IFN-α genes by transfected IFN-α genes……..185
Figure App.1.6. Network of induction of other IFN-α subtypes by transfected IFN-α genes……...……...186
Figure App.1.7. Reovirus replication in transfected primary cardiac myocyte and cardiac fibroblast cultures……..……..187
Figure App.1.8. Induction of ISG56 and IRF-7 by the transfected pORF-mcs…….188

Appendix 2: Proteomic Study of T3D-Infected Primary Cardiac Myocyte Cultures at Different Time Points by Two Dimensional Difference Gel Electrophoresis (2D-DIGE)

Figure App.2.1. Annotated preparative gel ("pick gel") image for T3D time-point comparison……198
Figure App.2.2. Differentially expressed proteins at different times following reovirus T3D infection of primary cardiac myocyte cultures……..199
Figure App.2.3. Principle Component Analysis (PCA) of mock- or T3D-infected primary cardiac myocyte cultures……200
Figure App.2.4. Hierarchical clustering of spot maps……...201
Figure App.2.5. Cryptdin 4 protein (spot 854) at different times post-T3D infection of primary cardiac myocyte cultures……..205
Figure App.2.6. Peptide information for cryptdin 4 and sequence alignment to the cryptdin 4 RefSeq from GenBank……...……206

Appendix 3: Proteomic Study of T3D-Infected Primary Cardiac Myocyte Cultures at 18 Hours Post-Infection by LC-MS/MS

Figure App.3.1. Gel slice distribution on 1D-gel image……214

Appendix 4: Ingenuity Pathway Analysis (IPA) of Differentially Expressed Proteins 12 Hours Post-Reovirus Infection of Primary Cardiac Myocyte Cultures

Figure App.4.1. IPA symbols……...…….256

Figure App.4.2. Network of differentially expressed proteins involved in cell cycle, cancer, and drug metabolism in 8B-infected primary cardiac myocyte cultures……...257
Figure App.4.3. Network of differentially expressed proteins involved in cardiovascular system development and function, skeletal and muscular system development and function, and tissue development in T3D-infected primary cardiac myocyte cultures…….258
Figure App.4.4. Network of differentially expressed proteins involved in cellular function and maintenance, amino acid metabolism, and post-translational modification in 8B-infected primary cardiac myocyte cultures…….259
Figure App.4.5. Network of differentially expressed proteins involved in cell-mediated immune responses, immunological disease, and drug metabolism in T3D-infected primary cardiac myocyte cultures……260
Figure App.4.6. Network of differentially expressed proteins involved in lipid metabolism, small molecule biochemistry, and nucleic acid metabolism in 8B-infected primary cardiac myocyte cultures……..…….261
Figure App.4.7. Network of differentially expressed proteins involved in gene expression, cellular assembly and organization, and drug metabolism in T3D-infected primary cardiac myocyte cultures……...…….262
Figure App.4.8. Network of differentially expressed proteins involved in neurological disease, cell death, and hematological disease in 8B-infected primary cardiac myocyte cultures……..……263

Appendix 5: Over-Expression of Hsp27D and Hsp25 by Transfection of Primary Cardiac Fibroblast Cultures

Figure App.5.1. Full length cDNA sequence of Hsp27D with part of pCAGGs sequence……270
Figure App.5.2. Transfected Hsp27D / Hsp25 does not affect reovirus replication…….272
Figure App.5.3. Effects of transfected Hsp25 / Hsp27D on reovirus protein expression in wild type and ABRKO primary cardiac fibroblast cultures……..273

CHAPTER 1

BACKGROUND

Orthoreovirus (reovirus)

Respiratory enteric orphan virus (reovirus) is a non-enveloped RNA virus in the *Reoviridae* family that is primarily a respiratory and enteric virus under natural circumstances (253). Reoviruses can be isolated from a broad range of mammalian species, and reovirus infection of humans is universal (42, 43). It is reported that about 23% of infants and young children (aged from 1 month to 5-years old) are seropositive for reovirus antibody and that this increases in an age-dependent manner, which peaks in 5-6 years old at about 50% (278). Normally, reovirus infection does not cause severe consequences, and is frequently associated with few or no symptoms (254).

The genome of reovirus consists of 3 large (L1, L2 and L3), 3 medium (M1, M2 and M3), and 4 small (S1, S2 S3 and S4) segmented linear double stranded (ds) RNA (254). Each viral genome consists of a single copy of each segment (258) and each viral particle contains 8 structural proteins. To date, it is known that 8 segments encode for one protein each and 2 segments encode for 2 proteins each (254). L1 encodes the λ3 protein, which is an inner core protein (33) acting as an RNA-dependent RNA polymerase (154). L2 encodes the λ2 protein, which is an outer capsid (74) and core spike protein with guanylyltransferase (188) and methyltransferase activity (30, 185). L3 encodes the λ1 protein (14), which is an inner core protein (74) and functions as an NTPase (218), an RNA helicase (19), an RNA triphosphatase (19), and has the capacity to bind to dsRNA and dsDNA (162). M1 encodes

the μ2 protein (317), which is an inner core protein (74) and can bind to RNA (24). M2 encodes the μ1/μ1c protein (138, 318), which is an outer capsid protein (74) involved in penetration (55) and transcriptase activation (72, 82). M3 encodes the two nonstructural proteins: μNS (197) and μNSC (317). μNSC is a short version of μNS missing the part of the N-terminus (317). μNS protein is an essential component for inclusion body formation and is involved in viral genome transcription and replication (25, 153). Function of μNSC is not clear yet. S1 encodes σ1 and σ1s proteins (85, 212, 247). σ1 is a cell-attachment protein (298) and serves as the viral hemagglutinin and primary serotype determinant (65). σ1s is a nonstructural protein, which is involved in G2/M cell cycle arrest (231). S2 encodes the σ2 protein (197, 209), which is an inner core protein (74) with dsRNA binding ability and which may be involved in RNA synthesis (66). S3 encodes σNS (239), which is a nonstructural protein binding to single stranded RNA (127), and possesses poly(C)-dependent poly(G) polymerase activity probably playing roles in RNA assortment or replication (105). S4 encodes the σ3 protein (7), which is an outer capsid protein (74) very sensitive to protease degradation and which can bind to dsRNA to modulate cell factors which regulate cellular RNA synthesis and protein translation (100, 163, 255, 257).

Reovirus infection begins with virus attachment to the cell surface receptor, junctional adhesion molecule-A (JAM-A) and/or sialic acid, through the σ1 protein (15, 34, 149). Then the reovirus virion is internalized into cells through receptor-mediated endocytosis (23, 77, 186). Following internalization, virions undergo stepwise acidic- and endocytic protease-dependent disassembly of the viral outer capsid in cellular endosomes. This uncoating procedure removes the major outer-capsid protein σ3, exposes the membrane-

penetration mediator μ1 and causes a conformational change in attachment protein σ1, which produces infectious (or intermediate) subviral particles (ISVPs) (22). That ISVP further loses σ1 and autocleaved μ1 experiences further conformational changes which yields ISVP* (216), which can penetrate the endosomal membrane and send the virus core particle into the cytoplasm to begin transcription.

Reovirus infection causes tissue damage mainly through the induction of cell apoptosis and different reovirus strains possess different capacities to cause apoptosis. The prototype Type 3 (T3) reoviruses, Dearing (T3D) and Abney (T3A), are more potent than prototype Type 1 (T1) reoviruses, Lang (T1L) in L929 fibroblast (42, 43). Researchers identified that reovirus T3 S1 and M2 genes are associated with the ability to induce apoptosis (47, 57, 125, 241, 290, 291). The S1 gene-encoded σ1 protein is a cell attachment protein with a globular head facing outside of the virion, and a fibrous tail inserted into the virion (85, 212, 247, 298). The σ1 protein is a determinant of the strain-specific patterns of viral tropism, and has the potential to induce apoptosis. Since JAM-A, a member of the immunoglobulin superfamily, acts as a cell receptor to recognize and bind to the head of σ1 from both T1L and T3D (15, 149), cell surface receptor binding to the tails of T1 and T3 σ1 may determine the difference in inducing apoptosis. In contrast to the unknown receptors for the T1 σ1 tail, α-linked sialic acid acts as cell surface receptor for the T3 σ1 tail (34). By using isogenic reovirus mutants, T3SA+, which can bind to sialic acid, and T3SA-, which cannot, Connolly et al (47) confirmed that T3SA+ caused a much higher rate of apoptosis than T3SA- in Hela and L cells, and this difference was not because of viral protein synthesis or yield of new virus. They further identified that the binding of σ1 to sialic acid is an

essential prerequisite for reovirus-induced apoptosis since T3SA+-induced apoptosis was eradicated when sialic acid was removed from the cell surface, or T3SA+ was incubated with a trisaccharide containing lactose and sialic acid. Therefore, sialic acid binding is associated with reovirus strain-specific induction of apoptosis. However, this binding is not enough to induce apoptosis. Inhibition of σ1 binding to JAM-A diminished T3 reovirus-induced apoptosis (15). So σ1 binding to both JAM-A and sialic acid on the cell surface is required for reovirus to induce apoptosis(47).

Though another S1-encoded protein, σ1s, a non-structural protein, was demonstrated to be dispensable for reovirus-induced apoptosis in L929 and HEK293 cells (48, 231, 291), it was discovered σ1 is "a determinant of the magnitude and extent of reovirus-induced apoptosis in both the heart and central nervous system (CNS)" by Hoyt et al (125). They injected 2-day-old neonatal mice with T3σ1s+ or T3σ1s- reovirus, and found that with similar virus replication, T3σ1s+ reovirus-injected mice showed much higher levels of caspase-3 activation. This resulted in much more severe tissue damage, and increased cell apoptosis in both the brain and heart.

While the attachment of reovirus can activate the apoptosis pathway, the M2 gene, encoding the major viral outer capsid protein μ1/μ1c which mediates viral disassembly, was identified as another gene that is associated with the capacity of reovirus to induce apoptosis (48, 57, 290). By over-expressing T1L and T3D M2 in CHO and CV-1 cells, Coffey et al (44) demonstrated that the M2-encoded μ1 protein was able to induce apoptosis without reovirus infection. By using truncated constructs of different fragments: the amino(N)-terminal myristoylated fragment μ1N (residues 2 to 41); the central fragment δ (residues 42 to 582);

the C-terminal fragment Φ (residues 582 to 708); μ1δ (residues 2 to 582 plus the N-terminal, *N*-myristoyl group) and μ1C (residues 42 to 708), they identified that residues 582 to 675 in the Φ region of μ1 is the critical region determining induction of apoptosis. Danthi et al (56) investigated whether JAM-A and sialic acid binding are required for reovirus infection to cause apoptosis. They incubated reovirus virions with monoclonal antibodies against σ1 protein before infection of JAM-A-null, Fc-receptor-expressing CHO cells, and found that this antibody-mediated, σ1-independent reovirus infection can cause apoptosis, and acidic-dependent disassembly of reovirus in the endosomes is required for this apoptotic procedure. In order to further identify which region of μ1 is responsible for penetration of endosomes and induction of apoptosis, they used reverse genetics to generate a panel of reoviruses with point mutations in the δ region of μ1 and identified that single amino acid mutations (A319E, V425F, Q440L, and I442V) can decrease reovirus membrane penetration efficiency (57).

Reovirus infection can initiate both innate and adaptive immunity in the host. Adaptive immunity has been reviewed in detail (254) and is not relevant here. Instead, this section will focus on innate immunity, specifically the Type I interferon (IFN-α/β) system. IFN-α/β is an indispensable component of the innate immune response which plays a critical role as the first line of the host's defense against viral infection (279). Once an RNA virus, like reovirus, infects cells from a vertebrate, viral dsRNA is recognized by pattern recognition receptors (PRRs), such as retinoic acid-inducible gene-I (RIG-I) and melanoma differentiation-associated gene 5 (Mda 5) (178, 243). Recognition of viral RNA results in activation of IPS-1/MAVS/VISA/Cardif-mediated pathways and phosphorylation of TANK-binding kinase 1 (TBK1) and IκK-ε. Transcription factors IRF-3 and NF-κB are activated

and translocate into the nucleus. Accompanied by other co-activators, a transcription factor complex is formed and binds to the IFNα/β promoter (positive regulatory domains (PRDs) I and III, and PRD-like elements (PRD-LEs)). Then IFN-β transcription is activated and secreted IFN-β binds to the IFN-α/β receptor (IFNAR) on the cell surface, which activates the tyrosine kinases Tyk2 and Jak1, followed by the phosphorylation of signal transducers and activators of transcription (Stat), Stat1 and Stat2. Phosphorylated Stat1 and Stat2 form heterodimers and recruit IRF-9 to construct a transcription factor complex: IFN-stimulated gene factor 3 (ISGF3). ISGF3 then translocates into the nucleus and binds to IFN-stimulated regulatory elements (ISRE) to up-regulate thousands of IFN-stimulated genes (ISGs). Among the ISGs, IRF-7 is another transcription factor and it can be activated by virus infection. Phosphorylated IRF-7 is capable of further inducing IFN-β and activating transcription of other IFN-α subtypes, and thus an amplification loop is formed to amplify IFN-α/β productions.

IFN has been shown to be protective against reovirus infection *in vitro* and *in vivo* for a many years (61, 134, 217, 316). Nilsen et al (217) suggested that activation of RNase L, an endoribonuclease, following upregulation of 2',5'-oligoadenylate (2',5'-oligo(A)) by IFN treatment in Hela cells may contribute to IFN antiviral effects since reovirus mRNA was cleaved in IFN-treated cells, but not in un-treated cells. Samuel et al (245) believed that IFN-triggered phosphorylation of the alpha subunit of protein synthesis initiation factor eIF-2 (eIF-2α) should be associated with IFN's antiviral effects against reovirus in mouse L929 cells. Henry et al (121) further demonstrated that IFN induces the RNA-dependent protein kinase (PKR) to phosphorylate eIF2α for regulation of viral protein synthesis.

Reovirus sensitivity to IFN is strain-specific. Jacobs et al (134) demonstrated that with 1000U/ml IFN-β treatment, T3D replication decreased about 17 to 100 fold, while T1L replication decreased only 2 to 3 fold in mouse L cell cultures. Sherry et al (264) identified that myocarditic and non-myocarditic reoviruses are different in their sensitivities to IFN in primary murine cardiac cell cultures and neonatal mice as well. They further identified that reovirus sensitivity to IFN was associated with the M1, S2 and L2 genes encoding viral core proteins.

Like other viruses (101, 139, 167, 232, 268, 284, 306), reovirus has also evolved mechanisms to counteract IFN antiviral effects. Imani et al (131) demonstrated that reovirus T1L can inhibit the activation of PKR in mouse L cells, and this inhibition is associated with the viral σ3 protein. Recently, Zurney et al (335) proposed that reovirus counteracts IFN antiviral effects by suppressing IFN induction of a subset of ISGs. This suppression is associated with the M1-encoded μ2 protein, which can retain one of the ISGF3 components, IRF9 in the nucleus, thus affecting both the amplification loop and induction of ISGs.

Myocarditis

Myocarditis is a cardiac disease defined as inflammation and injury of the myocardium, and viruses are the most common pathogen causing myocarditis (51, 80). More than 5% of the human population has experienced some form of viral myocarditis (80, 321). It has been demonstrated that over 20 viruses can cause viral myocarditis, such as coxsackieviruses, adenoviruses, influenza viruses, human immunodeficiency virus, parvovirus, hepatitis C virus, Epstein-Barr virus, cytomegalovirus, human herpesvirus 6, and

others (51, 80, 107). Since cardiac myocytes, which are responsible for contraction of the heart, are not readily replenished, with only 1% cell renewal in the average human lifetime (18), damage to these cells caused by viral infection can result in a serious prognosis. Myocarditis can be fatal in infants and young children, and about 20% of sudden unexpected deaths of young children is from myocarditis (73). Moreover, >50% of sudden deaths in young adults are due to cardiac causes with >10% of those due to myocarditis (71, 235). In addition, viral and post-viral myocarditis are the major causes of acute and chronic dilated cardiomyopathy (DCM) (51), for which there is no effective treatment but heart transplantation.

There are three mechanisms involved in the pathogenesis of viral myocarditis: immune-response-mediated myocardial injury, autoimmune-mediated myocardial injury, and direct virus-induced myocardial injury (80). Murine cytomegalovirus (MCMV) -induced myocarditis likely reflects predominantly immune-mediated damage (164), reovirus-induced myocarditis reflects direct viral cytopathogenic effect in cardiac cells (16, 263), while coxsackievirus B (CVB)-induced myocarditis reflects both direct and immune-mediated pathology (126, 315). Esfandiarei reviews the three mechanisms in great detail (80). Here I will focus on reovirus-induced myocarditis. Our laboratory and others have demonstrated that reovirus-induced viral myocarditis is due to direct virus-induced apoptosis. Evidence that damage is due to a direct viral effect rather than immune-mediated damage includes: 1) reovirus 8B-induced myocarditis required neither T cells (263) nor B cells (262) in either nude mice (deficient of cytotoxic T cells) or SCID mice (deficient of T and B cells), and 2) reovirus 8B induced cytopathic effect in primary cardiac myocyte cultures (16). Evidence

that damage is apoptotic includes: 1) hearts from reovirus 8B-infected neonatal mice showed only mild to moderate inflammatory infiltrate (rather than the massive infiltrate associated with coxsackievirus-induced myocarditis), and the damaged area was TUNEL-positive and reovirus antigen-positive (63, 263); 2) DNA extracted from hearts of 8B-infected neonatal mice demonstrated oligonucleosomal-length ladders, strongly indicating apoptosis (63); 3) inhibition of calpain, a cysteine protease which is known to play an important role in apoptosis and is activated by reovirus infection, was protective against 8B-induced myocarditis in neonatal mice (63); 4) caspase-3 was activated after reovirus infection both in the heart and in cardiac myocyte cultures, and moreover, inhibition of caspase activity reduced 8B-induced myocardial cell injury both *in vitro* and *in vivo* (64); and 5) inhibition of caspases prevented reovirus-induced heart damage (63, 64).

The reovirus genes and possible virus-host interaction which are responsible for reovirus myocarditic potentials are currently under investigation. Using reassortant viruses generated between the strongly myocarditic reovirus 8B and non-myocarditic reovirus strains, the M1 and L2 genes, both encoding viral core proteins, were identified as determining reovirus myoarditic potential (261). Additional studies using other reovirus strains identified those two genes, and also the L1 gene, which encodes another core protein, and the S1 gene, which encodes the viral attachment protein (260). One model was that the S1 gene determines the efficiency of virus attachment to cardiac myocytes, and then genes encoding viral core proteins determine efficiency of RNA synthesis which could affect induction of IFN. Indeed, later studies demonstrated that the S1 gene does determine the efficiency of infection of primary cultures of cardiac myocytes, and that the genes encoding core proteins

are associated with different rates of viral RNA synthesis in those cells (259). Moreover, genes encoding viral core proteins determine reovirus induction of IFN in cardiac myocytes, and a non-myocarditic reovirus induces myocarditis in mice depleted of IFN (264). Together, the data suggest that several virus-host interactions determine efficiency of infection and viral replication in cardiac myocytes which modulates the cardiac IFN response and determines viral myocarditic potential.

Antiviral treatment of viral myocarditis in experimental animals has been carried out for decades. Ribavirin, an antiviral agent with broad spectrum activity, has been tested for the treatment of encephalomyocarditis (EMC) virus or coxsackievirus B3 virus-induced viral myocarditis since the 1980's both in a mouse model in vivo (150, 195) and in heart cell cultures in vitro (117), and it was demonstrated to be effective in reducing virus replication and heart damage, elongating survival time, and increasing survival rate. However, ribavirin did not show therapeutic effects in the clinic in the treatment of influenza virus-associated fulminant myocarditis(238). Recombinant IFN-α has been used in the treatment of viral myocarditis as well. In animal experiments, IFN-α was effective in the therapy of encephalomyocarditis virus or coxsackievirus B3 virus-induced myocarditis in the mouse showing reduced virus replication, less heart damage, and less inflammation (150, 193, 194, 307). IFN-α is used in the clinic and has been demonstrated to be effective. Favorable signs were observed in the treatment of enterovirus-induced myocarditis (54, 118). IFN-β has been proven to be effective in treating viral myocarditis both in animal models(307) and in the clinic. Injectable IFN-β was capable of reducing left ventricle (LV) end diastolic diameter and LV end systolic diameter in persistently virus- infected patients with chronic, stable

cardiomyopathy (156). Recently, a Chinese herb, Qihong, was identified as a potent antiviral agent in the treatment of coxsackievirus B3 (CVB3)-induced myocarditis both in vivo and in vitro (271).

However, since antiviral agents are not available for the viruses most frequently associated with myocarditis, effective clinical therapy is still not available for myocarditis. Treatment of symptoms is the only choice. Patients with myocarditis presenting with acute dilated cardiomyopathy are required to be treated according to current guidelines from the American Heart Association, the American College of Cardiology, the European Society of Cardiology, and the Heart Failure Society of America (69, 116, 129). For acute myocarditis with left ventricular dysfunction, supportive therapy, including bed rest, is the major therapy. In both acute and chronic myocarditis, diuretic therapy, vasodilators, and inotropic support are used to optimize intracardiac filling pressures and increase cardiac output. It is recommended to start treatment with angiotensin-converting enzyme (ACE) inhibitors or angiotensin II (AII) receptor blockers (51, 79). For patients who do not respond to conventional therapy, aggressive mechanical assistance devices are adopted as a bridge to recovery or heart transplantation.

Interferon regulatory factors (IRFs)

IRFs are transcription factors in a growing family. Some are induced by IFN and all play a crucial role in regulating the induction of IFN and / or ISGs. There are a total of 10 members in the IRF family at present (187), and they are classified into four groups according to their transcriptional functions (187, 215, 248, 281). Class I, which induces ISGs,

includes IRF-1, IRF-3, and IRF-9 (also called ISGF3γ/p48). Class II, which represses ISGs, includes IRF-8 (ICSBP) and vIRF (a viral homolog of IRFs encoded by some herpesviruses). Class III, which both activates and represses ISGs, includes IRF-2, IRF-4 (Pip/LSIRF/ICSAT), and IRF-7. Class IV, with unknown functions, includes IRF-5 (is not well characterized) and IRF-6. All of these IRFs share a significantly homologous DNA-binding domain residing in the N-terminal 115 amino acids, which contains a characteristic repeat of five tryptophan residues separated by 10 -18 amino acid intervals. Through this DNA-binding domain, IRFs can bind to conserved DNA motifs, such as the interferon stimulated response element (ISRE, existing in most IFN-inducible gene promoters and whose conserved sequence is AGTTTCNNCNY), the interferon consensus sequence (ICS, which is the ICSBP recognition site found in the MHC class I promoter, and whose conserved sequence is G/A G/C TTTC), and the IFN regulatory element (IRF-E or positive regulatory domains [PRDs] I and III in the IFN-β promoters, whose conserved sequence is G(A)AAAG/CT/CGAAAG/CT/C). Recently, virally encoded IRFs have been found, e.g., the human herpes virus 8 / kaposi sarcoma herpes virus possessing 4 open reading frames homologous to cellular IRFs. The following sections will focus on IRF-3, -7 and -9.

IRF-3 was first identified as a homolog of IRF-1 and IRF-2 in a search of an EST database (8). It maps to 19q13.3-q13.4 in the human genome. IRF-3 is expressed constitutively in cells, and is not induced by virus infection or IFN treatment (8). Expression of IRF-3 inhibits IRF-1-induced activation of murine IRF-α4, so it was believed that IRF-3 is a repressor of IFN gene expression at first (249). However, it was shown that IRF-3 can cooperate with RelA(p65), one of the NF-kB family members, to induce IFN-β transcription

(124). Normally, IRF-3 is located in the cytoplasm. Upon virus infection, IRF-3 is activated by phosphorylation, translocates into the nucleus, and binds CBP/P300 to induce transcription of the IFN-β gene. Substitution and deletion mutation studies both showed that phosphorylation of Ser385 and Ser386 in the carboxyl-terminal region of IRF-3 are essential for its activation (330).

IRF-7 was first discovered as a protein that binds and represses the Qp promoter of the Epstein-Bar Virus-encoded gene EBNA-1, which has an ISRE-like element (333). IRF-7 maps to 11p15.5 in the human genome. It is not expressed constitutively in cells, but instead can be induced by virus infection, LPS and IFN (187). Like IRF-3, it is located in the cytoplasm and translocates to the nucleus when activated by virus-stimulated phosphorylation. Mutation studies showed that phosphorylation of Ser425 and Ser 426 are essential for the activation of IRF-7 (190).

IRF-9 was originally referred to as ISGF3γ (interferon-stimulated gene factor-3 gamma) or p48. It maps to 14q11.2 in the human genome. It is constitutively expressed in the cell and is located in both the nucleus and cytoplasm, but translocates to and accumulates in the nucleus upon IFN-α/β treatment (147). IFN-γ and virus infection both can induce IRF-9 expression (145, 297). Treatment of cells with IFN-α or IFN-β triggers phosphorylation of signal transducer and activator of transcription-1 (STAT1) or -2 (STAT2), which then bind to IRF-9 to form a trimeric transcription factor complex (ISGF3) (274). IRF-9 recognizes and binds to various ISREs, but does not function as a transcriptional activator except when complexed with STATs. It is an essential DNA binding domain subunit of ISGF3.

IRF-3 and IRF-7 have been demonstrated to be key regulators of induction of IFNs against virus infection (248). Together with IRF-9, these three factors act cooperatively and form a positive feedback loop of IFN-α and IFN–β production during the cellular antiviral response. IFN-α and IFN–β induction is cell-type specific in IRF-9 deficient mice. In IRF-$9^{-/-}$ MEFs, NDV induction of IFN-α and IFN-β mRNA expression was reduced about 40 and 2-fold respectively (113). The antiviral response can be divided into two phases which together form the positive feedback loop (248). In the early phase, upon initial virus infection, constitutively expressed IRF-3 in the cytoplasm is phosphorylated. The phosphorylated IRF-3 dimerizes and translocates to the nucleus, where it binds to other transcription factors, such as CBP/P300, to induce transcription of the IFN-β gene and IFN-α4 by binding to their IRF-E / PRDI elements. IFN–β and IFN-α4 are secreted and bind to the type I IFN receptors on the cell surface, causing phosphorylation of STAT1 and STAT2 and their binding to IRF-9 to form the trimeric transcription activator ISGF3. ISGF3 translocates to the nucleus and binds to ISREs to induce transcription of ISGs, including IRF-7. In the late phase which occurs as virus spreads, IRF-7 is activated by virus-induced phosphorylation, and IRF-3 and IRF-7 are both translocated into the nucleus. IRF-3 continues to form homodimers and induce IFN-β and IFN-α4 transcription, but IRF-3 also combines with IRF-7 to form heterodimers, binding to the IRF-Es of other IFN-α genes and inducing their transcription. The secreted IFN-α and IFN–β then again bind to the type I interferon receptors and induce more ISG expression to amplify the antiviral response.

Interferon alpha (IFN-α)

IFN-α is a cytokine belonging to the Type I interferon family, which includes IFN-α, -β, -ω, -κ, -δ, and –τ (114, 295). IFN-α is expressed in many if not all mammalian species [320]. The IFN-α gene is composed of a cluster of highly conserved intron-less genes (311). To date, it has been found that murine IFN-α possesses 14 functional subtype genes and 3 pseudogenes (114, 295), human IFN-α has at least 13 functional subtype genes and 1 pseudogene (68), porcine IFN-α has 14 functional subtype genes (37), and feline IFN-α has at least 13 functional subtype genes (210). Individual IFN-α subtypes share extremely high homology, e.g., DNA sequences of porcine IFN-α subtypes share 96.0 to 99.8% conserved nucleotide sequence, protein sequence of feline IFN-α subtypes share 95.9 to 100% similarity, and murine IFN-α subtypes share >80% DNA and protein similarity (114, 295). The following discussion will be focused on murine IFN-α subtypes.

Murine IFN-α genes are clustered on chromosome 4, near the central-proximal region (295). Van Pesch et al (295) screened the mouse genome sequence from the National Center for Biotechnology Information (NCBI), and found 14 functional IFN-α subtype genes and 3 pseudogenes. They determined that the previously named IFN-α6 and IFN-α8 share more than 99% similarity in BALB/c or Swiss mice, as do IFN-α7 and IFN-α10. Therefore they concluded that IFN-α6 and –α8 are the same gene named twice, and that –α7 and –α10 are as well. They referred to IFN-α6 and –α8 as "IFN-α8/6", and IFN-α7 and –α10 as "IFN-α7/10". All of the IFN-α subtype genes were similar between alleles from 129/Sv and C57BL/6 mice, except for IFN-α1, -α-7/10, -α 8/6 and –α11, which showed significant differences. All of the

IFN-α subtypes were stable upon pH 2 treatment, characteristic of Type I but not other IFNs, and all demonstrated antiviral function against Mengo virus infection.

Individual IFN-α subtypes display differential antiviral function. It was found that for antiviral activities against Mengo virus in BALB/3T3 cells, IFN-α11 and –α12 were the highest, IFN-α4 was moderate, and others were about equivalent, except for IFN-α7/10, especially –α7/10 from C57BL/6 mice, which showed much lower antiviral effects (295). IFN-α4 displayed highest antiviral activity compared to IFN-α1, -α2, and -α6 when it was transfected into COS cells and the supernatants were tested for protection of L929 and CHO cells against challenge with vesicular stomatitis virus (294). But purified recombinant murine IFN-α1 and -α4 showed no difference in their antiviral effect against encephalomyocarditis virus infection of J2E cells and L929 cells (276). Though all of IFN-α1, -α4 or -α9 transgenes reduced MCMV replication in mice, IFN-α1 was the most effective (328). When IFN transgenes were applied vaginally to mice before challenge with HSV-2, IFN-α1, -α5 and -β were protective while -α4, -α6 and -α9 were not (10). Finally when mice were injected with constructs expressing IFN-α subtypes and challenged with influenza virus, -α5 and -α6 were most and -α1 least protective (136). Together, the data suggest that the antiviral activity of murine IFN-α subtypes may be both virus- and tissue-specific. Similar differences in antiviral activity have been seen for human IFN-α subtypes (91, 155, 160, 251).

Differential viral induction of IFN-α subtypes has been known for a long time. Newcastle disease virus (NDV) was demonstrated to induce IFN-α4, -α5 and –α6, but not –

α1 in L cells, and IFN-α4 was the predominant subtype to be induced (146). Sendai virus infection can increase IFN-α5 expression in Hepatitis C virus-infected peripheral blood mononuclear cells (PBMC) (159). Induction of IFN-α2, -α6, -α8 and –α13/1 by NDV, respiratory synthytial virus (RSV) and inactivated Herpes simplex virus (HSV) in PBMC was monitored and IFN-α13/1 and -α2 were the major subtypes induced, then IFN-α8, and the lowest was IFN-α6 (181). IFN-α1, -α4, -α8/6, and -α11 were upregulated in influenza A/NWS/33-infected L929 cells, and only IFN-α4 was upregulated in influenza B/Lee/40-infected L929 cells (94). In addition, Van Pesch et al (295) found that IFN-α induction by NDV and Rift Valley fever virus (RVFV) was subtype-specific, with IFN-α4 as the major subtype, IFN-α5 and 2 as minor subtypes, and no other subtypes induced. Therefore viral induction of IFN-α is subtype-, virus, and cell-type-specific.

As described above, IRF-3, -7, and -9 play critical roles in the viral induction of IFN-α expression (45, 165, 190, 270, 327). IFN-α expression is also controlled by other mechanisms, such as suppression. Suppression of IFN-α expression can occur at either the transcriptional or translational level. It has been proposed that the proximal virus responsive element-A (VRE-A) and a 20 bp distal negative regulatory element (DNRE), which is located upstream of VRE-A, is associated with the repression of viral induction of IFN–α11 (180). Though they identified a similar DNRE in the highly induced IFN-α4 promoter region as well, a central anti-silencer region between VRE-A and DNRE was also discovered in IFN-α4, which they believed can overcome the DNRE suppression effect. In later experiments, pituitary homeobox 1 (Ptx1 or Pitx1) (179) and POU transcription factor Oct-1 (200) were demonstrated to bind to the DNRE region and suppress IFN-α11 and –α5

production. Moreover, physical interaction between Ptx1, IRF-3 and IRF-7 was discovered (132). Ptx1 was able to inhibit IRF-3 and IRF-7 transcriptional activity on IFN-α5 and –α11, but IRF-3 was able to bind to the central anti-silencer region of IFN-α4 to counteract the Ptx1 suppressor activity. Though both Ptx1 and Oct-1 bind to the DNRE, direct physical interaction between them was not found (200). Translational suppression was also determined to regulate type I IFN expression. Colina et al (45) determined that translational repressors 4E-BP1 and 4E-BP2 play vital roles in the control of type I IFN production, through translational suppression of IRF-7 expression.

Proteomics

As more complete genome sequences have been made available, it has become more clear that the theory of one gene encoding one protein is no longer true. RNA editing, mRNA alternative splicing, protein post-translational modification, and additional mechanisms result in a more complex set of proteins than genes in an organism (110). For example, Scheler et al (252) demonstrated that the small heat shock protein 27kD (Hsp27) can exist as up to 59 protein species (the smallest unit of the proteome by its chemical structure (141)) due to different protein modifications. Moreover, since proteins are the functional effector and the direct targets for drug development, the need for studies of protein expression is becoming more urgent. In 1995, Wilkins proposed the concept of "proteome", which is defined as "the total protein complement of a genome" (309, 319). Following that, "the study of protein properties (expression level, post-translational modification, interactions etc.) on a large scale to obtain a global, integrated view of disease processes, cellular processes and networks at

the protein level" was called proteomics (20). Two-dimensional (2D) polyacrylamide gel-electrophoresis (151, 219) for protein separation and mass spectrometry (MS) (325) for protein identification provide two essential tools for proteomic studies.

MS is an analytical technique for the determination of the elemental composition of a sample or molecule based on its mass to charge ratio. MS has become an increasingly sensitive and accurate technique to identify proteins (325). The mass spectrometer is composed of three major parts: an ion source, a mass analyzer and an ion detector. The ion source converts molecules into gas-phase ions. Electrospray ionization (ESI) (88) and matrix-assisted laser desorption/ionization (MALDI) (123, 143) are two commonly applied ionization techniques. ESI is used for molecules from a solution and MALDI is for molecules from a solid phase. The mass analyzer sorts the ions based on their mass-to-charge ratio in an electromagnetic field. The ion detector generates data that is used for the identification of each ion presented. Protein identification is accomplished by peptide mass fingerprinting (PMF) (13) database searching, in which a series of peptide masses obtained from MS analysis are compared with theoretical peptide masses derived from *in silico* digestions using protein and nucleotide sequence databases. In order to achieve more accurate protein identifications, tandem MS (MS/MS) technology (50, 70, 128, 300), which utilizes two-stage MS instruments, is also used very frequently. In MS/MS, the first MS selects a random ionized peptide falling within parameters defined by the user, and subjects the peptide to collision-induced dissociation. The second MS analyzes the resulting fragments. In this way, MS/MS provides direct sequence information. Triple quadrupole mass spectrometry,

quadrupole ion trap mass spectrometry, reflectron time-of-flight mass spectrometry, and matrix-assisted laser desorption ionization-time of flight-time of flight (MALDI-TOF-TOF) spectrometry are popular MS/MS technologies for accurate protein identification.

Two-dimensional gel-electrophoresis (2-DE) and shotgun proteomics

Two-DE was developed more than 30 years ago (151, 219), and provides a powerful tool to separate different proteins. It is still the most common choice for current applied proteomics projects (106, 236). The pipeline for 2DE is shown in Figure 1.1. 2-DE is based on separating different proteins by their charge (isoelectric point, pI) in the first dimension by isoelectric focusing (IEF), and by their molecular weight on the second dimension by sodium dodecyl sulfate polyacrylamide gel electrophoresis (SDS-PAGE). Visualization of protein spots on 2-DE gel is dependent on Coomassie blue or silver staining. 2-DE provides extremely powerful resolution. Each 2-DE gel can present over 10,000 individual protein spots (152). This can not be achieved by other protein separation methods. 2-DE is sensitive enough to detect less than 1 ng of protein per spot. Another advantage of 2-DE is that it can detect protein post-translational modifications (PTMs), such as phosphorylation. This is very important since some proteins, for example kinases, are not functional until they express a PTM. 2-DE is a high-throughput technology, allowing up to 12 different gels to be run simultaneously using commercially available devices. Since 2-DE has been in use for a long time, tremendous reagents and devices are available commercially, providing researchers many choices. Finally, protein identification by 2-DE is based on peptide mass fingerprinting,

so it does not require a high quality detection device, i.e., it does not require MS/MS for protein identification, and instead can work with just MS.

However, 2-DE is not perfect. First, while 2-DE is sensitive to some extent (the more sensitive silver staining procedure detects 1 ng protein), it is not sensitive enough to detect very low abundance proteins. Second, it cannot detect hydrophobic and very high molecular weight proteins. They are retained near their pI during electromigration (202, 246). Third, proteins with extreme pIs, *i.e.*, those that are too acidic or too basic, cannot be detected if they are outside of the IEF range (183, 225). Fourth, protein with molecular weights less than 10kD are barely detectable on 2-DE gels. Fifth, it is labor-intensive to run the multiple gels required to compare gel spots between different gels for quantitation. Sixth, variation between 2-DE gels can be large, i.e., the reproducibility can be low. This can result from sample preparation, devices, users, the environment, and other variables. Seventh, multiple proteins may co-resolve in the same spot. Some modifications can be applied to solve this problem. For example, by using an intermediate (pH 4 to 7 or 6 to 9)-range pH gradient IEF gel, 2-DE can separate proteins which may comigrate on traditional 2D gels (ph 3 to 10) (199). Lastly, while one major advantage of 2-DE is identification of PTMs, the disadvantage is that it is difficult to identify all possible forms of the protein and therefore it is difficult to determine the total amount, including all modified forms, of a protein.

Shotgun proteomics refers to a gel-free method which combines high performance liquid chromatography with mass spectrometry to identify proteins in complex mixtures (325). The pipeline of shotgun proteomics is outlined in Figure 1.1. In summary, shotgun proteomics consists of four parts: sample preparation, multidimensional chromatography, MS,

and proteomic analysis (277). Compared to traditional gel-based proteomics, shotgun proteomics has the advantage of enabling detection of extremely acidic or basic proteins, hydrophobic proteins, extremely high or low molecular weight proteins, and very low abundance proteins (308, 322). When the samples are chemically or metabolically labeled with stable isotopes before multidimensional chromatography (49, 109), shotgun proteomics is quantitative. However, because the complex mixture of proteins has not been separated at the "front" end, shotgun proteomics requires greater resolution at the "back" end. Therfore, shotgun proteomics requires much higher quality MS, specifically MS/MS. Another shortage of shotgun proteomics is that it does not allow parallel studies, i.e., 2-DE or 2D-DIGE allows multiple gels to be running at the same time, but shotgun proteomics does not have this capability. The most obvious disadvantage of shotgun proteomics is that it cannot detect PTMs, which is a critical component determining protein function.

2D difference gel electrophoresis (2D-DIGE)

Two-dimensional difference gel electrophoresis (2D-DIGE) is a modification of the traditional 2-DE first applied by Unlu et al (292). The pipeline for 2D-DIGE is shown in Figure 1.2. The principle of 2D-DIGE is based on pre-labeling proteins with fluorescent dyes before gel electrophoresis, so that instead of each gel containing proteins from only one sample, it can include up to three different samples by using different fluorescent dyes (292). In general in 2-DE, a gel contains samples from two different treatments which are labeled with Cy3 and Cy5, and a pool of multiple samples which is labeled with Cy2 as an internal control for quantitative comparisons between different gels (4).

In addition to allowing comparisons between gels, the fluorescent dyes enable 2D-DIGE to be more sensitive and to cover a broader dynamic range (286, 292, 324). The dyes are N-hydroxy succinimidyl ester derivatives of fluorescent cyanine(Cy) dyes, known as Cydye DIGE fluors, including Cy3, Cy5 and Cy2. They express distinct spectra but are charge and mass-matched (292). Currently, Amersham Biosciences (part of GE Healthcare), which owns the license to the 2D-DIGE technology, provides two kinds of Cydyes: Cydye DIGE fluor minimal and Cydye DIGE fluor saturation (191). The Cydye DIGE fluor minimal dyes include Cy2, Cy3, and Cy5, and label Lysine residues to identify differentially expressed proteins on analytical gels when at least 50 μg total protein is loaded per gel (191). Cy2 minimal dye allows detection of as little as 75 pg protein, Cy3 25 pg, and Cy5 25 pg. For these minimal dyes, the only protein molecules detected are those that are labeled with only one dye molecule, therefore very small amounts of the minimal dyes are used since Lysine residues are abundant in most proteins. The result is that about 3 to 5% of total protein is detected. In contrast, the Cydye DIGE fluor saturation dyes include Cy3 and Cy5, and label all available Cysteine residues in the protein and to detect differentially expressed low-abundant proteins on analytical gels which are loaded with only 5 μg total protein per gel. The saturation dyes Cy3 and Cy5 each allow detection of as little as 15 pg of protein, and are thus more sensitive than the minimal dyes. The dynamic range for both the minimal and saturation Cydyes is over 3.6 orders of magnitude, and is therefore much broader than that for silver staining (191).

Use of an internal control, often labeled by Cy2, makes 2D-DIGE an accurate quantitative proteomics tool (4). The internal control is a pool of equal amounts of protein

from each sample, and is loaded onto each gel. Since each gel contains the same amount of the internal control, the relative amount of each protein from one sample on each gel can be normalized to it, allowing comparisons both within the same gel and between different gels. While differences between samples on the same gel would be expected to reflect mainly biological effects, there is significant variation between 2-DE gels. Therefore, normalization to the internal standard is essential for comparisons between gels, and allows precise quantitation.

A Typhoon mode imager is used to scan the gel without disassembling the glass plates. This avoids contamination and provides sensitive and linear detection in a broad dynamic range (324). DeCyder 2D software is then used for data analysis. DeCyder 2D software is a completely automated image analysis software which enables detection, quantitation, matching and analysis of DIGE system gels. DeCyder 2D software includes a Differential In-gel Analysis module (DIA), which is for spot detection and quantitation from a single gel; a Biological Variation Analysis (BVA) module, which is for matching spots among different gels and comparing protein expression across multiple gels quantitatively; and a Batch Processor, which applies both the DIA and BVA modules to perform all stages of the 2-D DIGE analysis process. In addition to the DeCyder 2D software, the DeCyder Extended Data Analysis module (EDA) was developed to perform a more comparative and systematic data analysis for the 2D-DIGE gel. In the EDA analysis, different calculations can be performed, including: 1) differential expression analysis, which identifies proteins expressed differently between different samples; 2) principle component analysis (PCA), which can be calculated for any data set generated by the differential expression analysis but

is usually calculated only for sets where differential expression is statistically significant. PCA analysis provides a rough comparison of the relationship between spot maps and proteins, and indicates the reproducibility among 2D-DIGE gels; 3) pattern analysis, which groups proteins with similar expression patterns; and 4) discriminant analysis, which includes marker selection, classifier creation and classification.

Heart Proteomics

Heart diseases are diverse, and include coronary heart disease, cardiomyopathy, cardiovascular disease, ischaemic heart disease, heart failure, hypertensive heart disease, inflammatory heart disease, and valvular heart disease among others. Heart disease is currently the leading cause of death world-wide (3). Therefore there is an urgent need to identify the molecular mechanisms underlying these different heart diseases and to identify potential biomarkers for evaluation of heart health (272). Heart proteomics, which is defined as "a systematic study of global protein properties to gain insight into mechanisms of cardiac function in health and diseases" (170) is thus becoming an increasingly valuable approach.

Heart proteomic studies started in the 1990's. Currently, there are four 2-DE heart protein databases available, including HP-2DPAGE (for human ventricle) (206), HEART-2DPAGE (for human ventricle and atrium) (228), HSC-2DPAGE (for human, rat, dog and mouse ventricle) (12, 81), and RAT HEART-2DPAGE (for rat heart) (169). New 2-DE proteomics data have been added to the construction of these databases (84, 89, 158, 265, 269, 314). There are about 400 proteins identified, of which most are disease-related proteins

(233). These databases provide useful bases for comparison for researchers who are studying heart proteomics.

Heart proteomic studies can be carried out using specimens from human patients, animal models and cultured cardiac myocytes. Currently, proteomics studies on isolated heart cells, which can differentiate cell responses among different cell types, are rare and online databases are not available (135). Few publications have reported using mouse cardiac myocytes (40), neonatal (5) or adult (6) rat cardiac myocytes, and human cardiac myocytes (52, 293) for heart proteomic studies. Animal models provide useful tools for heart proteomics research. At present, several animal models mimicking human heart diseases are available, including a dog model for human idiopathic dilated cardiomyopathy (120), a bovine model for dilated cardiomyopathy (161, 310), a rat model for toxicity induced by chronic ethanol intake (223), and others.

Currently, most proteomic studies on the human heart are focused on dilated cardiomyopathy (DCM) (83, 199). DCM involves heart failure with an unclear etiology. Several factors may contribute to DCM, including genetic factors, viral infections, cardiac-specific antibodies, and toxic agents such as alcohol. Proteomic studies on DCM started in the 1990's with 2-DE (12, 140). About 100 cardiac proteins have been reported to be differentially expressed when comparing DCM hearts to the normal heart (198), and they can be classified into three major categories: cytoskeletal and myofibril proteins (such as actin and vimentin) (52), mitochondrial and energy production-related proteins (such as ATP synthase and creatine kinase) (52, 142), and stress response proteins (such as Hsp27, HSP60, and HSP70) (52). Proteomic studies on other heart diseases are rare. One study on ventricular

hypertrophy (275) and two studies on coronary artery disease in patients with heart transplantation (161, 313) were reported in the 1990's.

Some heart proteomic studies are focused on specific "subproteomes" of the heart, such as mitochondrial proteins (67, 283) or protein kinase C-ε (PKC-ε)-related proteins (11, 75, 168, 226, 301, 332). Mitochondria are vital organelles in the cells playing diverse biological roles, such as ATP production and regulation of apoptosis. Most importantly here, mitochondrial changes are correlated closely with heart disease (38). Taylor et al (283) applied sucrose gradient centrifugation coupled with one-dimensional PAGE and MS peptide mass fingerprinting to identify 615 mitochondria proteins from the normal human heart. Except for approximately 19% of the identified proteins which are of unknown function, most of the proteins are involved in RNA, DNA, and protein synthesis, signaling, ion transportation, and lipid metabolism. Though this study was of healthy hearts, it provides a comprehensive resource for other researchers who study heart mitochondrial functions and pathways during disease. Devreese et al (67) investigated the human heart enzymes of the mitochondrial oxidative phosphorylation system (OXPHOS) using blue-native polyacrylamide gel electrophoresis (BNPAGE) (250) as the first-dimension and tricine SDS-PAGE as the second-dimension for protein separation and MALDI TOF for protein identification. They detected all of the individual subunits of the five OXPHOS multienzyme complexes, providing valuable information for the diagnosis of diseases caused by disorders in the oxidative phosphorylation system. A proteomic study related to PKC-ε heart protective effects was carried out by Ping's group (11, 75, 168, 226, 301, 332). They found that at least 93 proteins in the mouse heart that interact with PKC-ε, and a complex of PKC-ε / AKT /

endothelial NO synthase (eNOS) are associated with heart protection. Though these "subproteome" studies are in their infant stage, they provide helpful information to guide future research on heart diseases.

Heat shock proteins (HSPs)

HSPs, which belong to the stress protein superfamily, are a group of highly conserved proteins produced in response to mild environmental challenges such as heat shock, heavy metals, infection, ischemia, and radiation (133, 174). HSPs were first identified by Ritossa et al in 1962 in the salivary gland in *Drosophila* flies as chromosome puffs (sites of active transcription) in response to high temperature stress (240). In 1974, studies on HSPs progressed to the protein level (285). Researchers demonstrated that HSPs are survival proteins that help cells to adjust to gradual environmental changes and to survive under lethal conditions. HSPs are characterized by their molecular chaperone function (31, 32) and anti-apoptotic role (326), and most of them are involved in tumorogenesis (204) as well. Classification of HSPs is based on their size and corresponding function. Criteria from the Cold Spring Harbor Meeting of 1996 (122) state that the family name should be written in capital letters, e.g. HSP60, and members of a family should be written as Hsp, e.g. Hsp27. Mammalian HSPs are classified into six major families: HSP110, 90, 70, 60, 40 and small HSPs (111, 288). Previously, HSPs were considered to be located only intracellularly, in the cytoplasm, nucleus, endoplasmic reticula or mitochondria (111). However recent studies determined that some HSPs are expressed extra-cellularly and on the cell surface membrane as well (208, 305). It is believed that the intracellular HSPs serve as molecular chaperones

and are responsible for cytoprotection, while the extracellular and membrane-bound HSPs play important immunological functions (208). The following sections will focus on a small HSP, Hsp25, which is identified in our proteomics project, and the HSP70 family, which plays an important protective role in the heart.

Hsp25

Rodent 25kD heat shock protein (Hsp25) and its human homolog Hsp27 belong to the small HSP subfamily, and are ATP-independent chaperones. They are constitutively expressed in the cytoplasm under physiological conditions (1) in some tissues and organs, such as the skin, lung, heart, and skeletal muscle, and in some cells, such as smooth, skeletal, and cardiac muscle cells (304). In the adult mouse heart, Hsp25 comprises approximately 0.2% of the heart protein (99). Upon heat shock or other stress, it translocates almost entirely into the nucleus (1). Hsp25/Hsp27 can form oligomeric structures up to 800 kD (28), and the dimer of Hsp25/Hsp27 is thought to be the building block for multimeric complexes (256). Hsp25/Hsp27 is a survival protein, and it possesses diverse biological potentials. Its main chaperone function is to prevent non-native protein aggregation (78). It plays important roles in protecting cells and organs from heat shock or other stresses by inhibiting apoptosis through different mechanisms, such as sequestering both pro-caspase-3 and cytochrome c (27, 46, 224), inhibiting cytochrome c-dependent activation of procaspase-9 (96), inhibiting caspase-3 proteolytic activation (302), and regulating Akt activation (237). Hsp25/Hsp27 is also critical in stabilizing actin microfilaments by preventing heat-induced aggregation of F-actin by forming soluble complexes with denatured actin (227) . Hsp25/Hsp27 plays a

protective role in neuronal cells (92, 323) and cardiac myocytes (21, 53, 119, 157, 166, 176, 182, 296, 331). It is involved in embryonic development (99, 280) and is correlated with tumorogenesis (102, 108) as well.

Hsp25/Hsp27 can undergo phosphorylation in response to stimuli, mainly by mitogen-activated protein kinase (MAPK)-activated protein kinase-2/3 (MK2/3) and p38-activated / regulated kinase (PRAK) through the p38-MAPK pathway (184, 214, 273), and sometimes through protein kinase c (144) as well. The phosphorylation sites for Hsp25 have been identified as Ser15 and Ser86 (95). Phosphorylation of Hsp25 results in the dissociation of larger oligomers into smaller ones (192, 242). Whether phosphorylation of Hsp25 is required for its protective and anti-apoptotic function is in conflict. Some studies found that large oligomers, which consist of non-phosphorylation Hsp25, are the major player in its anti-apoptotic effect and phosphorylation is not required (28). Moreover, phosphorylation can also attenuate its anti-apoptotic and chaperone action (234, 242). Others demonstrated that phosphorylation is required for Hsp25 to play its anti-apoptotic and protective roles (17, 21, 35, 166). Over-expression of Hsp25/Hsp27 provides protection against ischemia / reperfusion-induced cardiac dysfunction both *in vitro* and *in vivo (157, 182, 296, 331)*, and the protection is correlated with Hsp25/Hsp27 phosphorylation (21, 166).

Besides phosphorylation, Hsp27 can be methylglyoxal (MG) modified as well (97, 211, 221, 244). MG is the aldehyde form of pyruvic acid ($C_3H_4O_2$) and the major source of MG is glycolysis. It has been demonstrated that MG is the most important precursor for forming advanced glycation end-products (AGE) (266). MG can react with free arginine and lysine residues (2). For Hsp27 MG modification, MG occurs on Arg188 and to generate

argpyrimidine (244). In brunescent cataractous lenses, phosphorylated Hsp27 was identified as the major MG modified substrate to form argpyrimidine (221). MG modification can increase the chaperone function of both Hsp27 (211, 221) and phosphorylated Hsp27 (221), and can enhance their anti-apoptotic roles as well (221, 244). Oya-Ito et al further identified that MG modification of Hsp27 can reduce caspase-9 activity, and the same modification of phosphorylated Hsp27 can reduce both the caspase-9 and -3 activities (221).

Whether Hsp25/Hsp27 expresses an anti-viral role and whether its phosphorylation is correlated with this anti-viral role have not been well-studied. Currently, members of seven different virus families were found to induce Hsp25/Hsp27 expression or phosphorylation, including Herpesviridae (90, 93, 103, 104), Papillomaviridae (41, 177), Hepadnaviridae (112, 173), Paramyxoviridae (267, 329), Flaviviridae (39, 87, 172), Togaviridae (213), and Retroviridae (171, 303). However, only one study on HIV addressed Hsp27 anti-viral activity, finding that it inhibits HIV Vpr, and proposed that it may contribute to cellular intrinsic immunity against HIV infection (171).

HSP70

HSP70 is the most conserved HSP protein family discovered to date (174). The DNA sequence homology is 74% when compared between yeast and Drosophila and 85% between mouse and Drosophila. All eukaryotes possess multiple genes encoding highly homologous HSP70 proteins, for example one fungus species has 10 (98), yeast has 8 (312), and human has at least 11 (282). All members of the HSP70 family possess a conserved amino-terminal adenine nucleotide-binding domain (NBD or ATPase) and a carboxy-terminal substrate /

peptide-binding domain (SBD or PBD). The latter region is further split into two domains: the β-sandwich domain responsible for substrate binding, and the α-domain responsible for determining substrate-binding affinity (196). Based on the length of the loop between the β-sandwich domain and the α-domain, HSP70s are further classified into three subfamilies: the classic DnaK/Hsp70, the Sse/Hsp110 and the Lhs1/Grp170 (196). Functions of HSP70s have been investigated widely, and are reviewed well (9, 59, 203, 207). In brief, house-keeping functions of HSP70s are involved in transportation, degradation, regulation, folding and refolding proteins, and immune responses. Interestingly, some HSP70s enhance virus infectivity, replication and entry into cells. Parent et al (222) found that the heat shock cognate protein 70 (Hsc70) interacts with the E2 envelope protein of HCV and co-localizes with core and E2 proteins in lipid droplets. Anti-Hsc70 antibody decreased HCV infectivity, and RNA interference of Hsc70 decreased lipid droplet volume. Therefore it is thought that Hsc70 can regulate HCV infectivity and virus release, related in some way to lipid droplets. Hsc70 was also demonstrated to be able to compete with viral P protein for binding with viral X protein of Borna disease virus to modulate virus replication (115). Hsp70 serves as a putative receptor for Japanese encephalitis virus (JEV) by interacting with the viral envelope (E) protein on mouse neuroblastoma (Neuro2a) cells (58). Pogany et al reported that Hsp70 is required for *in vitro* assembly of a fully functional replicase complex of Tomato bushy stunt virus (TBSV) (230).

HSPs and the heart

Several HSPs were identified to be involved in heart development and play cardioprotective roles against stress. Among these, Hsp20 (86, 334), Hsp25, and the HSP70s have been investigated widely. The following discussion will be focused on the cardioprotective role of Hsp25/Hsp27 and the HSP70s.

Hsp25/Hsp27 is involved in cardiogenesis and myogenesis (26, 29, 60, 176). In *Xenopus laevis*, it has been demonstrated that Hsp27 possesses the capability of regulating actin dynamics to affect cell motility or adhesion during cardiogenesis, and is therefore necessary for heart tube formation (26). Hsp25 was demonstrated to play a critical role in the differentiation of the multipotent embryonal carcinoma cell line, P19, into cardiomyocytes (60).

Hsp25/Hsp27 also plays a critical protective role in the heart. Efthymiou et al (76) first discovered that over-expression of Hsp27 in mice can decrease the ischemia / reperfusion (IR)-induced infarct size, demonstrating that Hsp27 possesses a protective role in lethal IR in the heart. Lu et al (182) determined that IR causes cardiac troponin I (cTnI) and troponin T (cTnT) degradation, which decreases myofilament responses to Ca(2+) and impairs cardiac contractile function. Over-expression of Hsp27 in rat heart and cardiomyocytes can prevent cTnI and cTnT degradation by interacting with them directly to inhibit their proteolytic cleavage. Different groups discovered that Hsp27 plays an important role in protecting against congestive heart failure induced by doxorubicin (DOX), which is used for cancer therapy. Ilangovan ‘s group determined that Hsp27 reduces DOX-mediated oxidant-induced cardiac toxicity by behaving as an anti-apoptotic protein, to decrease

reactive oxygen species (ROS) production and the Bax to Bcl2 ratio (299). The same group also found that in mouse fibroblasts and embryonic rat heart-derived cardiac H9c2 cells, protection effect of Hsp27 against DOX-induced cardiac toxicity is dose-dependent, and depletion of Hsp27 results in lower cell viability in DOX-treated cells (289). Using Hsp27 transgenic mice, Liu et al (175) also found the same protective effects of Hsp27. They observed that over-expression of Hsp27 significantly decreased the 5-day mortality, cardiac dysfunction and cardiomyocyte apoptosis rates caused by DOX treatment compared to wild type mice. Moreover, they demonstrated that Hsp27 protects against endotoxin-induced cardiac dysfunction as well (331).

Phosphorylation of Hsp27 is required for its cardioprotective role in some instances. Using a hyperglycemia rat model, Chen et al demonstrated that rats with type I diabetes possess higher resistance to ischemia and better heart function recovery than non-diabetic rats, and that this is correlated with Hsp27 phosphorylation (36). The diphosphorylated form of Hsp27 was found to be localized in blood vessels of cardiac transplanted patients without cardiac allograft vasculopathy (CAV), which is a severe complication after cardiac transplantation, but not in patients with CAV. Therefore it is believed that diphosphorylated Hsp27 plays a critical role in maintaining blood vessel health in cardiac transplantation patients (62). It was discovered that morphine, which is used for cardiovascular anesthesia and for the emergency treatment of cardiac infarction, prevents cardiac injury through stimulating phosphorylation of Hsp27 in a rat model (205). The phosphorylated form of Hsp27 was able to reduce DOX-induced cardiac toxicity by stabilizing F-actin remodeling

(299). Finally, Hsp27 phosphorylation induced by low doses of H2O2 is protective against IR injury by preventing desmin degradation (21).

Members of the HSP70 family were demonstrated to play cardioprotective roles earlier than Hsp25/Hsp27, with much research carried out during the mid 1990's (130, 189, 201, 229, 287). Plumier et al transfected human inducible Hsp70 into mice, and monitored cardiac function post-IR injury. They found that Hsp27 transgenic mice demonstrated much better recovery of contractile force, rate of contraction and relaxation, and much lower creatine kinase activity, which indicates cell injury, compared to non-transgenic mice (229). Almost at the same time, Marber et al over-expressed rat inducible Hsp70 in mice and evaluated Hsp70 protective function in isolated hearts from transgenic mice after IR. They found that over-expression of Hsp70 reduced the infarct size and efflux of creatine kinase, and increased the contractile function during recovery from IR injury (189). The ability of Hsp70 to reduce infarct size was further confirmed *in vivo* in Hsp70 transgenic mice and rat (130, 220). Trost et al demonstrated that inducible Hsp70 in transgenic mice improved cardiac function after IR *in vivo* later as well (287). Jayakumar infused rat hearts with Hsp70 and then transplanted them into recipient rats, and found that the over-expressed Hsp70 improved both cardiac mechanical and endothelial cell function following IR injury (137). Finally, double null mice for Hsp70-3 and Hsp70-1 were much more susceptible to IR-induced cardiac dysfunction and cell damage, further demonstrating Hsp70's cardioprotective role (148).

Questions and approaches

IFN-α and IFN-β belong to the type I IFN family and they bind the same cell surface receptor. Reovirus induction of and sensitivity to IFN-β in cardiac cells is an important determinant of protection against myocarditis in a mouse model. Therefore, we investigated reovirus induction of and sensitivity to IFN-α subtypes in cardiac cells. While previous studies investigated virus induction of IFN-α expression in other cell types, they focused mainly on the entire IFN-α family rather than differentiating between individual IFN-α subtypes because of their high sequence conservation. Currently, there are still no commercially available reagents to differentiate among the different IFN-α subtypes. In addition, there have been no previous investigations of viral induction of individual IFN-α subtypes or of their antiviral roles in cardiac cells. Here we developed a new approach by designing primers for quantititative Real-Time PCR, which enables the accurate and specific quantitation of individual IFN-α subtypes induced by reovirus infection of primary cardiac myocyte and cardiac fibroblast cultures. Chapter 2 will describe this method and its application. However, this new method did not allow us to investigate the antiviral effects of each IFN-α subtype. At that time, there was no source of purified IFN-α subtypes or specific antibodies that distinguished between IFN-α subtypes. Therefore, we over-expressed several IFN-α subtypes in transfected primary cardiac myocyte and cardiac fibroblast cultures, and those investigations are described in Appendix I. Unfortunately, the transfection process itself induced genes downstream of IFN, and therefore this approach was not appropriate for our purposes. Fortunately, PBL Inc. offered to provide us with purified IFN-α subtypes

before their commercial availability, so we were able to use those reagents to investigate IFN-α antiviral effects, as described in Chapter 2.

The IFN system plays a critical antiviral role in innate immunity, and components in the IFN pathway have been widely investigated. However despite major progress, there has always remained the possibility that other players remain to be revealed. In addition, since the heart is a complex and vital organ that is continuously exposed to viral challenges, we hypothesized that there must be protective antiviral mechanisms in addition to the IFN system. Microarray technology offers a powerful high-throughput approach for discovery of new genes induced or repressed by viral infection. However, since proteins are the final effector molecules, and since post-translational modifications (PTMs) have proven to be very important in at least one innate response pathway (IFN), microarray technology, which detects differences in mRNA expression, seemed poorly suited for our goals. By comparison, proteomic approaches which can be used to detect stimulus effects on protein expression and PTMs, seemed a promising choice. Selection of the appropriate proteomic technology was critical for our investigations, which required quantitative comparison between multiple samples (generated using a small panel of viruses, which vary in their inductions of myocarditis and IFN-β), and which required the ability to detect PTMs. The technology 2D-DIGE seemed the best option.

All viruses induce changes in cell protein expression over time. In order to identify the optimal time post-infection to capture many cell protein changes, a preliminary 2D-DIGE experiment was conducted comparing cardiac myocyte lysates at several times post-infection with a single reovirus strain (T3D). This experiment is described in Appendix 2. Based on

these results, a single time-point was selected for the main study which was to compare proteome changes induced by four reovirus strains. Those results are discussed in Chapter 3. However, we found that T3D induced an interesting protein (cryptdin 4) in the first study (Appendix 2) but failed to induce it in the second study (Chapter 3). Therefore, in order to determine whether T3D induction of cryptdin 4 was reproducible, we used 1D gel electrophoresis followed by LC-MS/MS as a simpler approach to analyze infected lysates. While results indicated that T3D induction of cryptdin 4 is not reproducible, the study provided useful information documented in Appendix 3. Returning to our main study using 2D-DIGE to compare cardiac myocyte lysates infected with different reovirus strains, we used Ingenuity Pathway Analysis (IPA) to identify pathways and protein-protein interactions for the proteins which were identified as differentially expressed between infections. Although multiple interesting pathways and protein-protein interaction networks were identified, these preliminary results were difficult to interpret. Therefore, instead of including them in Chapter 3, they are provided in Appendix 4. Finally, Chapter 3 describes our identification of Hsp25 as an interesting protein modulated by virus infection. In order to determine whether Hsp25 or its phosphorylated form provide antiviral function, we over-expressed Hsp25 or Hsp27D (a phospho-mimetic version of the human isoform) in transfected cardiac myocytes, as described in Appendix 5. While concerns with this approach left results difficult to interpret, the studies provide the foundation for future attempts to over-express Hsp25 or its analogs in cardiac cells.

REFERENCES

1. **Adhikari, A. S., K. Sridhar Rao, N. Rangaraj, V. K. Parnaik, and C. Mohan Rao.** 2004. Heat stress-induced localization of small heat shock proteins in mouse myoblasts: intranuclear lamin A/C speckles as target for alphaB-crystallin and Hsp25. Exp Cell Res **299:**393-403.

2. **Ahmed, M. U., E. Brinkmann Frye, T. P. Degenhardt, S. R. Thorpe, and J. W. Baynes.** 1997. N-epsilon-(carboxyethyl)lysine, a product of the chemical modification of proteins by methylglyoxal, increases with age in human lens proteins. Biochem J **324 (Pt 2):**565-70.

3. **Ahmed, N., G. Barker, K. Oliva, D. Garfin, K. Talmadge, H. Georgiou, M. Quinn, and G. Rice.** 2003. An approach to remove albumin for the proteomic analysis of low abundance biomarkers in human serum. Proteomics **3:**1980-7.

4. **Alban, A., S. O. David, L. Bjorkesten, C. Andersson, E. Sloge, S. Lewis, and I. Currie.** 2003. A novel experimental design for comparative two-dimensional gel analysis: two-dimensional difference gel electrophoresis incorporating a pooled internal standard. Proteomics **3:**36-44.

5. **Arnott, D., K. L. O'Connell, K. L. King, and J. T. Stults.** 1998. An integrated approach to proteome analysis: identification of proteins associated with cardiac hypertrophy. Anal Biochem **258:**1-18.

6. **Arrell, D. K., I. Neverova, H. Fraser, E. Marban, and J. E. Van Eyk.** 2001. Proteomic analysis of pharmacologically preconditioned cardiomyocytes reveals novel phosphorylation of myosin light chain 1. Circ Res **89:**480-7.

7. **Atwater, J. A., S. M. Munemitsu, and C. E. Samuel.** 1986. Biosynthesis of reovirus-specified polypeptides. Molecular cDNA cloning and nucleotide sequence of the reovirus serotype 1 Lang strain s4 mRNA which encodes the major capsid surface polypeptide sigma 3. Biochem Biophys Res Commun **136:**183-92.

8. **Au WC, M. P., LowtherW, Juang YT, Pitha PM.** 1995. Identification of a member of the interferon regulatory factor family that binds to the interferon-stimulated response element and activates expression of interferon-induced genes. . Proc. Natl. Acad. Sci. USA **92:**11657–61.

9. **Aufricht, C.** 2005. Heat-shock protein 70: molecular supertool? Pediatr Nephrol **20:**707-13.

10. **Austin, B. A., C. M. James, P. Harle, and D. J. Carr.** 2006. Direct application of plasmid DNA containing type I interferon transgenes to vaginal mucosa inhibits HSV-2 mediated mortality. Biol Proced Online **8:**55-62.

11. **Baines, C. P., J. Zhang, G. W. Wang, Y. T. Zheng, J. X. Xiu, E. M. Cardwell, R. Bolli, and P. Ping.** 2002. Mitochondrial PKCepsilon and MAPK form signaling modules in the murine heart: enhanced mitochondrial PKCepsilon-MAPK interactions and differential MAPK activation in PKCepsilon-induced cardioprotection. Circ Res **90:**390-7.

12. **Baker, C. S., J. M. Corbett, A. J. May, M. H. Yacoub, and M. J. Dunn.** 1992. A human myocardial two-dimensional electrophoresis database: protein characterisation by microsequencing and immunoblotting. Electrophoresis **13:**723-6.

13. **Banks, R. E., M. J. Dunn, D. F. Hochstrasser, J. C. Sanchez, W. Blackstock, D. J. Pappin, and P. J. Selby.** 2000. Proteomics: new perspectives, new biomedical opportunities. Lancet **356:**1749-56.

14. **Bartlett, J. A., and W. K. Joklik.** 1988. The sequence of the reovirus serotype 3 L3 genome segment which encodes the major core protein lambda 1. Virology **167:**31-7.

15. **Barton, E. S., J. C. Forrest, J. L. Connolly, J. D. Chappell, Y. Liu, F. J. Schnell, A. Nusrat, C. A. Parkos, and T. S. Dermody.** 2001. Junction adhesion molecule is a receptor for reovirus. Cell **104:**441-51.

16. **Baty, C. J., and B. Sherry.** 1993. Cytopathogenic effect in cardiac myocytes but not in cardiac fibroblasts is correlated with reovirus-induced acute myocarditis. J Virol **67:**6295-8.

17. **Benn, S. C., D. Perrelet, A. C. Kato, J. Scholz, I. Decosterd, R. J. Mannion, J. C. Bakowska, and C. J. Woolf.** 2002. Hsp27 upregulation and phosphorylation is required for injured sensory and motor neuron survival. Neuron **36:**45-56.

18. **Bergmann, O., R. D. Bhardwaj, S. Bernard, S. Zdunek, F. Barnabe-Heider, S. Walsh, J. Zupicich, K. Alkass, B. A. Buchholz, H. Druid, S. Jovinge, and J. Frisen.** 2009. Evidence for cardiomyocyte renewal in humans. Science **324:**98-102.

19. **Bisaillon, M., J. Bergeron, and G. Lemay.** 1997. Characterization of the nucleoside triphosphate phosphohydrolase and helicase activities of the reovirus lambda1 protein. J Biol Chem **272:**18298-303.

20. **Blackstock, W. P., and M. P. Weir.** 1999. Proteomics: quantitative and physical mapping of cellular proteins. Trends Biotechnol **17:**121-7.

21. **Blunt, B. C., A. T. Creek, D. C. Henderson, and P. A. Hofmann.** 2007. H2O2 activation of HSP25/27 protects desmin from calpain proteolysis in rat ventricular myocytes. Am J Physiol Heart Circ Physiol **293:**H1518-25.

22. **Borsa, J., T. P. Copps, M. D. Sargent, D. G. Long, and J. D. Chapman.** 1973. New intermediate subviral particles in the in vitro uncoating of reovirus virions by chymotrypsin. J Virol **11:**552-64.

23. **Borsa, J., B. D. Morash, M. D. Sargent, T. P. Copps, P. A. Lievaart, and J. G. Szekely.** 1979. Two modes of entry of reovirus particles into L cells. J Gen Virol **45:**161-70.

24. **Brentano, L., D. L. Noah, E. G. Brown, and B. Sherry.** 1998. The reovirus protein mu2, encoded by the M1 gene, is an RNA-binding protein. J Virol **72:**8354-7.

25. **Broering, T. J., A. M. McCutcheon, V. E. Centonze, and M. L. Nibert.** 2000. Reovirus nonstructural protein muNS binds to core particles but does not inhibit their transcription and capping activities. J Virol **74:**5516-24.

26. **Brown, D. D., K. S. Christine, C. Showell, and F. L. Conlon.** 2007. Small heat shock protein Hsp27 is required for proper heart tube formation. Genesis **45:**667-78.

27. **Bruey, J. M., C. Ducasse, P. Bonniaud, L. Ravagnan, S. A. Susin, C. Diaz-Latoud, S. Gurbuxani, A. P. Arrigo, G. Kroemer, E. Solary, and C. Garrido.** 2000. Hsp27 negatively regulates cell death by interacting with cytochrome c. Nat Cell Biol **2:**645-52.

28. **Bruey, J. M., C. Paul, A. Fromentin, S. Hilpert, A. P. Arrigo, E. Solary, and C. Garrido.** 2000. Differential regulation of HSP27 oligomerization in tumor cells grown in vitro and in vivo. Oncogene **19:**4855-63.

29. **Brundel, B. J., A. Shiroshita-Takeshita, X. Qi, Y. H. Yeh, D. Chartier, I. C. van Gelder, R. H. Henning, H. H. Kampinga, and S. Nattel.** 2006. Induction of heat shock response protects the heart against atrial fibrillation. Circ Res **99:**1394-402.

30. **Bujnicki, J. M., and L. Rychlewski.** 2001. Reassignment of specificities of two cap methyltransferase domains in the reovirus lambda 2 protein. Genome Biol **2:**RESEARCH0038.

31. **Bukau, B., J. Weissman, and A. Horwich.** 2006. Molecular chaperones and protein quality control. Cell **125:**443-51.

32. **Burel, C., V. Mezger, M. Pinto, M. Rallu, S. Trigon, and M. Morange.** 1992. Mammalian heat shock protein families. Expression and functions. Experientia **48:**629-34.

33. **Cashdollar, L. W.** 1994. Characterization and structural localization of the reovirus lambda 3 protein. Res Virol **145:**277-85.

34. **Chappell, J. D., J. L. Duong, B. W. Wright, and T. S. Dermody.** 2000. Identification of carbohydrate-binding domains in the attachment proteins of type 1 and type 3 reoviruses. J Virol **74:**8472-9.

35. **Charette, S. J., J. N. Lavoie, H. Lambert, and J. Landry.** 2000. Inhibition of Daxx-mediated apoptosis by heat shock protein 27. Mol Cell Biol **20:**7602-12.

36. **Chen, H., X. J. Wu, X. Y. Lu, L. Zhu, L. P. Wang, H. T. Yang, H. Z. Chen, and W. J. Yuan.** 2005. Phosphorylated heat shock protein 27 is involved in enhanced heart tolerance to ischemia in short-term type 1 diabetic rats. Acta Pharmacol Sin **26:**806-12.

37. **Cheng, G., W. Chen, Z. Li, W. Yan, X. Zhao, J. Xie, M. Liu, H. Zhang, Y. Zhong, and Z. Zheng.** 2006. Characterization of the porcine alpha interferon multigene family. Gene **382:**28-38.

38. **Chinnery, P. F., N. Howell, R. M. Andrews, and D. M. Turnbull.** 1999. Clinical mitochondrial genetics. J Med Genet **36:**425-36.

39. **Choi, Y. W., Y. J. Tan, S. G. Lim, W. Hong, and P. Y. Goh.** 2004. Proteomic approach identifies HSP27 as an interacting partner of the hepatitis C virus NS5A protein. Biochem Biophys Res Commun **318:**514-9.

40. **Chu, G., G. F. Egnaczyk, W. Zhao, S. H. Jo, G. C. Fan, J. E. Maggio, R. P. Xiao, and E. G. Kranias.** 2004. Phosphoproteome analysis of cardiomyocytes subjected to beta-adrenergic stimulation: identification and characterization of a cardiac heat shock protein p20. Circ Res **94:**184-93.

41. **Ciocca, D. R., G. Lo Castro, L. V. Alonio, M. F. Cobo, H. Lotfi, and A. Teyssie.** 1992. Effect of human papillomavirus infection on estrogen receptor and heat shock protein hsp27 phenotype in human cervix and vagina. Int J Gynecol Pathol **11:**113-21.

42. **Clarke, P., S. M. Richardson-Burns, R. L. DeBiasi, and K. L. Tyler.** 2005. Mechanisms of apoptosis during reovirus infection. Curr Top Microbiol Immunol **289:**1-24.

43. **Clarke, P., and K. L. Tyler.** 2003. Reovirus-induced apoptosis: A minireview. Apoptosis **8:**141-50.

44. **Coffey, C. M., A. Sheh, I. S. Kim, K. Chandran, M. L. Nibert, and J. S. Parker.** 2006. Reovirus outer capsid protein micro1 induces apoptosis and associates with lipid droplets, endoplasmic reticulum, and mitochondria. J Virol **80:**8422-38.

45. **Colina, R., M. Costa-Mattioli, R. J. Dowling, M. Jaramillo, L. H. Tai, C. J. Breitbach, Y. Martineau, O. Larsson, L. Rong, Y. V. Svitkin, A. P. Makrigiannis, J. C. Bell, and N. Sonenberg.** 2008. Translational control of the innate immune response through IRF-7. Nature **452:**323-8.

46. **Concannon, C. G., S. Orrenius, and A. Samali.** 2001. Hsp27 inhibits cytochrome c-mediated caspase activation by sequestering both pro-caspase-3 and cytochrome c. Gene Expr **9:**195-201.

47. **Connolly, J. L., E. S. Barton, and T. S. Dermody.** 2001. Reovirus binding to cell surface sialic acid potentiates virus-induced apoptosis. J Virol **75:**4029-39.

48. **Connolly, J. L., and T. S. Dermody.** 2002. Virion disassembly is required for apoptosis induced by reovirus. J Virol **76:**1632-41.

49. **Conrads, T. P., K. Alving, T. D. Veenstra, M. E. Belov, G. A. Anderson, D. J. Anderson, M. S. Lipton, L. Pasa-Tolic, H. R. Udseth, W. B. Chrisler, B. D. Thrall, and R. D. Smith.** 2001. Quantitative analysis of bacterial and mammalian proteomes using a combination of cysteine affinity tags and 15N-metabolic labeling. Anal Chem **73:**2132-9.

50. **Coon, J. J., J. E. Syka, J. Shabanowitz, and D. F. Hunt.** 2005. Tandem mass spectrometry for peptide and protein sequence analysis. Biotechniques **38:**519, 521, 523.

51. **Cooper, L. T., Jr.** 2009. Myocarditis. N Engl J Med **360:**1526-38.

52. **Corbett, J. M., H. J. Why, C. H. Wheeler, P. J. Richardson, L. C. Archard, M. H. Yacoub, and M. J. Dunn.** 1998. Cardiac protein abnormalities in dilated cardiomyopathy detected by two-dimensional polyacrylamide gel electrophoresis. Electrophoresis **19:**2031-42.

53. **Cullingford, T. E., R. Wait, A. Clerk, and P. H. Sugden.** 2006. Effects of oxidative stress on the cardiac myocyte proteome: modifications to peroxiredoxins and small heat shock proteins. J Mol Cell Cardiol **40:**157-72.

54. **Daliento, L., F. Calabrese, F. Tona, A. L. Caforio, G. Tarsia, A. Angelini, and G. Thiene.** 2003. Successful treatment of enterovirus-induced myocarditis with interferon-alpha. J Heart Lung Transplant **22:**214-7.

55. **Danthi, P., C. M. Coffey, J. S. Parker, T. W. Abel, and T. S. Dermody.** 2008. Independent regulation of reovirus membrane penetration and apoptosis by the mu1 phi domain. PLoS Pathog **4:**e1000248.

56. **Danthi, P., M. W. Hansberger, J. A. Campbell, J. C. Forrest, and T. S. Dermody.** 2006. JAM-A-independent, antibody-mediated uptake of reovirus into cells leads to apoptosis. J Virol **80:**1261-70.

57. **Danthi, P., T. Kobayashi, G. H. Holm, M. W. Hansberger, T. W. Abel, and T. S. Dermody.** 2008. Reovirus apoptosis and virulence are regulated by host cell membrane penetration efficiency. J Virol **82:**161-72.

58. **Das, S., S. V. Laxminarayana, N. Chandra, V. Ravi, and A. Desai.** 2009. Heat shock protein 70 on Neuro2a cells is a putative receptor for Japanese encephalitis virus. Virology **385:**47-57.

59. **Daugaard, M., M. Rohde, and M. Jaattela.** 2007. The heat shock protein 70 family: Highly homologous proteins with overlapping and distinct functions. FEBS Lett **581:**3702-10.

60. **Davidson, S. M., and M. Morange.** 2000. Hsp25 and the p38 MAPK pathway are involved in differentiation of cardiomyocytes. Dev Biol **218:**146-60.

61. **De Benedetti, A., G. J. Williams, L. Comeau, and C. Baglioni.** 1985. Inhibition of viral mRNA translation in interferon-treated L cells infected with reovirus. J Virol **55:**588-93.

62. **De Souza, A. I., R. Wait, A. G. Mitchell, N. R. Banner, M. J. Dunn, and M. L. Rose.** 2005. Heat shock protein 27 is associated with freedom from graft vasculopathy after human cardiac transplantation. Circ Res **97:**192-8.

63. **DeBiasi, R. L., C. L. Edelstein, B. Sherry, and K. L. Tyler.** 2001. Calpain inhibition protects against virus-induced apoptotic myocardial injury. J Virol **75:**351-61.

64. **DeBiasi, R. L., B. A. Robinson, B. Sherry, R. Bouchard, R. D. Brown, M. Rizeq, C. Long, and K. L. Tyler.** 2004. Caspase inhibition protects against reovirus-induced myocardial injury in vitro and in vivo. J Virol **78:**11040-50.

65. **Dermody, T. S., M. L. Nibert, R. Bassel-Duby, and B. N. Fields.** 1990. A sigma 1 region important for hemagglutination by serotype 3 reovirus strains. J Virol **64:**5173-6.

66. **Dermody, T. S., L. A. Schiff, M. L. Nibert, K. M. Coombs, and B. N. Fields.** 1991. The S2 gene nucleotide sequences of prototype strains of the three reovirus serotypes: characterization of reovirus core protein sigma 2. J Virol **65:**5721-31.

67. **Devreese, B., F. Vanrobaeys, J. Smet, J. Van Beeumen, and R. Van Coster.** 2002. Mass spectrometric identification of mitochondrial oxidative phosphorylation subunits separated by two-dimensional blue-native polyacrylamide gel electrophoresis. Electrophoresis **23:**2525-33.

68. **Diaz, M. O., H. M. Pomykala, S. K. Bohlander, E. Maltepe, K. Malik, B. Brownstein, and O. I. Olopade.** 1994. Structure of the human type-I interferon gene cluster determined from a YAC clone contig. Genomics **22:**540-52.

69. **Dickstein, K., A. Cohen-Solal, G. Filippatos, J. J. McMurray, P. Ponikowski, P. A. Poole-Wilson, A. Stromberg, D. J. van Veldhuisen, D. Atar, A. W. Hoes, A. Keren, A. Mebazaa, M. Nieminen, S. G. Priori, K. Swedberg, A. Vahanian, J. Camm, R. De Caterina, V. Dean, K. Dickstein, G. Filippatos, C. Funck-Brentano, I. Hellemans, S. D. Kristensen, K. McGregor, U. Sechtem, S. Silber, M. Tendera, P. Widimsky, J. L. Zamorano, M. Tendera, A. Auricchio, J. Bax, M. Bohm, U. Corra, P. della Bella, P. M. Elliott, F. Follath, M. Gheorghiade, Y. Hasin, A. Hernborg, T. Jaarsma, M. Komajda, R. Kornowski, M. Piepoli, B. Prendergast, L. Tavazzi, J. L. Vachiery, F. W. Verheugt, J. L. Zamorano, and F. Zannad.** 2008. ESC guidelines for the diagnosis and treatment of acute and chronic heart failure 2008: the Task Force for the diagnosis and treatment of acute and chronic heart failure 2008 of the European Society of Cardiology. Developed in collaboration with the Heart Failure Association of the ESC (HFA) and endorsed by the European Society of Intensive Care Medicine (ESICM). Eur J Heart Fail **10:**933-89.

70. **Dongre, A. R., J. K. Eng, and J. R. Yates, 3rd.** 1997. Emerging tandem-mass-spectrometry techniques for the rapid identification of proteins. Trends Biotechnol **15:**418-25.

71. **Doolan, A., N. Langlois, and C. Semsarian.** 2004. Causes of sudden cardiac death in young Australians. Med J Aust **180:**110-2.

72. **Drayna, D., and B. N. Fields.** 1982. Activation and characterization of the reovirus transcriptase: genetic analysis. J Virol **41:**110-8.

73. **Drory, Y., Y. Turetz, Y. Hiss, B. Lev, E. Z. Fisman, A. Pines, and M. R. Kramer.** 1991. Sudden unexpected death in persons less than 40 years of age. Am J Cardiol **68:**1388-92.

74. **Dryden, K. A., G. Wang, M. Yeager, M. L. Nibert, K. M. Coombs, D. B. Furlong, B. N. Fields, and T. S. Baker.** 1993. Early steps in reovirus infection are associated with dramatic changes in supramolecular structure and protein conformation: analysis of virions and subviral particles by cryoelectron microscopy and image reconstruction. J Cell Biol **122:**1023-41.

75. **Edmondson, R. D., T. M. Vondriska, K. J. Biederman, J. Zhang, R. C. Jones, Y. Zheng, D. L. Allen, J. X. Xiu, E. M. Cardwell, M. R. Pisano, and P. Ping.** 2002. Protein kinase C epsilon signaling complexes include metabolism- and transcription/translation-related proteins: complimentary separation techniques with LC/MS/MS. Mol Cell Proteomics **1:**421-33.

76. **Efthymiou, C. A., M. M. Mocanu, J. de Belleroche, D. J. Wells, D. S. Latchmann, and D. M. Yellon.** 2004. Heat shock protein 27 protects the heart against myocardial infarction. Basic Res Cardiol **99:**392-4.

77. **Ehrlich, M., W. Boll, A. Van Oijen, R. Hariharan, K. Chandran, M. L. Nibert, and T. Kirchhausen.** 2004. Endocytosis by random initiation and stabilization of clathrin-coated pits. Cell **118:**591-605.

78. **Ehrnsperger, M., S. Graber, M. Gaestel, and J. Buchner.** 1997. Binding of non-native protein to Hsp25 during heat shock creates a reservoir of folding intermediates for reactivation. Embo J **16:**221-9.

79. **Ellis, C. R., and T. Di Salvo.** 2007. Myocarditis: basic and clinical aspects. Cardiol Rev **15:**170-7.

80. **Esfandiarei, M., and B. M. McManus.** 2008. Molecular biology and pathogenesis of viral myocarditis. Annu Rev Pathol **3:**127-55.

81. **Evans, G., C. H. Wheeler, J. M. Corbett, and M. J. Dunn.** 1997. Construction of HSC-2DPAGE: a two-dimensional gel electrophoresis database of heart proteins. Electrophoresis **18:**471-9.

82. **Ewing, D. D., M. D. Sargent, and J. Borsa.** 1985. Switch-on of transcriptase function in reovirus: analysis of polypeptide changes using 2-D gels. Virology **144:**448-56.

83. **Faber, M. J., G. Agnetti, K. Bezstarosti, I. M. Lankhuizen, M. Dalinghaus, C. Guarnieri, C. M. Caldarera, W. A. Helbing, and J. M. Lamers.** 2006. Recent developments in proteomics: implications for the study of cardiac hypertrophy and failure. Cell Biochem Biophys **44:**11-29.

84. **Fae, K. C., D. Diefenbach da Silva, A. M. Bilate, A. C. Tanaka, P. M. Pomerantzeff, M. H. Kiss, C. A. Silva, E. Cunha-Neto, J. Kalil, and L. Guilherme.** 2008. PDIA3, HSPA5 and vimentin, proteins identified by 2-DE in the valvular tissue, are the target antigens of peripheral and heart infiltrating T cells from chronic rheumatic heart disease patients. J Autoimmun **31:**136-41.

85. **Fajardo, E., and A. J. Shatkin.** 1990. Expression of the two reovirus S1 gene products in transfected mammalian cells. Virology **178:**223-31.

86. **Fan, G. C., Q. Yuan, G. Song, Y. Wang, G. Chen, J. Qian, X. Zhou, Y. J. Lee, M. Ashraf, and E. G. Kranias.** 2006. Small heat-shock protein Hsp20 attenuates beta-agonist-mediated cardiac remodeling through apoptosis signal-regulating kinase 1. Circ Res **99:**1233-42.

87. **Fang, C., Z. Yi, F. Liu, S. Lan, J. Wang, H. Lu, P. Yang, and Z. Yuan.** 2006. Proteome analysis of human liver carcinoma Huh7 cells harboring hepatitis C virus subgenomic replicon. Proteomics **6:**519-27.

88. **Fenn, J. B., M. Mann, C. K. Meng, S. F. Wong, and C. M. Whitehouse.** 1989. Electrospray ionization for mass spectrometry of large biomolecules. Science **246:**64-71.

89. **Fert-Bober, J., R. S. Basran, J. Sawicka, and G. Sawicki.** 2008. Effect of duration of ischemia on myocardial proteome in ischemia/reperfusion injury. Proteomics **8:**2543-55.

90. **Forsman, A., U. Ruetschi, J. Ekholm, and L. Rymo.** 2008. Identification of intracellular proteins associated with the EBV-encoded nuclear antigen 5 using an efficient TAP procedure and FT-ICR mass spectrometry. J Proteome Res **7:**2309-19.

91. **Foster, G. R., O. Rodrigues, F. Ghouze, E. Schulte-Frohlinde, D. Testa, M. J. Liao, G. R. Stark, L. Leadbeater, and H. C. Thomas.** 1996. Different relative activities of human cell-derived interferon-alpha subtypes: IFN-alpha 8 has very high antiviral potency. J Interferon Cytokine Res **16:**1027-33.

92. **Franklin, T. B., A. M. Krueger-Naug, D. B. Clarke, A. P. Arrigo, and R. W. Currie.** 2005. The role of heat shock proteins Hsp70 and Hsp27 in cellular protection of the central nervous system. Int J Hyperthermia **21:**379-92.

93. **Fukagawa, Y., J. Nishikawa, Y. Kuramitsu, D. Iwakiri, K. Takada, S. Imai, M. Satake, T. Okamoto, M. Fujimoto, K. Okita, K. Nakamura, and I. Sakaida.** 2008. Epstein-Barr virus upregulates phosphorylated heat shock protein 27 kDa in carcinoma cells using the phosphoinositide 3-kinase/Akt pathway. Electrophoresis **29:**3192-200.

94. **Fung, M. C., S. F. Sia, K. N. Leung, and N. K. Mak.** 2004. Detection of differential expression of mouse interferon-alpha subtypes by polymerase chain reaction using specific primers. J Immunol Methods **284:**177-86.

95. **Gaestel, M., W. Schroder, R. Benndorf, C. Lippmann, K. Buchner, F. Hucho, V. A. Erdmann, and H. Bielka.** 1991. Identification of the phosphorylation sites of the murine small heat shock protein hsp25. J Biol Chem **266:**14721-4.

96. **Garrido, C., J. M. Bruey, A. Fromentin, A. Hammann, A. P. Arrigo, and E. Solary.** 1999. HSP27 inhibits cytochrome c-dependent activation of procaspase-9. Faseb J **13:**2061-70.

97. **Gawlowski, T., B. Stratmann, I. Stork, B. Engelbrecht, A. Brodehl, K. Niehaus, R. Korfer, D. Tschoepe, and H. Milting.** 2009. Heat Shock Protein 27 Modification is Increased in the Human Diabetic Failing Heart. Horm Metab Res.

98. **Georg Rde, C., and S. L. Gomes.** 2007. Comparative expression analysis of members of the Hsp70 family in the chytridiomycete Blastocladiella emersonii. Gene **386:**24-34.

99. **Gernold, M., U. Knauf, M. Gaestel, J. Stahl, and P. M. Kloetzel.** 1993. Development and tissue-specific distribution of mouse small heat shock protein hsp25. Dev Genet **14:**103-11.

100. **Giantini, M., and A. J. Shatkin.** 1989. Stimulation of chloramphenicol acetyltransferase mRNA translation by reovirus capsid polypeptide sigma 3 in cotransfected COS cells. J Virol **63:**2415-21.

101. **Gil, J., J. Rullas, J. Alcami, and M. Esteban.** 2001. MC159L protein from the poxvirus molluscum contagiosum virus inhibits NF-kappaB activation and apoptosis induced by PKR. J Gen Virol **82:**3027-34.

102. **Glaessgen, A., S. Jonmarker, A. Lindberg, B. Nilsson, R. Lewensohn, P. Ekman, A. Valdman, and L. Egevad.** 2008. Heat shock proteins 27, 60 and 70 as prognostic markers of prostate cancer. Apmis **116:**888-95.

103. **Gober, M. D., J. M. Laing, J. W. Burnett, and L. Aurelian.** 2007. The Herpes simplex virus gene Pol expressed in herpes-associated erythema multiforme lesions upregulates/activates SP1 and inflammatory cytokines. Dermatology **215:**97-106.

104. **Gober, M. D., S. Q. Wales, and L. Aurelian.** 2005. Herpes simplex virus type 2 encodes a heat shock protein homologue with apoptosis regulatory functions. Front Biosci **10:**2788-803.

105. **Gomatos, P. J., O. Prakash, and N. M. Stamatos.** 1981. Small reovirus particle composed solely of sigma NS with specificity for binding different nucleic acids. J Virol **39:**115-24.

106. **Gorg, A., W. Weiss, and M. J. Dunn.** 2004. Current two-dimensional electrophoresis technology for proteomics. Proteomics **4:**3665-85.

107. **Grist, N. R., and D. Reid.** 1997. Organisms in myocarditis/endocarditis viruses. J Infect **34:**155.

108. **Guo, K., N. X. Kang, Y. Li, L. Sun, L. Gan, F. J. Cui, M. D. Gao, and K. Y. Liu.** 2009. Regulation of HSP27 on NF-kappaB pathway activation may be involved in metastatic hepatocellular carcinoma cells apoptosis. BMC Cancer **9:**100.

109. **Gygi, S. P., B. Rist, S. A. Gerber, F. Turecek, M. H. Gelb, and R. Aebersold.** 1999. Quantitative analysis of complex protein mixtures using isotope-coded affinity tags. Nat Biotechnol **17:**994-9.

110. **Gygi, S. P., Y. Rochon, B. R. Franza, and R. Aebersold.** 1999. Correlation between protein and mRNA abundance in yeast. Mol Cell Biol **19:**1720-30.

111. **Habich, C., and V. Burkart.** 2007. Heat shock protein 60: regulatory role on innate immune cells. Cell Mol Life Sci **64:**742-51.

112. **Han, J., H. Y. Yoo, B. H. Choi, and H. M. Rho.** 2000. Selective transcriptional regulations in the human liver cell by hepatitis B viral X protein. Biochem Biophys Res Commun **272:**525-30.

113. **Harada H, M. M., Sato M, Kashiwazaki Y, Kimura T, Kitagawa M, Yokochi T, Tan RS, Takasugi T, Kadokawa Y, Schindler C, Schreiber RD, Noguchi S,TaniguchiT. 1996. .** 1996. Regulation of IFN-a /b genes: evidence for a dual

function of the transcription factor complex ISGF3 in the production and action of IFN-a / b. . Genes Cells **1:**995-1005.

114. **Hardy, M. P., C. M. Owczarek, L. S. Jermiin, M. Ejdeback, and P. J. Hertzog.** 2004. Characterization of the type I interferon locus and identification of novel genes. Genomics **84:**331-45.

115. **Hayashi, Y., M. Horie, T. Daito, T. Honda, K. Ikuta, and K. Tomonaga.** 2009. Heat shock cognate protein 70 controls Borna disease virus replication via interaction with the viral non-structural protein X. Microbes Infect **11:**394-402.

116. **Heart Failure Society Of, A.** 2006. HFSA 2006 Comprehensive Heart Failure Practice Guideline. J Card Fail **12:**e1-2.

117. **Heim, A., I. Grumbach, P. Pring-Akerblom, M. Stille-Siegener, G. Muller, R. Kandolf, and H. R. Figulla.** 1997. Inhibition of coxsackievirus B3 carrier state infection of cultured human myocardial fibroblasts by ribavirin and human natural interferon-alpha. Antiviral Res **34:**101-11.

118. **Heim, A., M. Stille-Siegener, R. Kandolf, H. Kreuzer, and H. R. Figulla.** 1994. Enterovirus-induced myocarditis: hemodynamic deterioration with immunosuppressive therapy and successful application of interferon-alpha. Clin Cardiol **17:**563-5.

119. **Heimrath, O., A. Oxner, T. Myers, and J. F. Legare.** 2009. Heat shock treatment prior to myocardial infarction results in reduced ventricular remodeling. J Invest Surg **22:**9-15.

120. **Heinke, M. Y., C. H. Wheeler, D. Chang, R. Einstein, A. Drake-Holland, M. J. Dunn, and C. G. dos Remedios.** 1998. Protein changes observed in pacing-induced heart failure using two-dimensional electrophoresis. Electrophoresis **19:**2021-30.

121. **Henry, G. L., S. J. McCormack, D. C. Thomis, and C. E. Samuel.** 1994. Mechanism of interferon action. Translational control and the RNA-dependent protein kinase (PKR): antagonists of PKR enhance the translational activity of mRNAs that include a 161 nucleotide region from reovirus S1 mRNA. J Biol Regul Homeost Agents **8:**15-24.

122. **Hightower, L. E., and L. M. Hendershot.** 1997. Molecular chaperones and the heat shock response at Cold Spring Harbor. Cell Stress Chaperones **2:**1-11.

123. **Hillenkamp, F., and M. Karas.** 1990. Mass spectrometry of peptides and proteins by matrix-assisted ultraviolet laser desorption/ionization. Methods Enzymol **193:**280-95.

124. **Hiscott, J., Pitha, P., Ge´nin, P., Nguyen, H., Heylbroeck, C.,Mamane,Y., Algarte´, M., Lin, R., .** 1999. Triggering the interferon response:the role of IRF-3 transcription factor. . J. Interferon Cytokine Res. **19:**1–13.

125. **Hoyt, C. C., S. M. Richardson-Burns, R. J. Goody, B. A. Robinson, R. L. Debiasi, and K. L. Tyler.** 2005. Nonstructural protein sigma1s is a determinant of reovirus virulence and influences the kinetics and severity of apoptosis induction in the heart and central nervous system. J Virol **79:**2743-53.

126. **Huber, S.** 2008. Host immune responses to coxsackievirus B3. Curr Top Microbiol Immunol **323:**199-221.

127. **Huismans, H., and W. K. Joklik.** 1976. Reovirus-coded polypeptides in infected cells: isolation of two native monomeric polypeptides with affinity for single-stranded and double-stranded RNA, respectively. Virology **70:**411-24.

128. **Hunt, D. F., A. M. Buko, J. M. Ballard, J. Shabanowitz, and A. B. Giordani.** 1981. Sequence analysis of polypeptides by collision activated dissociation on a triple quadrupole mass spectrometer. Biomed Mass Spectrom **8:**397-408.

129. **Hunt, S. A.** 2005. ACC/AHA 2005 guideline update for the diagnosis and management of chronic heart failure in the adult: a report of the American College of Cardiology/American Heart Association Task Force on Practice Guidelines (Writing Committee to Update the 2001 Guidelines for the Evaluation and Management of Heart Failure). J Am Coll Cardiol **46:**e1-82.

130. **Hutter, J. J., R. Mestril, E. K. Tam, R. E. Sievers, W. H. Dillmann, and C. L. Wolfe.** 1996. Overexpression of heat shock protein 72 in transgenic mice decreases infarct size in vivo. Circulation **94:**1408-11.

131. **Imani, F., and B. L. Jacobs.** 1988. Inhibitory activity for the interferon-induced protein kinase is associated with the reovirus serotype 1 sigma 3 protein. Proc Natl Acad Sci U S A **85:**7887-91.

132. **Island, M. L., T. Mesplede, N. Darracq, M. T. Bandu, N. Christeff, P. Djian, J. Drouin, and S. Navarro.** 2002. Repression by homeoprotein pitx1 of virus-induced interferon a promoters is mediated by physical interaction and trans repression of IRF3 and IRF7. Mol Cell Biol **22:**7120-33.

133. **Jaattela, M.** 1999. Heat shock proteins as cellular lifeguards. Ann Med **31:**261-71.

134. **Jacobs, B. L., and R. E. Ferguson.** 1991. The Lang strain of reovirus serotype 1 and the Dearing strain of reovirus serotype 3 differ in their sensitivities to beta interferon. J Virol **65:**5102-4.

135. **Jager, D., P. R. Jungblut, and U. Muller-Werdan.** 2002. Separation and identification of human heart proteins. J Chromatogr B Analyt Technol Biomed Life Sci **771:**131-53.

136. **James, C. M., M. Y. Abdad, J. P. Mansfield, H. K. Jacobsen, A. R. Vind, P. A. Stumbles, and E. J. Bartlett.** 2007. Differential activities of alpha/beta IFN subtypes against influenza virus in vivo and enhancement of specific immune responses in DNA vaccinated mice expressing haemagglutinin and nucleoprotein. Vaccine **25:**1856-67.

137. **Jayakumar, J., K. Suzuki, M. Khan, R. T. Smolenski, A. Farrell, N. Latif, O. Raisky, H. Abunasra, I. A. Sammut, B. Murtuza, M. Amrani, and M. H. Yacoub.** 2000. Gene therapy for myocardial protection: transfection of donor hearts with heat shock protein 70 gene protects cardiac function against ischemia-reperfusion injury. Circulation **102:**III302-6.

138. **Jayasuriya, A. K., M. L. Nibert, and B. N. Fields.** 1988. Complete nucleotide sequence of the M2 gene segment of reovirus type 3 dearing and analysis of its protein product mu 1. Virology **163:**591-602.

139. **Juang, Y. T., W. Lowther, M. Kellum, W. C. Au, R. Lin, J. Hiscott, and P. M. Pitha.** 1998. Primary activation of interferon A and interferon B gene transcription by interferon regulatory factor 3. Proc Natl Acad Sci U S A **95:**9837-42.

140. **Jungblut, P., A. Otto, V. Regitz, E. Fleck, and B. Wittmann-Liebold.** 1992. Identification of human myocard proteins separated by two-dimensional electrophoresis. Electrophoresis **13:**739-41.

141. **Jungblut, P., B. Thiede, U. Zimny-Arndt, E. C. Muller, C. Scheler, B. Wittmann-Liebold, and A. Otto.** 1996. Resolution power of two-dimensional electrophoresis and identification of proteins from gels. Electrophoresis **17:**839-47.

142. **Jungblut, P. R., U. Zimny-Arndt, E. Zeindl-Eberhart, J. Stulik, K. Koupilova, K. P. Pleissner, A. Otto, E. C. Muller, W. Sokolowska-Kohler, G. Grabher, and G. Stoffler.** 1999. Proteomics in human disease: cancer, heart and infectious diseases. Electrophoresis **20:**2100-10.

143. **Karas, M., and F. Hillenkamp.** 1988. Laser desorption ionization of proteins with molecular masses exceeding 10,000 daltons. Anal Chem **60:**2299-301.

144. **Kato, K., H. Ito, I. Iwamoto, K. Lida, and Y. Inaguma.** 2001. Protein kinase inhibitors can suppress stress-induced dissociation of Hsp27. Cell Stress Chaperones **6:**16-20.

145. **Kawakami, T., Matsumoto, M., Sato, M., Harada, H.,Taniguchi, T. and Kitigawa, M., .** 1995. Possible involvement of the transcription factor ISGF37 in virus-induced expression of the 1FN-fl gene. . FEBS Lett, **358:**225-229.

146. **Kelley, K. A., and P. M. Pitha.** 1985. Characterization of a mouse interferon gene locus II. Differential expression of alpha-interferon genes. Nucleic Acids Res **13:**825-39.

147. **Kessler, D. S., Veals, S. A., Fu, X.-Y. and Levy, D.E.,.** 1990. Interferon- regulates nuclear translocation and DNA-binding affinity of ISGF3, a multimeric transcriptional activator. . Genes Dev., **4:**1753-1765.

148. **Kim, Y. K., J. Suarez, Y. Hu, P. M. McDonough, C. Boer, D. J. Dix, and W. H. Dillmann.** 2006. Deletion of the inducible 70-kDa heat shock protein genes in mice impairs cardiac contractile function and calcium handling associated with hypertrophy. Circulation **113:**2589-97.

149. **Kirchner, E., K. M. Guglielmi, H. M. Strauss, T. S. Dermody, and T. Stehle.** 2008. Structure of reovirus sigma1 in complex with its receptor junctional adhesion molecule-A. PLoS Pathog **4:**e1000235.

150. **Kishimoto, C., C. S. Crumpacker, and W. H. Abelmann.** 1988. Ribavirin treatment of murine coxsackievirus B3 myocarditis with analyses of lymphocyte subsets. J Am Coll Cardiol **12:**1334-41.

151. **Klose, J.** 1975. Protein mapping by combined isoelectric focusing and electrophoresis of mouse tissues. A novel approach to testing for induced point mutations in mammals. Humangenetik **26:**231-43.

152. **Klose, J., and U. Kobalz.** 1995. Two-dimensional electrophoresis of proteins: an updated protocol and implications for a functional analysis of the genome. Electrophoresis **16:**1034-59.

153. **Kobayashi, T., L. S. Ooms, J. D. Chappell, and T. S. Dermody.** 2009. Identification of functional domains in reovirus replication proteins muNS and mu2. J Virol **83:**2892-906.

154. **Koonin, E. V., A. E. Gorbalenya, and K. M. Chumakov.** 1989. Tentative identification of RNA-dependent RNA polymerases of dsRNA viruses and their relationship to positive strand RNA viral polymerases. FEBS Lett **252:**42-6.

155. **Koyama, T., N. Sakamoto, Y. Tanabe, M. Nakagawa, Y. Itsui, Y. Takeda, S. Kakinuma, Y. Sekine, S. Maekawa, Y. Yanai, M. Kurimoto, and M. Watanabe.** 2006. Divergent activities of interferon-alpha subtypes against intracellular hepatitis C virus replication. Hepatol Res **34:**41-9.

156. **Kuhl, U., M. Pauschinger, P. L. Schwimmbeck, B. Seeberg, C. Lober, M. Noutsias, W. Poller, and H. P. Schultheiss.** 2003. Interferon-beta treatment eliminates cardiotropic viruses and improves left ventricular function in patients with myocardial persistence of viral genomes and left ventricular dysfunction. Circulation **107:**2793-8.

157. **Kwon, J. H., J. B. Kim, K. H. Lee, S. M. Kang, N. Chung, Y. Jang, and J. H. Chung.** 2007. Protective effect of heat shock protein 27 using protein transduction domain-mediated delivery on ischemia/reperfusion heart injury. Biochem Biophys Res Commun **363:**399-404.

158. **Lam, L., J. Arthur, and C. Semsarian.** 2007. Proteome map of the normal murine ventricular myocardium. Proteomics **7:**3629-33.

159. **Larrea, E., A. Alberdi, Y. Castelruiz, P. Boya, M. P. Civeira, and J. Prieto.** 2001. Expression of interferon-alpha subtypes in peripheral mononuclear cells from patients with chronic hepatitis C: a role for interferon-alpha5. J Viral Hepat **8:**103-10.

160. **Larrea, E., R. Aldabe, J. I. Riezu-Boj, A. Guitart, M. P. Civeira, J. Prieto, and E. Baixeras.** 2004. IFN-alpha5 mediates stronger Tyk2-stat-dependent activation and higher expression of 2',5'-oligoadenylate synthetase than IFN-alpha2 in liver cells. J Interferon Cytokine Res **24:**497-503.

161. **Latif, N., M. L. Rose, M. H. Yacoub, and M. J. Dunn.** 1995. Association of pretransplantation antiheart antibodies with clinical course after heart transplantation. J Heart Lung Transplant **14:**119-26.

162. **Lemay, G., and C. Danis.** 1994. Reovirus lambda 1 protein: affinity for double-stranded nucleic acids by a small amino-terminal region of the protein independent from the zinc finger motif. J Gen Virol **75 (Pt 11):**3261-6.

163. **Lemieux, R., G. Lemay, and S. Millward.** 1987. The viral protein sigma 3 participates in translation of late viral mRNA in reovirus-infected L cells. J Virol **61:**2472-9.

164. **Lenzo, J. C., J. P. Mansfield, S. Sivamoorthy, V. S. Cull, and C. M. James.** 2003. Cytokine expression in murine cytomegalovirus-induced myocarditis: modulation with interferon-alpha therapy. Cell Immunol **223:**77-86.

165. **Levy, D. E., I. Marie, E. Smith, and A. Prakash.** 2002. Enhancement and diversification of IFN induction by IRF-7-mediated positive feedback. J Interferon Cytokine Res **22:**87-93.

166. **Li, G., I. S. Ali, and R. W. Currie.** 2008. Insulin-induced myocardial protection in isolated ischemic rat hearts requires p38 MAPK phosphorylation of Hsp27. Am J Physiol Heart Circ Physiol **294:**H74-87.

167. **Li, M., B. Damania, X. Alvarez, V. Ogryzko, K. Ozato, and J. U. Jung.** 2000. Inhibition of p300 histone acetyltransferase by viral interferon regulatory factor. Mol Cell Biol **20:**8254-63.

168. **Li, R. C., P. Ping, J. Zhang, W. B. Wead, X. Cao, J. Gao, Y. Zheng, S. Huang, J. Han, and R. Bolli.** 2000. PKCepsilon modulates NF-kappaB and AP-1 via mitogen-activated protein kinases in adult rabbit cardiomyocytes. Am J Physiol Heart Circ Physiol **279:**H1679-89.

169. **Li, X. P., K. P. Pleissner, C. Scheler, V. Regitz-Zagrosek, J. Salnikow, and P. R. Jungblut.** 1999. A two-dimensional electrophoresis database of rat heart proteins. Electrophoresis **20:**891-7.

170. **Li, Z. B., P. W. Flint, and M. O. Boluyt.** 2005. Evaluation of several two-dimensional gel electrophoresis techniques in cardiac proteomics. Electrophoresis **26:**3572-85.

171. **Liang, D., Z. Benko, E. Agbottah, M. Bukrinsky, and R. Y. Zhao.** 2007. Anti-vpr activities of heat shock protein 27. Mol Med **13:**229-39.

172. **Liew, K. J., and V. T. Chow.** 2006. Microarray and real-time RT-PCR analyses of a novel set of differentially expressed human genes in ECV304 endothelial-like cells infected with dengue virus type 2. J Virol Methods **131:**47-57.

173. **Lim, S. O., S. G. Park, J. H. Yoo, Y. M. Park, H. J. Kim, K. T. Jang, J. W. Cho, B. C. Yoo, G. H. Jung, and C. K. Park.** 2005. Expression of heat shock proteins (HSP27, HSP60, HSP70, HSP90, GRP78, GRP94) in hepatitis B virus-related hepatocellular carcinomas and dysplastic nodules. World J Gastroenterol **11:**2072-9.

174. **Lindquist, S., and E. A. Craig.** 1988. The heat-shock proteins. Annu Rev Genet **22:**631-77.

175. **Liu, L., X. Zhang, B. Qian, X. Min, X. Gao, C. Li, Y. Cheng, and J. Huang.** 2007. Over-expression of heat shock protein 27 attenuates doxorubicin-induced cardiac dysfunction in mice. Eur J Heart Fail **9:**762-9.

176. **Liu, L., X. J. Zhang, S. R. Jiang, Z. N. Ding, G. X. Ding, J. Huang, and Y. L. Cheng.** 2007. Heat shock protein 27 regulates oxidative stress-induced apoptosis in cardiomyocytes: mechanisms via reactive oxygen species generation and Akt activation. Chin Med J (Engl) **120:**2271-7.

177. **Lo, W. Y., C. C. Lai, C. H. Hua, M. H. Tsai, S. Y. Huang, C. H. Tsai, and F. J. Tsai.** 2007. S100A8 is identified as a biomarker of HPV18-infected oral squamous cell carcinomas by suppression subtraction hybridization, clinical proteomics analysis, and immunohistochemistry staining. J Proteome Res **6:**2143-51.

178. **Loo, Y. M., J. Fornek, N. Crochet, G. Bajwa, O. Perwitasari, L. Martinez-Sobrido, S. Akira, M. A. Gill, A. Garcia-Sastre, M. G. Katze, and M. Gale, Jr.** 2008. Distinct RIG-I and MDA5 signaling by RNA viruses in innate immunity. J Virol **82:**335-45.

179. **Lopez, S., M. L. Island, J. Drouin, M. T. Bandu, N. Christeff, N. Darracq, R. Barbey, J. Doly, D. Thomas, and S. Navarro.** 2000. Repression of virus-induced interferon A promoters by homeodomain transcription factor Ptx1. Mol Cell Biol **20:**7527-40.

180. **Lopez, S., R. Reeves, M. L. Island, M. T. Bandu, N. Christeff, J. Doly, and S. Navarro.** 1997. Silencer activity in the interferon-A gene promoters. J Biol Chem **272:**22788-99.

181. **Loseke, S., E. Grage-Griebenow, A. Wagner, K. Gehlhar, and A. Bufe.** 2003. Differential expression of IFN-alpha subtypes in human PBMC: evaluation of novel real-time PCR assays. J Immunol Methods **276:**207-22.

182. **Lu, X. Y., L. Chen, X. L. Cai, and H. T. Yang.** 2008. Overexpression of heat shock protein 27 protects against ischaemia/reperfusion-induced cardiac dysfunction via stabilization of troponin I and T. Cardiovasc Res **79:**500-8.

183. **Luche, S., H. Diemer, C. Tastet, M. Chevallet, A. Van Dorsselaer, E. Leize-Wagner, and T. Rabilloud.** 2004. About thiol derivatization and resolution of basic proteins in two-dimensional electrophoresis. Proteomics **4:**551-61.

184. **Ludwig, S., K. Engel, A. Hoffmeyer, G. Sithanandam, B. Neufeld, D. Palm, M. Gaestel, and U. R. Rapp.** 1996. 3pK, a novel mitogen-activated protein (MAP) kinase-activated protein kinase, is targeted by three MAP kinase pathways. Mol Cell Biol **16:**6687-97.

185. **Luongo, C. L., C. M. Contreras, D. L. Farsetta, and M. L. Nibert.** 1998. Binding site for S-adenosyl-L-methionine in a central region of mammalian reovirus lambda2 protein. Evidence for activities in mRNA cap methylation. J Biol Chem **273:**23773-80.

186. **Maginnis, M. S., J. C. Forrest, S. A. Kopecky-Bromberg, S. K. Dickeson, S. A. Santoro, M. M. Zutter, G. R. Nemerow, J. M. Bergelson, and T. S. Dermody.** 2006. Beta1 integrin mediates internalization of mammalian reovirus. J Virol **80:**2760-70.

187. **Mamane, Y., C. Heylbroeck, P. Genin, M. Algarte, M. J. Servant, C. LePage, C. DeLuca, H. Kwon, R. Lin, and J. Hiscott.** 1999. Interferon regulatory factors: the next generation. Gene **237:**1-14.

188. **Mao, Z. X., and W. K. Joklik.** 1991. Isolation and enzymatic characterization of protein lambda 2, the reovirus guanylyltransferase. Virology **185:**377-86.

189. **Marber, M. S., R. Mestril, S. H. Chi, M. R. Sayen, D. M. Yellon, and W. H. Dillmann.** 1995. Overexpression of the rat inducible 70-kD heat stress protein in a transgenic mouse increases the resistance of the heart to ischemic injury. J Clin Invest **95:**1446-56.

190. **Marie, I., Durbin, J.E., Levy, D.E., .** 1998. Differential viral induction of distinct interferon-a genes by positive feedback through interferon regulatory factor-7. EMBO J. **17:**6660–6669.

191. **Marouga, R., S. David, and E. Hawkins.** 2005. The development of the DIGE system: 2D fluorescence difference gel analysis technology. Anal Bioanal Chem **382:**669-78.

192. **Martin, J. L., E. Hickey, L. A. Weber, W. H. Dillmann, and R. Mestril.** 1999. Influence of phosphorylation and oligomerization on the protective role of the small heat shock protein 27 in rat adult cardiomyocytes. Gene Expr **7:**349-55.

193. **Matsumori, A., C. S. Crumpacker, and W. H. Abelmann.** 1987. Prevention of viral myocarditis with recombinant human leukocyte interferon alpha A/D in a murine model. J Am Coll Cardiol **9:**1320-5.

194. **Matsumori, A., N. Tomioka, and C. Kawai.** 1988. Protective effect of recombinant alpha interferon on coxsackievirus B3 myocarditis in mice. Am Heart J **115:**1229-32.

195. **Matsumori, A., H. Wang, W. H. Abelmann, and C. S. Crumpacker.** 1985. Treatment of viral myocarditis with ribavirin in an animal preparation. Circulation **71:**834-9.

196. **Mayer, M. P., D. Brehmer, C. S. Gassler, and B. Bukau.** 2001. Hsp70 chaperone machines. Adv Protein Chem **59:**1-44.

197. **McCrae, M. A., and W. K. Joklik.** 1978. The nature of the polypeptide encoded by each of the 10 double-stranded RNA segments of reovirus type 3. Virology **89:**578-93.

198. **McGregor, E., and M. J. Dunn.** 2003. Proteomics of heart disease. Hum Mol Genet **12 Spec No 2:**R135-44.

199. **McGregor, E., and M. J. Dunn.** 2006. Proteomics of the heart: unraveling disease. Circ Res **98:**309-21.

200. **Mesplede, T., M. L. Island, N. Christeff, F. Petek, J. Doly, and S. Navarro.** 2005. The POU transcription factor Oct-1 represses virus-induced interferon A gene expression. Mol Cell Biol **25:**8717-31.

201. **Mestril, R., F. J. Giordano, A. G. Conde, and W. H. Dillmann.** 1996. Adenovirus-mediated gene transfer of a heat shock protein 70 (hsp 70i) protects against simulated ischemia. J Mol Cell Cardiol **28:**2351-8.

202. **Molloy, M. P.** 2000. Two-dimensional electrophoresis of membrane proteins using immobilized pH gradients. Anal Biochem **280:**1-10.

203. **Morano, K. A.** 2007. New tricks for an old dog: the evolving world of Hsp70. Ann N Y Acad Sci **1113:**1-14.

204. **Mosser, D. D., and R. I. Morimoto.** 2004. Molecular chaperones and the stress of oncogenesis. Oncogene **23:**2907-18.

205. **Mourouzis, I., T. Saranteas, P. Perimenis, C. Tesseromatis, G. Kostopanagiotou, C. Pantos, and D. V. Cokkinos.** 2009. Morphine administration at reperfusion fails to improve postischaemic cardiac function but limits myocardial injury probably via heat-shock protein 27 phosphorylation. Eur J Anaesthesiol **26:**572-81.

206. **Muller, E. C., B. Thiede, U. Zimny-Arndt, C. Scheler, J. Prehm, U. Muller-Werdan, B. Wittmann-Liebold, A. Otto, and P. Jungblut.** 1996. High-performance human myocardial two-dimensional electrophoresis database: edition 1996. Electrophoresis **17:**1700-12.

207. **Multhoff, G.** 2009. Activation of natural killer cells by heat shock protein 70. Int J Hyperthermia **25:**169-75.

208. **Multhoff, G.** 2007. Heat shock protein 70 (Hsp70): membrane location, export and immunological relevance. Methods **43:**229-37.

209. **Mustoe, T. A., R. F. Ramig, A. H. Sharpe, and B. N. Fields.** 1978. Genetics of reovirus: identification of the ds RNA segments encoding the polypeptides of the mu and sigma size classes. Virology **89:**594-604.

210. **Nagai, A., O. Taira, M. Ishikawa, K. Hiramatsu, T. Hohdatsu, H. Koyama, S. Arai, H. Sato, K. Nakano, and N. Maehara.** 2004. Cloning of cDNAs encoding multiple subtypes of feline interferon-alpha from the feline epitherial cell line. J Vet Med Sci **66:**725-8.

211. **Nagaraj, R. H., T. Oya-Ito, P. S. Padayatti, R. Kumar, S. Mehta, K. West, B. Levison, J. Sun, J. W. Crabb, and A. K. Padival.** 2003. Enhancement of chaperone function of alpha-crystallin by methylglyoxal modification. Biochemistry **42:**10746-55.

212. **Nagata, L., S. A. Masri, D. C. Mah, and P. W. Lee.** 1984. Molecular cloning and sequencing of the reovirus (serotype 3) S1 gene which encodes the viral cell attachment protein sigma 1. Nucleic Acids Res **12:**8699-710.

213. **Nakatsue, T., I. Katoh, S. Nakamura, Y. Takahashi, Y. Ikawa, and Y. Yoshinaka.** 1998. Acute infection of Sindbis virus induces phosphorylation and intracellular translocation of small heat shock protein HSP27 and activation of p38 MAP kinase signaling pathway. Biochem Biophys Res Commun **253:**59-64.

214. **New, L., Y. Jiang, M. Zhao, K. Liu, W. Zhu, L. J. Flood, Y. Kato, G. C. Parry, and J. Han.** 1998. PRAK, a novel protein kinase regulated by the p38 MAP kinase. Embo J **17:**3372-84.

215. **Nguyen, H., J. Hiscott, and P. M. Pitha.** 1997. The growing family of interferon regulatory factors. Cytokine Growth Factor Rev **8:**293-312.

216. **Nibert, M. L., A. L. Odegard, M. A. Agosto, K. Chandran, and L. A. Schiff.** 2005. Putative autocleavage of reovirus mu1 protein in concert with outer-capsid disassembly and activation for membrane permeabilization. J Mol Biol **345:**461-74.

217. **Nilsen, T. W., P. A. Maroney, and C. Baglioni.** 1982. Synthesis of (2'-5')oligoadenylate and activation of an endoribonuclease in interferon-treated HeLa cells infected with reovirus. J Virol **42:**1039-45.

218. **Noble, S., and M. L. Nibert.** 1997. Characterization of an ATPase activity in reovirus cores and its genetic association with core-shell protein lambda1. J Virol **71:**2182-91.

219. **O'Farrell, P. H.** 1975. High resolution two-dimensional electrophoresis of proteins. J Biol Chem **250:**4007-21.

220. **Okubo, S., O. Wildner, M. R. Shah, J. C. Chelliah, M. L. Hess, and R. C. Kukreja.** 2001. Gene transfer of heat-shock protein 70 reduces infarct size in vivo after ischemia/reperfusion in the rabbit heart. Circulation **103:**877-81.

221. **Oya-Ito, T., B. F. Liu, and R. H. Nagaraj.** 2006. Effect of methylglyoxal modification and phosphorylation on the chaperone and anti-apoptotic properties of heat shock protein 27. J Cell Biochem **99:**279-91.

222. **Parent, R., X. Qu, M. A. Petit, and L. Beretta.** 2009. The heat shock cognate protein 70 is associated with hepatitis C virus particles and modulates virus infectivity. Hepatology **49:**1798-809.

223. **Patel, V. B., J. M. Corbett, M. J. Dunn, V. R. Winrow, B. Portmann, P. J. Richardson, and V. R. Preedy.** 1997. Protein profiling in cardiac tissue in response to the chronic effects of alcohol. Electrophoresis **18:**2788-94.

224. **Paul, C., F. Manero, S. Gonin, C. Kretz-Remy, S. Virot, and A. P. Arrigo.** 2002. Hsp27 as a negative regulator of cytochrome C release. Mol Cell Biol **22:**816-34.

225. **Pennington, K., E. McGregor, C. L. Beasley, I. Everall, D. Cotter, and M. J. Dunn.** 2004. Optimization of the first dimension for separation by two-dimensional gel electrophoresis of basic proteins from human brain tissue. Proteomics **4:**27-30.

226. **Ping, P., J. Zhang, W. M. Pierce, Jr., and R. Bolli.** 2001. Functional proteomic analysis of protein kinase C epsilon signaling complexes in the normal heart and during cardioprotection. Circ Res **88:**59-62.

227. **Pivovarova, A. V., N. A. Chebotareva, I. S. Chernik, N. B. Gusev, and D. I. Levitsky.** 2007. Small heat shock protein Hsp27 prevents heat-induced aggregation of F-actin by forming soluble complexes with denatured actin. Febs J **274:**5937-48.

228. **Pleissner, K. P., S. Sander, H. Oswald, V. Regitz-Zagrosek, and E. Fleck.** 1996. The construction of the World Wide Web-accessible myocardial two-dimensional gel electrophoresis protein database "HEART-2DPAGE": a practical approach. Electrophoresis **17:**1386-92.

229. **Plumier, J. C., B. M. Ross, R. W. Currie, C. E. Angelidis, H. Kazlaris, G. Kollias, and G. N. Pagoulatos.** 1995. Transgenic mice expressing the human heat shock protein 70 have improved post-ischemic myocardial recovery. J Clin Invest **95:**1854-60.

230. **Pogany, J., J. Stork, Z. Li, and P. D. Nagy.** 2008. In vitro assembly of the Tomato bushy stunt virus replicase requires the host Heat shock protein 70. Proc Natl Acad Sci U S A **105:**19956-61.

231. **Poggioli, G. J., C. Keefer, J. L. Connolly, T. S. Dermody, and K. L. Tyler.** 2000. Reovirus-induced G(2)/M cell cycle arrest requires sigma1s and occurs in the absence of apoptosis. J Virol **74:**9562-70.

232. **Poppers, J., M. Mulvey, D. Khoo, and I. Mohr.** 2000. Inhibition of PKR activation by the proline-rich RNA binding domain of the herpes simplex virus type 1 Us11 protein. J Virol **74:**11215-21.

233. **Prentice, H., and K. A. Webster.** 2004. Genomic and proteomic profiles of heart disease. Trends Cardiovasc Med **14:**282-8.

234. **Preville, X., H. Schultz, U. Knauf, M. Gaestel, and A. P. Arrigo.** 1998. Analysis of the role of Hsp25 phosphorylation reveals the importance of the oligomerization state of this small heat shock protein in its protective function against TNFalpha- and hydrogen peroxide-induced cell death. J Cell Biochem **69:**436-52.

235. **Puranik, R., C. K. Chow, J. A. Duflou, M. J. Kilborn, and M. A. McGuire.** 2005. Sudden death in the young. Heart Rhythm **2:**1277-82.

236. **Rabilloud, T.** 2002. Two-dimensional gel electrophoresis in proteomics: old, old fashioned, but it still climbs up the mountains. Proteomics **2:**3-10.

237. **Rane, M. J., Y. Pan, S. Singh, D. W. Powell, R. Wu, T. Cummins, Q. Chen, K. R. McLeish, and J. B. Klein.** 2003. Heat shock protein 27 controls apoptosis by regulating Akt activation. J Biol Chem **278:**27828-35.

238. **Ray, C. G., T. B. Icenogle, L. L. Minnich, J. G. Copeland, and T. M. Grogan.** 1989. The use of intravenous ribavirin to treat influenza virus-associated acute myocarditis. J Infect Dis **159:**829-36.

239. **Richardson, M. A., and Y. Furuichi.** 1983. Nucleotide sequence of reovirus genome segment S3, encoding non-structural protein sigma NS. Nucleic Acids Res **11:**6399-408.

240. **Ritossa, F.** 1962. A new puffing patterninduced by temperature shock and DNP in Drosophila. Experimentia **18:**571-573.

241. **Rodgers, S. E., E. S. Barton, S. M. Oberhaus, B. Pike, C. A. Gibson, K. L. Tyler, and T. S. Dermody.** 1997. Reovirus-induced apoptosis of MDCK cells is not linked to viral yield and is blocked by Bcl-2. J Virol **71:**2540-6.

242. **Rogalla, T., M. Ehrnsperger, X. Preville, A. Kotlyarov, G. Lutsch, C. Ducasse, C. Paul, M. Wieske, A. P. Arrigo, J. Buchner, and M. Gaestel.** 1999. Regulation of Hsp27 oligomerization, chaperone function, and protective activity against oxidative stress/tumor necrosis factor alpha by phosphorylation. J Biol Chem **274:**18947-56.

243. **Saito, T., and M. Gale, Jr.** 2008. Differential recognition of double-stranded RNA by RIG-I-like receptors in antiviral immunity. J Exp Med **205:**1523-7.

244. **Sakamoto, H., T. Mashima, K. Yamamoto, and T. Tsuruo.** 2002. Modulation of heat-shock protein 27 (Hsp27) anti-apoptotic activity by methylglyoxal modification. J Biol Chem **277:**45770-5.

245. **Samuel, C. E., R. Duncan, G. S. Knutson, and J. W. Hershey.** 1984. Mechanism of interferon action. Increased phosphorylation of protein synthesis initiation factor eIF-2 alpha in interferon-treated, reovirus-infected mouse L929 fibroblasts in vitro and in vivo. J Biol Chem **259:**13451-7.

246. **Santoni, V., M. Molloy, and T. Rabilloud.** 2000. Membrane proteins and proteomics: un amour impossible? Electrophoresis **21:**1054-70.

247. **Sarkar, G., J. Pelletier, R. Bassel-Duby, A. Jayasuriya, B. N. Fields, and N. Sonenberg.** 1985. Identification of a new polypeptide coded by reovirus gene S1. J Virol **54:**720-5.

248. **Sato, M., T. Taniguchi, and N. Tanaka.** 2001. The interferon system and interferon regulatory factor transcription factors -- studies from gene knockout mice. Cytokine Growth Factor Rev **12:**133-42.

249. **Schafer, S. L., Lin, R., Moore, P.A., Hiscott, J., Pitha, P.M., .** 1998. Regulation of type 1 interferon gene expression by interferon regulatory factor 3. . J. Biol. Chem. **273:**2714–2720.

250. **Schagger, H., and G. von Jagow.** 1991. Blue native electrophoresis for isolation of membrane protein complexes in enzymatically active form. Anal Biochem **199:**223-31.

251. **Schanen, C., V. Chieux, P. E. Lobert, J. Harvey, and D. Hober.** 2006. Correlation between the anti-virus-induced cytopathic effect activity of interferon-alpha subtypes and induction of MxA protein in vitro. Microbiol Immunol **50:**19-24.

252. **Scheler, C., E. C. Muller, J. Stahl, U. Muller-Werdan, J. Salnikow, and P. Jungblut.** 1997. Identification and characterization of heat shock protein 27 protein species in human myocardial two-dimensional electrophoresis patterns. Electrophoresis **18:**2823-31.

253. **Schiff, L. A., Nibert, M. L., Tyler, K. L.** 2007. Orthoreoviruses and their replication, p. 1853-1915. *In* D. M. Knipe and P. M. Howley (ed.), Fields virology, 5th ed, vol. 2. Lippincott Williams & Wilkins, Philadelphia, PA.

254. **Schiff LA, N. M., Tyler KL.** 2007. Orthoreoviruses and their repliation, 5th ed, vol. 2. Lippincott Williams & Wilkins, Philadelphia, PA.

255. **Schmechel, S., M. Chute, P. Skinner, R. Anderson, and L. Schiff.** 1997. Preferential translation of reovirus mRNA by a sigma3-dependent mechanism. Virology **232:**62-73.

256. **Schmitt, E., M. Gehrmann, M. Brunet, G. Multhoff, and C. Garrido.** 2007. Intracellular and extracellular functions of heat shock proteins: repercussions in cancer therapy. J Leukoc Biol **81:**15-27.

257. **Sharpe, A. H., and B. N. Fields.** 1982. Reovirus inhibition of cellular RNA and protein synthesis: role of the S4 gene. Virology **122:**381-91.

258. **Shatkin, A. J., J. D. Sipe, and P. Loh.** 1968. Separation of ten reovirus genome segments by polyacrylamide gel electrophoresis. J Virol **2:**986-91.

259. **Sherry, B., C. J. Baty, and M. A. Blum.** 1996. Reovirus-induced acute myocarditis in mice correlates with viral RNA synthesis rather than generation of infectious virus in cardiac myocytes. J Virol **70:**6709-15.

260. **Sherry, B., and M. A. Blum.** 1994. Multiple viral core proteins are determinants of reovirus-induced acute myocarditis. J Virol **68:**8461-5.

261. **Sherry, B., and B. N. Fields.** 1989. The reovirus M1 gene, encoding a viral core protein, is associated with the myocarditic phenotype of a reovirus variant. J Virol **63:**4850-6.

262. **Sherry, B., X. Y. Li, K. L. Tyler, J. M. Cullen, and H. W. t. Virgin.** 1993. Lymphocytes protect against and are not required for reovirus-induced myocarditis. J Virol **67:**6119-24.

263. **Sherry, B., F. J. Schoen, E. Wenske, and B. N. Fields.** 1989. Derivation and characterization of an efficiently myocarditic reovirus variant. J Virol **63:**4840-9.

264. **Sherry, B., J. Torres, and M. A. Blum.** 1998. Reovirus induction of and sensitivity to beta interferon in cardiac myocyte cultures correlate with induction of myocarditis and are determined by viral core proteins. J Virol **72:**1314-23.

265. **Shi, Q., J. Feng, H. Qu, and Y. Y. Cheng.** 2008. A proteomic study of S-nitrosylation in the rat cardiac proteins in vitro. Biol Pharm Bull **31:**1536-40.

266. **Shinohara, M., P. J. Thornalley, I. Giardino, P. Beisswenger, S. R. Thorpe, J. Onorato, and M. Brownlee.** 1998. Overexpression of glyoxalase-I in bovine endothelial cells inhibits intracellular advanced glycation endproduct formation and prevents hyperglycemia-induced increases in macromolecular endocytosis. J Clin Invest **101:**1142-7.

267. **Singh, D., K. L. McCann, and F. Imani.** 2007. MAPK and heat shock protein 27 activation are associated with respiratory syncytial virus induction of human bronchial epithelial monolayer disruption. Am J Physiol Lung Cell Mol Physiol **293:**L436-45.

268. **Smith, E. J., I. Marie, A. Prakash, A. Garcia-Sastre, and D. E. Levy.** 2001. IRF3 and IRF7 phosphorylation in virus-infected cells does not require double-stranded RNA-dependent protein kinase R or Ikappa B kinase but is blocked by Vaccinia virus E3L protein. J Biol Chem **276:**8951-7.

269. **Smith, J. R., I. R. Matus, D. A. Beard, and A. S. Greene.** 2008. Differential expression of cardiac mitochondrial proteins. Proteomics **8:**446-62.

270. **Solis, M., D. Goubau, R. Romieu-Mourez, P. Genin, A. Civas, and J. Hiscott.** 2006. Distinct functions of IRF-3 and IRF-7 in IFN-alpha gene regulation and control of anti-tumor activity in primary macrophages. Biochem Pharmacol **72:**1469-76.

271. **Song, X., Z. Liu, H. Wang, Y. Xin, X. Wang, J. Chen, Y. Shi, C. Zhang, and R. Hui.** 2007. QiHong prevents death in coxsackievirus B3 induced murine myocarditis through inhibition of virus attachment and penetration. Exp Biol Med (Maywood) **232:**1441-8.

272. **Stanley, B. A., R. L. Gundry, R. J. Cotter, and J. E. Van Eyk.** 2004. Heart disease, clinical proteomics and mass spectrometry. Dis Markers **20:**167-78.

273. **Stokoe, D., K. Engel, D. G. Campbell, P. Cohen, and M. Gaestel.** 1992. Identification of MAPKAP kinase 2 as a major enzyme responsible for the phosphorylation of the small mammalian heat shock proteins. FEBS Lett **313:**307-13.

274. **Suhara W, Y. M., Yonekawa H, Fujita T. .** 1996. Structure of mouse interferon stimulated gene factor 3 gamma (ISGF3 gamma/p48) cDNA and chromosomal localization of the gene. . J Biochem (Tokyo). **119:**231-4.

275. **Sutsch, G., U. T. Brunner, C. von Schulthess, H. O. Hirzel, O. M. Hess, M. Turina, H. P. Krayenbuehl, and M. C. Schaub.** 1992. Hemodynamic performance and myosin light chain-1 expression of the hypertrophied left ventricle in aortic valve disease before and after valve replacement. Circ Res **70:**1035-43.

276. **Swaminathan, N., C. M. Lai, M. W. Beilharz, S. J. Boyer, and S. P. Klinken.** 1992. Biological activities of recombinant murine interferons alpha 1 and alpha 4: large difference in antiproliferative effect. Antiviral Res **19:**149-59.

277. **Swanson, S. K., and M. P. Washburn.** 2005. The continuing evolution of shotgun proteomics. Drug Discov Today **10:**719-25.

278. **Tai, J. H., J. V. Williams, K. M. Edwards, P. F. Wright, J. E. Crowe, Jr., and T. S. Dermody.** 2005. Prevalence of reovirus-specific antibodies in young children in Nashville, Tennessee. J Infect Dis **191:**1221-4.

279. **Takaoka, A., and H. Yanai.** 2006. Interferon signalling network in innate defence. Cell Microbiol **8:**907-22.

280. **Tanguay, R. M., Y. Wu, and E. W. Khandjian.** 1993. Tissue-specific expression of heat shock proteins of the mouse in the absence of stress. Dev Genet **14:**112-8.

281. **Taniguchi, T., K. Ogasawara, A. Takaoka, and N. Tanaka.** 2001. IRF family of transcription factors as regulators of host defense. Annu Rev Immunol **19:**623-55.

282. **Tavaria, M., T. Gabriele, I. Kola, and R. L. Anderson.** 1996. A hitchhiker's guide to the human Hsp70 family. Cell Stress Chaperones **1:**23-8.

283. **Taylor, S. W., E. Fahy, B. Zhang, G. M. Glenn, D. E. Warnock, S. Wiley, A. N. Murphy, S. P. Gaucher, R. A. Capaldi, B. W. Gibson, and S. S. Ghosh.** 2003. Characterization of the human heart mitochondrial proteome. Nat Biotechnol **21:**281-6.

284. **Terstegen, L., P. Gatsios, S. Ludwig, S. Pleschka, W. Jahnen-Dechent, P. C. Heinrich, and L. Graeve.** 2001. The vesicular stomatitis virus matrix protein inhibits glycoprotein 130-dependent STAT activation. J Immunol **167:**5209-16.

285. **Tissieres, A., H. K. Mitchell, and U. M. Tracy.** 1974. Protein synthesis in salivary glands of Drosophila melanogaster: relation to chromosome puffs. J Mol Biol **84:**389-98.

286. **Tonge, R., J. Shaw, B. Middleton, R. Rowlinson, S. Rayner, J. Young, F. Pognan, E. Hawkins, I. Currie, and M. Davison.** 2001. Validation and development of fluorescence two-dimensional differential gel electrophoresis proteomics technology. Proteomics **1:**377-96.

287. **Trost, S. U., J. H. Omens, W. J. Karlon, M. Meyer, R. Mestril, J. W. Covell, and W. H. Dillmann.** 1998. Protection against myocardial dysfunction after a brief ischemic period in transgenic mice expressing inducible heat shock protein 70. J Clin Invest **101:**855-62.

288. **Tsan, M. F., and B. Gao.** 2004. Heat shock protein and innate immunity. Cell Mol Immunol **1:**274-9.

289. **Turakhia, S., C. D. Venkatakrishnan, K. Dunsmore, H. Wong, P. Kuppusamy, J. L. Zweier, and G. Ilangovan.** 2007. Doxorubicin-induced cardiotoxicity: direct correlation of cardiac fibroblast and H9c2 cell survival and aconitase activity with heat shock protein 27. Am J Physiol Heart Circ Physiol **293:**H3111-21.

290. **Tyler, K. L., M. K. Squier, A. L. Brown, B. Pike, D. Willis, S. M. Oberhaus, T. S. Dermody, and J. J. Cohen.** 1996. Linkage between reovirus-induced apoptosis and inhibition of cellular DNA synthesis: role of the S1 and M2 genes. J Virol **70:**7984-91.

291. **Tyler, K. L., M. K. Squier, S. E. Rodgers, B. E. Schneider, S. M. Oberhaus, T. A. Grdina, J. J. Cohen, and T. S. Dermody.** 1995. Differences in the capacity of reovirus strains to induce apoptosis are determined by the viral attachment protein sigma 1. J Virol **69:**6972-9.

292. **Unlu, M., M. E. Morgan, and J. S. Minden.** 1997. Difference gel electrophoresis: a single gel method for detecting changes in protein extracts. Electrophoresis **18:**2071-7.

293. **van der Velden, J., Z. Papp, R. Zaremba, N. M. Boontje, J. W. de Jong, V. J. Owen, P. B. Burton, P. Goldmann, K. Jaquet, and G. J. Stienen.** 2003. Increased Ca2+-sensitivity of the contractile apparatus in end-stage human heart failure results from altered phosphorylation of contractile proteins. Cardiovasc Res **57:**37-47.

294. **Van Heuvel, M., I. J. Bosveld, A. A. Mooren, J. Trapman, and E. C. Zwarthoff.** 1986. Properties of natural and hybrid murine alpha interferons. J Gen Virol **67 (Pt 10):**2215-22.

295. **van Pesch, V., H. Lanaya, J. C. Renauld, and T. Michiels.** 2004. Characterization of the murine alpha interferon gene family. J Virol **78:**8219-28.

296. **Vander Heide, R. S.** 2002. Increased expression of HSP27 protects canine myocytes from simulated ischemia-reperfusion injury. Am J Physiol Heart Circ Physiol **282:**H935-41.

297. **Veals, S. A., Schindler, C., Leonard, D., Fu, X.-Y., Aebersold, R., Darnell, Jr. J. E. and Levy, D. E., .** 1992. Subunit of an alpha-interferon-responsive transcription factor is related to interferon regulatory factor and myb families of DNA-binding proteins. . Mol. Cell. Biol., **12:**3315-3324.

298. **Vedula, S. R., T. S. Lim, E. Kirchner, K. M. Guglielmi, T. S. Dermody, T. Stehle, W. Hunziker, and C. T. Lim.** 2008. A comparative molecular force spectroscopy study of homophilic JAM-A interactions and JAM-A interactions with reovirus attachment protein sigma1. J Mol Recognit **21:**210-6.

299. **Venkatakrishnan, C. D., A. K. Tewari, L. Moldovan, A. J. Cardounel, J. L. Zweier, P. Kuppusamy, and G. Ilangovan.** 2006. Heat shock protects cardiac cells from doxorubicin-induced toxicity by activating p38 MAPK and phosphorylation of small heat shock protein 27. Am J Physiol Heart Circ Physiol **291:**H2680-91.

300. **Vestal, M. L., and J. M. Campbell.** 2005. Tandem time-of-flight mass spectrometry. Methods Enzymol **402:**79-108.

301. **Vondriska, T. M., J. Zhang, C. Song, X. L. Tang, X. Cao, C. P. Baines, J. M. Pass, S. Wang, R. Bolli, and P. Ping.** 2001. Protein kinase C epsilon-Src modules direct signal transduction in nitric oxide-induced cardioprotection: complex formation as a means for cardioprotective signaling. Circ Res **88:**1306-13.

302. **Voss, O. H., S. Batra, S. J. Kolattukudy, M. E. Gonzalez-Mejia, J. B. Smith, and A. I. Doseff.** 2007. Binding of caspase-3 prodomain to heat shock protein 27 regulates monocyte apoptosis by inhibiting caspase-3 proteolytic activation. J Biol Chem **282:**25088-99.

303. **Wainberg, Z., M. Oliveira, S. Lerner, Y. Tao, and B. G. Brenner.** 1997. Modulation of stress protein (hsp27 and hsp70) expression in CD4+ lymphocytic cells following acute infection with human immunodeficiency virus type-1. Virology **233:**364-73.

304. **Wakayama, T., and S. Iseki.** 1998. Expression and cellular localization of the mRNA for the 25-kDa heat-shock protein in the mouse. Cell Biol Int **22:**295-304.

305. **Wallin, R. P., A. Lundqvist, S. H. More, A. von Bonin, R. Kiessling, and H. G. Ljunggren.** 2002. Heat-shock proteins as activators of the innate immune system. Trends Immunol **23:**130-5.

306. **Wang, X., M. Li, H. Zheng, T. Muster, P. Palese, A. A. Beg, and A. Garcia-Sastre.** 2000. Influenza A virus NS1 protein prevents activation of NF-kappaB and induction of alpha/beta interferon. J Virol **74:**11566-73.

307. **Wang, Y. X., V. da Cunha, J. Vincelette, K. White, S. Velichko, Y. Xu, C. Gross, R. M. Fitch, M. Halks-Miller, B. R. Larsen, T. Yajima, K. U. Knowlton, R. Vergona, M. E. Sullivan, and E. Croze.** 2007. Antiviral and myocyte protective effects of murine interferon-beta and -{alpha}2 in coxsackievirus B3-induced myocarditis and epicarditis in Balb/c mice. Am J Physiol Heart Circ Physiol **293:**H69-76.

308. **Washburn, M. P., D. Wolters, and J. R. Yates, 3rd.** 2001. Large-scale analysis of the yeast proteome by multidimensional protein identification technology. Nat Biotechnol **19:**242-7.

309. **Wasinger, V. C., S. J. Cordwell, A. Cerpa-Poljak, J. X. Yan, A. A. Gooley, M. R. Wilkins, M. W. Duncan, R. Harris, K. L. Williams, and I. Humphery-Smith.** 1995. Progress with gene-product mapping of the Mollicutes: Mycoplasma genitalium. Electrophoresis **16:**1090-4.

310. **Weekes, J., C. H. Wheeler, J. X. Yan, J. Weil, T. Eschenhagen, G. Scholtysik, and M. J. Dunn.** 1999. Bovine dilated cardiomyopathy: proteomic analysis of an animal model of human dilated cardiomyopathy. Electrophoresis **20:**898-906.

311. **Weissmann, C., and H. Weber.** 1986. The interferon genes. Prog Nucleic Acid Res Mol Biol **33:**251-300.

312. **Werner-Washburne, M., and E. A. Craig.** 1989. Expression of members of the Saccharomyces cerevisiae hsp70 multigene family. Genome **31:**684-9.

313. **Wheeler, C. H., A. Collins, M. J. Dunn, S. J. Crisp, M. H. Yacoub, and M. L. Rose.** 1995. Characterization of endothelial antigens associated with transplant-associated coronary artery disease. J Heart Lung Transplant **14:**S188-97.

314. **White, M. Y., A. S. Tchen, H. C. McCarron, B. D. Hambly, R. W. Jeremy, and S. J. Cordwell.** 2006. Proteomics of ischemia and reperfusion injuries in rabbit myocardium with and without intervention by an oxygen-free radical scavenger. Proteomics **6:**6221-33.

315. **Whitton, J. L.** 2002. Immunopathology during coxsackievirus infection. Springer Semin Immunopathol **24:**201-13.

316. **Wiebe, M. E., and T. W. Joklik.** 1975. The mechanism of inhibition of reovirus replication by interferon. Virology **66:**229-40.

317. **Wiener, J. R., J. A. Bartlett, and W. K. Joklik.** 1989. The sequences of reovirus serotype 3 genome segments M1 and M3 encoding the minor protein mu 2 and the major nonstructural protein mu NS, respectively. Virology **169:**293-304.

318. **Wiener, J. R., and W. K. Joklik.** 1988. Evolution of reovirus genes: a comparison of serotype 1, 2, and 3 M2 genome segments, which encode the major structural capsid protein mu 1C. Virology **163:**603-13.

319. **Wilkins, M. R., J. C. Sanchez, A. A. Gooley, R. D. Appel, I. Humphery-Smith, D. F. Hochstrasser, and K. L. Williams.** 1996. Progress with proteome projects: why all proteins expressed by a genome should be identified and how to do it. Biotechnol Genet Eng Rev **13:**19-50.

320. **Woelk, C. H., S. D. Frost, D. D. Richman, P. E. Higley, and S. L. Kosakovsky Pond.** 2007. Evolution of the interferon alpha gene family in eutherian mammals. Gene **397:**38-50.

321. **Woodruff, J. F.** 1980. Viral myocarditis. A review. Am J Pathol **101:**425-84.

322. **Wu, C. C., M. J. MacCoss, K. E. Howell, and J. R. Yates, 3rd.** 2003. A method for the comprehensive proteomic analysis of membrane proteins. Nat Biotechnol **21:**532-8.

323. **Wyttenbach, A., O. Sauvageot, J. Carmichael, C. Diaz-Latoud, A. P. Arrigo, and D. C. Rubinsztein.** 2002. Heat shock protein 27 prevents cellular polyglutamine toxicity and suppresses the increase of reactive oxygen species caused by huntingtin. Hum Mol Genet **11:**1137-51.

324. **Yan, J. X., A. T. Devenish, R. Wait, T. Stone, S. Lewis, and S. Fowler.** 2002. Fluorescence two-dimensional difference gel electrophoresis and mass spectrometry based proteomic analysis of Escherichia coli. Proteomics **2:**1682-98.

325. **Yates, J. R., 3rd.** 1998. Mass spectrometry and the age of the proteome. J Mass Spectrom **33:**1-19.

326. **Yenari, M. A., J. Liu, Z. Zheng, Z. S. Vexler, J. E. Lee, and R. G. Giffard.** 2005. Antiapoptotic and anti-inflammatory mechanisms of heat-shock protein protection. Ann N Y Acad Sci **1053:**74-83.

327. **Yeow, W. S., W. C. Au, Y. T. Juang, C. D. Fields, C. L. Dent, D. R. Gewert, and P. M. Pitha.** 2000. Reconstitution of virus-mediated expression of interferon alpha genes in human fibroblast cells by ectopic interferon regulatory factor-7. J Biol Chem **275:**6313-20.

328. **Yeow, W. S., C. M. Lawson, and M. W. Beilharz.** 1998. Antiviral activities of individual murine IFN-alpha subtypes in vivo: intramuscular injection of IFN expression constructs reduces cytomegalovirus replication. J Immunol **160:**2932-9.

329. **Yokota, S., N. Yokosawa, T. Kubota, T. Okabayashi, S. Arata, and N. Fujii.** 2003. Suppression of thermotolerance in mumps virus-infected cells is caused by lack of HSP27 induction contributed by STAT-1. J Biol Chem **278:**41654-60.

330. **Yoneyama, M., Suhara, W., Fukuhara, Y., Fukada, M., Nishida, E.,Fujita, T., .** 1998. Direct triggering of the type I interferon system by virus infection: activation of a transcription factor complex con-taining IRF-3 and CBP/p300. . EMBO J. **17:**1087–1095.

331. **You, W., X. Min, X. Zhang, B. Qian, S. Pang, Z. Ding, C. Li, X. Gao, R. Di, Y. Cheng, and L. Liu.** 2008. Cardiac Specific Expression of Heat Shock Protein 27 Attenuated Endotoxin-Induced Cardiac Dysfunction and Mortality in Mice through a PI3K/Akt Dependent Mechanism. Shock.

332. **Zhang, J., C. P. Baines, C. Zong, E. M. Cardwell, G. Wang, T. M. Vondriska, and P. Ping.** 2005. Functional proteomic analysis of a three-tier PKCepsilon-Akt-

eNOS signaling module in cardiac protection. Am J Physiol Heart Circ Physiol **288:**H954-61.

333. **Zhang L, P. J.** 1997. IRF-7, a new interferon regulatory factor associated with Epstein-Barr virus latency. . Mol. Cell. Biol. **17:**5748–57.

334. **Zhu, Y. H., and X. Wang.** 2005. Overexpression of heat-shock protein 20 in rat heart myogenic cells confers protection against simulated ischemia/reperfusion injury. Acta Pharmacol Sin **26:**1076-80.

335. **Zurney, J., T. Kobayashi, G. H. Holm, T. S. Dermody, and B. Sherry.** 2009. Reovirus mu2 protein inhibits interferon signaling through a novel mechanism involving nuclear accumulation of interferon regulatory factor 9. J Virol **83:**2178-87.

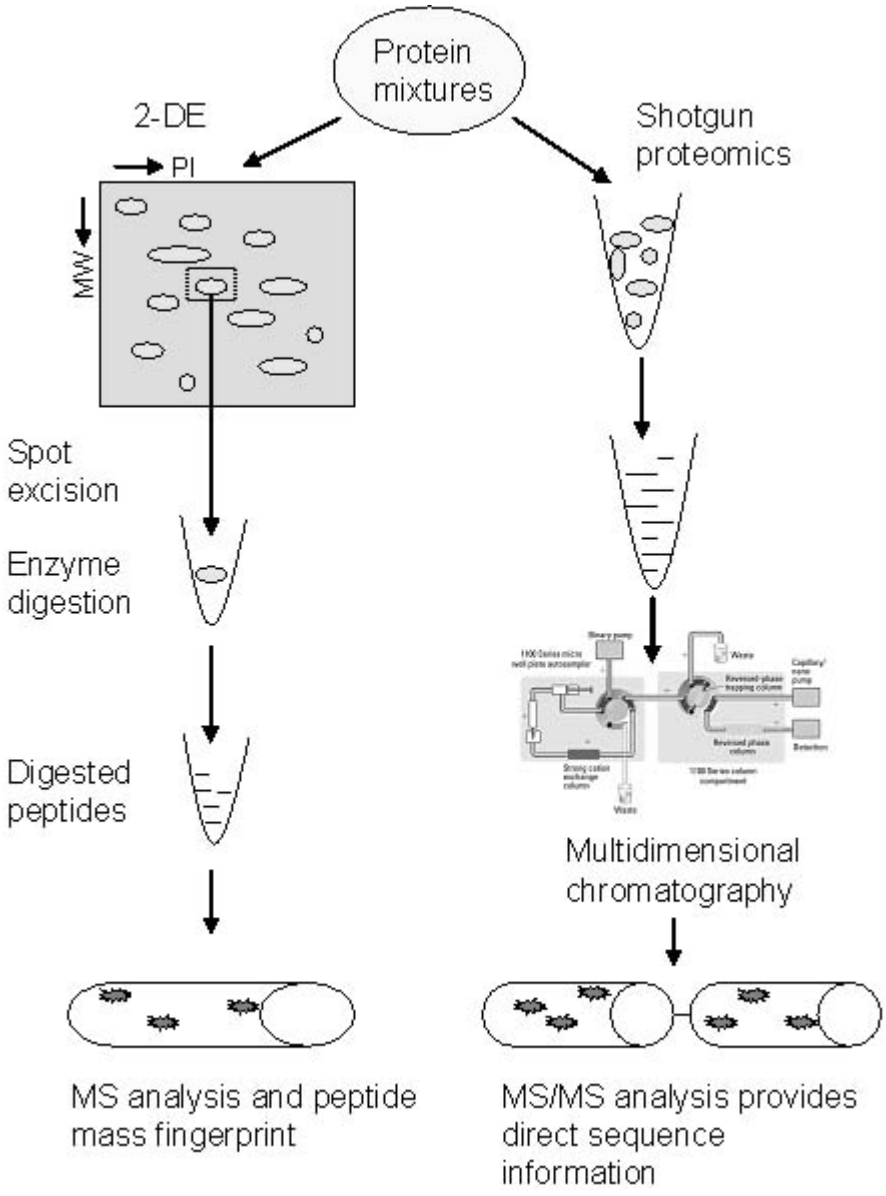

Figure 1.1. Comparison of proteomics coupled with traditional two-dimensional gel electrophoresis and shot gun proteomics.

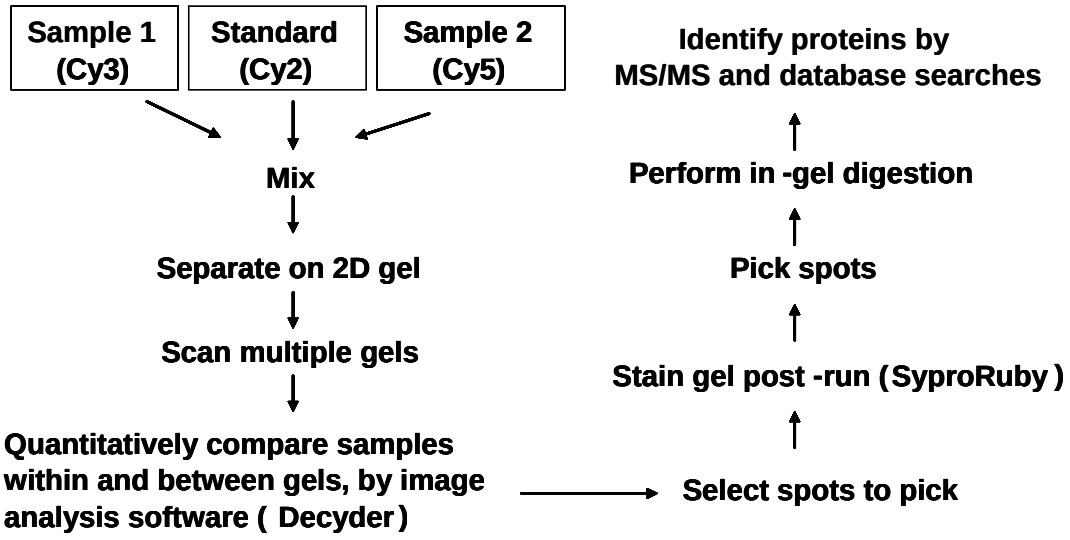

Figure 1.2. Schematic steps for two-dimensional difference gel electrophoresis (2D-DIGE).

CHAPTER 2

IFN-α Expression and Antiviral Effects are Subtype- and Cell Type-Specific in the Cardiac Response to Viral Infection

Lianna Li [1] and Barbara Sherry [1,2]

Departments of Molecular Biomedical Sciences [1] and Microbiology [2], North Carolina State University, Raleigh, North Carolina

Submitted for publication to Virology. Currently in review.

ABSTRACT

The interferon-β (IFN-β) response is critical for protection against viral myocarditis in several mouse models, and IFN-α or -β treatment is beneficial in the treatment of human viral myocarditis. The IFN-β response differs between cardiac myocytes and cardiac fibroblasts, and evidence suggests that the two cell types together form an integrated network for organ protection. However, there have been no studies comparing expression and antiviral effects of the different IFN-α subtypes in cardiac cells. We developed a quantitative RT-PCR assay that distinguishes between thirteen highly conserved IFN-α subtypes, and found that reovirus T3D induced five IFN-α subtypes in primary cultures of cardiac myocytes and fibroblasts: IFN-α1, -α2, -α4, -α5, and -α8/6. The levels of IFN-α expression were both higher and spanned a greater range in cardiac myocytes than in fibroblasts. Viral induction of IFN-α1, -α2, -α5, and -α8/6 required IFN-α/β signaling in both cell types, while induction of IFN-β and -α4 was more dependent on IFN signaling in myocytes than fibroblasts. Murine IFN-α1, -α2, -α4, or -α5 treatment induced IRF7 and ISG56 in both cardiac cell types, however induction was always greater in cardiac fibroblasts than in cardiac myocytes consistent with our previous reports for IFN-β. Finally, each IFN-α subtype inhibited reovirus T3D replication in both cell types, but protection was subtype-specific. This first investigation of viral induction of IFN-α in cardiac cells for any virus demonstrates that IFN-α is induced in cardiac cells, that it is both subtype- and cell type-specific, and that it is likely important in the antiviral cardiac response.

INTRODUCTION

Many viruses infect the heart, and >5% of the human population has experienced some form of viral myocarditis (19, 74). Moreover, >50% of sudden deaths in young adults are due to cardiac causes with >10% of those due to myocarditis (17, 53). Unfortunately, cardiac myocytes are not readily replenished, with a recent report suggesting only 1% cell renewal in the average human lifetime (7). This cardiac vulnerability likely necessitates a uniquely effective cardiac response to limit virus spread through the heart until immune defenses can be deployed. The cytokine IFN-β could provide this critical first line of defense (51), and indeed, we have shown that IFN-β is a determinant of protection against reovirus-induced myocarditis in a mouse model (60). That is, differences in the capacity of reovirus strains to induce myocarditis correlate with differences in viral induction of IFN-β and viral sensitivity to the antiviral effects of IFN-α/β in primary cultures of cardiac myocytes. In addition, a non-myocarditic reovirus induces cardiac lesions in mice lacking IFN-α/β function (60). Reovirus-induced myocarditis reflects direct viral cytopathogenic effect in cardiac cells (5), while coxsackievirus B (CVB)-induced myocarditis reflects both direct and immune-mediated pathology (31, 72), and murine cytomegalovirus-induced myocarditis (MCMV) likely reflects predominantly immune-mediated damage (44). IFN-α/β provides protection against myocarditis induced by CVB(71) and MCMV (4, 12) as well, suggesting that regardless of mechanism, the IFN response plays an important antiviral role. Importantly,

IFN-β treatment clears virus from the heart and improves cardiac function in patients with persistent viral myocarditis (40, 41).

IFN-β is expressed and secreted by most cell types in response to viral infection or other stimuli (36). Binding to the IFN-α/β-receptor (IFNAR) stimulates a signal transduction cascade to induce hundreds of interferon-stimulated genes (ISGs) (37), some of which have antiviral function (55), and one of which is a transcription factor (IRF7) which can further induce IFN-β and IFN-α4 in a positive amplification loop (30, 47, 56). However this signaling cascade is clearly cell type-specific (13, 68). Previously, we found that cardiac myocytes and cardiac fibroblasts differ in their basal expression of components in the IFN pathway, resulting in differences in their IFN-β response to viral infection (63, 77). Our results suggested that high basal IFN-β expression in cardiac myocytes pre-arms this vulnerable, non-replenishable cell type, while high basal expression of latent components in the IFN response path in adjacent cardiac fibroblasts renders these cells more responsive to IFN and prevents them from inadvertently serving as a reservoir for viral replication and spread to cardiac myocytes. These studies provided the first indication of an integrated network of cell type-specific innate immune components for organ protection, and confirmed the importance of investigating the IFN response in cell types relevant to the disease of interest.

Both IFN-α and IFN-β bind the IFN-α/β-receptor but with different affinities, resulting in induction of an overlapping but distinct set of ISGs (34). While IFN-β is expressed by most cell types in response to viral infection or other stimuli, dendritic cells are likely the

predominant cells expressing IFN-α as an early step in maturation of the adaptive immune response (62). Nonetheless, IFN-α expression has been detected in many cell types, suggesting that direct protection against pathogens is also an important function for IFN-α. Indeed, IFN-α is a component of the most effective antiviral regimen currently available for treatment of Hepatitis C virus infection, and IFN-α has also been beneficial to patients with viral myocarditis (14, 48, 64). Given that IFN-α and IFN-β bind the same cell receptor and given the importance of both IFN-α and IFN-β in protection against viral myocarditis, we wished to investigate IFN-α expression and function in primary cultures of murine cardiac cells.

IFN-α is expressed in many if not all mammalian species (73). While IFN-β is encoded by a single gene, mouse IFN-α is encoded by at least 13 functional genes which share >80% DNA and protein similarity (26, 70). This has limited the reagents and technologies available for discernment of individual IFN-α subtypes to determine their roles in protection against pathogens. To differentiate between thirteen highly conserved murine IFN-α subtypes, we developed a 3'-base mismatch approach to design primer pairs specific for each IFN-α subtype in quantitative RT-PCR. We used this novel assay and purified preparations of individual IFN-α subtypes to investigate IFN-α subtype expression and function in cardiac myocytes and fibroblasts. This first investigation of viral induction of IFN-α in cardiac cells for any virus demonstrates that IFN-α is induced in cardiac cells, that it is both subtype- and cell type-specific, and that it is likely important in the antiviral cardiac response.

MATERIALS AND METHODS

Mice. Timed-pregnant Cr:NIH(S) mice were purchased from the National Cancer Institute. IFN-α/β-receptor-null mice (51) were maintained as breeding colonies to generate neonates and fetuses for generation of primary cell cultures. Mouse facilities were accredited by the Association for Assessment and Accreditation of Laboratory Animal Care, and all procedures were approved by the North Carolina State University institutional animal care and use committee.

Primary cell cultures. Primary cardiac myocyte cultures and primary cardiac fibroblast cultures were generated from 1- or 2-day-old neonatal or term fetal mice according to the method described previously (5). Briefly, the apical two-thirds of the hearts from euthanized neonates or fetuses were removed and trypsinized. Cells were suspended in Dulbecco's modified Eagle's medium (DMEM; Gibco BRL, Gaithersburg, MD) supplemented with 7% fetal calf serum and 10 μg of gentamicin (Sigma Co.) per ml (cDMEM). Cells were plated in 6-well clusters, and incubated for 2 hours for separation by differential adhesion. Cardiac myocytes were harvested from the supernatant and the adherent cardiac fibroblasts were harvested by trypsinization. Following centrifugation, cardiac myocytes were suspended in cDMEM plus 0.06% thymidine (Sigma Co., St. Louis, MO), cardiac fibroblasts were suspended in cDMEM, and both cultures were incubated in a 37ºC, 5% CO_2 incubator. Cells were never passaged before use. By immunofluorescent staining, myocyte cultures contained <5% fibroblasts while fibroblast cultures contained <1% myocytes (77) .

Viruses and cell lines. Reovirus type 3 Dearing (T3D (58)) was plaque purified and amplified in mouse L929 cells, which were maintained in a suspension system in sMEM (SAFC Biosciences, Denver, PA) supplemented with 5% fetal calf serum (Atlanta Biologicals, Atalanta, GA) and 2mM L-glutamine (Mediatech Inc., Herndon, VA). Virus was purified by CsCl gradient centrifugation (61) for use in all experiments.

Infection for T3D induction of IFN-α. Cardiac myocytes from Cr:NIH(S) mice were plated at 1×10^6 cells per well and cardiac fibroblasts were plated at 5×10^5 cells per well in 2 ml media in 24-well clusters. Cardiac fibroblasts were assumed to double after two day's incubation. All cultures were washed twice, and duplicate wells were infected at an moi of 10 pfu per cell two days post-plating. Virus suspended in 700 μl of cDMEM with or without thymidine was added to each well, and cells were incubated in 37ºC, 5% CO_2 incubator for 1 hour. Then an additional 1000 μl cDMEM with or without thymidine was added to each well. Mock-infected cells were treated identically except the inocula lacked virus.

Cardiac myocytes from IFN-α/β-receptor-null mice were plated at 5×10^5 cells per well and cardiac fibroblasts were plated at 2.5×10^5 cells per well in 1 ml media in 48-well clusters. Infections were as above, except that virus inoculum was 350 μl per well, and an additional 500 μl media was added after the 1 hour incubation.

Infection for T3D sensitivity to IFN-α. Cardiac myocytes from Cr:NIH(S) mice were plated at 1.5×10^5 cells per well and cardiac fibroblasts were plated at 7.5×10^4 cells per well in 300μl media in 96-well clusters. Cardiac fibroblasts were assumed to double after two day's incubation. Twenty-four hours post-plating, cells were washed once, and overlying medium was replaced with 300 μl of IFN-β, -α1, -α2, -α4 or -α5 at 100 or 1000U per ml in

cDMEM with or without thymidine in triplicate wells (IFN-β: cat # 12400-1; IFN-α subtypes: a gift of purified recombinant preparations quantified in a standard IFN assay measuring protection of L929 cells against encephalomyocarditis virus challenge; both from PBL Biomedical Laboratories, Piscataway, NJ). . After an additional overnight incubation, cells were washed twice, infected with T3D at an moi of 10 pfu per cell in 100 µl inoculum, and incubated for 1 hour in a 37ºC, 5% CO2 incubator. Cells were washed once, and the appropriate IFN at 100 or 1000U per ml in 250µl cDMEM with or without thymidine was added to each well. Control cells lacked IFN treatment, but were infected with T3D as above. After 20 hours incubation, cultures were stored at -80°C, frozen and thawed an additional two times, and supplemented to a final 0.5% Nonidet P-40 (Sigma). Serial dilutions were used to infect L929 cells in a standard plaque assay (59).

Harvesting cultures for RNA and ELISA. Supernatants and RNA were harvested at indicated times post-infection or post-treatment with IFN (from PBL as above). Supernatants were stored at -35ºC, and remaining cells were lysed directly on the plate using cell lysis buffer from an RNeasy Kit (Qiagen, Inc., Valencia, CA) supplemented with 1% β-mercaptoethanol. Cell lysates were homogenized using Qiashredders (Qiagen, Inc.), and total RNA was isolated using the RNeasy Kit according to the manufacturer's instructions. Genomic DNA was removed using RNase-free DNase I (Qiagen, Inc.). The isolated RNA was stored at -80ºC.

Reverse transcription (RT) and Quantitative (q)RT-PCR. To generate cDNA, one third of the RNA harvested from each well in a 24-well cluster or two thirds from a 48-well cluster was used as template in a 100 µl reaction containing 5µM oligo(dT) (Invitrogen Corp.,

Carlsbad, CA), 1× Taq buffer (Promega corp., Madison, WI), 7.5 mM $MgCl_2$ (Promega corp.), 1 mM dithiothreitol (Promega corp.), 1 mM each dNTP (Roche, Indianapolis, IN), 0.67 U/µl RNasin (Promega Corp., Madison, WI), and 0.20 U/µl of AMV reverse transcriptase (Promega Corp.).

Gene expression was quantified using a Sybergreen system on an iCycler iQ fluorescence thermocycler (Bio-Rad Laboratories, Hercules, CA). Each 25 µl reaction contained 5% of the RT product, 1× Quantitech master mix (Qiagen, Inc.), 10 nM fluorescein (Invitrogen Corp., Carlsbad, CA), and 0.3µM each of the forward and reverse primers (IFN-β forward: 5'-GGAGATGACGGAGAAGATGC-3' and reverse: 5'- CCCAGTGCTGGAGAAATTGT; GAPDH forward: 5'- GGGTGTGAACCACGAGAAAT-3' and reverse: 5'-CCTTCCACAATGCCAAAGTT-3'; IFN-α as indicated in Table 2.1). iCyclerTM iQ Optional System Software, version 3.0 (Bio-Rad Laboratories) was used to analyze the data. Gene-of-interest expression was normalized to GAPDH gene expression, and standard curves (generated from serial dilutions of known concentrations of purified PCR products) were used to quantify copy number. Individual cDNA standards for each IFN-α subtype were purified PCR products, using primers to generate products that contain the primers indicated in Table 2.1, as follows: IFN-α1 (334bp) Forward: 5'-GGAACAAGAGAGCCTTGACA-3' and reverse: 5'-CTCACAGCCAGCAGGGCAT-3'; IFN-α2 (626bp) forward: 5'-TCTGTGCTTTCCTCGTGATG-3' and reverse: 5'-GATGCAGTTTCTAGTCCAGG -3' ; IFN-α4 (295bp) forward: 5'-CTGCTGGCTGTGAGGACATA-3' and reverse: 5'-TTGCTCAAGATTGCTGAAACA-3'; IFN-α5 (603bp) forward: 5'-AGAGCCTTAACCCTCCTGGT-3' and reverse: 5'-CGCTCAAGATTGCTGAAACA - 3';

IFN-α8/6 (240bp) forward: 5'-CCTGATGGTTTTGGTGGTGT-3' and reverse: 5'-ATCTGCTGGGTCAGCTCAG-3'.

Pyrosequencing to confirm qRT-PCR products. qRT-PCR products were generated as above, except that one primer of the primer pair was biotinylated at its 5' terminus (Invitrogen). A 50% slurry of Streptavidin Sepharose™ High Performance beads (GE Heathcare, Piscataway, NJ) was suspended in Binding buffer (10 mM Tris-HCl pH 7.6, 2 M NaCl, 1 mM EDTA, 0.1% Tween 20; Biotage, Charlottesville, VA) for a final 5% slurry. Primers for pyrosequencing were suspended in annealing buffer (20 mM Tris-acetate pH 7.6, 2 mM Mg-acetate; Biotage) at a final concentration of 0.4μM. Ten μl (40%) of qRT-PCR products were mixed with the streptavidin beads in 96-well clusters (Corning, NY), and then transferred to PSQ 96 Sample Prep Thermoplates (Low; Biotage) for Pyrosequencing, using Pyro Gold Reagents (Biotage) according to the manufacturer's instructions. Primers for pyrosequencing were: GAPDH (5'-GGTCTACATGTTCCAGTATG-3'); IFN-β (5'-CGGAGAAGATGCAGAAGAGT-3'); IFN-α2 (5'- ATTCCCCCTGGAGAAGGTG -3'); IFN-α4 (5'-CTGGAGAGCCCTCTCTTCCT-3'), and IFN-α5 (5'-AGCCTGTGTGATGCAACAGG-3').

ELISA. Expression of IFN-α protein was determined using a mouse IFN-α ELISA kit (PBL Biomedical Laboratories) according to the manufacturer's instructions. Briefly, 100 μl supernatant from each sample (24-well clusters) was measured. A standard curve was constructed ranging from 0-500 pg/ml, using serial dilutions of a mouse IFN-α standard provided with the kit. Absorbance was detected at 450nm on a Tecan Sunrise Microplate Reader (Tecan Systems Inc., San Jose, CA).

Statistical analysis. A Student's two-sample *t*-test (pooled variance) was applied (Systat 9.0). Results were considered significant at $P < 0.05$.

RESULTS

Design of qRT-PCR primer pairs and confirmation of IFN-α subtype specificity. To differentiate between thirteen highly conserved IFN-α subtypes, a 3'-base mismatch approach was adopted to design qRT-PCR primer pairs. This method is based on the extreme specificity of the 3' terminal nucleotide for primer extension, i.e., cDNA synthesis can be extended only when its 3' terminal nucleotide is complementary to the template nucleotide. Since IFN-α gene sequences for Cr:NIH(S) mice are unavailable, fifteen primer pairs were designed using alternative mouse sequences from GenBank, and then Cr:NIH(S) mouse genomic DNA was used in qPCR to confirm that the primer pairs could amplify products from this heterologous mouse strain (Table 2.1). Each primer pair generated a single peak in a standard melt-curve analysis (data not shown), indicating amplification of a single product. Next, total cell RNA was harvested from T3D-infected primary cardiac myocyte and primary cardiac fibroblast cultures, and was used as template for oligo-dT-primed cDNA synthesis and qRT-PCR. Finally, qRT-PCR products for IFN-α2, -α4 and α5 were sequenced using pyrosequencing technology, confirming the subtype-specificity for these primer pairs (examples in Figure. 2.1).

Basal and reovirus T3D-induced expression of IFN-α is subtype- and cell type-specific in cardiac cells. In order to determine whether T3D infection induces IFN-α and whether

induction is subtype-specific in cardiac cells, primary cardiac myocyte cultures and primary cardiac fibroblast cultures were mock-infected or infected with T3D, and RNA was harvested at 8 hours post-infection for qRT-PCR. As reported previously (60, 63, 77), T3D induced IFN-β in both cell types. Results indicated that five of the thirteen IFN-α subtypes were induced in both cell types: IFN-α1, -α2, -α4, -α5, and -α8/6 (Table 2.2). Other IFN-α subtypes were either undetectable or the induction was less than 2-fold relative to mock-infected cultures. Therefore, additional experiments focused on these five IFN-α subtypes only.

IFN-β and IFN-α4 were both expressed at higher basal levels in cardiac myocytes than in cardiac fibroblasts (Figure. 2.2A), suggesting that the two genes may be regulated by a common cell type-specific mechanism. In contrast, IFN-α1, -α2, -α5, and -α8/6 were expressed at similar basal levels in the two cardiac cell types (Figure. 2.2A). Finally, IFN-α8/6 was expressed at significantly higher basal levels than IFN-β or any other IFN-α subtype (*P* values < 0.05 in all cases, except for IFN-α4 in myocytes), suggesting unique regulation of its basal expression by a mechanism common to both cardiac cell types.

At 8 hours post-infection with T3D, as previously seen for IFN-β (77), all five IFN-α subtypes were induced to higher expression in cardiac myocytes than in cardiac fibroblasts (Figure 2.2B). In T3D-infected cardiac myocyte cultures (Figure. 2.2B), IFN-β expression was the highest and was approximately 3-fold higher than IFN-α4 expression. All other IFN-α subtypes were expressed at significantly lower levels than IFN-α4, with a relative order of expression of IFN-α2 = IFN-α5 > IFN-α8/6 = IFN-α1. In T3D-infected cardiac

fibroblast cultures (Figure 2.2B), IFN-β expression was also the highest and was approximately twice as high as IFN-α4 expression. While the remaining IFN-α subtypes were expressed at significantly lower levels as observed for cardiac myocytes, the relative order of expression differed: IFN-α5 > IFN-α8/6 ≥ IFN-α1 ≥ IFN-α2. The most apparent difference was for IFN-α2, which was among the most highly expressed IFN-α subtypes in cardiac myocytes but among the least expressed in cardiac fibroblasts.

To compare relative expression of the different IFN-α subtypes, expression for each IFN-α subtype was calculated as a percentage of IFN-β expression (Figure 2.2C). The relative expression of each IFN-α subtype was significantly different between cardiac myocytes and cardiac fibroblasts except for IFN-α2. Notably, while IFN-α1, IFN-α2, IFN-α5 and IFN-α8/6 were expressed at 6 – 26% the level of IFN-β in cardiac fibroblasts, these same IFN-α subtypes were expressed at only 0.5 – 2% the level of IFN-β in cardiac myocytes; a ten-fold difference between cell types. Together, the data suggest that the Type I IFNs induced by viral infection are predominantly IFN-β and IFN-α4 in cardiac myocytes, but IFN-β and multiple IFN-α subtypes in cardiac fibroblasts.

To identify possible differences in the cell response to viral infection, T3D induction of IFN was calculated as fold induction relative to basal expression (Figure 2.2D). As previously seen for IFN-β (77), T3D infection resulted in a significantly greater fold induction for each of the five IFN-α subtypes in cardiac myocytes than in cardiac fibroblasts. Moreover, while the range of induction in cardiac myocytes for IFN-β, -α2, -α4, and -α5 spanned a >16-fold difference (448-fold for IFN-α5 to 7467-fold for IFN-β), the range for those same IFN types

in cardiac fibroblasts spanned only a <3-fold difference (259-fold for IFN-α5 to 712-fold for IFN-β). Finally, although the magnitude and range for fold induction differed dramatically between the two cell types the relative order was very similar. For cardiac myocytes, the fold induction was IFN-β > IFN-α2 > IFN-α4 > IFN-α5 > IFN-α1 > IFN-α8/6, while in cardiac fibroblasts, it was IFN-β > IFN-α2 = IFN-α4 = IFN-α5 > IFN-α1 > IFN-α8/6. Together, the data suggest that cardiac cell type-specific differences in the cell response to viral infection are likely more quantitative than qualitative.

To investigate IFN-α induction over time, RNA was harvested from primary cardiac cell cultures at 4 – 24 hours post-infection with T3D. The four most abundantly induced IFN-α subtypes were quantified by qRT-PCR (Figure 2.3). The trends in relative expression levels for the different IFN-α subtypes were very similar to the single 8 hr time-points in Figure 2.2. Expression peaked at 8 to 12 hrs post-infection for all IFN-α subtypes in cardiac myocytes and for IFN-α2, -α5 and α8/6 in cardiac fibroblasts. Interestingly, IFN-α4 expression in cardiac fibroblasts continued to increase at 24 hours post-infection, in contrast to the other IFN-α subtypes or IFN-β (77) in that cell type, and in contrast to any IFN-α subtype or IFN-β (77) in cardiac myocytes. Together, the data suggest again both subtype- and cell type-specific differences for viral induction of IFN-α in cardiac cells.

To investigate secreted IFN-α, supernatants were harvested between 4 and 24 hours post-infection of primary cardiac cell cultures, and total IFN-α was quantified by ELISA (Figure 2.4). T3D induction of secreted IFN-α was significant starting at 8 hours post-infection for cardiac myocytes ($P < 0.001$) but only at 24 hours post-infection for cardiac fibroblasts ($P =$

0.002). Secreted IFN-α increased over time for both cultures, and was significantly higher for cardiac myocytes than cardiac fibroblasts at 12 and 24 hours post-infection ($P = 0.05$ and 0.002, respectively). Therefore, reovirus T3D induction of secreted IFN-α, like IFN-α mRNA, is cell type-specific.

Reovirus T3D induction of IFN is both direct and indirect, and is subtype- and cell type-specific in cardiac cells. In some cell types, viral infection of cells induces initial synthesis and secretion of IFN-β and IFN-α4, which then signal through the IFN-α/β receptor and JAK-Stat to induce IRF7 for subsequent further induction of IFN-β, IFN-α4 and other IFN-α subtypes (30, 47, 56). To determine whether reovirus T3D induction of IFN-α is direct or mediated by IFN-α or -β, primary cardiac cell cultures were generated from IFN-α/β-receptor-null mice, and reovirus T3D induction of IFN-α and IFN-β at 8 hours post-infection was quantified by qRT-PCR. Basal expression of IFN mRNA was either undetectable or very low in IFN-α/β-receptor-null cells (data not shown) relative to wild-type cells (Figure 2.2A), and suggested a ≥5-fold decrease in IFN-β, IFN-α4, and IFN-α8/6 in cardiac myocytes and a ≥5-fold decrease in IFN-α8/6 in cardiac fibroblasts (data not shown). Basal expression of other IFN mRNA types was too low in wild-type cells (Figure 2.2A) to extrapolate reduction in IFN-α/β-receptor-null cells. T3D induced IFN-β and IFN-α4 significantly in IFN-α/β-receptor null cultures, but expression was dramatically decreased in both cardiac cell types relative to wild type cardiac cell cultures (Figure 2.5). Interestingly, while the reduction in expression was greater in cardiac myocytes than cardiac fibroblasts for both IFN-β and IFN-α4, the reduction was most dramatic for T3D-induced IFN-α4

expression in cardiac myocytes (Figure 2.5B), resulting in an inversion where cardiac fibroblasts expressed more IFN-α4 than cardiac myocytes. Reduction in expression for other IFN-α subtypes ranged from 10- to 100-fold (data not shown) or was not possible to extrapolate given the low expression in wild type cultures (Figure 2.2B). Together the data suggest that IFN-mediated amplification is more critical for T3D-induced IFN-α expression, in particular for IFN-α4, than for IFN-β expression in cardiac myocytes. In contrast, T3D-induced type I IFN in cardiac fibroblasts is less dependent on IFN-mediated amplification.

Virus is a critical component for IFNα/β-mediated induction of IFN-α and -β in cardiac cells. To determine whether IFN-α or IFN-β in the absence of viral infection induces Type I IFN in cardiac cells, primary cardiac myocyte and cardiac fibroblast cultures were treated with murine IFN-β or individual IFN-α subtypes at 1000 U/ml. Total RNA was harvested at 2 and 5 hours post-treatment, and IFN-β and IFN-α subtype expression was assessed by qRT-PCR (data not shown). Results from duplicate experiments indicated that neither IFN-β nor any of the IFN-α subtypes tested induce Type I IFN in cardiac cells in the absence of viral infection.

IFN induction of ISG expression is subtype- and cell type-specific. To determine whether individual IFN-α subtypes can signal in cardiac cells, IFN-α induction of two ISGs was assessed by qRT-PCR. The ISG IRF-7 was chosen for its importance as a transcription factor critical in the positive feedback loop for IFN induction (30, 47, 56), and the ISG 56 was chosen as one representative antiviral ISG. Primary cardiac cell cultures were treated with 1000 U/ml of the indicated IFN type, RNA was harvested between 2 and 8 hours post-

treatment for qRT-PCR analysis (Figure 2.6). In all cases, IFN-α induction of ISGs was greater in cardiac fibroblasts than in cardiac myocytes, consistent with previous results for IFN-β in these cell types (63, 77). At 8 hours post-treatment, the trend for IRF7 expression was similar in cardiac myocytes and cardiac fibroblasts, with the greatest induction by IFN-β and IFN-α4, followed by IFN-α1 and IFN-α5, and the lowest induction by IFN-α2. A similar trend was seen for ISG 56 expression, except that expression decreased by 8 hours post-treatment in cardiac myocytes. Thus cardiac myocytes and cardiac fibroblasts are differentially sensitive to IFN-α treatment as previously seen for IFN-β(77), and IFN signaling in cardiac cells is IFN-α subtype-specific.

Reovirus T3D sensitivity to IFN-α is subtype-specific in cardiac cells. To determine whether individual IFN-α subtypes can provide antiviral protection to cardiac cells, primary cardiac cell cultures were treated with IFN-α1, -α2, -α4, -α5 or -β at 100 or 1000U/ml and then challenged with reovirus T3D 24 hours later. After 20 hours infection, viral titers were determined by plaque assay (Figure 2.7). In both cardiac myocytes and cardiac fibroblasts, each IFN-α subtype tested was antiviral at 1000 U/ml, with decreased effects at 100 U/ml. And in both cell types, IFN-β provided the greatest antiviral protection, IFN-α4 and IFN-α5 provided the next greatest protection, and IFN-α1 and IFN-α2 provided the least protection.

DISCUSSION

IFN-α and IFN-β bind a shared receptor to induce expression of an overlapping set of antiviral genes (34), and both cytokines have been used successfully in the treatment of human viral myocarditis (40, 41) (14, 48, 64) . However, the only investigation measuring expression of different IFN-α subytpes in the heart during murine viral myocarditis used CVB3 [59], which induces both direct and immune-mediated damage (31, 72). Therefore, the IFN-α in that study likely reflected contributions from both cardiac and inflammatory cells. Similarly, there has been only one investigation comparing the efficacy of different IFN-α subtypes in protection against murine viral myocarditis (12), and that study also used a virus that mediates cardiac damage primarily through immune-mediated rather than direct mechanisms (MCMV (44)). There have been no studies comparing cardiac expression of the different IFN-α subtypes using a virus that mediates direct damage to the heart, or using cardiac cells to assess expression of different IFN-α subtypes and their relative importance in the cardiac protective response. Results here demonstrate that IFN-α is induced in cardiac cells, that it is both subtype- and cell type-specific, and that it is likely important in the antiviral cardiac response.

Investigations comparing expression for the different IFN-α subtypes have been hindered by the >80% DNA homology between genes (26, 70). Early semi-quantitative approaches used subtype-specific probes for S1 nuclease mapping (29), *in situ* hybridization (24), and hybridization to PCR products generated using consensus primers (32, 42). In a later labor-

intensive approach, consensus primers were used to generate PCR products which were then cloned and sequenced to quantify the frequency of IFN-α subtype expression (3, 8, 15, 47). Several more recent studies have used IFN-α subtype-specific primers for PCR, but have provided only semi-quantitative electrophoresis-based results (10, 22, 45). Finally, several studies have provided more quantitative assessments. One used fluorescein-labeled probes in a heteroduplex analysis of PCR products generated from consensus primers (16). Several others used IFN-α subtype-specific primers, one for Taqman-based qRT-PCR (46) and two for Sybergreen-based qRT-PCR (2, 33). Here, we took advantage of the extreme specificity of the 3' terminal nucleotide for primer extension to design primers that could be used for Sybergreen-based qRT-PCR, a much less expensive option than Taqman-based qRT-PCR. We also used pyrosequencing in a novel approach to validate the specificity of qRT-PCR products without the need for subcloning. Results provide not only insights into differential IFN-α subtype expression in cardiac cells, but also a method for quantitatively comparing and validating expression from closely related genes.

IFN-α is expressed at detectable levels in some tissues even without stimulation (8, 47, 67, 76) and may play a role in embryo development (18, 54) and prevention of cell transformation (9). Importantly, constitutive expression of IFN-α also plays a critical role in the host response to viral infection. To enhance innate immune responses, high basal expression of IFN-α can directly protect cells from virus infection (6) and can determine high basal expression of IRF7 and thereby increase viral induction of IFN through a positive amplification loop (27). To enhance adaptive immunity, high basal IFN-α can stimulate

maturation and activation of dendritic cells (50) and can augment cell responses to IFN-γ (66) and IL-6 (49). Here, we found that basal expression of IFN-α was both subtype- and cell type-specific in cardiac cells. We previously demonstrated that high basal Type I IFN expression in cardiac myocytes stimulates high basal ISG expression relative to cardiac fibroblasts, resulting in a pre-arming in cardiac myocytes from both protective ISGs and latent IRF7 expression (77). Results here indicate that this Type I IFN could be comprised of both IFN-β and IFN-α4, but not IFN-α1, -α2, -α5 or -α8/6 since they were expressed at basal levels that were equivalent in the two cell types (Figure 2.2). In addition, results here confirm that as in other cell types, IRF7 is not active in cardiac myocytes in the absence of viral infection, since high basal IRF7 expression in cardiac myocytes did not result in higher basal expression of downstream IFN-α subtypes in that cell type. The mechanism underlying high basal expression of IFN-β and IFN-α4 in cardiac myocytes remains unclear. Type I IFN expression is enhanced by an IRF7-mediated positive amplification loop (30, 47, 56) and cell type-specific differences in IRF7 expression can therefore determine viral induction of IFN-α. Indeed, differences in virus-induced expression for two different human IFN-α subtypes reflects differences in organization of IRF elements in the promoters of their genes (11, 23). Constitutive IRF7 levels correlate with levels of both IFN-α4 and IFN-non-α4 (using consensus primers) induced by influenza virus in spleen cells compared to fibroblasts or in plasmacytoid dendritic cells compared to myeloid dendritic cells, and high constitutive IRF7 overcomes the requirement for the positive amplification loop for expression of both IFN-α classes (52). West Nile Virus induction of IFN-α (consensus) is

reduced in multiple primary cell types deficient in IRF7, but interestingly, IFN-β is not (13). However, no previous studies have addressed the impact of IRF7 expression levels on viral induction of different IFN-α subtypes. Previously, we found that reovirus T3D induces greater IRF7 in cardiac fibroblasts than in cardiac myocytes (63), consistent with the greater responsiveness of the former than the latter to IFN signaling (77). Here, we found that while IFN-β and IFN-α4 comprised the majority of Type I IFN induced by reovirus in both cardiac myocytes and cardiac fibroblasts, the relative contribution from the other subtypes differed dramatically, providing only 4% of the total Type I IFN in cardiac myocytes but 27% of the total in cardiac fibroblasts (Figure 2.2B). Moreover, reovirus induced IFN-non-α4 subtypes to a combined level of only 6% that of IFN-β in cardiac myocytes, but 56% the level of IFN-β in cardiac fibroblasts (Figure 2.2C). These data would suggest that cell type-specific differences in virus-induced IRF7 levels (63) correlate with differences in viral induction of IFN-α subtypes downstream of IRF7. However in contrast, viral induction of IFN-α4 and IFN-β in cells lacking IFN-α/β signaling was reduced much more in cardiac myocytes than in cardiac fibroblasts (Figure 2.5; other subtypes were below the limits of detection and therefore could not be assessed). These data would suggest that, as for West Nile Virus comparisons between total IFN-α and IFN-β (13), the role of IRF7 in reovirus induction of Type I IFN varies between IFN types and is cell type-specific.

IFN-α subtypes differ in their antiviral activity both *in vitro* and *in vivo*. When COS cells were transfected with constructs expressing murine IFN-α1, -α2, -α4 and -α6, and then supernatants were tested for protection of L929 and CHO cells against challenge with

vesicular stomatitis virus, IFN-α4 was most effective (69). But when purified recombinant IFN-α1 and -α4 were tested for protection of L929 and J2E cells against encephalomyocarditis virus challenge, the two subtypes were equivalent (65). IFN-α1, -α4 or -α9 transgenes introduced into regenerating muscles of mice each reduced MCMV replication, with IFN-α1 providing the most protection (75). When IFN transgenes were applied vaginally to mice before challenge with HSV-2, IFN-α1, -α5 and -β were protective while -α4, -α6 and -α9 were not (1). Finally when mice were injected with constructs expressing IFN-α subtypes and challenged with influenza virus, -α5 and -α6 were most and -α1 least protective (35). Together, the data suggest that the antiviral activity of murine IFN-α subtypes may be both virus- and tissue-specific. Similar differences in antiviral activity have been seen for human IFN-α subtypes (21, 39, 43, 57). Interestingly, IFN-α subtypes may differ in antiviral activity but not anti-proliferative function, or *vice versa* (20, 65). Here, we found that the relative antiviral activity for Type I IFNs was the same for cardiac myocytes and cardiac fibroblasts: IFN-β provided the greatest protection, -α4 and -α5 were intermediate, and -α1 and -α2 provided the least protection (Figure 2.7). These relative antiviral effects parallel relative IFN subtype-specific induction of ISGs (Figure 2.6; 8 hours post-treatment), perhaps reflecting differences in affinity for the IFN-α/β-receptor (34). Finally, IFN-β, -α4 and -α5 were expressed at higher levels than IFN-α1 and -α2 in cardiac fibroblasts after reovirus infection (Figure 2.2B), potentially contributing even further to their protective functions in the heart.

Viral induction of IFN (Figure 2.2), IFN induction of ISGs (Figure 2.6), and IFN antiviral activity (Figure 2.7) was always greater for IFN-β than for any IFN-α subtype. This is consistent with previous evidence for greater activation of the JAK-Stat pathway (25) and greater antiviral activity of IFN-β than IFN-α (pooled preparations) against CVB3 (28) in human cardiac fibroblasts. Indeed, IFN-β provides protection against influenza virus in mice that cannot be provided by IFN-α alone (38). Nonetheless, while the combined expression of IFN-α subtypes was only 26% of the total IFN in infected cardiac myocytes, it was 52% of the total in infected cardiac fibroblasts (Figure 2.2B). Given that cardiac fibroblasts are more responsive than cardiac myocytes to both IFN-α (Figure 2.6) and IFN-β (63, 77), this contribution of IFN-α could be particularly important in cardiac fibroblasts. Finally, although combined antiviral effects cannot be extrapolated from the data, IFN-α4 and -α5 each expressed 15% of the antiviral activity of IFN-β in cardiac myocytes, and 16 to 23% the activity in cardiac fibroblasts (Figure 2.7B). Together, the data indicate that IFN-α subtypes are likely to play an important role in protecting the heart from viral infection.

ACKNOWLEDGEMENTS

We thank Lindsey Jones, Susan Irvin and Jennifer Zurney for insightful discussions, Wrennie Edwards for technical assistance, and Ronald G. Jubin and colleagues at PBL Biomedical Laboratories for their gift of IFN-α preparations. This research was supported by NIH award R01 AI062657 and graduate student support from the North Carolina State University Genomics Graduate Program (L.L.).

REFERENCES

1. **Austin, B. A., C. M. James, P. Harle, and D. J. Carr.** 2006. Direct application of plasmid DNA containing type I interferon transgenes to vaginal mucosa inhibits HSV-2 mediated mortality. Biol Proced Online **8:**55-62.

2. **Baig, E., and E. N. Fish.** 2008. Distinct signature type I interferon responses are determined by the infecting virus and the target cell. Antivir Ther **13:**409-22.

3. **Barchet, W., M. Cella, B. Odermatt, C. Asselin-Paturel, M. Colonna, and U. Kalinke.** 2002. Virus-induced interferon alpha production by a dendritic cell subset in the absence of feedback signaling in vivo. J Exp Med **195:**507-16.

4. **Bartlett, E. J., J. C. Lenzo, S. Sivamoorthy, J. P. Mansfield, V. S. Cull, and C. M. James.** 2004. Type I IFN-beta gene therapy suppresses cardiac CD8+ T-cell infiltration during autoimmune myocarditis. Immunol Cell Biol **82:**119-26.

5. **Baty, C. J., and B. Sherry.** 1993. Cytopathogenic effect in cardiac myocytes but not in cardiac fibroblasts is correlated with reovirus-induced acute myocarditis. J Virol **67:**6295-8.

6. **Bautista, E. M., G. S. Ferman, D. Gregg, M. C. Brum, M. J. Grubman, and W. T. Golde.** 2005. Constitutive expression of alpha interferon by skin dendritic cells confers resistance to infection by foot-and-mouth disease virus. J Virol **79:**4838-47.

7. **Bergmann, O., R. D. Bhardwaj, S. Bernard, S. Zdunek, F. Barnabe-Heider, S. Walsh, J. Zupicich, K. Alkass, B. A. Buchholz, H. Druid, S. Jovinge, and J. Frisen.** 2009. Evidence for cardiomyocyte renewal in humans. Science **324:**98-102.

8. **Brandt, E. R., A. W. Linnane, and R. J. Devenish.** 1994. Expression of IFN A genes in subpopulations of peripheral blood cells. Br J Haematol **86:**717-25.

9. **Chen, H. M., N. Tanaka, Y. Mitani, E. Oda, H. Nozawa, J. Z. Chen, H. Yanai, H. Negishi, M. K. Choi, T. Iwasaki, H. Yamamoto, T. Taniguchi, and A. Takaoka.** 2009. Critical role for constitutive type I interferon signaling in the prevention of cellular transformation. Cancer Sci **100:**449-56.

10. **Cheng, G., X. Zhao, W. Chen, W. Yan, M. Liu, J. Chen, and Z. Zheng.** 2007. Detection of differential expression of porcine IFN-alpha subtypes by reverse transcription polymerase chain reaction. J Interferon Cytokine Res **27:**579-87.

11. **Civas, A., P. Genin, P. Morin, R. Lin, and J. Hiscott.** 2006. Promoter organization of the interferon-A genes differentially affects virus-induced expression and responsiveness to TBK1 and IKKepsilon. J Biol Chem **281:**4856-66.

12. **Cull, V. S., E. J. Bartlett, and C. M. James.** 2002. Type I interferon gene therapy protects against cytomegalovirus-induced myocarditis. Immunology **106:**428-37.

13. **Daffis, S., M. A. Samuel, M. S. Suthar, B. C. Keller, M. Gale, Jr., and M. S. Diamond.** 2008. Interferon regulatory factor IRF-7 induces the antiviral alpha interferon response and protects against lethal West Nile virus infection. J Virol **82:**8465-75.

14. **Daliento, L., F. Calabrese, F. Tona, A. L. Caforio, G. Tarsia, A. Angelini, and G. Thiene.** 2003. Successful treatment of enterovirus-induced myocarditis with interferon-alpha. J Heart Lung Transplant **22:**214-7.

15. **Delhaye, S., S. Paul, G. Blakqori, M. Minet, F. Weber, P. Staeheli, and T. Michiels.** 2006. Neurons produce type I interferon during viral encephalitis. Proc Natl Acad Sci U S A **103:**7835-40.

16. **Demoulins, T., M. L. Baron, N. Kettaf, A. Abdallah, E. Sharif-Askari, and R. P. Sekaly.** 2009. Poly (I:C) induced immune response in lymphoid tissues involves three sequential waves of type I IFN expression. Virology **386:**225-36.

17. **Doolan, A., N. Langlois, and C. Semsarian.** 2004. Causes of sudden cardiac death in young Australians. Med J Aust **180:**110-2.

18. **Duc-Goiran, P., B. Robert, S. Navarro, A. Civas, I. Cerutti, C. Rudant, M. Maury, H. Condamine, and J. Doly.** 1994. Developmental control of IFN-alpha expression in murine embryos. Exp Cell Res **214:**570-83.

19. **Esfandiarei, M., and B. M. McManus.** 2008. Molecular biology and pathogenesis of viral myocarditis. Annu Rev Pathol **3:**127-55.

20. **Foster, G. R., S. H. Masri, R. David, M. Jones, A. Datta, G. Lombardi, L. Runkell, C. de Dios, I. Sizing, M. J. James, and F. M. Marelli-Berg.** 2004. IFN-alpha subtypes differentially affect human T cell motility. J Immunol **173:**1663-70.

21. **Foster, G. R., O. Rodrigues, F. Ghouze, E. Schulte-Frohlinde, D. Testa, M. J. Liao, G. R. Stark, L. Leadbeater, and H. C. Thomas.** 1996. Different relative activities of human cell-derived interferon-alpha subtypes: IFN-alpha 8 has very high antiviral potency. J Interferon Cytokine Res **16:**1027-33.

22. **Fung, M. C., S. F. Sia, K. N. Leung, and N. K. Mak.** 2004. Detection of differential expression of mouse interferon-alpha subtypes by polymerase chain reaction using specific primers. J Immunol Methods **284:**177-86.

23. **Genin, P., R. Lin, J. Hiscott, and A. Civas.** 2009. Differential Regulation of Human Interferon-A Genes Expression by Interferon Regulatory Factor 3 and 7. Mol Cell Biol.

24. **Gobl, A. E., K. Funa, and G. V. Alm.** 1988. Different induction patterns of mRNA for IFN-alpha and -beta in human mononuclear leukocytes after in vitro stimulation with herpes simplex virus-infected fibroblasts and Sendai virus. J Immunol **140:**3605-9.

25. **Grumbach, I. M., E. N. Fish, S. Uddin, B. Majchrzak, O. R. Colamonici, H. R. Figulla, A. Heim, and L. C. Platanias.** 1999. Activation of the Jak-Stat pathway in cells that exhibit selective sensitivity to the antiviral effects of IFN-beta compared with IFN-alpha. J Interferon Cytokine Res **19:**797-801.

26. **Hardy, M. P., C. M. Owczarek, L. S. Jermiin, M. Ejdeback, and P. J. Hertzog.** 2004. Characterization of the type I interferon locus and identification of novel genes. Genomics **84:**331-45.

27. **Hata, N., M. Sato, A. Takaoka, M. Asagiri, N. Tanaka, and T. Taniguchi.** 2001. Constitutive IFN-alpha/beta signal for efficient IFN-alpha/beta gene induction by virus. Biochem Biophys Res Commun **285:**518-25.

28. **Heim, A., and S. Weiss.** 2004. Interferons in enteroviral heart disease: modulation of cytokine expression and antiviral activity. Med Microbiol Immunol **193:**149-54.

29. **Hiscott, J., K. Cantell, and C. Weissmann.** 1984. Differential expression of human interferon genes. Nucleic Acids Res **12:**3727-46.

30. **Honda, K., H. Yanai, H. Negishi, M. Asagiri, M. Sato, T. Mizutani, N. Shimada, Y. Ohba, A. Takaoka, N. Yoshida, and T. Taniguchi.** 2005. IRF-7 is the master regulator of type-I interferon-dependent immune responses. Nature **434:**772-7.

31. **Huber, S.** 2008. Host immune responses to coxsackievirus B3. Curr Top Microbiol Immunol **323:**199-221.

32. **Hughes, T. K., Jr., R. Chin, S. K. Tyring, and P. L. Rady.** 1994. Distinction of mouse interferon-alpha subtypes by polymerase chain reaction utilizing consensus primers and type-specific oligonucleotide probes. J Interferon Res **14:**117-20.

33. **Izaguirre, A., B. J. Barnes, S. Amrute, W. S. Yeow, N. Megjugorac, J. Dai, D. Feng, E. Chung, P. M. Pitha, and P. Fitzgerald-Bocarsly.** 2003. Comparative analysis of IRF and IFN-alpha expression in human plasmacytoid and monocyte-derived dendritic cells. J Leukoc Biol **74:**1125-38.

34. **Jaks, E., M. Gavutis, G. Uze, J. Martal, and J. Piehler.** 2007. Differential receptor subunit affinities of type I interferons govern differential signal activation. J Mol Biol **366:**525-39.

35. **James, C. M., M. Y. Abdad, J. P. Mansfield, H. K. Jacobsen, A. R. Vind, P. A. Stumbles, and E. J. Bartlett.** 2007. Differential activities of alpha/beta IFN subtypes against influenza virus in vivo and enhancement of specific immune responses in DNA vaccinated mice expressing haemagglutinin and nucleoprotein. Vaccine **25:**1856-67.

36. **Kawai, T., and S. Akira.** 2008. Toll-like receptor and RIG-I-like receptor signaling. Ann N Y Acad Sci **1143:**1-20.

37. **Khabar, K. S., L. Al-Haj, F. Al-Zoghaibi, M. Marie, M. Dhalla, S. J. Polyak, and B. R. Williams.** 2004. Expressed gene clusters associated with cellular sensitivity and resistance towards anti-viral and anti-proliferative actions of interferon. J Mol Biol **342:**833-46.

38. **Koerner, I., G. Kochs, U. Kalinke, S. Weiss, and P. Staeheli.** 2007. Protective role of beta interferon in host defense against influenza A virus. J Virol **81:**2025-30.

39. **Koyama, T., N. Sakamoto, Y. Tanabe, M. Nakagawa, Y. Itsui, Y. Takeda, S. Kakinuma, Y. Sekine, S. Maekawa, Y. Yanai, M. Kurimoto, and M. Watanabe.** 2006. Divergent activities of interferon-alpha subtypes against intracellular hepatitis C virus replication. Hepatol Res **34:**41-9.

40. **Kuhl, U., M. Pauschinger, W. Poller, and H. P. Schultheiss.** 2006. Anti-viral treatment in patients with virus-induced cardiomyopathy. Ernst Schering Res Found Workshop**:**323-42.

41. **Kuhl, U., M. Pauschinger, P. L. Schwimmbeck, B. Seeberg, C. Lober, M. Noutsias, W. Poller, and H. P. Schultheiss.** 2003. Interferon-beta treatment eliminates cardiotropic viruses and improves left ventricular function in patients with myocardial persistence of viral genomes and left ventricular dysfunction. Circulation **107:**2793-8.

42. **Lai, M. C., W. S. Yeow, S. J. Boyer, and M. W. Beilharz.** 1994. Differential expression patterns of type I interferon subtypes in mouse embryo fibroblasts: influence of genotype and viral inducer. Antiviral Res **24:**327-40.

43. **Larrea, E., R. Aldabe, J. I. Riezu-Boj, A. Guitart, M. P. Civeira, J. Prieto, and E. Baixeras.** 2004. IFN-alpha5 mediates stronger Tyk2-stat-dependent activation and higher expression of 2',5'-oligoadenylate synthetase than IFN-alpha2 in liver cells. J Interferon Cytokine Res **24:**497-503.

44. **Lenzo, J. C., J. P. Mansfield, S. Sivamoorthy, V. S. Cull, and C. M. James.** 2003. Cytokine expression in murine cytomegalovirus-induced myocarditis: modulation with interferon-alpha therapy. Cell Immunol **223:**77-86.

45. **Lienenklaus, S., R. Walisko, A. te Boekhorst, T. May, C. Samuelsson, T. Michiels, and S. Weiss.** 2008. PCR-based simultaneous analysis of the interferon-alpha family reveals distinct kinetics for early interferons. J Interferon Cytokine Res **28:**653-60.

46. **Loseke, S., E. Grage-Griebenow, A. Wagner, K. Gehlhar, and A. Bufe.** 2003. Differential expression of IFN-alpha subtypes in human PBMC: evaluation of novel real-time PCR assays. J Immunol Methods **276:**207-22.

47. **Marie, I., J. E. Durbin, and D. E. Levy.** 1998. Differential viral induction of distinct interferon-alpha genes by positive feedback through interferon regulatory factor-7. Embo J **17:**6660-9.

48. **Miric, M., J. Vasiljevic, M. Bojic, Z. Popovic, N. Keserovic, and M. Pesic.** 1996. Long-term follow up of patients with dilated heart muscle disease treated with human leucocytic interferon alpha or thymic hormones initial results. Heart **75:**596-601.

49. **Mitani, Y., A. Takaoka, S. H. Kim, Y. Kato, T. Yokochi, N. Tanaka, and T. Taniguchi.** 2001. Cross talk of the interferon-alpha/beta signalling complex with gp130 for effective interleukin-6 signalling. Genes Cells **6:**631-40.

50. **Montoya, M., G. Schiavoni, F. Mattei, I. Gresser, F. Belardelli, P. Borrow, and D. F. Tough.** 2002. Type I interferons produced by dendritic cells promote their phenotypic and functional activation. Blood **99:**3263-71.

51. **Muller, U., U. Steinhoff, L. F. Reis, S. Hemmi, J. Pavlovic, R. M. Zinkernagel, and M. Aguet.** 1994. Functional role of type I and type II interferons in antiviral defense. Science **264:**1918-21.

52. **Prakash, A., E. Smith, C. K. Lee, and D. E. Levy.** 2005. Tissue-specific positive feedback requirements for production of type I interferon following virus infection. J Biol Chem **280:**18651-7.

53. **Puranik, R., C. K. Chow, J. A. Duflou, M. J. Kilborn, and M. A. McGuire.** 2005. Sudden death in the young. Heart Rhythm **2:**1277-82.

54. **Riego, E., A. Perez, R. Martinez, F. O. Castro, R. Lleonart, and J. de la Fuente.** 1995. Differential constitutive expression of interferon genes in early mouse embryos. Mol Reprod Dev **41:**157-66.

55. **Sadler, A. J., and B. R. Williams.** 2008. Interferon-inducible antiviral effectors. Nat Rev Immunol **8:**559-68.

56. **Sato, M., N. Hata, M. Asagiri, T. Nakaya, T. Taniguchi, and N. Tanaka.** 1998. Positive feedback regulation of type I IFN genes by the IFN-inducible transcription factor IRF-7. FEBS Lett **441:**106-10.

57. **Schanen, C., V. Chieux, P. E. Lobert, J. Harvey, and D. Hober.** 2006. Correlation between the anti-virus-induced cytopathic effect activity of interferon-alpha subtypes and induction of MxA protein in vitro. Microbiol Immunol **50:**19-24.

58. **Schiff, L. A., M. L. Nibert, and K. L. Tyler.** 2007. Orthoreoviruses and their replication, p. 1853-1915. *In* D. M. Knipe and P. M. Howley (ed.), Fields virology, 5th ed, vol. 2. Lippincott Williams & Wilkins, Philadelphia, PA.

59. **Sherry, B., C. J. Baty, and M. A. Blum.** 1996. Reovirus-induced acute myocarditis in mice correlates with viral RNA synthesis rather than generation of infectious virus in cardiac myocytes. J Virol **70:**6709-15.

60. **Sherry, B., J. Torres, and M. A. Blum.** 1998. Reovirus induction of and sensitivity to beta interferon in cardiac myocyte cultures correlate with induction of myocarditis and are determined by viral core proteins. J Virol **72:**1314-23.

61. **Smith, R. E., H. J. Zweerink, and W. K. Joklik.** 1969. Polypeptide components of virions, top component and cores of reovirus type 3. Virology **39:**791-810.

62. **Steinman, R. M., and H. Hemmi.** 2006. Dendritic cells: translating innate to adaptive immunity. Curr Top Microbiol Immunol **311:**17-58.

63. **Stewart, M. J., K. Smoak, M. A. Blum, and B. Sherry.** 2005. Basal and reovirus-induced beta interferon (IFN-beta) and IFN-beta-stimulated gene expression are cell type specific in the cardiac protective response. J Virol **79:**2979-87.

64. **Stille-Siegener, M., A. Heim, and H. R. Figulla.** 1995. Subclassification of dilated cardiomyopathy and interferon treatment. Eur Heart J **16 Suppl O:**147-9.

65. **Swaminathan, N., C. M. Lai, M. W. Beilharz, S. J. Boyer, and S. P. Klinken.** 1992. Biological activities of recombinant murine interferons alpha 1 and alpha 4: large difference in antiproliferative effect. Antiviral Res **19:**149-59.

66. **Takaoka, A., Y. Mitani, H. Suemori, M. Sato, T. Yokochi, S. Noguchi, N. Tanaka, and T. Taniguchi.** 2000. Cross talk between interferon-gamma and -alpha/beta signaling components in caveolar membrane domains. Science **288:**2357-60.

67. **Tovey, M. G., M. Streuli, I. Gresser, J. Gugenheim, B. Blanchard, J. Guymarho, F. Vignaux, and M. Gigou.** 1987. Interferon messenger RNA is produced constitutively in the organs of normal individuals. Proc Natl Acad Sci U S A **84:**5038-42.

68. **van Boxel-Dezaire, A. H., M. R. Rani, and G. R. Stark.** 2006. Complex modulation of cell type-specific signaling in response to type I interferons. Immunity **25:**361-72.

69. **Van Heuvel, M., I. J. Bosveld, A. A. Mooren, J. Trapman, and E. C. Zwarthoff.** 1986. Properties of natural and hybrid murine alpha interferons. J Gen Virol **67 (Pt 10):**2215-22.

70. **van Pesch, V., H. Lanaya, J. C. Renauld, and T. Michiels.** 2004. Characterization of the murine alpha interferon gene family. J Virol **78:**8219-28.

71. **Wang, Y. X., V. da Cunha, J. Vincelette, K. White, S. Velichko, Y. Xu, C. Gross, R. M. Fitch, M. Halks-Miller, B. R. Larsen, T. Yajima, K. U. Knowlton, R. Vergona, M. E. Sullivan, and E. Croze.** 2007. Antiviral and myocyte protective effects of murine interferon-beta and -{alpha}2 in coxsackievirus B3-induced myocarditis and epicarditis in Balb/c mice. Am J Physiol Heart Circ Physiol **293:**H69-76.

72. **Whitton, J. L.** 2002. Immunopathology during coxsackievirus infection. Springer Semin Immunopathol **24:**201-13.

73. **Woelk, C. H., S. D. Frost, D. D. Richman, P. E. Higley, and S. L. Kosakovsky Pond.** 2007. Evolution of the interferon alpha gene family in eutherian mammals. Gene **397:**38-50.

74. **Woodruff, J. F.** 1980. Viral myocarditis. A review. Am J Pathol **101:**425-84.

75. **Yeow, W. S., C. M. Lawson, and M. W. Beilharz.** 1998. Antiviral activities of individual murine IFN-alpha subtypes in vivo: intramuscular injection of IFN expression constructs reduces cytomegalovirus replication. J Immunol **160:**2932-9.

76. **Zoumbos, N. C., P. Gascon, J. Y. Djeu, and N. S. Young.** 1985. Interferon is a mediator of hematopoietic suppression in aplastic anemia in vitro and possibly in vivo. Proc Natl Acad Sci U S A **82:**188-92.

77. **Zurney, J., K. E. Howard, and B. Sherry.** 2007. Basal expression levels of IFNAR and Jak-STAT components are determinants of cell-type-specific differences in cardiac antiviral responses. J Virol **81:**13668-80.

Table 2.1. Primers for subtype-specific detection of IFN-α [1]

IFN-α subtype [2]	Accession No. [3]		Primer sequence (5' → 3')	Product size
IFN-α1 BALB/c	X01974	Forward	TAATTCCTACGTCTTTTCTTT	81
		Reverse	TATGCCTGATCCCTGAACAGT	
IFN-α1 129/Sv	NM_010502	Forward	TGAAGGACAGGAAGGACTTTG	167
		Reverse	GAATGAGTCTAGGAGGGTTGT	
IFN-α2 BALB/c	X01969	Forward	TTGAAGGTCCTGGCACAG	160
		Reverse	GAGGTTCAAGGTCTGCTGA	
IFN-α4 BALB/c	X01973	Forward	GCAGAAGTCTGGAGAGCCCTC	122
		Reverse	TGAGATGCAGTGTTCTGGTCC	
IFN-α5 BALB/c	X01971	Forward	CTCAAAGCCTGTGTGATGCAA	123
		Reverse	GTGTTTCTTCTCTCTCAGGTA	
IFN-α6T 129/Sv	AY220465	Forward	CCCTGAAGATCCAGAAAGAGA	118
		Reverse	GTATCTAGGAGGGTTGCATCC	
IFN-α7 C57BL/6	AY225952	Forward	CATCTGCTGCTTGGGATGGAT	125
		Reverse	TTCCTGGGTCAGAGGAGGTTC	
IFN-α7/10 Swiss	M13710	Forward	AGGTGGGGGTGCAGGAACTTT	97
		Reverse	TTCTTCTCTCTCAGGAACACA	
IFN-α8/6 C57BL/6	AY225953	Forward	TCATAACCTCAGGAACAAGAA	81
		Reverse	TCCACCTTCTCCAAGGGGAAT	
IFN-α8/6 BALB/c	X01972	Forward	CTCATTACCTTCAGTGTGAAC	93
		Reverse	AGATACAAAAGTGGCTATACA	
IFN-α9 BALB/c	M13660	Forward	CCTGACCCAGGAAGACTCCCA	114
		Reverse	ACTTCTGCTCTGACCACCTCC	
IFN-α11 Swiss	M68944	Forward	GAGAAGAGATCAAGAAAAATG	111
		Reverse	TCCCAGGACTGGCTTATGAGG	
IFN-α12 C57BL/6	NM_177361	Forward	CAGCAGGTGGGGGTGCAGGAG	102
		Reverse	TTTCTTCTCTCTCAGGTACAC	
IFN-α13 C57BL/6	AY190047	Forward	GGTGGTCAGAGCAGAAGTCCA	112
		Reverse	GTTCAGAAGAGTCCTCTCCAC	
IFN-α14 129/Sv	AY220462	Forward	TTCTGCAATGACCTCAACACT	119
		Reverse	AAGTATTTCCTCACAGCCAGC	

[1] Genomic DNA from Cr:NIH(S) mice was subjected to qRT-PCR using the indicated primer pairs. Single peaks in a standard melt-curve analysis indicated amplification of a single product.
[2] Mouse strains used for sequence information are as indicated.
[3] Many sequences / accession numbers are as originally suggested in van Pesch et al., 2004.

A.

IFN-α Subtype	Sequence alignment to detect IFN-α4
IFN-α1 BALB/c	GAGCCCTGTCTTCCTC**TG**CCAA**T**GTGCTGGGAAGACTGAGAGAAGAGAAATGA
IFN-α2 BALB/c	GAGCCCTGTCTTCCTCA**GT**CAACTTGCTGCCAAGACTGAGTGAAGAGAAGGAG
IFN-α4 BALB/c	***gagccctgtcttcct*CAACCAAC**TTGCTGGCAAGACTGAGTGAGGAGAAGGAG
IFN-α5 BALB/c	GAGCCCTGTCTTCCTCA**GTT**AACTTGCTGGCAAGATTGAGCAAGGAGGAGTGA
IFN-α6T 129/Sv	GAGCCCTGTCTTCCTC**TG**CCAA**T**GTGCTGGGAAGACTGAGAGAAGAGAAATGA
IFN-α7 C57BL/6	GAGCCCTGTCTTCCTCA**G**CCAA**G**TTGCTGGCAAGATTGAGTGAGAAGAAGGAG
IFN-α8/6 BALB/c	GAGCCCTGTCTTCCTCA**G**CCAA**G**TTGCTGGCAAGACTGAATGAGGACGAGTGA
IFN-α8/6 C57BL/6	GAGCCCTGTCTTCCTCA**G**CCAA**G**TTGCTGGCAAGACTGAGTGAGGACGAGTGA
IFN-α9 BALB/c	GAGCCCTGTCTTCCTCA**GTT**AACTTGCTGGCAAGACTGAGTGAGGAGAAG-GA
IFN-α11 Swiss	GAGCCCTGTCTTCCTCA**GTT**AACTTGCTGGCAAGATTGAGTGAAGAGAAGGCT
IFN-α12 C57BL/6	GAACCCTGTCTTCCTCA**G**CT**A**A**G**TTGCTGGCAAGACTGAGTGAGAAGGAGTGA
IFN-α13 C57BL/6	GAACCCTGTCTTCCTCA**G**CCAACTTGCTGGCAAGACTGAGCAAGGAGGAGTGA
IFN-α14 129/Sv	GAGCCCTGTCTTCCTCA**G**CCAA**G**TTGCTGACCAGCCTGAAAGAAGAGAAGTGA

B.

IFN-α Subtype	Sequence alignment to detect IFN-α5
IFN-α1 BALB/c	GCTCAATGACCTGCAAGGCTGTCTGATGCAGCAGGT**G**GGGGTGCAGGAATTTC
IFN-α2 BALB/c	GCTCAATGACCTGCAAACCTGTCTGATGCAGCAGGT**G**GGGGTGCAGGAACCTC
IFN-α4 BALB/c	GCTCAATGATCTCAAAGCCTGTGTGATGCAG----------GAACCTC
IFN-α5 BALB/c	GCTCAATGACCTCAA***agcctgtgtgatgcaacagg*TCGGGGTGCA**GGAATCTC
IFN-α6T 129/Sv	GCTCAATGACCTGCAAGCCTGTCTAGTGCAGCAGGT**GA**GG**T**GCAGGAACCTC
IFN-α7 C57BL/6	GCTCAATGACCTGCAAGGCTGTCTGATGCAGCAGGT**G**GGGGTGCAGGAACCTC
IFN-α8/6 BALB/c	GCTCAATGACCTGCAAGGCTGTCTGATGCAGCAGGT**A**G**A**GA**T**ACAGGCACTTC
IFN-α8/6 C57BL/6	GCTCAATGACCTCAAAGCCTGTGTGATGCAGGAGGT**G**GGGGTGCAGGAATCTC
IFN-α9 BALB/c	GCTCAATGACCTGCAAGGCTGTCTGATGCAGCTGGTCGGG**A**TG**A**AGGAACTGC
IFN-α11 Swiss	GCTCAATGACCTGCAAGGCTGTCTGATGCAGCAGGT**G**GGGGTGCAGGAACCTC
IFN-α12 C57BL/6	GCTCAATGACCTGCAAGGCTGTCTGATGCAGCAGGT**G**GGGGTGCAGGAGCCTC
IFN-α13 C57BL/6	GCTCAATGACCTCAAAGCTTGTCTGATGCAGCAGGTT**G**GGGTGCAGGAATTTC
IFN-α14 129/Sv	GCTCAATGACCTGCAAGGCTGTCTGATGCAGCAGGT**A**G**A**GA**T**ACAGGCACCTC

C

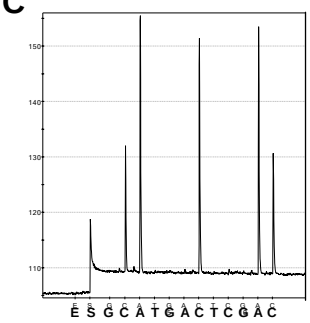

D

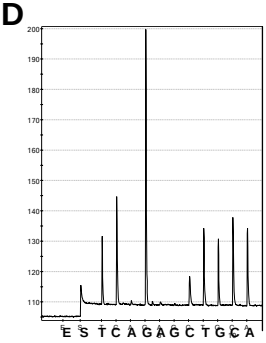

Figure 2.1. Pyrosequencing confirmation of IFN-α products. The indicated IFN-α sequences (accession numbers provided in Table 1) were aligned by ClustalW2. Regions recognized by pyrosequencing primers for IFN-α4 (A) and -α5 (B) are indicated. Bold italic lower case indicates primer sequences, bold uppercase (unshaded) indicates the region sequenced for each product, and bold shaded uppercase indicates IFN-α subtype-specific sequence polymorphisms. Representative spectra using primers specific for IFN-α4 (C) and -α5 (D) are provided. The nucleotides provided during successive pyrosequencing cycles are indicated on the X axis, and sequence is interpreted from the height of the peak. For example, in (C), following the E (enzyme) and S (substrate), the sequence is C (single peak), AA (double peak, specific for IFN-α4), no T (indicating no IFN-α2, -α5, -α9, -α11 or -α12), no G, no A, CC (double peak), no T, no C, no G, AA (double peak), C (indicating no IFN-α1, -α6T, -α7, -α8/6, -α12, or α-14).

Table 2.2. Reovirus T3D induction of IFN-α is subtype-specific in primary cardiac myocyte and cardiac fibroblast cultures [1]

IFN-α Subtype [2]	Induction [3]		IFN-α Subtype [2]	Induction [3]
IFN-α1 BALB/c	√		IFN-α8/6 BALB/c	√
IFN-α1 129/Sv	√		IFN-α8/6 C57BL/6	× [4]
IFN-α2 BALB/c	√		IFN-α9 BALB/c	×
IFN-α4 BALB/c	√		IFN-α11 Swiss	×
IFN-α5 BALB/c	√		IFN-α12 C57BL/6	×
IFN-α6T 129/Sv	×		IFN-α13 C57BL/6	×
IFN-α7/10 Swiss	×		IFN-α14 129/Sv	×
IFN-α7 C57BL/6	×			

[1] Primary cardiac myocyte and cardiac fibroblast cultures were infected with reovirus T3D at an moi of 10 pfu per cell. Total cell RNA was extracted 8 hours post-infection and results from qRT-PCR using the indicated primer pairs in at least two independent experiments are summarized here.
[2] Primers are as indicated in Table 2.1.
[3] A single peak by standard melt-curve analysis and >2-fold change relative to mock-infected cultures were together considered evidence of IFN-α induction (√); absence of an identifiable peak or <2-fold change were interpreted as insignificant IFN-α induction (×).
[4] While IFN-α8/6 BALB/c primers indicated induction by T3D infection, IFN-α8/6 C57BL/6 primers did not, despite both recognizing Cr:NIH(S) genomic DNA (Table 1). Possible mouse strain-specific sequence polymorphisms within the primer-binding region could have allowed detection of IFN-α8/6 genomic DNA but not mRNA given its relatively low copy number (Figure 2.1).

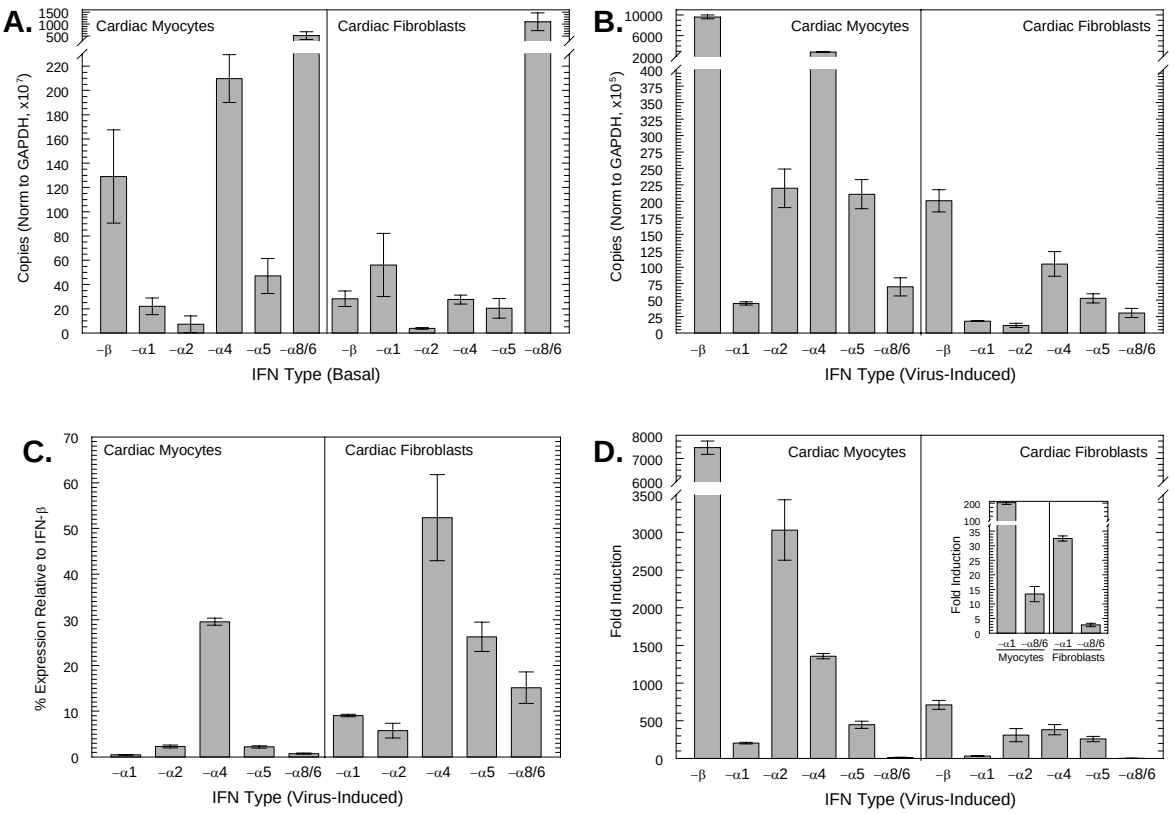

Figure 2.2. Basal and reovirus T3D-induced expression of IFN-α is subtype- and cell type-specific in cardiac cells. Primary cardiac cell cultures were mock-infected or infected with reovirus T3D at an moi of 10 pfu per cell. Total cell RNA was extracted from replicate culture wells at 8 hours post-infection for qRT-PCR. Copy number for each gene of interest was normalized to GAPDH, and then further normalized to compensate for differences in GAPDH expression between cardiac myocytes and cardiac fibroblasts. Results are the mean of replicate samples ± SEM, and are representative of two (A) or three (B) independent experiments. (A) Basal expression in mock-infected cultures. (B) T3D-induced expression. (C) T3D-induced expression for each IFN-α subtype relative to IFN-β in that cell type (calculated from panel B). (D) Fold induction, calculated from data in panels (A) and (B). Inset presents a subset of the same data on an amplified scale.

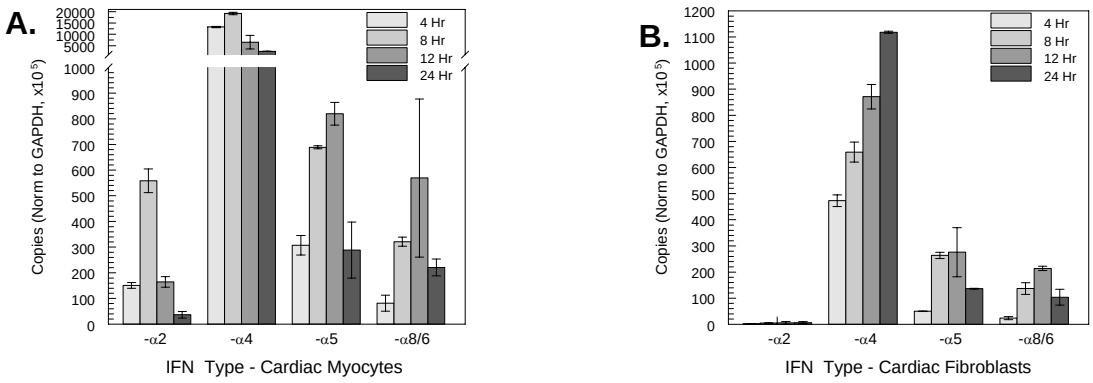

Figure 2.3. Peak time of IFN-α induction by reovirus T3D is cell type- and subtype-specific. Primary cardiac cell cultures were infected as for Figure 2. Total cell RNA was extracted from replicate culture wells at the indicated time post-infection for qRT-PCR, and analyzed as for Figure 2. Results are the mean of replicate samples ± SEM, and are representative of three independent experiments. (A) Cardiac myocyte cultures. (B) Cardiac fibroblast cultures.

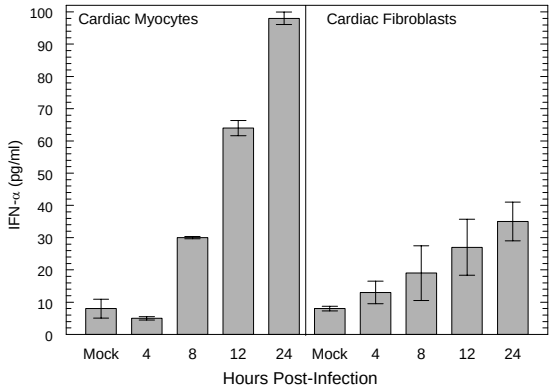

Figure 2.4. Reovirus T3D induction of secreted IFN-α is cell type-specific. Primary cardiac cell cultures were infected as for Figure 2, and supernatants from duplicate wells were harvested at 4, 8, 12 and 24 hours post infection for quantification of secreted total IFN-α by ELISA. Data are expressed as mean ± SD.

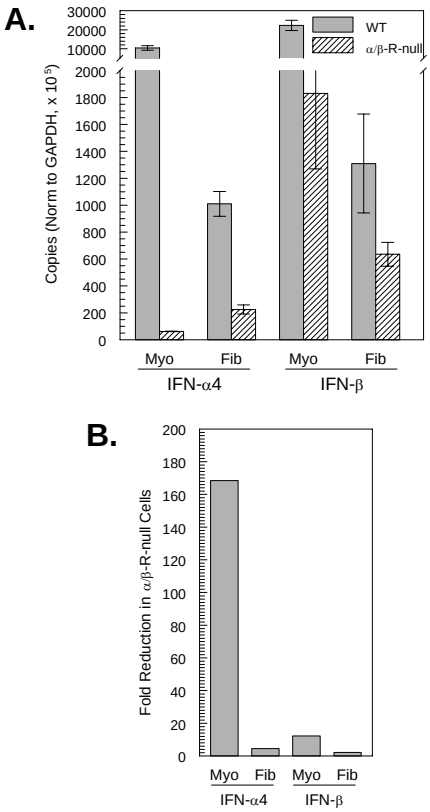

Figure 2.5. The role of IFN-mediated amplification in T3D induction of Type I IFN is cell type-specific. Primary cardiac cell cultures were generated from IFN-α/β-receptor-null and wild-type mice. Cultures were infected and RNA was harvested and analyzed as for Figure 2. (A) Results are the mean of duplicate samples from each of two experiments ± SEM. (B) Results in (A) from wild-type cells were divided by those from IFN-α/β-receptor-null cells.

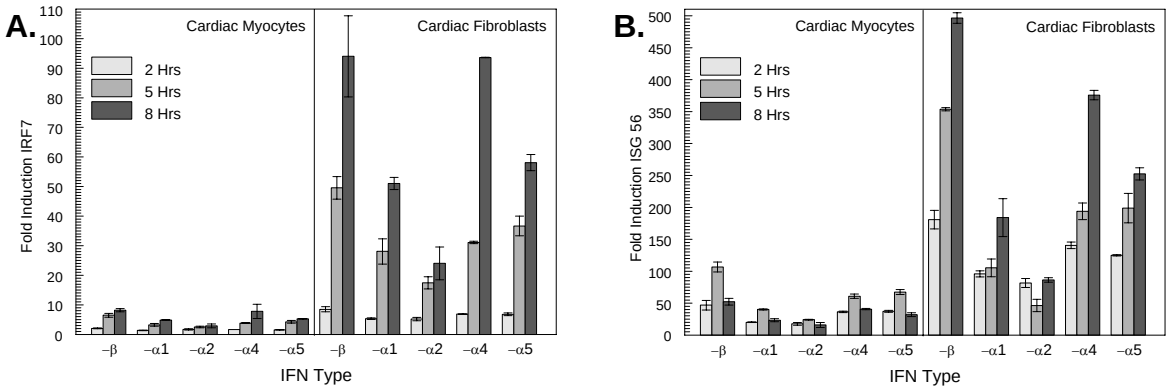

Figure 2.6. IFN-α induction of ISG mRNA is subtype- and cell type-specific. Primary cardiac cell cultures were treated with media or 1000 U/ml of the indicated IFN type, and RNA was harvested at the indicated time post-treatment for qRT-PCR analysis. Copy number for each sample was normalized to GAPDH expression, and then divided by copy number in replicate media-treated cultures harvested at the same time to calculate fold induction. Results are expressed as the mean of duplicate samples ± SD, and are representative of three independent experiments. (A) IRF7 expression. (B) ISG 56 expression.

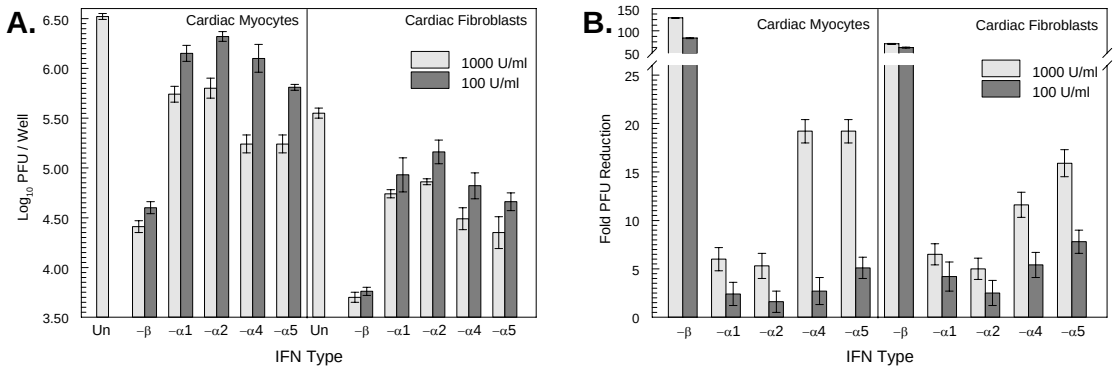

Figure 2.7. Reovirus T3D sensitivity to IFN-α is subtype-specific in cardiac cells. Primary cardiac myocyte cultures and primary cardiac fibroblast cultures were treated with IFN-α1, -α2, -α4, -α5 or -β at 100 or 1000 U/ml, incubated for 24 hours, challenged with reovirus T3D at an moi of 10 pfu per cell, and then incubated an additional 20 hours. Viral titers were determined by plaque assay (Figure 8A, expressed as mean ± SD from triplet samples), and fold inhibition by IFN treatment was determined (Figure 8B, expressed as IFN-treated relative to mock-treated samples). Results are representative of two independent experiments. In each cell type at 1000 U/ml, relative inhibition of viral titers were IFN-β > α5 = α4 > α2 = α1 ($P < 0.05$).

CHAPTER 3

Proteomic analysis reveals virus-specific Hsp25 modulation during the cardiac myocyte antiviral response

Lianna Li[1], Joel Sevinsky[2], James L. Stephenson, Jr.[2], Barbara Sherry[1]

[1] Dept. of Molecular Biomedical Sciences, North Carolina State University, Raleigh NC 27606

[2] Proteomics Research Group, Research Triangle Institute, Research Triangle Park, NC 27709

Manuscript in preparation

ABSTRACT

Viruses frequently infect the heart but clinical myocarditis is rare, suggesting that the cardiac antiviral response is uniquely effective. Indeed, the Type I interferon (IFN) response is cardiac cell type-specific and provides one integrated network of protection for the heart. Here, a proteomic approach was used to identify additional proteins that may be involved in the cardiac antiviral response. Reovirus-induced murine myocarditis reflects direct viral apoptotic damage to cardiac cells, and offers an excellent system for study. Primary cultures of murine cardiac myocytes were infected with myocarditic or non-myocarditic reovirus strains, and whole cell lysates were compared by two-dimensional difference gel electrophoresis (2D-DIGE) and matrix absorption laser desorption ionization-time of flight-time of flight (MALDI-TOF-TOF) mass spectrometry. Results were quantitative and reproducible, and demonstrated that whole proteome changes clustered according to viral pathogenic phenotype. Moreover, results suggest that the heat shock protein Hsp25 is modulated differentially by myocarditic and non-myocarditic reoviruses and may play a role in the cardiac antiviral response. Members of seven virus families modulate Hsp25 or Hsp27 expression in a variety of cell types, suggesting that Hsp25 participation in the antiviral response may be widespread. However, results here provide the first evidence for a virus-induced decrease in Hsp25/27, and suggest that viruses may have evolved a mechanism to subvert this protective response, as they have for IFN.

INTRODUCTION

Viruses are the most common pathogen causing myocarditis, with random autopsies suggesting that between 5 and 20% of the population has suffered a viral infection in the heart (14, 22, 89). While most cases are asymptomatic, myocarditis is frequently fatal in infants, and adult infections can progress to dilated cardiomyopathy requiring heart transplantation [22, 54]. Moreover, greater than 50% of sudden deaths in young adults are due to cardiac causes with greater than 10% of those due to myocarditis (20, 65). While immune-mediated pathology can occur, immunosuppressive therapy is not beneficial (52), suggesting that most damage reflects direct viral cytopathic effect (CPE). Most virus families have been implicated in human viral myocarditis, with adenoviruses and coxsackieviruses indicated most often (9, 50). However, coxsackieviruses induce both direct and immune-mediated pathology in mice (36), and adenovirus-induced myocarditis remains poorly studied in an animal model (7). In contrast, reovirus-induced myocarditis in neonatal mice involves only direct viral CPE reflecting virus-induced apoptosis, providing a well-characterized model system for study (4, 16, 17, 57, 74, 75).

Virus-induced pathology is particularly problematic in the heart because only 1% of cardiac myocytes are renewed in the average human lifetime (6). While the blood-brain barrier protects the similarly vulnerable central nervous system from pathogens, there is no identifiable cell architecture protecting the heart. Instead, it is likely that cardiac cells have evolved uniquely effective innate responses to limit virus spread through the heart until

immune cells can react. Indeed, the cytokine IFN-β is a determinant of protection against reovirus-induced murine myocarditis (76). That is, virus strain-specific differences in the capacity to induce myocarditis correlate with differences in viral induction of IFN-β and viral sensitivity to the antiviral effects of IFN-α/β in primary cultures of cardiac myocytes. Moreover, a non-myocarditic reovirus induces cardiac lesions in mice lacking IFN-α/β function (76). It seems unlikely, however, that the heart would have evolved only a single antiviral strategy given its constant exposure to viral pathogens. To identify additional proteins that may be involved in the cardiac antiviral response, a proteomic approach was used here to compare cardiac myocyte responses to infection with myocarditic and non-myocarditic reoviruses. Assessing primary cardiac myocyte cultures rather than hearts from infected mice ensured measurement of the innate cardiac myocyte response rather than that of a mix of cardiac and inflammatory cells.

While microarray technology offers an excellent tool to compare mRNA levels between samples, the prevalence of post-transcriptional regulation in eukaryotic cells precludes accurate predictions about final protein expression. Accordingly, proteomic approaches have become increasingly popular and have provided a useful catalog of cardiac protein expression (24) and (37) and (24, 55). Two-dimensional difference gel electrophoresis (2D-DIGE) (83) is a powerful tool that builds on traditional 2D polyacrylamide gel electrophoresis (2DE), which provided one of the earliest methods to separate closely-related proteins (31, 60). Indeed, 2D-DIGE has been used to investigate differences between healthy and diseased hearts for a number of conditions, however none have examined viral infections and none have investigated purified cardiac myocytes (18, 33,

53, 56, 61, 69). The two major strengths of 2DE are that it allows both separation of thousands of proteins simultaneously and identification of post-translational modifications. In particular, the use of intermediate ranges of pH gradients (i.e. pH 4 to 7 or 6 to 9) in the isoelectric focusing (IEF) dimension of the gel greatly enhances separation of proteins which would otherwise co-migrate in a traditional 2D gel (ph 3 to 10). In 2D-DIGE, proteins are labeled with fluorescent cyanine (Cy) dyes before electrophoresis, to both increase the sensitivity and broaden the dynamic range of protein quantification (84, 90). Because proteins are labeled after cells are harvested, there is no risk of perturbing the cell environment and affecting cell responses. Moreover, labeling samples from different treatments with Cy3 and Cy5 and labeling a pool of multiple samples with Cy2 as an internal control allows quantitative comparison among an unlimited number of samples on different gels (1). Once gel spots are selected, they are proteolytically digested and analyzed by tandem mass spectrometry (MS/MS) for protein identification (86).

Studies here demonstrate that 2D-DIGE analysis of primary cardiac myocyte cultures provides quantitative and reproducible results, and that proteome changes cluster according to viral pathogenic phenotype. Moreover, results suggest that the heat shock protein Hsp25 is modulated differentially by myocarditic and non-myocarditic reoviruses and may play a role in the cardiac antiviral response.

RESULTS

2D-DIGE analysis. The four reoviruses selected for comparison are comprised of

two prototypes strains (T1L and T3D (71)), a potently myocarditic reassortant virus generated in vivo during a mixed infection with T1L and T3D (8B (75)), and a non-myocarditic reassortant virus derived from 8B (DB93A (73)) (Table 3.1). Together, they allow comparisons relating to both viral myocarditic potential and viral induction of IFN-β. A preliminary experiment comparing mock- and T3D-infected cultures at 8, 12 and 18 hours post-infection indicated that the greatest differences between mock- and virus-infected cultures were captured at 12 hours post-infection (data not shown), and therefore this single time-point was selected for further 2D-DIGE studies. Triplicate lysates from mock- or virus-infected primary cardiac myocyte cultures were labeled and electrophoresed with an internal control on a total of 8 gels (Figure 3.1 and Supp Table 3.1). The scanned 2D-DIGE gel images were analyzed using DeCyder 2D Software with exclusion filters set manually. The total number of protein spots detected on the 8 gels ranged from 5,617 to 7,408 per gel, with the master gel selected as the one with the greatest number of protein spots. A total of 3,000 protein spots were selected for comparisons based on their abundance exceeding a filter-set threshold, and 197 differentially expressed protein spots were detected in the EDA module with One-Way ANOVA and $P < 0.01$ as the threshold.

Principle component analysis (PCA), which is a statistical method to eliminate redundant variables and reduce data complexity, was performed on the 197 differentially expressed proteins (Figure 3.2). Triplicate samples for each infection were tightly clustered, indicating high reproducibility between primary cardiac myocyte culture wells and between gels. Reovirus-infected samples were most distantly segregated from mock-infected samples. The two viruses that induce IFN-β poorly (T1L and DB93A) were clustered closely. The two

other viruses, 8B and T3D, were segregated by myocarditic potential. Thus, global proteome changes correlated well with viral phenotypes.

Protein identification by MALDI-TOF-TOF and pathway analysis. The 3000 protein spots were re-analyzed by One-way Anova at a lower threshold of significance ($P < 0.05$) to increase the pool of proteins for subsequent analyses. This identified 227 differentially expressed protein spots, which were then picked for identification by MALDI-TOF-TOF and database searches. Of the 227 protein spots, 194 achieved a score higher than 64 in the Swiss-Prot database or 60 in the IPI database, and 124 of those corresponded to unique proteins (rather than hypothetical proteins or post-translational modifications of the same protein). Proteins fell into many groupings, based on whether they were up-regulated or down-regulated in viral infections, and whether accumulation was virus strain-specific or segregated by previously characterized viral phenotypes (e.g. induction of IFN, or induction of myocarditis). Supp Table 3.2 provides an example of proteins that are uniquely altered in T3D-infected cultures, 8B-infected cultures, or both, and groups them by biological function. Not surprisingly, the number of biological functions altered by both viruses is much greater than the number altered by just one virus.

The 124 differentially expressed proteins also participate in diverse pathways, including those for calcium signaling, ERK/ MAPK signaling, protein ubiquitination, mitochondrial dysfunction, oxidative stress, and amino acid metabolism (data not shown). Of interest, the potently myocarditic reovirus 8B uniquely modulated proteins involved in mitochondrial dysfunction, endoplasmic reticulum stress, and phospholipid degradation, consistent with this virus' extreme cytopathogenicity.

Analysis of post-translational modifications identifies Hsp25 phosphorylation. We found 18 cases where a single protein was identified in multiple spots with the same molecular weight but different pIs, suggestive of post-translational modifications. One of these proteins was Hsp25, the mouse homolog of human Hsp27 (Supp. Figure 3.1). Three gel spots were identified as this protein by extremely high scores from searches of the Swiss-Prot and IPI databases (459, 388 and 359 on Swiss-Prot, and 461, 389 and 361 on IPI). Each gel spot included high coverage for Hsp25 by peptide mass fingerprinting, and included sufficient MS-MS data for sequence confirmation (Supp. Tables 3.3 – 3.5). By comparing the pool of un-matched peptide masses to Hsp25 theoretical peptide masses using Protein Prospector, two un-matched peptides were identified as potentially phosphorylated (Supp. Tables 3.4, 3.5). The predicted mono-phosphorylated peptide was absent from the most basic spot but present in the two more acidic spots, as would be predicted for successive phosphorylation. And, as would be expected, the potentially di-phosphorylated peptide was present in only the most acidic spot. Moreover, phosphorylation predictive software (NetPhos 2.0 Server) suggested phosphorylation of Hsp25 on those two peptides; on serine-15 (ser15), corresponding to the novel peptide in both mono- and di-phosphorylated Hsp25, and on ser86, corresponding to the novel peptide found only in di-phosphorylated Hsp25. Importantly, these two Hsp25 residues have previously been reported to be phosphorylated by various stimuli (28, 80). Western blot analyses confirmed these gel spot identifications (see below).

Quantification and confirmation of Hsp25. Protein abundance was determined for the predicted unphosphorylated, mono-phosphorylated and di-phosphorylated Hsp25 gel

spots (Figure 3.3). Unphosphorylated Hsp25 was most abundant in mock-infected samples ($P < 0.03$ to 0.001) and least abundant in 8B-infected samples ($P < 0.01$ to 0.002, Figure 3.3A). Unphosphorylated Hsp25 was also less abundant in T3D- relative to DB93A- and T1L-infected samples ($P < 0.02$). One simple interpretation is that viral infection stimulates phosphorylation of Hsp25 resulting in decreased unphosphorylated Hsp25, and that the extent of phosphorylation is virus-specific. Indeed, di-phosphorylated Hsp25 was more abundant in reovirus- than mock-infected samples ($P < 0.028$ to 0.001 for the four viruses), and was more abundant in cultures infected with than non-myocarditic (T3D, DB93A) than myocarditic (8B, T1L) viruses (Figure 3.3C, $P < 0.02$ for each of the four comparisons). Finally, mono-phosphorylated Hsp25 was similar between mock- and virus-infected cultures consistent with efficient further phosphorylation to the di-phosphorylated state, except for 8B ($P < 0.04$, Figure 3.3B). The lower unphosphorylated and mono-phosphorylated Hsp25 in 8B-infected cultures without a corresponding increase in di-phosphorylated Hsp25 suggested that this potently myocarditic virus might induce degradation of Hsp25, or reduce its synthesis or stability.

In order to confirm protein identifications, primary cardiac myocyte cultures were infected as for 2D-DIGE and lysates were electrophoresed and probed by Western blot (Figure 3.4A). Antisera recognizing total Hsp25 confirmed Hsp25 expression in cardiac myocytes, and confirmed that total Hsp25 was least abundant in 8B-infected cultures. Since this antibody recognizes both unphosphorylated and phosphorylated Hsp25, it is not surprising that relative Hsp25 levels here were not the same as those for unphosphorylated Hsp25 by 2D-DIGE (Figure 3.3). Antisera specific for Hsp25 phosphorylated on ser15 and

ser86 confirmed virus-induced phosphorylation for each of those residues. Moreover, Hsp25-ser86-P levels were greater for all four virus- relative to mock-infections, consistent with 2D-DIGE results for di-phosphorylated Hsp25 (Figure 3.3). The experiment was repeated in cardiac myocytes generated from mice lacking the IFN-α/β-receptor to increase viral replication. Results emphasized the reduction of Hsp25 in 8B-infected cultures, and the increased Hsp25 phosphorylation specifically in cultures infected with non-myocarditic reoviruses T3D and DB93A (Figure 3.4B). Quantitative RT-PCR confirmed that reovirus modulation of Hsp25 levels is post-transcriptional (Supp. Figure 3.2). Together the data confirm both 2D-DIGE identification and quantification of Hsp25 and phosphorylated forms, and demostrate that stimulation of Hsp25 phosphorylation or reduction of Hsp25 accumulation is virus strain-specific.

Reovirus-induced Hsp25 phosphorylation and reduction of Hsp25 accumulation is virus strain-specific, p38-MAPK-dependent, and IFN-independent. To confirm that differences in virus-induced Hsp25 phosphorylation and reduction of Hsp25 accumulation are virus strain-specific, lysates from cardiac myocyte cultures were probed at a range of times post-infection (Figure 3.5). Both T3D and 8B induced phosphorylation of Hsp25 at 8 and 12 hours post-infection, but while phosphorylated Hsp25 remained elevated in T3D-infected cultures at 18 and 24 hours post-infection, it was reduced in 8B-infected cultures to levels below those in mock-infected cultures (Figure 3.5A). And while levels of total Hsp25 remained relatively constant in T3D-infected cultures over time, Hsp25 was successively reduced in 8B-infected cultures (Figure 3.5B). Together results suggest that both reovirus strains induce initial Hsp25 phosphorylation, but then 8B reduces accumulation of Hsp25.

Hsp25 phosphorylation can be mediated through the p38-MAPK pathway. To determine whether reovirus-induced phosphorylation of Hsp25 is p38-MAPK-dependent, primary cardiac myocyte cultures were treated with the p38-MAPK inhibitor SB203580 for 1 hour and then mock- or reovirus-infected for 13 hours (Figure 3.6). As expected in the absence of inhibitor, T3D and 8B induced Hsp25 phosphorylation relative to mock-infected cultures (Figure 3.6A). The p38-MAPK inhibitor reduced Hsp25 phosphorylation in both T3D and 8B-infected cultures, indicating reovirus use of this pathway. Residual detectable phosphorylation suggested reovirus may use pathways in addition to p38-MAPK. To determine the role of Type I IFN, cardiac myocytes were generated from mice lacking the IFN-α/β-receptor. Efficient reovirus-induced phosphorylation of Hsp25 in these cells demonstrates that it is IFN-independent (Figures. 3.4B and 3.6B). IFN can stimulate p38-MAPK (3) , however the p38-MAPK inhibitor reduced Hsp25 phosphorylation, confirming that reovirus-induced Hsp25 phosphorylation is p38-MAPK-dependent and IFN-independent (Figure 3.6C).

Reovirus does not induce Hsp25 nuclear translocation. Stress can induce Hsp25 nuclear translocation. Whole cell lysates can under-represent the nuclear fraction, and therefore separate cytoplasmic and nuclear fractions were generated. Neither T3D nor 8B induced nuclear accumulation of Hsp25 (Figure 3.7), confirming that the reduced accumulation of Hsp25 in 8B-infected cells was not due to nuclear sequestration.

Expression of Hsp25 is cell type-specific in the heart. Cardiac myocytes are surrounded by cardiac fibroblasts in the heart, and their IFN responses are cell type-specific for an integrated antiviral response (92). To determine possible cardiac cell type-specificity

for reovirus modulation of Hsp25, primary cultures of cardiac myocytes and cardiac fibroblasts were infected and lysates were subjected to SDS-PAGE and Western blot analysis (Figure 3.8A). Surprisingly, Hsp25 was undetectable in either mock- or reovirus-infected cardiac fibroblast cultures, regardless of the reovirus strain tested. To confirm that this did not reflect alterations in Hsp25 during cell culture, mouse cardiac sections were probed for Hsp25 by immunofluorescent microscopy (Figure 3.8B). Indeed, Hsp25 was readily detected in cardiac myocytes, identified by co-expression of myomesin, but was not detected in cardiac fibroblasts, identified by strong co-expression of vimentin. Together, results indicate that Hsp25 expression is cell type-specific in the heart.

Inhibition of p38-MAPK increases T3D- and 8B-induced CPE in cardiac myocytes. Phosphorylation of Hsp25 can increase or decrease Hsp25 anti-apoptotic function. To probe the role of Hsp25 phosphorylation in reovirus-induced CPE, cardiac myocyte cultures generated from wild type or IFN-α/β-receptor-null mice were treated with the p38-MAPK inhibitor SB203580 for 1 hour, and then mock- or reovirus-infected. T3D induces high levels of IFN-β and is highly sensitive to the antiviral effects of IFN-α/β in cardiac myocytes (76), therefore potential antiviral effects of Hsp25 against this virus might be more apparent in IFN-α/β-receptor-null cells. Inhibition of p38-MAPK increased 8B-induced CPE in wild type cells, and increased T3D-induced CPE in IFN-α/β-receptor-null cells (Figure 3.9). Results are consistent with an antiviral role for phosphorylated Hsp25.

DISCUSSION

To identify novel proteins involved in the cardiac antiviral response, the proteomes of primary cultures of cardiac myocytes infected with different reovirus strains were compared by 2D-DIGE. Results were reproducible between replicate cultures and provided a good correlation between known viral phenotypes and whole proteome changes. Hsp25 was identified as one candidate antiviral protein. While non-myocarditic reovirus strains induced Hsp25 phosphorylation, which is a well-characterized protective response in stressed cardiac myocytes (see below), a potently myocarditic reovirus strain induced Hsp25 degradation. Hsp25 degradation does not occur in stressed cardiac myocytes or failing hearts. Viral activation and then degradation of a cell response is reminiscent of the interplay between viruses and cells during the protective IFN response, and suggests that Hsp25 may serve not just as a marker of virus-induced cytopathology, but as an active participant in the antiviral response.

Members of seven different virus families induce Hsp25/Hsp27 expression or phosphorylation, including Herpesviridae(26, 27, 29, 30), Papillomaviridae(12, 46), Hepadnaviridae(34, 45), Paramyxoviridae(77, 91), Flaviviridae(11, 25, 44), Togaviridae(59), and Retroviridae(43, 87). However, only one study has addressed possible Hsp25/27 antiviral activity, finding that while HIV1 induces Hsp27 expression, Hsp27 can inhibit HIV1-induced cell cycle arrest and apoptosis (43). HIV1 induction of Hsp27 and Hsp27 inhibition of HIV1 damage to the cell are similar to virus induction of IFN and IFN inhibition of viral damage. While viral infection of most cells can induce expression and secretion of Type I IFN (47, 68,

70, 72), viruses have evolved many mechanisms to sabotage this potent protective response (32, 39, 66). Indeed, reoviruses have evolved a novel mechanism to repress IFN signaling (93). However to date, there has been no evidence that, by analogy, viruses might subvert the Hsp25/Hsp27 response. Results here demonstrate that while all four reovirus strains tested, regardless of potential to induce disease, induce phosphorylation of Hsp25, only the potently myocarditic reovirus 8B induces Hsp25 degradation. Together, the data suggest that Hsp25 participates in the antiviral response and that some reovirus strains have evolved to subvert this Hsp25 function.

Murine Hsp25 and its human homolog Hsp27 are members of the small HSP family, and can inhibit apoptosis both up- and downstream of cytochrome c release from mitochondria (2). Hsp25 is expressed at greater basal levels in muscle (heart, skeletal muscle) and the gastrointestinal and respiratory tracts than in other tissues (38, 82, 88). However, a variety of stimuli induce Hsp25/27 expression or phosphorylation as a critical protective response in many cell types. The frequency with which microarray and proteomic approaches have identified variations in Hsp25/27 expression raises questions about the validity of these identifications, and emphasizes the importance of confirmation using complementary techniques such as qRT-PCR and Western blots (63). Results here demonstrate that reovirus modulation of Hsp25 expression in cardiac myocytes is post-transcriptional (qRT-PCR, Supp. Figure 3.2), unlike reovirus modulation of other HSPs in other cell types (15, 78). Indeed, reovirus modulation of Hsp25 would have remained undetected without proteomic approaches.

Hsp27 phosphorylation is increased in hearts from patients with ischemia (oxygen

deprivation) / reperfusion (oxygen restoration) damage or dilated cardiomyopathy (49), and in hearts from dogs with congestive heart failure (19). Ischemia / reperfusion is modeled *in vitro* in hearts and in primary cardiac myocyte cultures, and induces apoptosis similar to that in patients. Oxidative stress activates p38-MAPK to phosphorylate and activate MAPKAPK2 (MK2), which then phosphorylates Hsp25/27 in cardiac myocytes (8). The p38-MAPK / MK2 pathway also mediates Hsp25/27 phosphorylation following other stresses such as TNF-α addition to cardiac cells (5), and stresses in other cell types (23, 40, 62, 81). Hsp25/27 can also be phosphorylated through other pathways (23), and Type I IFN can activate p38-MAPK (3), providing IFN-mediated mechanisms for Hsp25/27 phosphorylation. Thus the mechanism for Hsp25/27 phosphorylation is both stimulus- and cell type-specific. Results here demonstrate that reovirus-induced Hsp25 phosphorylation in cardiac myocytes is p38-MAPK-dependent and IFN-independent, but do not exclude involvement of other pathways (Figure 3.6). Inhibition of p38-MAPK increased reovirus-induced CPE in cardiac myocytes (Figure 3.9), consistent with impairment of a protective response normally mediated by phosphorylated Hsp25.

Over-expressed Hsp25/27 is protective against ischemic damage in cardiac myocytes (21, 48, 85). Stress induces phosphorylation of two Hsp25 residues (ser15 and -86) (28, 80), and while some studies suggest that phosphorylation is protective (41, 42) and implicate the p38-MAPK pathway (8, 13), others suggest phosphorylation is irrelevant to protection (35, 51, 67). In addition, while some studies suggest that unphosphorylated Hsp25/27 exists as very large multimers which are protective and that phosphorylated Hsp25 is dissociated to dimers or tetramers which are not protective (64, 67), other studies suggest that

phosphorylation does not always prevent formation of large oligomers nor does it always limit protective function (10). The relationship between phosphorylation, oligomerization and protection is likely to be cell type-specific, and to depend on the Hsp25/27 function assayed. Results here demonstrate that both non-myocarditic and myocarditic reoviruses induce phosphorylation of Hsp25 in cardiac myocytes, likely reflecting a general stress response in those cells. However both unphosphorylated and phosphorylated Hsp25, and both multimeric and oligomeric Hsp25 were degraded in cardiac myocyte cultures infected with the potently myocarditic reovirus 8B, suggesting that all forms can be viral targets.

MATERIALS AND METHODS

Mice and primary cell cultures. Timed-pregnant Cr:NIH(S) mice were purchased from the National Cancer Institute. IFN-α/β-receptor-null (58) mice were maintained as breeding colonies to generate neonates and fetuses for generation of primary cell cultures. Mice were housed according to the recommendations of the Association for Assessment and Accreditation of Laboratory Animal Care, and all procedures were approved by the North Carolina State University institutional animal care and use committee. Primary cardiac myocyte cultures were generated from 1- or 2-day old neonatal or term fetal mice as described previously (4). Briefly, the apical two-thirds of the hearts from euthanized neonates or fetuses were removed and trypsinized. Cells were suspended in Dulbecco's modified Eagle's medium (DMEM; Gibco BRL, Gaithersburg, MD) supplemented with 7% fetal calf serum and 10 μg of gentamicin (Sigma Co.) per ml (cDMEM). Cells were plated in 6-well

clusters, and incubated for 2 hours for separation by differential adhesion. Cardiac myocytes were harvested from the supernatant and the adherent cardiac fibroblasts were harvested by trypsinization. Following centrifugation, cardiac myocytes were suspended in cDMEM supplemented with 0.06% thymidine (Sigma Co., St. Louis, MO), cardiac fibroblasts were suspended in cDMEM, and both cultures were incubated in a 37ºC, 5% CO_2 incubator. All infections and incubations were in these media at 37°C unless otherwise indicated. Cells were never passaged before use. By immunofluorescent staining, the myocyte cultures contained <5% fibroblasts (92).

Viruses and cell lines. Reovirus type 3 Dearing (T3D) and type 1 Lang (T1L) were plaque purified and amplified in mouse L929 cells, which are maintained in a suspension system in sMEM (SAFC Biosciences, Denver, PA) supplemented with 5% fetal calf serum (Atlanta Biologicals, Atalanta, GA) and 2mM L-glutamine (Mediatech Inc., Herndon, VA). Reovirus 8B is a reassortant virus derived from a mouse infected with T3D and T1L (75). DB93A was derived from mouse L929 cells infected with 8B and a reassortant virus (EB121) derived from T3D and T1L (73). All viruses were purified by CsCl gradient centrifugation (79).

Infections. All primary cardiac cell cultures were incubated for two days before infection. For 2D-DIGE, cardiac myocytes were plated at 2×10^6 cells per well in 12-well clusters. Triplicate wells were infected with media or virus at 10 pfu per cell in 1400 μl for 1 hour, and then supplemented with an additional 2 ml media. Cultures were harvested 12 hours post-infection. For MTT assays, cardiac myocytes were plated at 1.5×10^5 cells per well in 96-well clusters. Triplicate wells were treated with 50 μM p38 MAPK inhibitor

SB203580 (EMD CalBiochem, cat #559389) or vehicle for 1 hour, infected with media or virus at 25 pfu per cell in 100 μl for 1 hour, and then supplemented with an additional 100 μl media. Cultures were harvested 48 to 72 hours post-infection. For Western blots, cardiac myocytes were plated at 1×10^6 cells and cardiac fibroblasts at 5×10^5 cells per well in 24-well clusters. Duplicate wells were infected with media or virus at 10 pfu per cell in 700μl for 1 hour, and then supplemented with an additional 1000 μl media. Cultures were harvested 8 to 48 hours post-infection. For qRT-PCR, cardiac myocytes were plated and infected as for Western blots, and harvested 30 minutes to 24 hours post-infection.

Reagents for 2-dimensional difference gel electrophoresis (2D-DIGE). Sodium chloride, Trizma base, bromophenol blue, chloroform, DMF, phosphatase inhibitor, sodium carbonate, sodium bicarbonate, ammonium bicarbonate, ammonium monobasic phosphate, L-lysine, and α-cyano-4-hydroxycinnamic acid were obtained from Sigma Aldrich. Urea, thiourea, SDS, DTT, Tris, and iodoacetamide were purchased from GE Healthcare. CHAPS was obtained from USB. Complete Mini Protease Inhibitor Cocktail Tablets were obtained from Roche Applied Science. Methanol, acetonitrile, and HPLC grade water were obtained from Burdick & Jackson. Acetic acid was obtained from J.T. Baker.

Sample Preparation and Protein Labeling. Total cell protein harvest procedures and protein concentration determinations were as for SDS-PAGE. Protein disulfide bonds were reduced in 2mM DTT. For each sample, 85 μg protein was precipitated using 4:1 methanol:chloroform, washed once with methanol, and resuspended in L-buffer (7M Urea, 2M Thiourea, 4% CHAPS, 30 mM Tris, pH 8.5). An internal standard was created by pooling 35.3 μg of each of the 15 samples. In order to create an even number of samples, 26

μl of the pool was used to create a 16th sample. Then, 26 μl of each of the 16 samples was labeled with 4.25 pmol of either Cy3 or Cy5 dye per μg protein. In order to avoid dye binding bias, two samples from each virus infection were labeled with one of the two dyes and the third sample was labeled with the other dye. The internal pooled standard was labeled using 3.32 pmol / μg Cy2. Reactions were stopped by adding 10 mM lysine in a volume equal to that of the dye. For each gel, a Cy3- and a Cy5-labeled sample was mixed with an equal volume (30 μl) of Cy2-labeled standard. Samples were then reduced and denatured in R-buffer (7M urea, 2M Thiourea, 4% CHAPS, 13mM DTT) at 10:1 v:v with ampholytes (IPG Buffer, pH 4-7, GE Healthcare). The samples were then applied to a 24 cm, pH 4-7 Immobiline DryStrip (GE Healthcare).

2-dimensional difference gel electrophoresis (2D-DIGE). Gels were loaded with different combinations of the 15 samples such that no two infections were ever directly compared more than once. First dimension isoelectric focusing was performed using an Ettan IPGphor3 (GE Healthcare) for a total focusing time of 64.5kVHrs. at 20ºC and 75μA / strip max. After focusing was complete, each strip was equilibrated for 15 minutes with 10 ml equilibration buffer (6M Urea, 75 mM Tris pH 8.8, 29.3% Glycerol, 2% SDS, 0.002% bromophenol blue) supplemented with 10 mg/ml DTT. The strips were then equilibrated for 15 minutes with 10 ml equilibration buffer supplemented with 25 mg/ml iodoacetamide. The strips were briefly washed with 1x Running Buffer (NextGen Sciences) to remove any excess equilibration buffer, and then loaded onto 12% Homogenous SDS-PAGE gels (NextGen Sciences). Electrophoresis was performed on an Ettan DALTtwelve System Separation Unit (Amersham Biosciences) at 0.5W/gel until the bromophenol blue dye front had just run off

the bottom of the gel. Gels were scanned at 488 nm(Cy2), 532 nm(Cy3), and 633 nm(Cy5) using a Typhoon Trio Variable Mode Imager (GE Healthcare).

DIGE image analysis. DeCyder 2D Software, Version 6.5 from GE Healthcare was applied to visualize and resize the digitalized images from the scanner (84, 90). Protein spots were identified in differential in-gel analysis (DIA) module, and gels were matched to the master gel in the biological variation analysis (BVA) module. DeCyder Extended Data Analysis (EDA) module Version 1.0 was applied to carry out the DIA analysis, principle component analysis (PCA) and pattern analysis. Protein spots were selected for identification based on their differential expression among different groups ($P < 0.05$ using one-way ANOVA) and their relative abundance in 3D visualization.

Protein Identifications. A fraction of each of the 15 samples was used to generate a pool of 356 μg protein for preparative 2D-gel electrophoresis. The gel was stained for 1 hour with Deep Purple Total Protein Stain (1:200, GE Healthcare), and the image was imported for DIGE analysis using DeCyder software. After matching back to the master gel, gel plugs corresponding to differentially expressed proteins were isolated using an Ettan Spot Picker (GE Healthcare). Destained and dehydrated gel spots were digested overnight in Trypsin Gold (Promega), and then desalted and concentrated using C18 P10 ZipTips (Millipore). One third of each sample was loaded onto a ZipTip by pipetting up and down five times using a fresh 96-well plate. Samples (in ZipTips) were washed four times with 10 μL of 0.1% TFA and eluted with 2 μL of 50% acetonitrile / 0.1% trifluoroacetic acid. A total of 1 μL of eluate was pipetted onto a clean MALDI plate and covered with 1μL of α-cyano-4-hydroxycinnamic acid MALDI matrix. Mass spectra for each spot were acquired using an

Applied Biosystems 4700 Proteomics Analyzer MALDI-TOF-TOF. Data-dependent MS/MS analysis was performed on the top 10 peaks from each MS spectrum. GPS explorer™ workstation, the Applied Biosystem/MDS SCIEX 400 series MALDI-TOF analyzer, was used for the peptide mass fingerprints database match searching in two databases: Swiss-Prot (for proteins from all organisms) and IPI (for proteins from mouse) with carbamidomethyl (C) and oxidation (M) as fixed modification. A protein score higher than 64 in the Swiss-Prot search and 60 in IPI search was considered significant.

Software applied. Protein-protein interaction and pathway analysis were assessed using Ingenuity Pathways Analysis (IPA 5.0; Ingenuity® Systems, www.ingenuity.com). Theoretical protein digestion was performed using ProteinProspector from University of California, San Francisco (http://169.230.19.26:8080/cgi-bin/msform.cgi?form=msdigest). Predictions of protein phosphorylation sites were performed using NetPhos 2.0 Server (http://www.cbs.dtu.dk/services/NetPhos/).

SDS-PAGE and Western blot analysis. Infected cardiac myocyte cultures were washed four times with ice-cold 1x PBS. Total cell protein was harvested at the indicated times by incubation in TNE lysis buffer (50 mM Tris HCl pH 7.6, 150 mM NaCl, 2 mM EDTA pH 8.0, 1% [v/v] NP-40 containing a cocktail of protease and phosphatase inhibitors [Sigma Co.; P8340 and P2850]) on ice for 30 minutes with shaking. Lysates were centrifuged at 10,000 x g for 10 minutes at 4ºC to remove cellular debris. For Figure 3.7, cytoplasmic and nuclear protein was harvested at 17 hours post-infection by NE-PER kit (Pierce, Rockford, IL). Protein concentrations were determined using a bicinchoninic acid kit (Pierce, Rockford, IL), and 40 μg was boiled for 5 minutes in 1x Laemmli sample buffer

and subjected to 10% sodium dodecyl sulfate-polyacrylamide gel electrophoresis (SDS-PAGE). Gels were transferred to nitrocellulose membranes, and membranes were blocked for 1 hour at room temperature in 3% milk in Tris-buffered saline (20 mM Tris [pH 7.6], 137 mM NaCl) containing 0.05% Tween 20 (TBS-T) and then probed overnight at 4°C with the indicated primary antibody (1:1000 of Hsp25 polyclonal antibody, cat. # SPA-801; 1:1000 of Hsp27-phospho-Ser82 polyclonal antibody, cat. # SPA-524; 1:500 of Hsp27-phospho-Ser15 polyclonal antibody, cat. # SPA-525; Assay Designs, Ann Arbor, Michigan). Membranes were washed for 5 minutes twice in TBS-T, incubated for 1.5 hours at room temperature in goat anti-rabbit HRP-conjugated secondary antibody (Millipore, Catlog # AP132P), and then washed for 10 minutes three times in TBS-T. Antibody-labeled proteins were detected according to manufacturer's recommendations (Amersham^{TM} ECL^{TM} or ECL^{TM} Plus Western Blotting Detection reagent, GE Healthcare, Buckinghamshire, United Kingdom). Western blots were exposed to film and converted to digital format using an HP Scanjet 5470c.

Cell viability (MTT assay). At 48 or 72 hours post-infection, 20 μl of 0.6% MTT(catalog #M-5655; Sigma) in cDMEM was added to each well and cultures were incubated for 4 hours at 37°C. Culture plates were centrifuged at 750 x g for 8 minutes, supernatants were removed, and 100 μl of 0.04 N HCl in isopropanol was added to each well. Plates were incubated at room temperature for 15 minutes, 100 μl H2O was added to each well and the optical densities at 570 and 630 nm were determined on a Tecan Sunrise Microplate Reader (Tecan Systems Inc., San Jose, CA). Results are expressed as signal (OD_{570}) minus background (OD_{630}).

Indirect immunofluorescence. Procedure was as described previously (92). In brief, hearts from adult Cr:NIH(S) mice were washed in ice-cold 1x PBS and snap frozen in liquid nitrogen-cooled isopentane (Fisher Scientific Co.). Tissue samples were mounted frozen on a metal chuck using a small volume of Tissue-Tek OCT (Ted Pella, Inc., Redding, CA) in a cryostat (Leica CM1850) at -20°C. Transverse cryosections (1 μm) were collected on SuperFrost/Plus slides (Fisher Scientific) and stored at -80°C. Sections were thawed and blocked for 1 hour at room temperature with 10% donkey serum (Sigma) and 10% goat serum (Sigma Co.) in 1x phosphate-buffered saline (PBS) plus 0.1% Triton X-100 (PBST) for vimentin, or with 10% donkey serum in PBST for myomesin, and then probed overnight at 4°C with a mix of rabbit anti-Hsp25 (1:1000) and goat anti-myomesin (1:50, cat. # 30384, Santa Cruz Biotechnology, Inc.) or chicken anti-vimentin (1:5,000, Affinity Bioreagents Inc., Golden, CO) antibodies in 1 x PBS with 0.3% IgG-free, protease-free bovine serum albumin (BSA)(Jackson ImmunoResearch Laboratories, Inc., West Grove, PA). Slides were washed three times in 1 x PBS, and then incubated for 2 hours at room temperature with a mix of Alexa fluor 594 goat anti-chicken IgG (Invitrogen, SKU# A-11042, 1:1000) plus Alexa fluor 488 donkey anti-rabit IgG(Invitrogen, SKU# A-21206,1:1000) for detection of vimentin and Hsp25, or alexa fluor 594 donkey anti-goat IgG (Invitrogen, SKU# A-11058, 1:1000) plus Alexa fluor 488 donkey anti-rabbit IgG (1:1000) in 1xPBS with 0.3% IgG-free, protease-free BSA for detection of myomesin and Hsp25. Slides were washed in 1 x PBS, coverslips were mounted with Prolong Gold reagent (Invitrogen), and slides were analyzed using a Nikon TE-200 inverted epifluorescence microscope. Images were captured using a 100x objective under oil immersion, and were collected digitally (SPOT, Jr.; Diagnostics Instruments, Inc.,

Sterling Heights, MI) and processed using the manufacturer's instructions and Adobe Photoshop (with no change in content).

SUPPLEMENTAL MATERIALS AND METHODS

Reverse transcription (RT) and Quantitative (q)RT-PCR. Cells were harvested at the indicated times post-infection using cell lysis buffer from an RNeasy Kit (Qiagen, Inc., Valencia, CA) supplemented with 1% β-mercaptoethanol, and homogenized using Qiashredders (Qiagen, Inc.), and total RNA was isolated using the RNeasy Kit according to the manufacturer's instructions. Genomic DNA was removed using RNase-free DNase I (Qiagen, Inc.). The isolated RNA was stored at -80ºC. To generate cDNA, one third of the RNA harvested from each well in a 24-well cluster or two thirds from a 48-well cluster was used as template in a 100 µl reaction containing 5 µM oligo(dT) (Invitrogen Corp., Carlsbad, CA), 1× Taq buffer (Promega corp., Madison, WI), 7.5 mM MgCl2 (Promega corp.), 1 mM dithiothreitol (Promega corp.), 1 mM each dNTP (Roche, Indianapolis, IN), 0.67 U/µl RNasin (Promega Corp., Madison, WI), and 0.20 U/µl of AMV reverse transcriptase (Promega Corp.). Gene expression was quantified using a Sybergreen system on an iCycler iQ fluorescence thermocycler (Bio-Rad Laboratories, Hercules, CA). Each 25 µl reaction contained 5% of the RT product, 1× Quantitech master mix (Qiagen, Inc.), 10 nM fluorescein (Invitrogen Corp., Carlsbad, CA), and 0.3µM each of the forward and reverse primers (GAPDH forward: 5'- GGGTGTGAACCACGAGAAAT-3' and reverse: 5'-CCTTCCACAATGCCAAAGTT-3'; HSP25 Forward: 5'-

GAAGAAAGGCAGGACGAACA-3' and reverse: 5'-CTCAGGGGATAGGGAAGAGG-3'). iCyclerTM iQ Optional System Software, version 3.0 (Bio-Rad Laboratories) was used to analyze the data. Gene-of-interest expression was normalized to GAPDH gene expression.

ACKNOWLEDGEMENTS

We thank Megan Rowland for her help at RTI, Susan Irvin, Jennifer Zurney, Kevin Blackburn and Michael Goshe for insightful discussions, and Wrennie Edwards for technical assistance. This research was supported by NIH award R01 AI062657 and graduate student support from the North Carolina State University Genomics Graduate Program (L.L.).

REFERENCES

1. **Alban, A., S. O. David, L. Bjorkesten, C. Andersson, E. Sloge, S. Lewis, and I. Currie.** 2003. A novel experimental design for comparative two-dimensional gel analysis: two-dimensional difference gel electrophoresis incorporating a pooled internal standard. Proteomics **3:**36-44.

2. **Arya, R., M. Mallik, and S. C. Lakhotia.** 2007. Heat shock genes - integrating cell survival and death. J Biosci **32:**595-610.

3. **Barca, O., J. A. Costoya, R. M. Senaris, and V. M. Arce.** 2008. Interferon-beta protects astrocytes against tumour necrosis factor-induced apoptosis via activation of p38 mitogen-activated protein kinase. Exp Cell Res **314:**2231-7.

4. **Baty, C. J., and B. Sherry.** 1993. Cytopathogenic effect in cardiac myocytes but not in cardiac fibroblasts is correlated with reovirus-induced acute myocarditis. J Virol **67:**6295-8.

5. **Bellahcene, M., S. Jacquet, X. B. Cao, M. Tanno, R. S. Haworth, J. Layland, A. M. Kabir, M. Gaestel, R. J. Davis, R. A. Flavell, A. M. Shah, M. Avkiran, and M. S. Marber.** 2006. Activation of p38 mitogen-activated protein kinase contributes to the early cardiodepressant action of tumor necrosis factor. J Am Coll Cardiol **48:**545-55.

6. **Bergmann, O., R. D. Bhardwaj, S. Bernard, S. Zdunek, F. Barnabe-Heider, S. Walsh, J. Zupicich, K. Alkass, B. A. Buchholz, H. Druid, S. Jovinge, and J. Frisen.** 2009. Evidence for cardiomyocyte renewal in humans. Science **324:**98-102.

7. **Blailock, Z. R., E. R. Rabin, and J. L. Melnick.** 1968. Adenovirus myocarditis in mice. An electron microscopic study. Exp Mol Pathol **9:**84-96.

8. **Blunt, B. C., A. T. Creek, D. C. Henderson, and P. A. Hofmann.** 2007. H2O2 activation of HSP25/27 protects desmin from calpain proteolysis in rat ventricular myocytes. Am J Physiol Heart Circ Physiol **293:**H1518-25.

9. **Bowles, N. E., J. Ni, D. L. Kearney, M. Pauschinger, H. P. Schultheiss, R. McCarthy, J. Hare, J. T. Bricker, K. R. Bowles, and J. A. Towbin.** 2003. Detection of viruses in myocardial tissues by polymerase chain reaction. evidence of adenovirus as a common cause of myocarditis in children and adults. J Am Coll Cardiol **42:**466-72.

10. **Bruey, J. M., C. Paul, A. Fromentin, S. Hilpert, A. P. Arrigo, E. Solary, and C. Garrido.** 2000. Differential regulation of HSP27 oligomerization in tumor cells grown in vitro and in vivo. Oncogene **19:**4855-63.

11. **Choi, Y. W., Y. J. Tan, S. G. Lim, W. Hong, and P. Y. Goh.** 2004. Proteomic approach identifies HSP27 as an interacting partner of the hepatitis C virus NS5A protein. Biochem Biophys Res Commun **318:**514-9.

12. **Ciocca, D. R., G. Lo Castro, L. V. Alonio, M. F. Cobo, H. Lotfi, and A. Teyssie.** 1992. Effect of human papillomavirus infection on estrogen receptor and heat shock protein hsp27 phenotype in human cervix and vagina. Int J Gynecol Pathol **11:**113-21.

13. **Clerk, A., A. Michael, and P. H. Sugden.** 1998. Stimulation of multiple mitogen-activated protein kinase sub-families by oxidative stress and phosphorylation of the small heat shock protein, HSP25/27, in neonatal ventricular myocytes. Biochem J **333 (Pt 3):**581-9.

14. **Cooper, L. T., Jr.** 2009. Myocarditis. N Engl J Med **360:**1526-38.

15. **DeBiasi, R. L., P. Clarke, S. Meintzer, R. Jotte, B. K. Kleinschmidt-Demasters, G. L. Johnson, and K. L. Tyler.** 2003. Reovirus-induced alteration in expression of apoptosis and DNA repair genes with potential roles in viral pathogenesis. J Virol **77:**8934-47.

16. **DeBiasi, R. L., C. L. Edelstein, B. Sherry, and K. L. Tyler.** 2001. Calpain inhibition protects against virus-induced apoptotic myocardial injury. J Virol **75:**351-61.

17. **DeBiasi, R. L., B. A. Robinson, B. Sherry, R. Bouchard, R. D. Brown, M. Rizeq, C. Long, and K. L. Tyler.** 2004. Caspase inhibition protects against reovirus-induced myocardial injury in vitro and in vivo. J Virol **78:**11040-50.

18. **Dekkers, D. H., K. Bezstarosti, N. Gurusamy, K. Luijk, A. J. Verhoeven, E. J. Rijkers, J. A. Demmers, J. M. Lamers, N. Maulik, and D. K. Das.** 2008. Identification by a differential proteomic approach of the induced stress and redox proteins by resveratrol in the normal and diabetic rat heart. J Cell Mol Med **12:**1677-89.

19. **Dohke, T., A. Wada, T. Isono, M. Fujii, T. Yamamoto, T. Tsutamoto, and M. Horie.** 2006. Proteomic analysis reveals significant alternations of cardiac small heat shock protein expression in congestive heart failure. J Card Fail **12:**77-84.

20. **Doolan, A., N. Langlois, and C. Semsarian.** 2004. Causes of sudden cardiac death in young Australians. Med J Aust **180:**110-2.

21. **Efthymiou, C. A., M. M. Mocanu, J. de Belleroche, D. J. Wells, D. S. Latchmann, and D. M. Yellon.** 2004. Heat shock protein 27 protects the heart against myocardial infarction. Basic Res Cardiol **99:**392-4.

22. **Esfandiarei, M., and B. M. McManus.** 2008. Molecular biology and pathogenesis of viral myocarditis. Annu Rev Pathol **3:**127-55.

23. **Evans, I. M., G. Britton, and I. C. Zachary.** 2008. Vascular endothelial growth factor induces heat shock protein (HSP) 27 serine 82 phosphorylation and endothelial tubulogenesis via protein kinase D and independent of p38 kinase. Cell Signal **20:**1375-84.

24. **Faber, M. J., G. Agnetti, K. Bezstarosti, I. M. Lankhuizen, M. Dalinghaus, C. Guarnieri, C. M. Caldarera, W. A. Helbing, and J. M. Lamers.** 2006. Recent developments in proteomics: implications for the study of cardiac hypertrophy and failure. Cell Biochem Biophys **44:**11-29.

25. **Fang, C., Z. Yi, F. Liu, S. Lan, J. Wang, H. Lu, P. Yang, and Z. Yuan.** 2006. Proteome analysis of human liver carcinoma Huh7 cells harboring hepatitis C virus subgenomic replicon. Proteomics **6:**519-27.

26. **Forsman, A., U. Ruetschi, J. Ekholm, and L. Rymo.** 2008. Identification of intracellular proteins associated with the EBV-encoded nuclear antigen 5 using an efficient TAP procedure and FT-ICR mass spectrometry. J Proteome Res **7:**2309-19.

27. **Fukagawa, Y., J. Nishikawa, Y. Kuramitsu, D. Iwakiri, K. Takada, S. Imai, M. Satake, T. Okamoto, M. Fujimoto, K. Okita, K. Nakamura, and I. Sakaida.** 2008. Epstein-Barr virus upregulates phosphorylated heat shock protein 27 kDa in carcinoma cells using the phosphoinositide 3-kinase/Akt pathway. Electrophoresis **29:**3192-200.

28. **Gaestel, M., W. Schroder, R. Benndorf, C. Lippmann, K. Buchner, F. Hucho, V. A. Erdmann, and H. Bielka.** 1991. Identification of the phosphorylation sites of the murine small heat shock protein hsp25. J Biol Chem **266:**14721-4.

29. **Gober, M. D., J. M. Laing, J. W. Burnett, and L. Aurelian.** 2007. The Herpes simplex virus gene Pol expressed in herpes-associated erythema multiforme lesions upregulates/activates SP1 and inflammatory cytokines. Dermatology **215:**97-106.

30. **Gober, M. D., S. Q. Wales, and L. Aurelian.** 2005. Herpes simplex virus type 2 encodes a heat shock protein homologue with apoptosis regulatory functions. Front Biosci **10:**2788-803.

31. **Gorg, A., W. Weiss, and M. J. Dunn.** 2004. Current two-dimensional electrophoresis technology for proteomics. Proteomics **4:**3665-85.

32. **Haller, O., G. Kochs, and F. Weber.** 2006. The interferon response circuit: induction and suppression by pathogenic viruses. Virology **344:**119-30.

33. **Hamblin, M., D. B. Friedman, S. Hill, R. M. Caprioli, H. M. Smith, and M. F. Hill.** 2007. Alterations in the diabetic myocardial proteome coupled with increased myocardial oxidative stress underlies diabetic cardiomyopathy. J Mol Cell Cardiol **42:**884-95.

34. **Han, J., H. Y. Yoo, B. H. Choi, and H. M. Rho.** 2000. Selective transcriptional regulations in the human liver cell by hepatitis B viral X protein. Biochem Biophys Res Commun **272:**525-30.

35. **Hollander, J. M., J. L. Martin, D. D. Belke, B. T. Scott, E. Swanson, V. Krishnamoorthy, and W. H. Dillmann.** 2004. Overexpression of wild-type heat shock protein 27 and a nonphosphorylatable heat shock protein 27 mutant protects against ischemia/reperfusion injury in a transgenic mouse model. Circulation **110:**3544-52.

36. **Huber, S.** 2008. Host immune responses to coxsackievirus B3. Curr Top Microbiol Immunol **323:**199-221.

37. **Jager, D., P. R. Jungblut, and U. Muller-Werdan.** 2002. Separation and identification of human heart proteins. J Chromatogr B Analyt Technol Biomed Life Sci **771:**131-53.

38. **Kato, K., H. Ito, I. Iwamoto, K. Lida, and Y. Inaguma.** 2001. Protein kinase inhibitors can suppress stress-induced dissociation of Hsp27. Cell Stress Chaperones **6:**16-20.

39. **Komuro, A., D. Bamming, and C. M. Horvath.** 2008. Negative regulation of cytoplasmic RNA-mediated antiviral signaling. Cytokine **43:**350-8.

40. **Kotlyarov, A., A. Neininger, C. Schubert, R. Eckert, C. Birchmeier, H. D. Volk, and M. Gaestel.** 1999. MAPKAP kinase 2 is essential for LPS-induced TNF-alpha biosynthesis. Nat Cell Biol **1:**94-7.

41. **Kwon, J. H., J. B. Kim, K. H. Lee, S. M. Kang, N. Chung, Y. Jang, and J. H. Chung.** 2007. Protective effect of heat shock protein 27 using protein transduction domain-mediated delivery on ischemia/reperfusion heart injury. Biochem Biophys Res Commun **363:**399-404.

42. **Li, G., I. S. Ali, and R. W. Currie.** 2008. Insulin-induced myocardial protection in isolated ischemic rat hearts requires p38 MAPK phosphorylation of Hsp27. Am J Physiol Heart Circ Physiol **294:**H74-87.

43. **Liang, D., Z. Benko, E. Agbottah, M. Bukrinsky, and R. Y. Zhao.** 2007. Anti-vpr activities of heat shock protein 27. Mol Med **13:**229-39.

44. **Liew, K. J., and V. T. Chow.** 2006. Microarray and real-time RT-PCR analyses of a novel set of differentially expressed human genes in ECV304 endothelial-like cells infected with dengue virus type 2. J Virol Methods **131:**47-57.

45. **Lim, S. O., S. G. Park, J. H. Yoo, Y. M. Park, H. J. Kim, K. T. Jang, J. W. Cho, B. C. Yoo, G. H. Jung, and C. K. Park.** 2005. Expression of heat shock proteins (HSP27, HSP60, HSP70, HSP90, GRP78, GRP94) in hepatitis B virus-related hepatocellular carcinomas and dysplastic nodules. World J Gastroenterol **11:**2072-9.

46. **Lo, W. Y., C. C. Lai, C. H. Hua, M. H. Tsai, S. Y. Huang, C. H. Tsai, and F. J. Tsai.** 2007. S100A8 is identified as a biomarker of HPV18-infected oral squamous cell carcinomas by suppression subtraction hybridization, clinical proteomics analysis, and immunohistochemistry staining. J Proteome Res **6:**2143-51.

47. **Loo, Y. M., J. Fornek, N. Crochet, G. Bajwa, O. Perwitasari, L. Martinez-Sobrido, S. Akira, M. A. Gill, A. Garcia-Sastre, M. G. Katze, and M. Gale, Jr.** 2008. Distinct RIG-I and MDA5 signaling by RNA viruses in innate immunity. J Virol **82:**335-45.

48. **Lu, X. Y., L. Chen, X. L. Cai, and H. T. Yang.** 2008. Overexpression of heat shock protein 27 protects against ischaemia/reperfusion-induced cardiac dysfunction via stabilization of troponin I and T. Cardiovasc Res **79:**500-8.

49. **Lutsch, G., R. Vetter, U. Offhauss, M. Wieske, H. J. Grone, R. Klemenz, I. Schimke, J. Stahl, and R. Benndorf.** 1997. Abundance and location of the small heat shock proteins HSP25 and alphaB-crystallin in rat and human heart. Circulation **96:**3466-76.

50. **Martin, A. B., S. Webber, F. J. Fricker, R. Jaffe, G. Demmler, D. Kearney, Y. H. Zhang, J. Bodurtha, B. Gelb, J. Ni, and et al.** 1994. Acute myocarditis. Rapid diagnosis by PCR in children. Circulation **90:**330-9.

51. **Martin, J. L., E. Hickey, L. A. Weber, W. H. Dillmann, and R. Mestril.** 1999. Influence of phosphorylation and oligomerization on the protective role of the small heat shock protein 27 in rat adult cardiomyocytes. Gene Expr **7:**349-55.

52. **Mason, J. W., J. B. O'Connell, A. Herskowitz, N. R. Rose, B. M. McManus, M. E. Billingham, and T. E. Moon.** 1995. A clinical trial of immunosuppressive therapy for myocarditis. The Myocarditis Treatment Trial Investigators. N Engl J Med **333:**269-75.

53. **Mayr, M., D. Liem, J. Zhang, X. Li, N. K. Avliyakulov, J. I. Yang, G. Young, T. M. Vondriska, C. Ladroue, B. Madhu, J. R. Griffiths, A. Gomes, Q. Xu, and P. Ping.** 2009. Proteomic and metabolomic analysis of cardioprotection: Interplay between protein kinase C epsilon and delta in regulating glucose metabolism of murine hearts. J Mol Cell Cardiol **46:**268-77.

54. **McCarthy, R. E., 3rd, J. P. Boehmer, R. H. Hruban, G. M. Hutchins, E. K. Kasper, J. M. Hare, and K. L. Baughman.** 2000. Long-term outcome of fulminant myocarditis as compared with acute (nonfulminant) myocarditis. N Engl J Med **342:**690-5.

55. **McGregor, E., and M. J. Dunn.** 2006. Proteomics of the heart: unraveling disease. Circ Res **98:**309-21.

56. **Meng, C., X. Jin, L. Xia, S. M. Shen, X. L. Wang, J. Cai, G. Q. Chen, L. S. Wang, and N. Y. Fang.** 2009. Alterations of mitochondrial enzymes contribute to cardiac hypertrophy before hypertension development in spontaneously hypertensive rats. J Proteome Res **8:**2463-75.

57. **Miyamoto, S. D., R. D. Brown, B. A. Robinson, K. L. Tyler, C. S. Long, and R. L. Debiasi.** 2009. Cardiac cell specific apoptotic and cytokine response to reovirus infection: determinants of myocarditic phenotype. Journal of cardiac failure.

58. **Muller, U., U. Steinhoff, L. F. Reis, S. Hemmi, J. Pavlovic, R. M. Zinkernagel, and M. Aguet.** 1994. Functional role of type I and type II interferons in antiviral defense. Science **264:**1918-21.

59. **Nakatsue, T., I. Katoh, S. Nakamura, Y. Takahashi, Y. Ikawa, and Y. Yoshinaka.** 1998. Acute infection of Sindbis virus induces phosphorylation and intracellular translocation of small heat shock protein HSP27 and activation of p38 MAP kinase signaling pathway. Biochem Biophys Res Commun **253:**59-64.

60. **O'Farrell, P. H.** 1975. High resolution two-dimensional electrophoresis of proteins. J Biol Chem **250:**4007-21.

61. **Page, B., R. Young, V. Iyer, G. Suzuki, M. Lis, L. Korotchkina, M. S. Patel, K. M. Blumenthal, J. A. Fallavollita, and J. M. Canty, Jr.** 2008. Persistent regional downregulation in mitochondrial enzymes and upregulation of stress proteins in swine with chronic hibernating myocardium. Circ Res **102:**103-12.

62. **Park, J. K., N. Ronkina, A. Hoft, C. Prohl, J. Menne, M. Gaestel, H. Haller, and M. Meier.** 2008. Deletion of MK2 signalling in vivo inhibits small Hsp phosphorylation but not diabetic nephropathy. Nephrol Dial Transplant **23:**1844-53.

63. **Petrak, J., R. Ivanek, O. Toman, R. Cmejla, J. Cmejlova, D. Vyoral, J. Zivny, and C. D. Vulpe.** 2008. Deja vu in proteomics. A hit parade of repeatedly identified differentially expressed proteins. Proteomics **8:**1744-9.

64. **Preville, X., H. Schultz, U. Knauf, M. Gaestel, and A. P. Arrigo.** 1998. Analysis of the role of Hsp25 phosphorylation reveals the importance of the oligomerization state of this small heat shock protein in its protective function against TNFalpha- and hydrogen peroxide-induced cell death. J Cell Biochem **69:**436-52.

65. **Puranik, R., C. K. Chow, J. A. Duflou, M. J. Kilborn, and M. A. McGuire.** 2005. Sudden death in the young. Heart Rhythm **2:**1277-82.

66. **Randall, R. E., and S. Goodbourn.** 2008. Interferons and viruses: an interplay between induction, signalling, antiviral responses and virus countermeasures. J Gen Virol **89:**1-47.

67. **Rogalla, T., M. Ehrnsperger, X. Preville, A. Kotlyarov, G. Lutsch, C. Ducasse, C. Paul, M. Wieske, A. P. Arrigo, J. Buchner, and M. Gaestel.** 1999. Regulation of Hsp27 oligomerization, chaperone function, and protective activity against oxidative stress/tumor necrosis factor alpha by phosphorylation. J Biol Chem **274:**18947-56.

68. **Sadler, A. J., and B. R. Williams.** 2008. Interferon-inducible antiviral effectors. Nat Rev Immunol **8:**559-68.

69. **Sakai, J., H. Ishikawa, H. Satoh, S. Yamamoto, S. Kojima, and M. Kanaoka.** 2007. Two-dimensional differential gel electrophoresis of rat heart proteins in ischemia and ischemia-reperfusion. Methods Mol Biol **357:**33-43.

70. **Samuel, C. E.** 2007. Innate immunity minireview series: making biochemical sense of nucleic acid sensors that trigger antiviral innate immunity. J Biol Chem **282:**15313-4.

71. **Schiff LA, N. M., Tyler KL.** 2007. Orthoreoviruses and their repliation, 5 ed, vol. 2. Lippincott Williams & Wilkins, Philadelphia, PA.

72. **Schindler, C., D. E. Levy, and T. Decker.** 2007. JAK-STAT signaling: from interferons to cytokines. J Biol Chem **282:**20059-63.

73. **Sherry, B., and B. N. Fields.** 1989. The reovirus M1 gene, encoding a viral core protein, is associated with the myocarditic phenotype of a reovirus variant. J Virol **63:**4850-6.

74. **Sherry, B., X. Y. Li, K. L. Tyler, J. M. Cullen, and H. W. t. Virgin.** 1993. Lymphocytes protect against and are not required for reovirus-induced myocarditis. J Virol **67:**6119-24.

75. **Sherry, B., F. J. Schoen, E. Wenske, and B. N. Fields.** 1989. Derivation and characterization of an efficiently myocarditic reovirus variant. J Virol **63:**4840-9.

76. **Sherry, B., J. Torres, and M. A. Blum.** 1998. Reovirus induction of and sensitivity to beta interferon in cardiac myocyte cultures correlate with induction of myocarditis and are determined by viral core proteins. J Virol **72:**1314-23.

77. **Singh, D., K. L. McCann, and F. Imani.** 2007. MAPK and heat shock protein 27 activation are associated with respiratory syncytial virus induction of human bronchial epithelial monolayer disruption. Am J Physiol Lung Cell Mol Physiol **293:**L436-45.

78. **Smith, J. A., S. C. Schmechel, A. Raghavan, M. Abelson, C. Reilly, M. G. Katze, R. J. Kaufman, P. R. Bohjanen, and L. A. Schiff.** 2006. Reovirus induces and benefits from an integrated cellular stress response. J Virol **80:**2019-33.

79. **Smith, R. E., H. J. Zweerink, and W. K. Joklik.** 1969. Polypeptide components of virions, top component and cores of reovirus type 3. Virology **39:**791-810.

80. **Stokoe, D., K. Engel, D. G. Campbell, P. Cohen, and M. Gaestel.** 1992. Identification of MAPKAP kinase 2 as a major enzyme responsible for the phosphorylation of the small mammalian heat shock proteins. FEBS Lett **313:**307-13.

81. **Su, X., L. Ao, N. Zou, Y. Song, X. Yang, G. Y. Cai, D. A. Fullerton, and X. Meng.** 2008. Post-transcriptional regulation of TNF-induced expression of ICAM-1 and IL-8 in human lung microvascular endothelial cells: an obligatory role for the p38 MAPK-MK2 pathway dissociated with HSP27. Biochim Biophys Acta **1783:**1623-31.

82. **Tanguay, R. M., Y. Wu, and E. W. Khandjian.** 1993. Tissue-specific expression of heat shock proteins of the mouse in the absence of stress. Dev Genet **14:**112-8.

83. **Timms, J. F., and R. Cramer.** 2008. Difference gel electrophoresis. Proteomics **8:**4886-97.

84. **Tonge, R., J. Shaw, B. Middleton, R. Rowlinson, S. Rayner, J. Young, F. Pognan, E. Hawkins, I. Currie, and M. Davison.** 2001. Validation and development of fluorescence two-dimensional differential gel electrophoresis proteomics technology. Proteomics **1:**377-96.

85. **Vander Heide, R. S.** 2002. Increased expression of HSP27 protects canine myocytes from simulated ischemia-reperfusion injury. Am J Physiol Heart Circ Physiol **282:**H935-41.

86. **Vestal, M. L., and J. M. Campbell.** 2005. Tandem time-of-flight mass spectrometry. Methods Enzymol **402:**79-108.

87. **Wainberg, Z., M. Oliveira, S. Lerner, Y. Tao, and B. G. Brenner.** 1997. Modulation of stress protein (hsp27 and hsp70) expression in CD4+ lymphocytic cells following acute infection with human immunodeficiency virus type-1. Virology **233:**364-73.

88. **Wakayama, T., and S. Iseki.** 1998. Expression and cellular localization of the mRNA for the 25-kDa heat-shock protein in the mouse. Cell Biol Int **22:**295-304.

89. **Woodruff, J. F.** 1980. Viral myocarditis. A review. Am J Pathol **101:**425-84.

90. **Yan, J. X., A. T. Devenish, R. Wait, T. Stone, S. Lewis, and S. Fowler.** 2002. Fluorescence two-dimensional difference gel electrophoresis and mass spectrometry based proteomic analysis of Escherichia coli. Proteomics **2:**1682-98.

91. **Yokota, S., N. Yokosawa, T. Kubota, T. Okabayashi, S. Arata, and N. Fujii.** 2003. Suppression of thermotolerance in mumps virus-infected cells is caused by lack of HSP27 induction contributed by STAT-1. J Biol Chem **278:**41654-60.

92. **Zurney, J., K. E. Howard, and B. Sherry.** 2007. Basal expression levels of IFNAR and Jak-STAT components are determinants of cell-type-specific differences in cardiac antiviral responses. J Virol **81:**13668-80.

93. **Zurney, J., T. Kobayashi, G. H. Holm, T. S. Dermody, and B. Sherry.** 2009. Reovirus mu2 protein inhibits interferon signaling through a novel mechanism involving nuclear accumulation of interferon regulatory factor 9. J Virol **83:**2178-87.

Table 3.1. Reovirus selected for infection of primary cardiac myocyte cultures

Reovirus strain	Causes myocarditis? [1]	Induces IFN-β? [2]
T3D	-	+++
DB93A	-	+/-
T1L	+	-
8B	+++	++

[1] Based on (73).
[2] Based on (76).

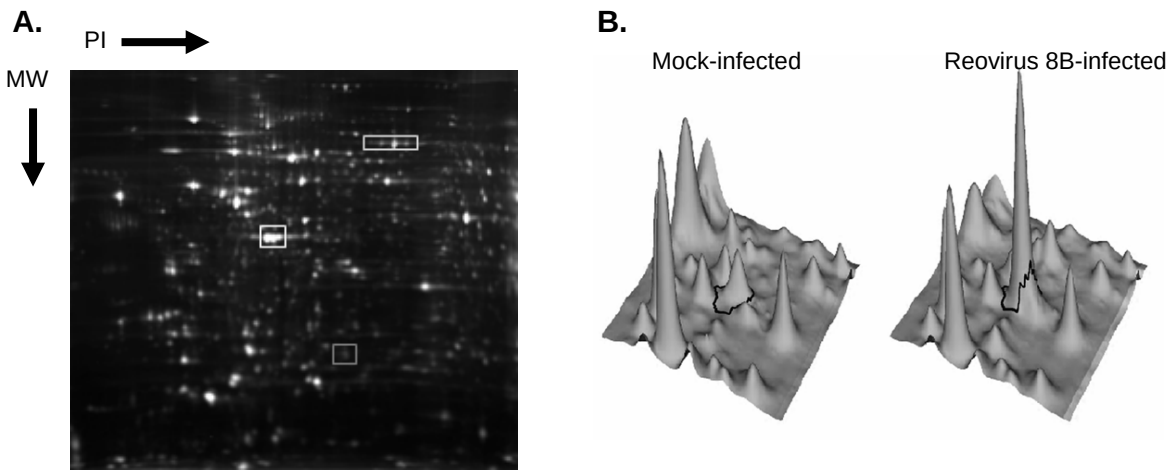

Figure 3.1. Representative 2D-DIGE gel image and 3D-view. Triplicate wells of primary cardiac myocyte cultures were mock- or reovirus-infected (moi 10 pfu per cell, Table 1), and whole cell lysates were harvested 12 hours post-infection for 2D-DIGE. A) Representative gel containing mock- (Cy3-labeled) and 8B- (Cy5-labeled) infected cardiac myocyte samples as well as an internal standard (Cy2-labeled) composed of a pool of all samples. While colors are not indicated here, in the original image, green indicates greater expression in the 8B- than in mock-infected sample, red indicates the converse, white indicates equivalent expression, and blue indicates presence in the pooled internal control but neither of the two samples. B) Example of 3D-view for Cy3 or Cy5 intensity for a selected protein spot (ringed in black).

Supplemental Table 3.1. Gel setup of the DIGE gels

Gel #	Cy3	Cy5
1	T3D-1	8B-1
2	T3D-3	T1L-1
3	DB93A-1	T3D-2
4	MOCK-1	8B-3
5	T1L-1	MOCK-2
6	8B-2	DB93A-2
7	DB93A-3	MOCK-3
8	T1L-3	POOL-CY5

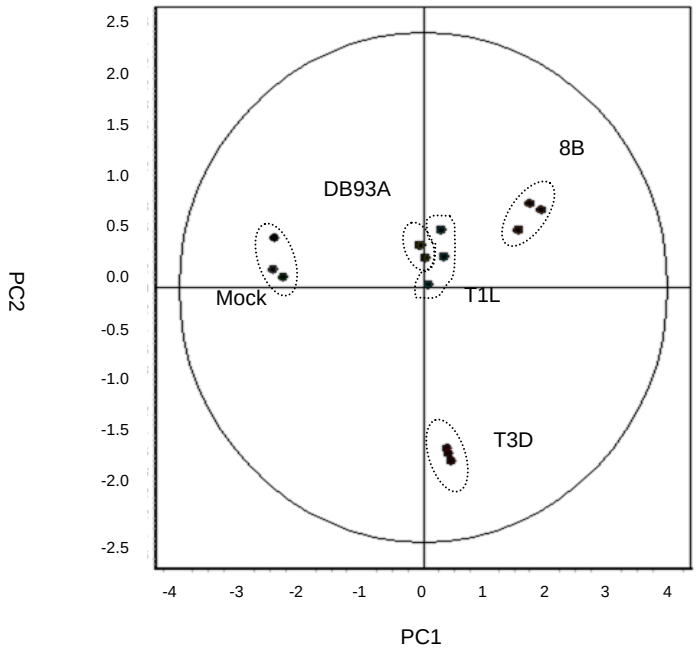

Figure 3.2. Principle Component Analysis (PCA). PCA was performed on the triplicate samples for the 197 differentially expressed proteins identified by 2D-DIGE. Each data point represents all 197 proteins for one sample. PC1 accounted for 55.8% of the variance, while PC2 accounted for 23.3% of the variance.

Supplemental Table 3.2. Biological function of differentially expressed proteins in T3D- and 8B-infected primary cardiac myocyte cultures

Category	Group	P-value	Molecules
Unique for T3D			
Organ Morphology	T3D	1.52E-04-2.82E-02	TPM1, HSP90B1, MYH6, TNNT2
Cell Signaling	T3D	2.38E-03-4.88E-02	NPM1 (includes EG:18148), TNNT2, PGM1, ANXA7
Vitamin and Mineral Metabolism	T3D	2.38E-03-1.13E-02	TNNT2, PGM1, ANXA7
Infection Mechanism	T3D	7.12E-03-4.66E-02	PDCD6IP
Lymphoid Tissue Structure and Development	T3D	2.82E-02-2.82E-02	HSP90B1
Renal and Urological System Development and Function	T3D	3.05E-02-3.05E-02	HSP90B1
Immune Cell Trafficking	T3D	4.36E-02-4.36E-02	PSME1, HSP90B1
For both T3D and 8B			
Cellular Assembly and Organization	T3D	2.11E-05-4.25E-02	TPM1, MYH6, ACTB, TNNT2, HOOK3, MYO1B, FSCN1, GORASP2, VCP, EIF3A, CALD1, ANXA7, PDCD6IP
	8B	2.75E-03-4.14E-02	MYH6, LCP1, HSPA1B, PDIA3, GFM1, RFC1, SEPT11, GSN, DCTN2, HOOK3, TOP1, MYO1B, PLS3, FSCN1, VCP, EIF3A, CALD1, ANXA7
Cellular Function and Maintenance	T3D	2.11E-05-4.66E-02	TPM1, HSP90B1, MYH6, FSCN1, VCP, ADK (includes EG:132), TNNT2, PGM1, ANXA7, LMNB1, HSPB1
	8B	2.28E-05-2.7E-02	LCP1, MYH6, HSPA1B, RFC1, HSPA5, GSN, DCTN2, DYNC1I2, NDUFS1, HSP90B1, PLS3, FSCN1, VCP, UQCRC1, HSPB1, PRKAR1A
Skeletal and Muscular System Development and Function	T3D	2.11E-05-3.51E-02	TPM1, HSP90B1, MYH6, TNNT2, CALD1, ANXA7
	8B	2.75E-03-3.63E-02	HSP90B1, MYH6, CALD1, ANXA7, GSN, PLOD3
Cardiovascular System Development and Function	T3D	2.73E-05-4.76E-03	TPM1, MYH6, TNNT2, ANXA7
	8B	1.05E-02-1.05E-02	ANXA7
Tissue Development	T3D	2.73E-05-2.82E-02	TPM1, HSP90B1, MYH6, TNNT2
	8B	2.75E-03-4.64E-02	MYH6, HSP90B1, LAMB1, PRKAR1A
Cell Death	T3D	1.98E-04-4.36E-02	TPM1, NPM1 (includes EG:18148), HSP90B1, IMMT, ACTB, TNNT2, VCP, ANXA7, PDCD6IP, LMNB1, EEF1D, HSPB1
	8B	6.72E-04-4.64E-02	UTP11L (includes EG:51118), SDHA (includes EG:6389), NPM1 (includes EG:18148), P4HB, HSPA1B, PDIA3, HSPA9, RFC1, HSPA5, MDH1, GSN, DCTN2, HSP90B1, GSPT1, TOP1, NDUFS1, ENO1, VCP, ANXA7, UBA1, RAD23B, HSPB1, PRKAR1A

Supplemental Table 3.2. Continued

Skeletal and Muscular Disorders	T3D	1.98E-04-1.65E-02	VCP, TNNT2, CALD1, EEF1D, HSPB1
	8B	2.98E-05-3.63E-02	SDHA (includes EG:6389), PLOD2, ENO3, PPP1CB, MDH1, LDHB, DCTN2, PDHA1 (includes EG:5160), P4HA1, COL1A1, TOP1, MYO1B, VCP, DLD, LAMB1, CALD1, UQCRC1, HSPB1
Cardiovascular Disease	T3D	4.43E-04-2.82E-02	TPM1, MYH6, TNNT2
	8B	2.98E-05-3.12E-02	PDHA1 (includes EG:5160), SDHA (includes EG:6389), COL1A1, MYH6, DLD
Cellular Compromise	T3D	1.02E-03-1.42E-02	TPM1, HSP90B1, HOOK3, GORASP2, VCP, HSPB1
	8B	9.57E-04-4.64E-02	SDHA (includes EG:6389), PLOD2, HSPA1B, NDUFA10 (includes EG:4705), PDIA3, SEPT11, GSN, HSPA5, ZNF791, HOOK3, HSP90B1, ATP5B, PDIA6, GORASP2, VCP, DLD, KARS, RNH1, UQCRC1, PLOD3, HSPB1
Tissue Morphology	T3D	1.02E-03-2.82E-02	TPM1, HSP90B1, MYH6, TNNT2, CALD1
	8B	5.27E-03-1.57E-02	HSP90B1, GSN, PLOD3
Neurological Disease	T3D	1.12E-03-4.2E-02	NPM1 (includes EG:18148), ACTB, HSPB1
	8B	2.98E-05-4.64E-02	NPM1 (includes EG:18148), STRN, HSPA1B, PDIA3, ENO3, PPP1CB, SEPT11, HSPA5, MDH1, LDHB, PDHA1 (includes EG:5160), TOP1, HSP90B1, MYO1B, ASPM, VCP, LAMB1, LASP1, SDHA (includes EG:6389), PLOD2, P4HB, GFM1, GSN, DCTN2, P4HA1, CAP2, DLD, UBA1, UQCRC1, PRKAR1A, HSPB1
Cancer	T3D	2.38E-03-4.43E-02	IFIT3, ALDH1B1, TPM1, HSP90B1, IMMT, FSCN1, GORASP2, VCP, ANXA7, PDCD6IP, LMNB1, HSPB1
	8B	3.03E-03-4.83E-02	HSPA1B, NDUFA10 (includes EG:4705), PDIA3, MDH1, HSPA5, PRKCSH, HSPA4, GSPT1, HSP90B1, TOP1, GORASP2, VCP, LASP1, PLOD3, PLOD2, IFIT3, ALDH1B1, P4HB, GSN, GLG1, P4HA1, COL1A1, ZNF791, ACOT2, ATP5B, PDIA6, ENO1, FSCN1, CALD1, UBA1, UQCRC1, PRKAR1A
Carbohydrate Metabolism	T3D	2.38E-03-2.38E-03	PPA1
	8B	5.27E-03-2.61E-02	PDIA3, GSN, PRKAR1A
Cell Cycle	T3D	2.38E-03-9.49E-03	TPM1, ASPM, GORASP2
	8B	5.27E-03-4.14E-02	COL1A1, TOP1, ASPM, GORASP2, DCTN2
Cell Morphology	T3D	2.38E-03-3.51E-02	TPM1, VCP, CALD1, ANXA7, PDCD6IP, LMNB1, HSPB1
	8B	5.27E-03-4.68E-02	HSPA4, COL1A1, TOP1, PDIA3, VCP, CALD1, GSN, HSPB1, DCTN2
Cell-To-Cell Signaling and Interaction	T3D	2.38E-03-4.36E-02	PSME1, HSP90B1, CALD1, ANXA7, PDCD6IP
	8B	5.27E-03-4.64E-02	HSP90B1, PDIA3, CALD1, ANXA7, PRKAR1A
Connective Tissue Development and Function	T3D	2.38E-03-4.66E-02	TPM1, NPM1 (includes EG:18148), ADK (includes EG:132), CALD1, EEF1D
	8B	1.05E-02-3.63E-02	COL1A1, GSN

Supplemental Table 3.2. Continued

DNA Replication, Recombination, and Repair	T3D	2.38E-03-4.2E-02	MYH6, VCP, ADK (includes EG:132), PDCD6IP
	8B	3.96E-03-4.14E-02	MYH6, TOP1, HSPA1B, ATP5B, PDIA3, VCP, ADK (includes EG:132), RAD23B, DCTN2
Molecular Transport	T3D	2.38E-03-4.88E-02	NPM1 (includes EG:18148), ADK (includes EG:132), VCP, PDCD6IP
	8B	1.39E-03-4.47E-02	NPM1 (includes EG:18148), COL1A1, ERP29, ATP5B, ENO1, PDIA3, ADK (includes EG:132), VCP, HSPA9, DLD, GSN
Nucleic Acid Metabolism	T3D	2.38E-03-4.2E-02	MYH6, ADK (includes EG:132), PPA1
	8B	4.17E-04-3.63E-02	NDUFS1, MYH6, ATP5B, ENO1, ADK (includes EG:132), DLD, PDHB (includes EG:5162)
RNA Trafficking	T3D	2.38E-03-1.42E-02	EIF3A, PDCD6IP
	8B	3.12E-02-3.12E-02	EIF3A
Reproductive System Disease	T3D	2.38E-03-4.43E-02	TPM1, GORASP2, ANXA7, PDCD6IP
	8B	5.27E-03-1.47E-02	P4HB, NDUFA10 (includes EG:4705), PDIA3, GSN, COL1A1, ZNF791, GSPT1, TOP1, HSP90B1, ATP5B, PDIA6, ENO1, GORASP2, FSCN1, UQCRC1, PLOD3
Small Molecule Biochemistry	T3D	2.38E-03-4.43E-02	MYH6, ADK (includes EG:132), PGM1, ANXA7, PDCD6IP, PPA1
	8B	5.58E-07-3.63E-02	SDHA (includes EG:6389), P4HB, MYH6, PDIA3, GSN, MDH1, P4HA1, NDUFS1, ATP5B, ACOT2, ENO1, ADK (includes EG:132), KARS, DLD, PDHB (includes EG:5162), PLOD3, PRKAR1A
Tumor Morphology	T3D	2.38E-03-3.05E-02	TPM1, HSP90B1, EEF1D
	8B	1.05E-02-2.09E-02	HSPA4, COL1A1
Protein Synthesis	T3D	4.23E-03-7.54E-03	NPM1 (includes EG:18148), TNNT2, VCP, EIF3A, HSPB1
	8B	1.9E-03-4.85E-02	NPM1 (includes EG:18148), VCP, KARS, EIF3A, SEPT11, HSPA5, HSPB1, PRKCSH
Embryonic Development	T3D	4.76E-03-2.12E-02	HSP90B1, ASPM
	8B	5.27E-03-4.64E-02	TOP1, HSP90B1, ASPM, GSN, PRKAR1A
Hepatic System Disease	T3D	4.76E-03-4.76E-03	ADK (includes EG:132)
	8B	1.05E-02-3.12E-02	ADK (includes EG:132), HSPA5, PRKCSH
Lipid Metabolism	T3D	4.76E-03-4.76E-03	PDCD6IP
	8B	1.2E-03-3.12E-02	SDHA (includes EG:6389), ACOT2, PDIA3, DLD, GSN, PDHB (includes EG:5162), PRKAR1A
Nervous System Development and Function	T3D	4.76E-03-3.74E-02	ASPM, HSPB1
	8B	1.05E-02-1.05E-02	PDIA3, ASPM
Genetic Disorder	T3D	7.12E-03-3.51E-02	MYH6, ACTB, VCP, HSPB1
	8B	2.98E-05-3.63E-02	SDHA (includes EG:6389), PLOD2, ENO3, PPP1CB, GSN, LDHB, PRKCSH, PDHA1 (includes EG:5160), COL1A1, P4HA1, TOP1, MYO1B, FSCN1, VCP, DLD, LAMB1, CALD1, UBA1, UQCRC1, HSPB1, PRKAR1A

Supplemental Table 3.2. Continued

Cell-mediated Immune Response	T3D	7.72E-03-2.59E-02	TPM1, HSP90B1, ANXA7, PDCD6IP, LMNB1, HSPB1
	8B	4.64E-02-4.64E-02	HSP90B1
Cellular Movement	T3D	9.49E-03-3.97E-02	TPM1, FSCN1
	8B	3.53E-03-3.63E-02	COL1A1, FSCN1, GSN
Connective Tissue Disorders	T3D	1.18E-02-1.18E-02	CALD1
	8B	5.27E-03-2.61E-02	PLOD2, COL1A1, HSPA1B, CALD1
Developmental Disorder	T3D	1.18E-02-1.18E-02	MYH6
	8B	9.61E-04-3.63E-02	COL1A1, MYH6, PLOD3, PRKAR1A
Infectious Disease	T3D	1.18E-02-1.18E-02	CALD1
	8B	8.94E-03-4.66E-02	PLOD2, NDUFA10 (includes EG:4705), PDIA3, PPP1CB, ZNF791, TOP1, ATP5B, PDIA6, KARS, CALD1, RNH1, UQCRC1, PLOD3
Inflammatory Disease	T3D	1.18E-02-2.82E-02	MYH6, CALD1
	8B	2.61E-02-2.61E-02	CALD1
Organismal Injury and Abnormalities	T3D	1.18E-02-2.36E-02	MYH6, TNNT2
	8B	5.27E-03-3.12E-02	COL1A1, MYH6, PLOD3
Protein Degradation	T3D	1.18E-02-1.18E-02	HSP90B1
	8B	2.71E-04-2.71E-04	HSP90B1, HSPA5
Gene Expression	T3D	1.42E-02-1.42E-02	EIF3A
	8B	5.27E-03-3.12E-02	TOP1, ENO1, EIF3A, RFC1
Metabolic Disease	T3D	1.65E-02-1.65E-02	VCP
	8B	1.05E-02-3.63E-02	PDHA1 (includes EG:5160), VCP, DLD, GSN
RNA Damage and Repair	T3D	1.65E-02-1.65E-02	DNAJB11
	8B	2.39E-03-3.63E-02	GSPT1, HSPA1B, APOBEC2
RNA Post-Transcriptional Modification	T3D	1.65E-02-4.03E-02	NPM1 (includes EG:18148), DNAJB11
	8B	5.27E-03-3.63E-02	APOBEC2, KARS
Cellular Development	T3D	1.89E-02-3.28E-02	TPM1, NPM1 (includes EG:18148), HSP90B1, MYH6
	8B	4.14E-02-4.14E-02	MYH6
Cellular Growth and Proliferation	T3D	2.12E-02-4.43E-02	TPM1, NPM1 (includes EG:18148), HSP90B1, ANXA7
	8B	9.34E-03-4.64E-02	NPM1 (includes EG:18148), IFIT3, LCP1, PDIA3, GFM1, RFC1, HSPA5, GSN, PRKCSH, COL1A1, HSP90B1, TOP1, ATP5B, ENO1, LAMB1, ANXA7, UBA1, PRKAR1A
Hematological System Development and Function	T3D	2.12E-02-4.36E-02	PSME1, HSP90B1, ANXA7
	8B	1.05E-02-4.64E-02	HSP90B1, GSN, DCTN2
Hematological Disease	T3D	2.59E-02-4.2E-02	HSP90B1
	8B	6.94E-06-1.57E-02	P4HB, ENO1, PDIA3, HSPA5, GSN, PRKAR1A
Immunological Disease	T3D	2.82E-02-4.36E-02	HSP90B1, MYH6, LMNB1, HSPB1
	8B	6.94E-06-4.14E-02	P4HB, ENO1, PDIA3, HSPA5, GSN

Supplemental Table 3.2. Continued

Protein Trafficking	T3D	2.85E-02-2.85E-02	NPM1 (includes EG:18148), VCP
	8B	5.16E-03-2.61E-02	COL1A1, ERP29, PDIA3, VCP, HSPA9
Dermatological Diseases and Conditions	T3D	3.97E-02-3.97E-02	FSCN1
	8B	3.53E-03-3.12E-02	COL1A1, FSCN1, GSN
Energy Production	T3D	4.2E-02-4.2E-02	MYH6
	8B	4.17E-04-4.14E-02	NDUFS1, MYH6, ATP5B, ENO1, ADK (includes EG:132), DLD, MDH1
Antigen Presentation	T3D	4.36E-02-4.36E-02	PSME1, HSP90B1
	8B	1.57E-02-3.63E-02	DCTN2
Unique for 8B			
Inflammatory Response	8B	1.05E-02-3.63E-02	GSN, DCTN2
Post-Translational Modification	8B	5.58E-07-1.05E-02	PLOD2, P4HB, PDIA3, PPP1CB, HSPA5, GSN, HSPA4, P4HA1, GSPT1, ERP29, PDIA6, UBA1, PLOD3
Protein Folding	8B	7.75E-03-7.75E-03	ERP29, PDIA6, HSPA5
Free Radical Scavenging	8B	1.57E-02-1.57E-02	GSN
Amino Acid Metabolism	8B	5.58E-07-5.27E-03	P4HA1, P4HB, PLOD3
Organismal Development	8B	5.27E-03-4.14E-02	TOP1, RAD23B, DCTN2, PRKAR1A
Reproductive System Development and Function	8B	2.09E-02-2.09E-02	TOP1
Organismal Functions	8B	1.57E-02-1.57E-02	DCTN2
Respiratory Disease	8B	6.94E-06-3.11E-02	ALDH1B1, P4HB, HSP90B1, TOP1, ENO1, PDIA3, HSPA5, GSN
Gastrointestinal Disease	8B	5.27E-03-3.43E-02	PLOD2, COL1A1, P4HA1, HSP90B1, P4HB, TOP1, FSCN1, CALD1, UBA1, HSPA5, GSN, GLG1
Renal and Urological Disease	8B	4.89E-03-2.09E-02	TOP1, HSPA1B, PRKAR1A

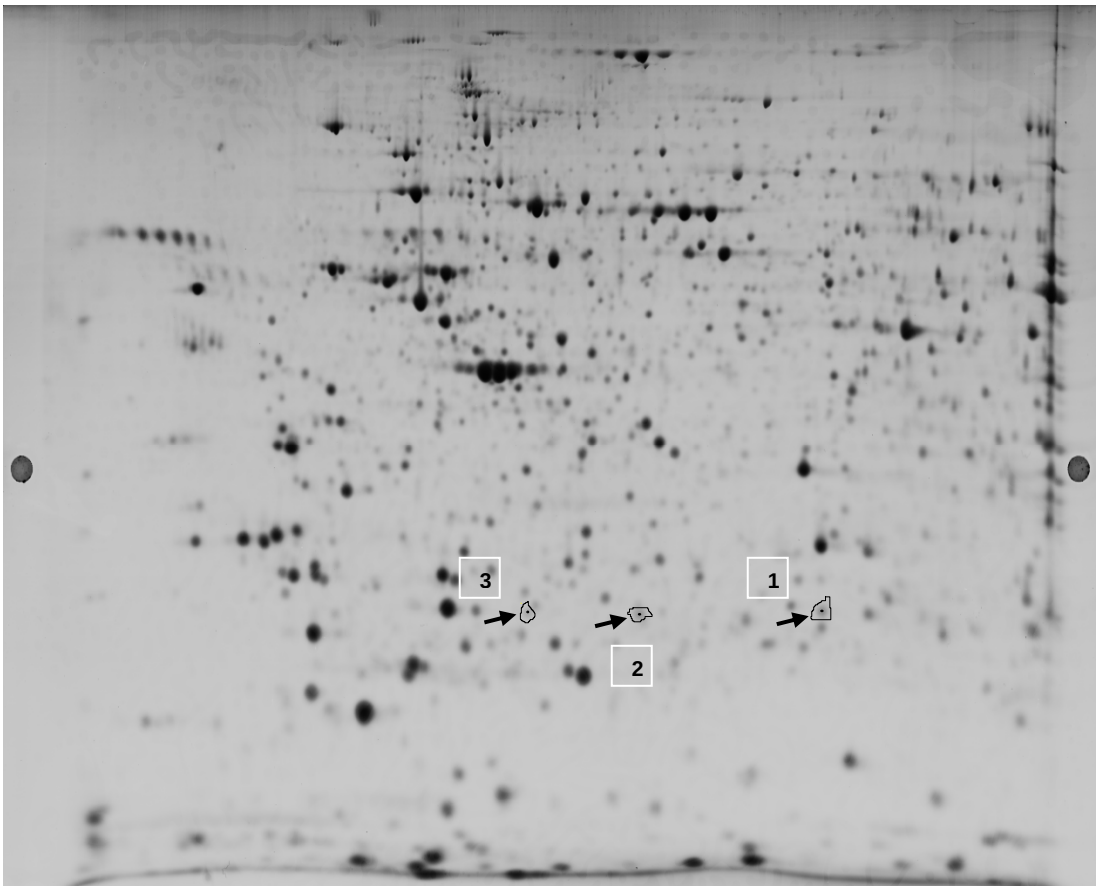

Supplemental Figure 3.1. Hsp25 2D-DIGE gel spots. The three gel spots picked and identified as Hsp25 are indicated on this image of the master gel. They have the same molecular weight, but vary from more basic (gel spot #1) to more acidic (gel spot #3).

Supplemental Table 3.3. Swiss-Prot analysis of Spot #1 (most basic spot; putative unphosphorylated Hsp25) [1]

Observed Mr [2]	Exper. Mr	Calc. Mr	Delta	AA Start	AA End	Miss	Ions	Peptide	Comment
927.60	926.59	926.48	0.11	193	202	0	-	AQIGGPEAGK	
931.60	930.59	930.50	0.09	119	127	0	-	EGVVEITGK	
1005.57	1004.56	1004.47	0.09	13	20	0	48	SPSWEPFR	
1005.57	1004.56	1004.47	0.09	13	20	0	-	SPSWEPFR	
1031.57	1030.56	1030.46	0.10	21	28	0	-	DWYPAHSR	
1031.57	1030.56	1030.46	0.10	21	28	0	49	DWYPAHSR	
1075.67	1074.67	1074.57	0.10	84	93	0	28	QLSSGVSEIR	
1075.67	1074.67	1074.57	0.10	84	93	0	-	QLSSGVSEIR	Oxidation (M)
1104.61	1103.60	1103.50	0.10	132	140	0	62	QDEHGYISR	
1104.61	1103.60	1103.50	0.10	132	140	0	-	QDEHGYISR	
1149.71	1148.71	1148.60	0.11	29	38	0	91	LFDQAFGVPR	
1149.71	1148.71	1148.60	0.11	29	38	0	-	LFDQAFGVPR	Oxidation (M)
1798.10	1797.10	1796.93	0.17	101	116	0	-	VSLDVNHFAPEELTVK	
1798.10	1797.10	1796.93	0.17	101	116	0	49	VSLDVNHFAPEELTVK	
1833.14	1832.13	1831.97	0.17	176	192	0	-	AVTQSAEITIPVTFEAR	
1833.14	1832.13	1831.97	0.17	176	192	0	81	AVTQSAEITIPVTFEAR	

[1] (P14602) Heat shock 27 kDa protein (Hsp 27, Hsp 25), Mass: 23000, Score: 459

[2] Additional peptides for which there was no match (and which could include post-translationally modified Hsp25 peptides): 1009.57, 1018.57, 1021.57, 1021.57, 1035.56, 1037.57, 1037.57, 1047.56, 1051.56, 1053.56, 1058.65, 1062.58, 1063.57, 1079.59, 1087.58, 1095.62, 1126.66, 1134.72, 1148.68, 1161.72, 1171.70, 1175.73, 1187.67, 1203.64, 1314.91, 1332.86, 1424.89, 1499.93, 1528.96, 1630.01, 1634.08, 1701.05, 1820.09, 1847.15, 1923.11, 1941.12, 1985.25, 1987.26, 2003.27, 2079.31, 2079.31, 2091.33, 2230.41, 2233.41, 2285.38, 2288.29, 2304.27, 2316.32, 2319.22, 2331.24, 2334.50, 2435.47, 2440.26, 2596.41, 2679.57, 3065.97, 3110.93, 3194.04, 3347.02

Supplemental Table 3.4. Swiss-Prot analysis of Spot #2 (middle spot; putative mono-phosphorylated Hsp25) [1]

Observed Mr [2]	Exper. Mr	Calc. Mr	Delta	AA Start	AA End	Miss	Ions	Peptide
927.58	926.58	926.48	0.09	193	202	0	----	AQIGGPEAGK
1005.56	1004.55	1004.47	0.08	13	20	0	36	SPSWEPFR
1005.56	1004.55	1004.47	0.08	13	20	0	----	SPSWEPFR
1031.55	1030.54	1030.46	0.08	21	28	0	----	DWYPAHSR
1031.55	1030.54	1030.46	0.08	21	28	0	51	DWYPAHSR
1075.66	1074.65	1074.57	0.08	84	93	0	2	QLSSGVSEIR
1075.66	1074.65	1074.57	0.08	84	93	0	----	QLSSGVSEIR
1104.59	1103.59	1103.50	0.09	132	140	0	60	QDEHGYISR
1104.59	1103.59	1103.50	0.09	132	140	0	----	QDEHGYISR
1149.70	1148.69	1148.60	0.09	29	38	0	----	LFDQAFGVPR
1149.70	1148.69	1148.60	0.09	29	38	0	73	LFDQAFGVPR
1798.08	1797.07	1796.93	0.14	101	116	0	----	VSLDVNHFAPEELTVK
1798.08	1797.07	1796.93	0.14	101	116	0	50	VSLDVNHFAPEELTVK
1833.11	1832.11	1831.97	0.14	176	192	0	74	AVTQSAEITIPVTFEAR
1833.11	1832.11	1831.97	0.14	176	192	0	----	AVTQSAEITIPVTFEAR

[1] (P14602) Heat shock 27 kDa protein (Hsp 27, Hsp 25), Mass: 23000, Score: 388

[2] Additional peptides for which there was no match (and which could include post-translationally modified Hsp25 peptides): 990.36, 1009.56, 1021.56, 1035.55, 1037.55, 1047.57, 1058.63, 1061.57, 1063.55, 1063.55, **1085.53**, 1087.56, 1089.56, 1101.52, 1117.52, 1126.65, 1148.65, 1165.68, 1171.69, 1175.72, 1187.65, 1194.75, 1203.62, 1314.87, 1345.85, 1424.88, 1528.93, 1569.98, 1629.97, 1634.06, 1701.03, 1720.99, 1794.95, 1820.07, 1923.07, 1941.10, 1969.21, 1987.23, 1987.23, 2003.23, 2079.28, 2079.28, 2091.30, 2230.38, 2265.22, 2297.39, 2316.30, 2317.24, 2334.47, 2408.25, 2564.39, 2663.59, 2679.56, 3065.95, 3094.89, 3111.90, 3194.05, 3339.01, 3346.95, 3355.06. The peptide in **bold** is absent in the putative non-phosphorylated Hsp25 (Supp. Table 3.3), is present in both this putative mono-phosphorylated Hsp25 and di-phosphorylated Hsp25 (Supp. Table 3.5), matches the Exper. Mr for a peptide comprised of residues 13 – 20 with a single phosphorylation, is predicted to be phosphorylated on serine 15 by NetPhos 2.0 software, and includes a serine residue previously shown by others to be phosphorylated (serine 15).

Supplemental Table 3.5. Swiss-Prot analysis of Spot #3 (most acidic spot; putative di-phosphorylated Hsp25) [1]

Observed Mr [2]	Exper. Mr	Calc. Mr	Delta	AA Start	AA End	Miss	Ions	Peptide
927.58	926.57	926.48	0.09	193	202	0	----	AQIGGPEAGK
931.59	930.58	930.50	0.08	119	127	0	----	EGVVEITGK
932.57	931.56	931.46	0.10	94	100	1	----	QTADRWR
1031.55	1030.55	1030.46	0.08	21	28	0	----	DWYPAHSR
1031.55	1030.55	1030.46	0.08	21	28	0	48	DWYPAHSR
1104.59	1103.59	1103.50	0.09	132	140	0	----	QDEHGYISR
1104.59	1103.59	1103.50	0.09	132	140	0	38	QDEHGYISR
1149.70	1148.69	1148.60	0.09	29	38	0	----	LFDQAFGVPR
1149.70	1148.69	1148.60	0.09	29	38	0	68	LFDQAFGVPR
1798.08	1797.07	1796.93	0.14	101	116	0	49	VSLDVNHFAPEELTVK
1798.08	1797.07	1796.93	0.14	101	116	0	----	VSLDVNHFAPEELTVK
1833.12	1832.11	1831.97	0.14	176	192	0	----	AVTQSAEITIPVTFEAR
1833.12	1832.11	1831.97	0.14	176	192	0	106	AVTQSAEITIPVTFEAR
2018.08	2017.08	2016.92	0.15	13	28	1	----	SPSWEPFRDWYPAHSR

[1] (P14602) Heat shock 27 kDa protein (Hsp 27, Hsp 25), Mass: 23000, Score: 359

[2] Additional peptides for which there was no match (and which could include post-translationally modified Hsp25 peptides): 1035.55, 1047.55, 1061.58, 1063.55, 1071.72, **1085.53**, 1087.56, 1089.56, 1101.53, 1108.64, 1117.52, 1126.65, 1148.67, **1155.63**, 1165.68, 1171.68, 1175.72, 1179.69, 1187.67, 1277.80, 1282.78, 1307.78, 1314.88, 1316.87, 1424.88, 1425.87, 1475.87, 1528.93, 1701.03, 1794.95, 1820.07, 1923.07, 1941.09, 1941.09, 1969.22, 1985.22, 1987.23, 1987.23, 2003.23, 2079.28, 2079.28, 2091.31, 2230.38, 2262.34, 2297.37, 2334.47, 2408.24, 2419.44, 2565.38, 2662.57, 2663.58, 2679.58, 2914.76, 3094.89, 3111.93, 3194.00, 3339.00, 3339.00, 3346.89, 3347.98, 3355.05. The peptides in **bold** include the one in supp. Table 3.4 (1085.53), but also a second one (1155.63) which is absent in both the putative non-phosphorylated Hsp25 (Supp. Table 3.3) and mono-phosphorylated Hsp25 (Supp. Table 3.4), matches the Exper. Mr for a peptide comprised of residues 84-93 with one phosphorylation, is predicted to be phosphorylated on serine 86 by NetPhos 2.0 software, and includes a serine residue previously shown by others to be phosphorylated (serine 86).

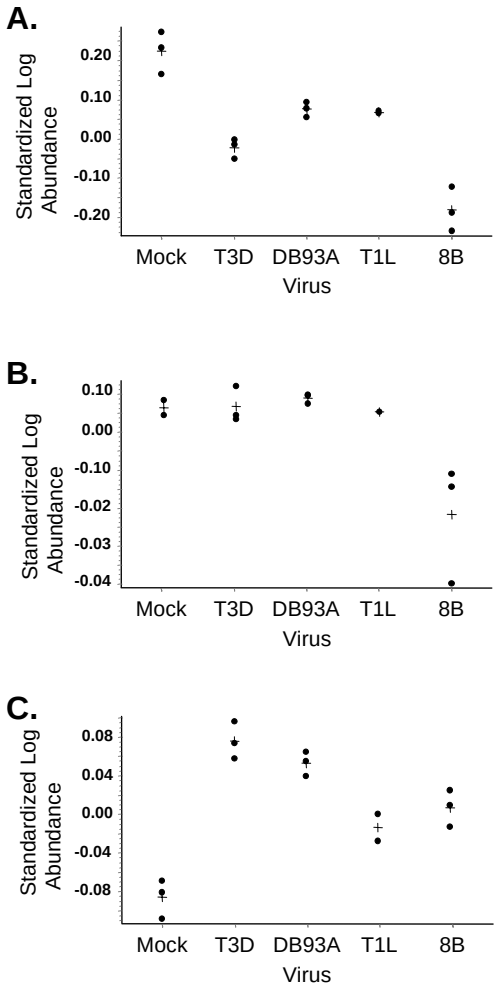

Figure 3.3. Quantification of Hsp25 by 2D-DIGE. Protein abundance was determined for each of the indicated gel spots using DeCyder software. A) Predicted unphosphorylated Hsp25 spot, B) Predicted mono-phosphorylated Hsp25 spot, C) Predicted di-phosphorylated Hsp25 spot. Results from triplicate samples are shown in each case except T1L, where only two (A and C) or one (B) protein spot was detectable on the gels. In some other cases, data-points lie directly on top of one another.

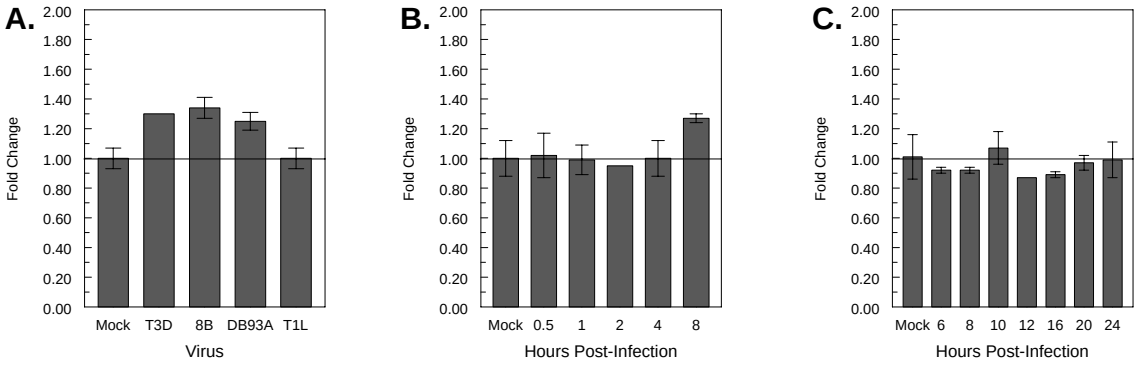

Supplemental Figure 3.2. Reovirus modulation of Hsp25 is post-transcriptional. Primary cardiac myocyte cultures were mock- or T3D infected, and RNA was harvested at the indicated times post-infection for qRT-PCR. Copy number for each sample was first normalized to GAPDH, and then samples from T3D-infected cultures were normalized to those from mock-infected cultures at that same time point. Results are expressed as the average of duplicate wells ± S.D.

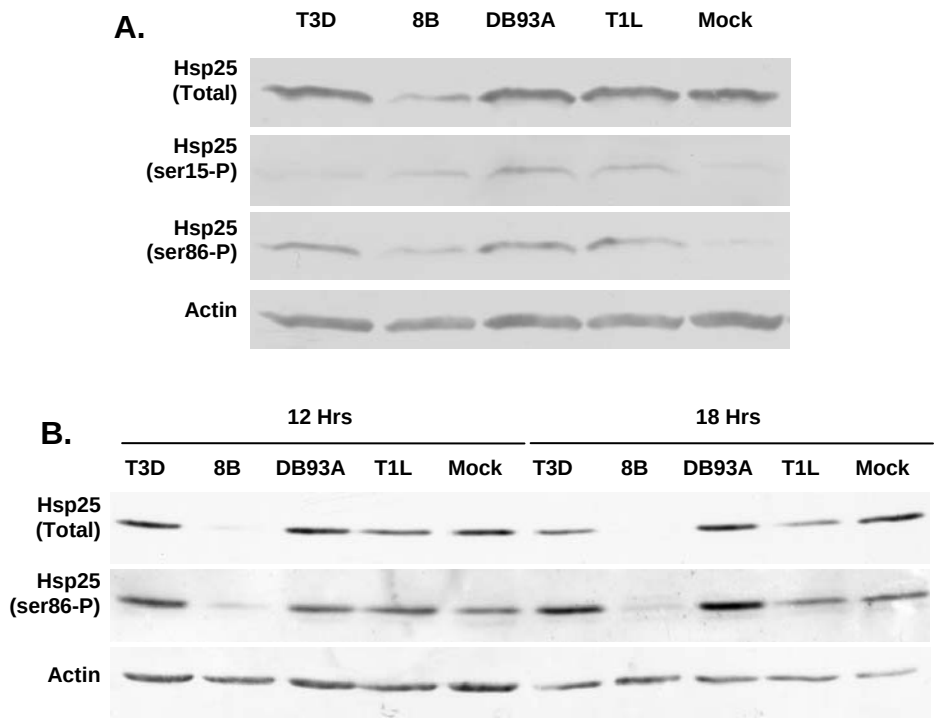

Figure 3.4. Confirmation of Hsp25 expression and phosphorylation by Western blot. Primary cardiac myocyte cultures generated from wild type (A) or IFN-α/β-receptor-null (B) mice were mock- or reovirus-infected as for Figure 1, and harvested 12 hours (A) or 12 and 18 hours (B) post-infection for SDS-PAGE and Western blot analysis using the indicated antibody probes. Results are representative of at least 3 independent experiments.

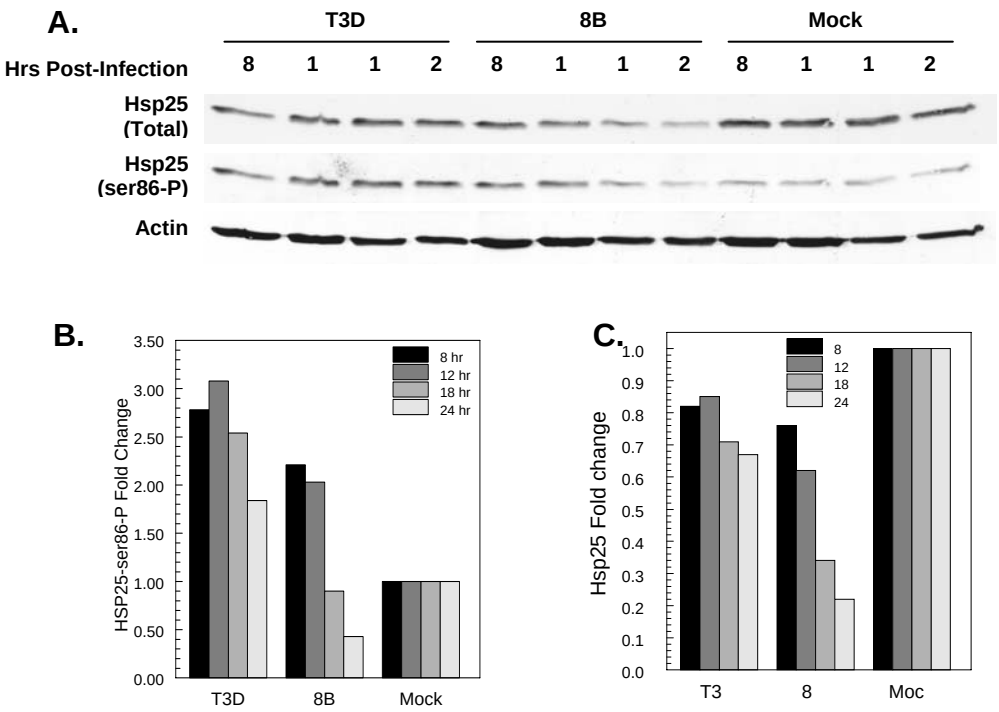

Figure 3.5. Reovirus-induced phosphorylation and degradation of Hsp25 is virus strain-specific. Primary cardiac myocyte cultures were mock-, T3D- or 8B-infected at an moi of 10 pfu per cell, and cultures were harvested for SDS-PAGE and Western blot at the indicated times post-infection. For each sample, the band intensity for Hsp25-Ser86-P (A) or Hsp25 (B) was first normalized to that for actin, and then normalized to the mock-infected sample at that same time-point. Each bar represents the single samples shown, and is representative of similar results from at least 3 independent independent experiments.

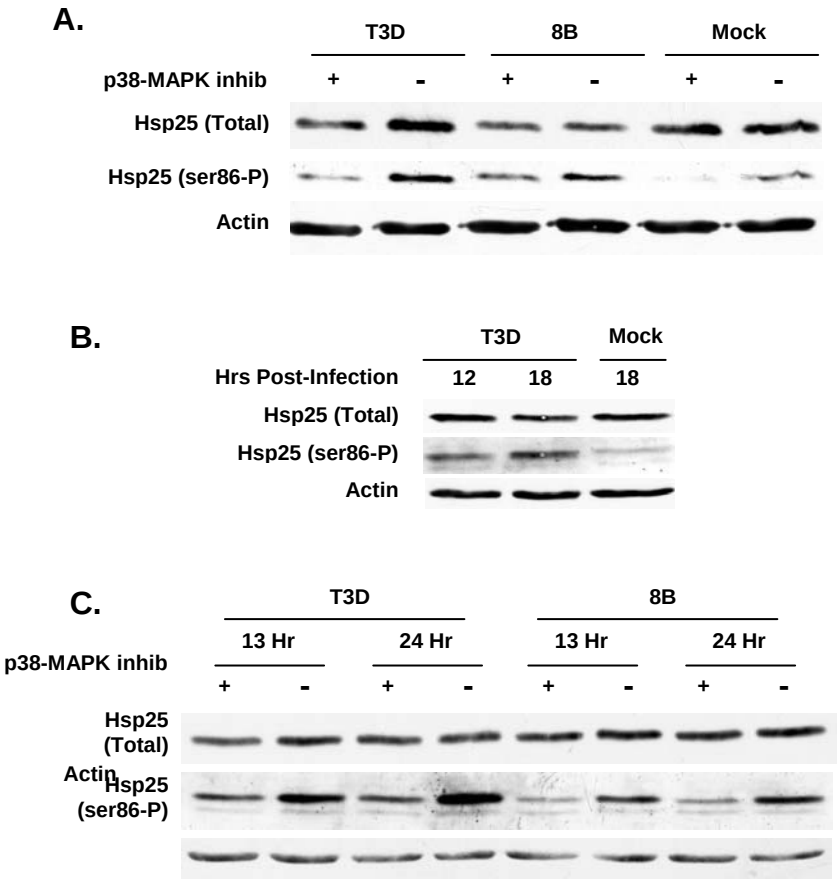

Figure 3.6. Reovirus-induced phosphorylation of Hsp25 is p38-MAPK-dependent and IFN-independent. Primary cardiac myocyte cultures were generated from wild type (A) or IFN-α/β-receptor-null (B, C) mice. Cultures were treated with 50 μM p38-MAPK inhibitor SB203580 for 1 hour as indicated (A, C) or left untreated (B), and then mock- or reovirus-infected (moi 10 pfu per cell) for 13 hours (A) or indicated hours. Total cell lysates were subjected to SDS-PAGE and then transferred to nitrocellulose for Western Blots. Results are representative of 2 experiments.

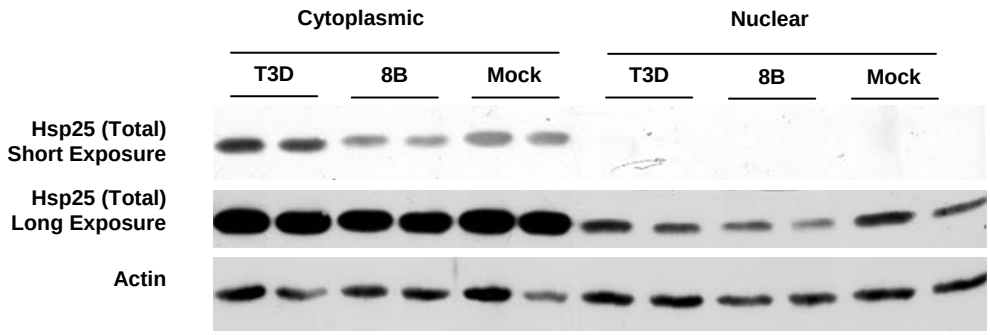

Figure 3.7. Reovirus does not induce nuclear translocation of Hsp25 . Primary cardiac myocyte cultures were mock- or reovirus-infected (moi 10 pfu per cell), and cytoplasmic and nuclear lysates were harvested from duplicate wells at 17 hours post-infection for SDS-PAGE and Western blot to detect total Hsp25 (short film exposure to emphasize cytoplasmic Hsp25 differences; long film exposure to detect nuclear Hsp25). Results are representative of 3 experiments.

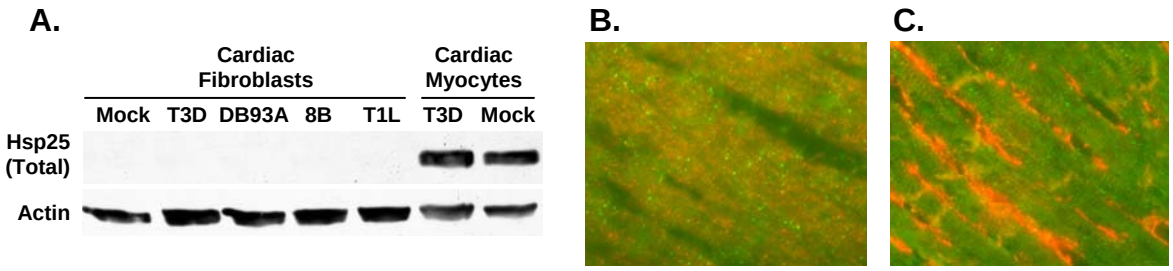

Figure 3.8. Expression of Hsp25 is cell type-specific in the heart. A) Primary cultures of cardiac myocytes and cardiac fibroblasts were mock- or reovirus-infected (moi 10 pfu per cell), and cultures were harvested at 12 hours post-infection for SDS-PAGE and Western blot analysis to detect total Hsp25. B) Cardiac sections from adult mice were stained for Hsp25 (green) and myomesin (red) to detect cardiac myocytes. C) As for (B), but stained for Hsp25 (green) and vimentin (red) to detect cardiac fibroblasts.

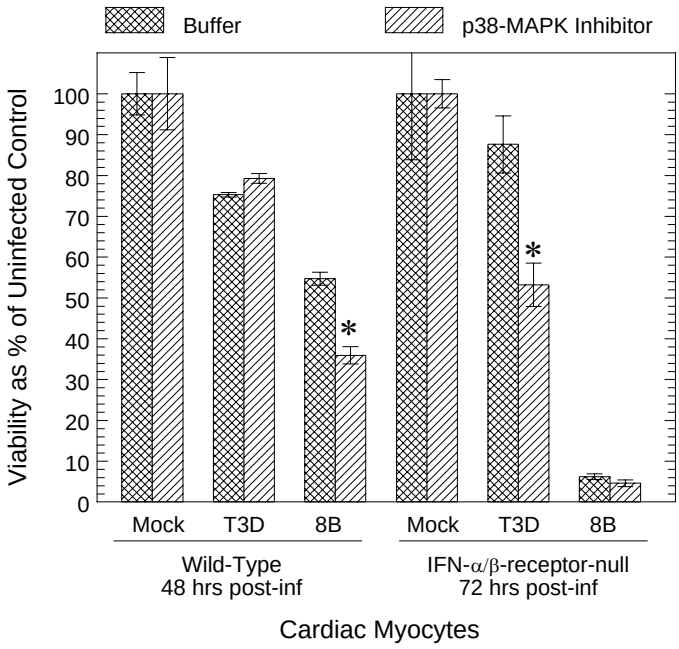

Figure 3.9. Inhibition of p38-MAPK increases T3D- and 8B-induced CPE in cardiac myocytes. Primary cardiac myocyte cultures were generated from wild type or IFN-α/β-receptor null mice, treated with buffer or the p38-MAPK inhibitor S203580 (50 μM) for 1 hour, and then mock- or reovirus-infected (moi 25 pfu per cell). At the indicated time post-infection, cell viability was determined by MTT assay. Results represent the average of triplicate wells ± SD, and are representative of 3 experiments.

APPENDIX 1

Over-Expression of IFN-α2, -α4 and –α5 in Primary Cardiac Myocyte and Fibroblast Cultures

INTRODUCTION

Murine IFN-α occurs as 14 functional subtype genes and 3 pseudogenes, and individual IFN-α subtypes share >80% DNA and protein similarity (3, 8). It has been reported that individual IFN-α subtypes display differential antiviral abilities (1, 5-9). Our Real-Time PCR results demonstrated that reovirus T3D induces IFN-α1, -α2, -α4, -α5, and –α8/6 in primary cultures of mouse cardiac myocytes and cardiac fibroblasts, and that IFN-α2, -α4, and –α5 were expressed at the highest levels. To determine whether they express different antiviral effects against reovirus infection, IFN-α2 and -α4 were cloned and an IFN-α5 construct was purchased, and all were over-expressed in cardiac cell cultures. However, results were unexpected in that even empty vector DNA induced the interferon stimulated genes (ISGs) ISG56 and IRF7, and the antiviral effects elicited by transfected DNA, regardless of content, were greater than any antiviral effects from over-expressed IFN-α2, -α4 and –α5.

MATERIALS AND METHODS

Plasmid construction. The empty plasmid pORF-mcs (catalog # porf-mcs) and pORF-mIFN-α (catalog # porf-mifnα) which over-expresses murine IFN-α5, were purchased from InvivoGen. Primers for amplifying IFN-α2 and -α4 full length cDNA were designed and restriction enzyme sites for EcoRI and NheI were added. Primers for IFN-α2 (593bp), forward: 5'- CGGCgaattcCTCTGCAAGACCCACA -3' (# 507) and reverse: 5'-GGCGgctagcACACTCACTCCTTCT-3' (#508); IFN-α4 (617bp), forward: 5'-CGGCgaattcCAGCATCTACAAGACCC-3' (#509) and reverse: GGCGgctagcGTCCAGAAAAGTCCT-3' (#510) (restriction enzyme sites in lower case letters). As a positive control, IFN-β full length cDNA was also cloned with primers, forward (#539): 5'-CGGCgaattcCCATCATGAACAACAGGTG-3' and reverse (#540): 5'-GGCGgctagcTCAGTTTTGGAAGTTTCTG-3'.

Protocol for cloning genes into pORF-mcs. Reaction components for amplifying genes of interest are shown in Table App.1.1 (using IFN-α2 as an example). PCR was carried out in the MJR thermal cycler (program LLNIFNA2) in a 0.5ml epp, with 50 μl mineral oil overlay. The PCR program was set up as:

Step 1: 98°C, 30"

Step 2: 98°C, 10"

Step 3: 52°C, 20"

Step 4: 72°C, 30"

Repeat Step 2 to 4 for 35 times

Step 5: 72°C, 5’

Step 6: 4°C, 24h

Eppendorf tubes were put onto the thermal cycler only when the temperature reached above 85ºC (as a “Hot Start” protocol). An analytic thin 1% agarose gel in 1 x TBE with 10-well narrow comb was used to verify the product size, and the PCR product was gel purified using QIAquick Gel Extraction Kit (catalog # 28704). After restriction enzyme digestion, the digested PCR mixture was purified with the Wizard SV Gel and PCR clean-up system (Promega, catalog A9281). For the empty vector, the digested mixture was gel purified using the QIAquick Gel Extaction Kit (catalog # 28704). T4 DNA ligase from Promega (catalog M180B) was used for ligation at room temperature for 3 hours (in 1X final ligase buffer diluted from 2X stock) or overnight (in 1X final ligase buffer diluted from 10X stock at 16ºC). The ligation products were transformed into DH5α cells according to the laboratory protocol.

Verification of over-expressed products. Plasmid DNA from MiniPreps were sequenced by the DNA Sequencing facility at the University of Chicago Cancer Research Center (http://cancer-seqbase.bsd.uchicago.edu/template2-36.html). To sequence the region that does not include the promoter region (very close to the start and end of the open reading frame), primers were designed as: Forward (#543): 5’- cgactactaaccttcttctc- 3’, and reverse (#544): 5' - GCATTCTAGTTGTGGTTTG - 3'. To sequence the region that includes promoter, primers were, forward (#583): 5'-CAAAATAGGCTGTCCCCAGT-3', and reverse (#582): 5’-CGGTCACAGCTTGGATCTG-3’.

Transfection of cardiac myocytes. MaxiPrep empty vector DNA pORF-mcs or plasmids containing the genes of interest were transfected into primary cultured cardiac myocytes using the Amaxa Nucleofector device. The Rat Cardiomyocyte-Neonatal Nucleofector^{TM} Kit (catalog # VPE-1002) and program G-07 were used. Briefly, cardiac myocytes were spun down at 340xg (340xg=1380 rpm on the microfuge, but the laboratory protocol lists it as 2000 rpm) for 1 minute. Each transfection included up to 2 x 10^6 cells in 100 µl Nucleofector^{TM} solution, and 2 µg plasmid DNA. Control transfections with a GFP-expressing plasmid suggest that this procedure transfects 1-2% of the cells, which although low, is the maximum for any technique the laboratory has attempted (data not shown).

Transfection of cardiac fibroblasts. Procedure was as above except for the following differences. The Basic Nucleofector Kit for primary mammalian fibroblasts (catalog # VPI-1002) and program U-12 were used. Briefly, cardiac fibroblasts were spun down at 100xg (800 rpm) for 10 minutes. Each transfection included up to 0.5-1 x 10^6 cells in 100 µl Nucleofector^{TM} solution, and 2 µg plasmid DNA. Control transfections with a GFP-expressing plasmid suggest that this procedure transfects 50% of the cells, which is the maximum for any technique the laboratory has attempted (data not shown).

Reverse transcription and Real-Time PCR. Total cell RNA was harvested and used for reverse transcription and Real-Time PCR by standard laboratory protocol. All primers were those used routinely in the laboratory, except for IFN-α4 primers: forward (#527): 5'-GATGAGCTACTACTGGTCAG-3' and reverse (#528): 5' -TTCTCCAAGGGGAATCCAAAA - 3'.

RESULTS

Confirmation of sequences of cloned IFN-α genes. Two colonies for each construct (IFN-α2, -α4 and –β) were selected for DNA sequencing. DNA sequence of IFN-α2 and –β were 100% identical to the RefSeq from GenBank (NM_010503.2 and NM_010510.1, respectively). IFN-α4 had 4 synonymous mutations, and IFN-α5, which was purchased from InVivogen (Figure App.1.1), had 2 non-synonymous mutations (Figure App.1.2).

Confirmation of IFN-α mRNA over-expression by Real-Time PCR. Cardiac myocytes and fibroblasts were transfected, and total cell RNA was harvested at the indicated times post-transfection. Real-Time PCR results demonstrated that the transfected genes were up-regulated dramatically compared to mock-transfected samples or samples transfected with the empty vector, pORF-mcs (Figure App.1.3).

Confirmation of IFN-α protein over-expression and secretion by ELISA. Cardiac myocytes and fibroblasts were transfected, and supernatants were harvested at the indicated times post-transfection. ELISA results demonstrated that IFN-α was up-regulated in a time-dependent manner (Figure App.1.4), and that it was undetectable in samples transfected with the empty vector, pORF-mcs (data not shown). There are no commercially available ELISAs to distinguish between different IFN-α subtypes.

Network of induction of other IFN-α subtypes by over-expressed genes. Real-Time PCR demonstrated that the over-expressed IFN-α genes can induce expression of other IFN-α subtyeps (selected transfection #11 as an example, Figure App.1.5). A network for this induction is summarized from at least 3 independent experiments Figure App.1.6.

Antiviral effects of individual IFN-α subtypes. While the fraction of cardiac myocytes and cardiac fibroblasts transfected was low (2% and 50%, respectively; see Materials and Methods), the induction of other IFN-α subtypes suggested that secreted IFN from the few transfected cells functioned in paracrine stimulation, and might be sufficient to induce antiviral effects in the culture population. To test this, primary cardiac myocyte and cardiac fibroblast cultures were transfected or left untreated (as a negative control), treated with buffer or IFN-β (as a positive control), and then infected with reovirus T3D (moi=1 pfu/cell) 24 hours post-transfection. The infection was incubated for 24 or 44 hours and viral titers were determined by plaque assay (Figure App.1.7). Surprisingly, in cardiac myocytes, transfection with the empty vector pORF-mcs ("mcs") inhibited reovirus replication 10 to 20-fold relative to untreated cells (bar set 1), indicating that the transfection process itself induced a potent antiviral response. Moreover, treatment with IFN-β increased the antiviral effects only approximately 4-fold (bar set 2 divided by bar set 1), indicating that even a potent antiviral treatment generated little antiviral effect relative to the transfection process. Not surprisingly then, cells transfected with the empty vector mcs were protected only 4-fold when treated with IFN-β (bar set 3), and this was similar to the effects of transfected IFN-β or IFN-α5 (bar sets 4 and 5, respectively). IFN-α2 and IFN-α4 had less than a 2-fold effect (data not shown). Together, the data indicate that the transfection process itself induces a potent antiviral response relative to treatment or transfection with Type I IFN in cardiac myocytes, and leaves this an inappropriate approach for characterizing the antiviral response for individual IFN-α subtypes in these cells. In cardiac fibroblasts, the results were more promising. Transfection with the empty vector mcs inhibited reovirus replication only 2-fold

relative to untreated cells (bar set 6), and treatment with IFN-β increased the antiviral effects more than 10-fold (bar set 7 divided by bar set 6). Consistent with these results, cardiac fibroblasts transfected with the empty vector mcs were protected more than 10-fold when treated with IFN-β (bar set 8), and this was similar to the effects of transfected IFN-β or IFN-α5 (bar sets 9 and 10, respectively). IFN-α4 and -α2 had lesser, but detectable, effects. Together, the data indicate that while the transfection process does induce some antiviral effects in cardiac fibroblasts, these effects are minimal compared to those provided by Type I IFN. Moreover, IFN-α5, -α4 and -α2 are each antiviral in this cell type, consistent with results using purified preparations of these cytokines (Chapter 3).

pORF-mcs transfection induces ISGs. Since pORF-mcs induced antiviral effects in cardiac myocytes and fibroblasts, pORF-mcs induction of IFN and ISGs was examined by Real-Time PCR. pORF-mcs did not induce IFN-β, IFN-α1, -α2, -α4, or -α5 in cardiac fibroblasts when examined at 16, 24, 40 and 64 hours post-transfection (data not shown). Data for cardiac myocytes were similar for 64 hours post-transfection, but were less clear at 24 and 40 hours post-transfection, with the possibility of a maximum 4 to 10-fold induction of IFN-β, IFN-α2 and -α5 (16 hours was not tested; data not shown). By comparison, transfection of cardiac myocytes with constructs expressing IFN-α genes induced heterologous IFN-α subtypes by much greater amounts; 40 – 900 (Figure App.1. 5). In contrast to this minimal or undetectable induction of Type I IFN by pORF-mcs, surprisingly, this empty vector induced ISG56 and IRF-7 expression, in some cases as effectively as transfected IFN-β did (Figure App.1.8A and 1.8B). It is unclear why pORF-mcs induced

ISGs slightly better in cardiac fibroblasts than in myocytes, and yet induced greater antiviral effects in cardiac myocytes and in fibroblasts (Figure App.1.7). It is also unclear how pORF-mcs induces these ISGs given that it induces IFN minimally or not at all. Nonetheless, the data suggest that the transfection process can induce antiviral genes (Figure App.1.8) and antiviral effects (Figure App.1.7) in cardiac cells.

DISCUSSION

It has been reported that transfected B form DNA from modified vaccinia virus Ankara (MVA) induces antiviral responses in MEFs (4). Transfected DNA can induce production of IFN-β and IFN-α and some chemokines as well, such as Cxcl10, Ccl5, Ccl2, and Ccl4. What's more, the induction is both toll like receptor (TLR) and RIG-I-independent. In another report, Cheng et al (2) found that transfected dsDNA can trigger the activation of the IFN-β promoter in a human hepatoma cell line (Huh-7), which is dependent on both RIG-I and the mitochondrial antiviral signaling protein (MAVS) pathways. In our experiments, the transfected double stranded plasmid DNA can induce the production of ISGs with little or no induction of either IFN-β or IFN-α. Therefore it likely triggers activation of pathways other than the IFN-pathway, and this dsDNA-activated antiviral response is dominant compared to the transfected genes of interest. Given these non-specific effects, this transfection approach is a poor choice for investigating the antiviral effects of candidate innate response proteins in cardiac cells.

REFERENCES

1. **Austin, B. A., C. M. James, P. Harle, and D. J. Carr.** 2006. Direct application of plasmid DNA containing type I interferon transgenes to vaginal mucosa inhibits HSV-2 mediated mortality. Biol Proced Online **8:**55-62.

2. **Cheng, G., J. Zhong, J. Chung, and F. V. Chisari.** 2007. Double-stranded DNA and double-stranded RNA induce a common antiviral signaling pathway in human cells. Proc Natl Acad Sci U S A **104:**9035-40.

3. **Hardy, M. P., C. M. Owczarek, L. S. Jermiin, M. Ejdeback, and P. J. Hertzog.** 2004. Characterization of the type I interferon locus and identification of novel genes. Genomics **84:**331-45.

4. **Ishii, K. J., C. Coban, H. Kato, K. Takahashi, Y. Torii, F. Takeshita, H. Ludwig, G. Sutter, K. Suzuki, H. Hemmi, S. Sato, M. Yamamoto, S. Uematsu, T. Kawai, O. Takeuchi, and S. Akira.** 2006. A Toll-like receptor-independent antiviral response induced by double-stranded B-form DNA. Nat Immunol **7:**40-8.

5. **James, C. M., M. Y. Abdad, J. P. Mansfield, H. K. Jacobsen, A. R. Vind, P. A. Stumbles, and E. J. Bartlett.** 2007. Differential activities of alpha/beta IFN subtypes against influenza virus in vivo and enhancement of specific immune responses in DNA vaccinated mice expressing haemagglutinin and nucleoprotein. Vaccine **25:**1856-67.

6. **Swaminathan, N., C. M. Lai, M. W. Beilharz, S. J. Boyer, and S. P. Klinken.** 1992. Biological activities of recombinant murine interferons alpha 1 and alpha 4: large difference in antiproliferative effect. Antiviral Res **19:**149-59.

7. **Van Heuvel, M., I. J. Bosveld, A. A. Mooren, J. Trapman, and E. C. Zwarthoff.** 1986. Properties of natural and hybrid murine alpha interferons. J Gen Virol **67 (Pt 10):**2215-22.

8. **van Pesch, V., H. Lanaya, J. C. Renauld, and T. Michiels.** 2004. Characterization of the murine alpha interferon gene family. J Virol **78:**8219-28.

9. **Yeow, W. S., C. M. Lawson, and M. W. Beilharz.** 1998. Antiviral activities of individual murine IFN-alpha subtypes in vivo: intramuscular injection of IFN expression constructs reduces cytomegalovirus replication. J Immunol **160:**2932-9.

Table App.1.1. Reaction components for amplifying full length cDNA of IFN-α2 by PCR

Reagent	Final Conc	Tube_1	Tube_2
52 µl ddH2O		√	√
20 µl 5x Phusion HF Buffer	1x	√	√
2 µl 10 mM dNTPs	0.2 mM	√	√
5 µl 10 µM upstream primer	0.5 µM	507	507
5 µl 10 µM downstream primer	0.5 µM	508	508
15 µl of cDNA or ddH2O [1]		DNA	H2O
1 ul Phusion DNA polymerase [2]	0.02U/ul	√	√
Final Volume	100µl		

[1] cDNA is reverse transcribed from T3D infected-myocyte RNA
[2] Phusion™ high-fidelity DNA polymerase (F-530 or F-540)

```
NM_010504.1 ATGGCTAGGCTCTGTGCTTTCCTCATGATCCTAGTAATGATGAGCTACTACTGGTCAGCC  60
            |||||||||||||||||||||||||||||||| ||||||||||||||||||||||||||
pORF-IFN-α4 ATGGCTAGGCTCTGTGCTTTCCTCATGATCCTGGTAATGATGAGCTACTACTGGTCAGCC  114

NM_010504.1 TGTTCTCTAGGATGTGACCTGCCTCACACTTATAACCTCGGGAACAAGAGGGCCTTGACA  120
            ||||||||||||||||||||||||||||||||||||||||||||||||||||||||||||
pORF-IFN-α4 TGTTCTCTAGGATGTGACCTGCCTCACACTTATAACCTCGGGAACAAGAGGGCCTTGACA  174

NM_010504.1 GTCCTGGAAGAAATGAGAAGACTCCCCCCTCTTTCCTGCCTGAAGGACAGGAAGGATTTT  180
            ||||||||||||||||||||||||||||||||||||||||||||||||||||||||||||
pORF-IFN-α4 GTCCTGGAAGAAATGAGAAGACTCCCCCCTCTTTCCTGCCTGAAGGACAGGAAGGATTTT  234

NM_010504.1 GGATTCCCCTTGGAGAAGGTGGATAACCAACAGATCCAGAAGGCTCAAGCCATCCTTGTG  240
            ||||||||||||||||||||||||||||||||||||||||||||||||||||||||||||
pORF-IFN-α4 GGATTCCCCTTGGAGAAGGTGGATAACCAACAGATCCAGAAGGCTCAAGCCATCCTTGTG  294

NM_010504.1 CTAAGAGATCTTACCCAGCAGATTTTGAACCTCTTCACATCAAAAGACTTGTCTGCTACT  300
            ||||||||||||||||||||||||||||||||||||||||||||||||||||||||||||
pORF-IFN-α4 CTAAGAGATCTTACCCAGCAGATTTTGAACCTCTTCACATCAAAAGACTTGTCTGCTACT  354

NM_010504.1 TGGAATGCAACTCTCCTAGACTCATTCTGCAATGACCTCCATCAGCAGCTCAATGATCTC  360
            |||||||||||||| ||||||||||||||||||||||||||||||||||||| |||
pORF-IFN-α4 TGGAATGCAACTCTACTAGACTCATTCTGCAATGACCTCCATCAGCAGCTCAATGACCTC  414

NM_010504.1 AAAGCCTGTGTGATGCAGGAACCTCCTCTGACCCAGGAAGACTCCCTGCTGGCTGTGAGG  420
            ||||||||||||||||||||||||||||||||||||||||||||||||||||||||||||
pORF-IFN-α4 AAAGCCTGTGTGATGCAGGAACCTCCTCTGACCCAGGAAGACTCCCTGCTGGCTGTGAGG  474

NM_010504.1 ACATACTTCCACAGGATCACTGTGTACCTGAGAAAGAAGAAACACAGCCTCTGTGCCTGG  480
            ||||||||||||||||||||||||||||||||||||||||||||||||||||||||||||
pORF-IFN-α4 ACATACTTCCACAGGATCACTGTGTACCTGAGAAAGAAGAAACACAGCCTCTGTGCCTGG  534

NM_010504.1 GAGGTGATCAGAGCAGAAGTCTGGAGAGCCCTCTCTTCCTCAACCAACTTGCTGGCAAGA  540
            ||||||||||||||||||||||||||||||||||||||||||||||||||||||||||||
pORF-IFN-α4 GAGGTGATCAGAGCAGAAGTCTGGAGAGCCCTCTCTTCCTCAACCAACTTGCTGGCAAGA  594

NM_010504.1 CTGAGTGAGGAGAAGGAGTGA  561
            ||||||||||||||||||||
pORF-IFN-α4 CTGAGTGAGGAGAAGGAGTGA  615
```

Figure App.1.1. Multiple sequence alignment results for pORF-IFNα4 (IFN-α4) against the RefSeq from NCBI (NM_010504.1). Shaded nucleotides indicate three synonymous mutations.

```
NM_010505.1 ATGGCTAGGCTCTGTGCTTTCCTGATGGTCCTGCCGGTGCTGAGCTACTGGCCAACCTGC  60
            ||||||||||||||||||||||||||||||||||||||||||||||||||||||||||
pORF-IFN-α5 ATGGCTAGGCTCTGTGCTTTCCTGATGGTCCTGGCGGTGCTGAGCTACTGGCCAACCTGC  77

NM_010505.1 TCTCTAGGATGTGACCTTCTTCAGACTCATAACCTCAGGAACAAGAGAGCCTTAACCCTC  120
            |||||||||||||||||| ||||||||||||||||||||||||||||||||||||||
pORF-IFN-α5 TCTCTAGGATGTGACCTTCCTCAGACTCATAACCTCAGGAACAAGAGAGCCTTAACCCTC  137

NM_010505.1 CTGGTAAAAATGAGGAGACTCTCCCCTCTCTCCTGCCTGAAGGACAGAAAGGACTTTGGA  180
            ||||||||||||||||||||||||||||||||||||||||||||||||||||||||||
pORF-IFN-α5 CTGGTAAAAATGAGGAGACTCTCCCCTCTCTCCTGCCTGAAGGACAGAAAGGACTTTGGA  197

NM_010505.1 TTCCCACAGGAGAAGGTGGGTGCCCAGCAGATCCAGGAGGCTCAAGCCATCCCTGTCCTG  240
            ||||||||||||||||||||||||||||||||||||||||||||||||||||||||||
pORF-IFN-α5 TTCCCACAGGAGAAGGTGGGTGCCCAGCAGATCCAGGAGGCTCAAGCCATCCCTGTCCTG  257

NM_010505.1 AGTGAGCTGACCCAGCAGGTCCTGAACATCTTCACATCAAAGGACTCATCTGCTGCATGG  300
            ||||||||||||||||||||||||||||||||||||||||||||||||||||||||||
pORF-IFN-α5 AGTGAGCTGACCCAGCAGGTCCTGAACATCTTCACATCAAAGGACTCATCTGCTGCATGG  317

NM_010505.1 AATGCAACCCTCCTAGACTCATTCTGCAATGAAGTCCATCAGCAGCTCAATGACCTCAAA  360
            ||||||||||||||||||||||||||||||||||||||||||||||||||||||||||
pORF-IFN-α5 AATGCAACCCTCCTAGACTCATTCTGCAATGAAGTCCATCAGCAGCTCAATGACCTCAAA  377

NM_010505.1 GCCTGTGTGATGCAACAGGTCGGGGTGCAGGAATCTCCCCTGACCCAGGAAGACTCCCTG  420
            ||||||||||||||||||||||||||||||||||||||||||||||||||||||||||
pORF-IFN-α5 GCCTGTGTGATGCAACAGGTCGGGGTGCAGGAATCTCCCCTGACCCAGGAAGACTCCCTG  437

NM_010505.1 CTGGCTGTGAGGAAATACTTCCACAGGATCACTGTGTACCTGAGAGAGAAGAAACACAGC  480
            ||||||||||||||||||||||||||||||||||||||||||||||||||||||||||
pORF-IFN-α5 CTGGCTGTGAGGAAATACTTCCACAGGATCACTGTGTACCTGAGAGAGAAGAAACACAGC  497

NM_010505.1 CCCTGTGCCTGGGAGGTGGTCAGAGCAGAAGTCTGGAGAGCCCTGTCTTCCTCAGTTAAC  540
            ||||||||||||||||||||||||||||||||||||||||||||||||||||||||||
pORF-IFN-α5 CCCTGTGCCTGGGAGGTGGTCAGAGCAGAAGTCTGGAGAGCCCTGTCTTCCTCAGTTAAC  557

NM_010505.1 TTGCTGGCAAGATTGAGCAAGGAGGAGTGA  570
            |||||||||||||||||||||||||||||
pORF-IFN-α5 TTGCTGGCAAGATTGAGCAAGGAGGAGTGA  587
```

Figure App.1.2. Multiple sequence alignment results for pORF-IFNα (IFN-α5) against the RefSeq (NM_010505.1) from NCBI. Shaded nucleotides indicate two non-synonymous mutations, which Ala is changed to Pro at amino acid 12 and Pro to Leu at 27.

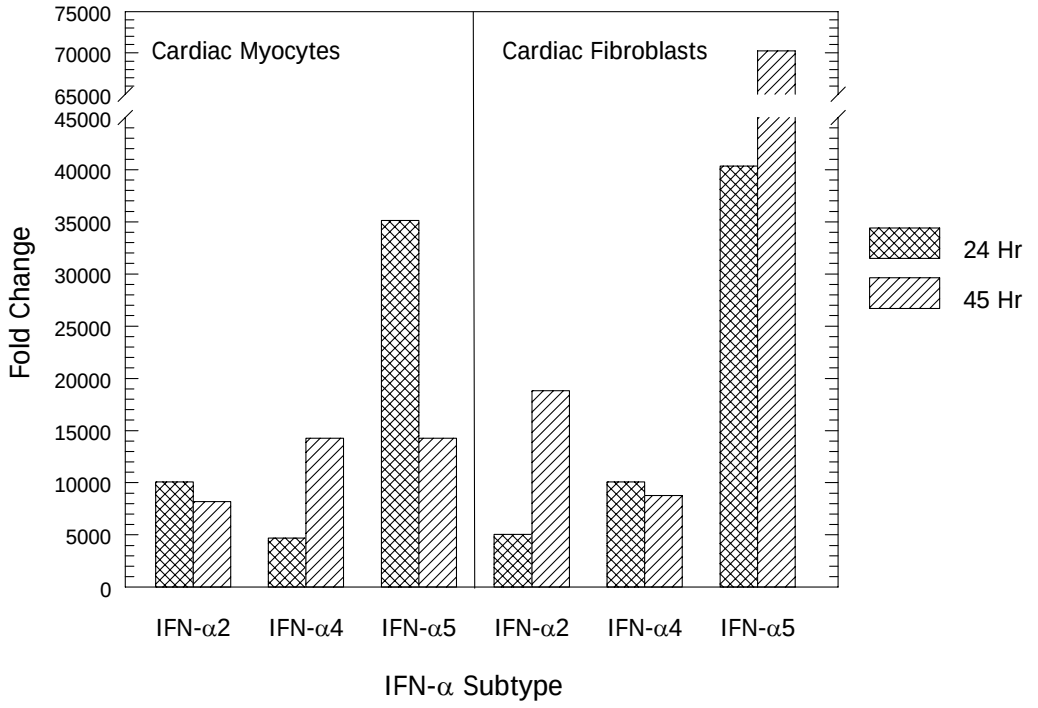

Figure App.1.3. Fold change of IFN-α mRNA expression in transfected primary cultures of cardiac myocytes and cardiac fibroblasts. Cardiac myocytes or fibroblasts were transfected with the indicated IFN-α construct, and total cell RNA was harvested at the indicated time post-transfection for reverse transcription and Real-Time PCR using the homologous IFN-α primers and GAPDH primers. The Ct number for each IFN-α gene was normalized to GAPDH, and then fold changes were calculated by comparing to mock-transfected samples at the same time point. Data are representative (transfection #11) of at least 3 independent experiments. While mcs-ORF was tested, fold changes were always <5, and therefore data were not included in this graph.

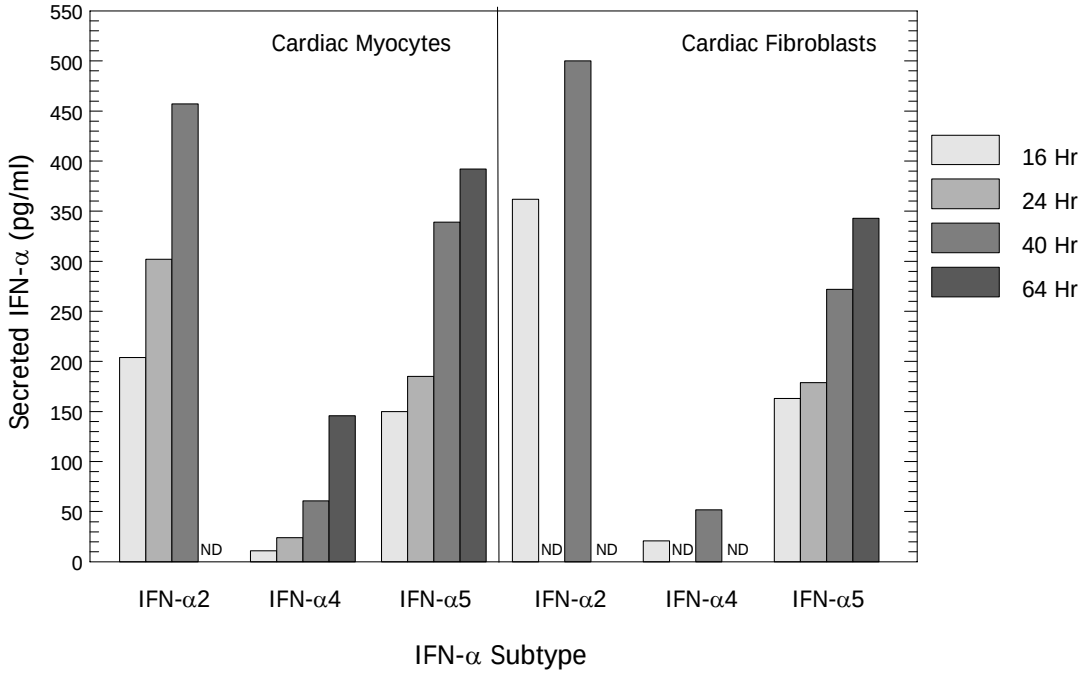

Figure App.1.4. Over-expression and secretion of IFN-α in transfected primary cultures of cardiac myocytes and cardiac fibroblasts. Cardiac myocytes or fibroblasts were transfected with the indicated IFN-α construct, and supernatant were harvested at the indicated times post-transection for ELISA using a commercial ELISA kit for mouse IFN-α (PBL). ND = not determined.

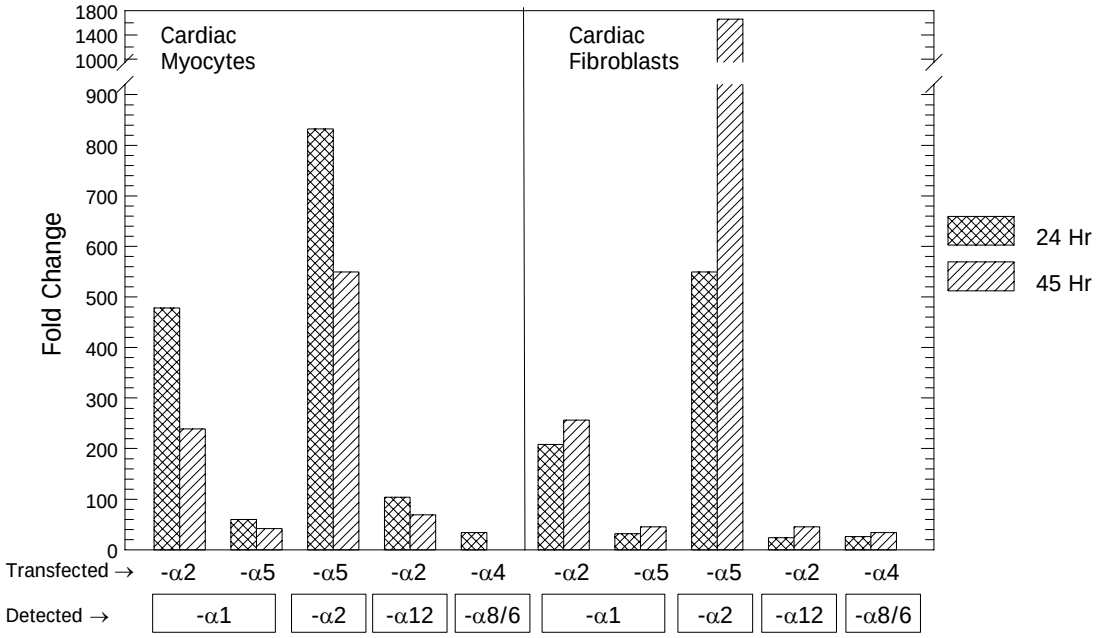

Figure App.1.5. Induction of heterologous IFN-α genes by transfected IFN-α genes. Cardiac myocytes or fibroblasts were transfected with the IFN-α construct indicated on the X axis, and total cell RNA was harvested at the indicated time post-transfection for reverse transcription and Real-Time PCR using heterologous IFN-α primers (IFN-α1, -α2, -α4, -α5, -α6T, -α7, -α7/10, -α8/6, -α9, -α11, -α12, -α13, -α14) and GAPDH primers. The Ct number for each IFN-α gene was normalized to GAPDH, and then fold changes were calculated by comparing to mock-transfected samples at the same time point. IFN-α subtypes that were detected are indicated by IFN-α names listed in boxes below the X axis. Data are representative (transfection #11) of at least 3 independent experiments.

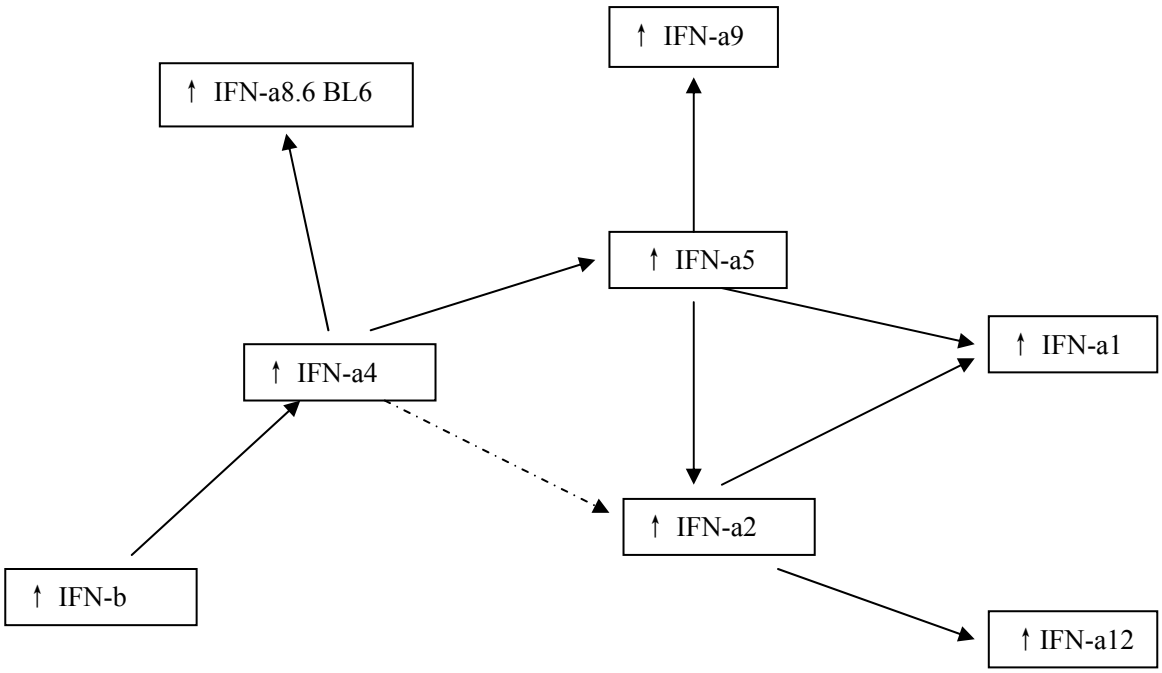

Figure App.1.6. Network of induction of other IFN-α subtypes by transfected IFN-α genes. Arrows with bold lines indicate reproducible upregulation. Arrows with dashed lines indicate upregulation was not reproduced in every experiment. The results were summarized from at least 3 independent experiments.

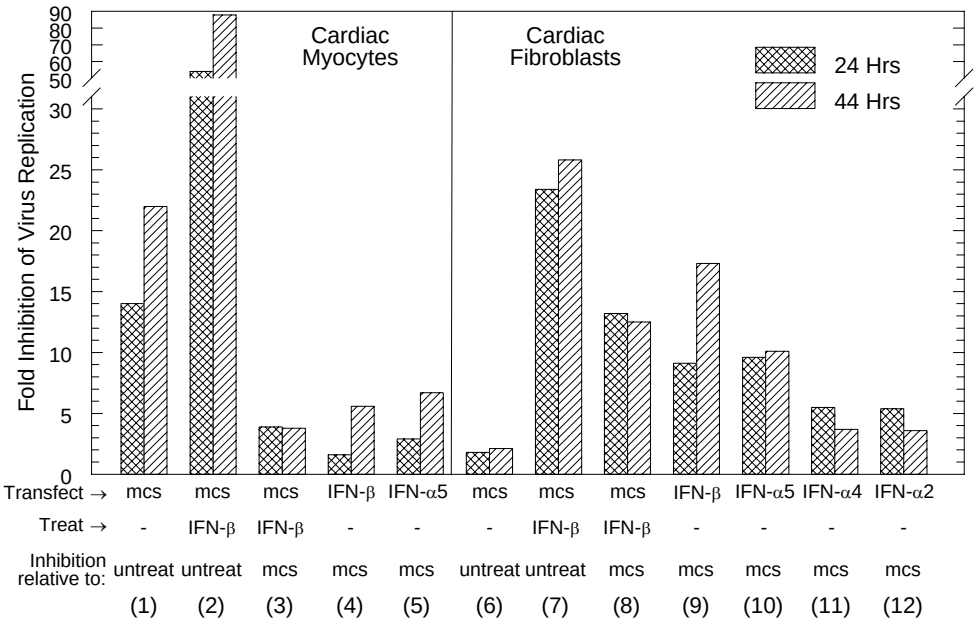

Figure App.1.7. Reovirus replication in transfected primary cardiac myocyte and cardiac fibroblast cultures. Primary cardiac myocyte and fibroblast cultures were transfected and infected as indicated in the text. Viral titers from triplicate wells were determined by plaque assay. Average titers from cultures transfected with pORF-mcs were divided by those from untransfected cultures that were not treated with IFN-β ("Inhibition relative to untreat") to determine the inhibitory effects of the transfection treatment alone or in combination with IFN-β treatment. Average titers from transfected cultures were divided by those from pORF-mcs-transfected cultures that were not treated with IFN-β ("Inhibition relative to mcs") to determine the inhibitory effects of IFN-β treatment or IFN expression from constructs.

Figure App.1.8. Induction of ISG56 and IRF-7 by the transfected pORF-mcs. Cardiac myocytes or fibroblasts were transfected with the indicated pORF-mcs or the construct expressing IFN-β, and total cell RNA was harvested at the indicated time post-transfection for reverse transcription and Real-Time PCR using primers for ISG56, IRF7, and GAPDH. The Ct numbers for ISG56 and IRF7 were normalized to GAPDH, and then fold changes were calculated by comparing to mock-transfected samples at the same time point. Data are averages from multiple experiments (transfections #3, 6, 7, 11, 13 and 14). 7A: Transfected with pORF-mcs; fold change calculated relative to mock-transfection. 7B: Transfected with pORF-mcs or IFN-β; fold change as above.

8A:

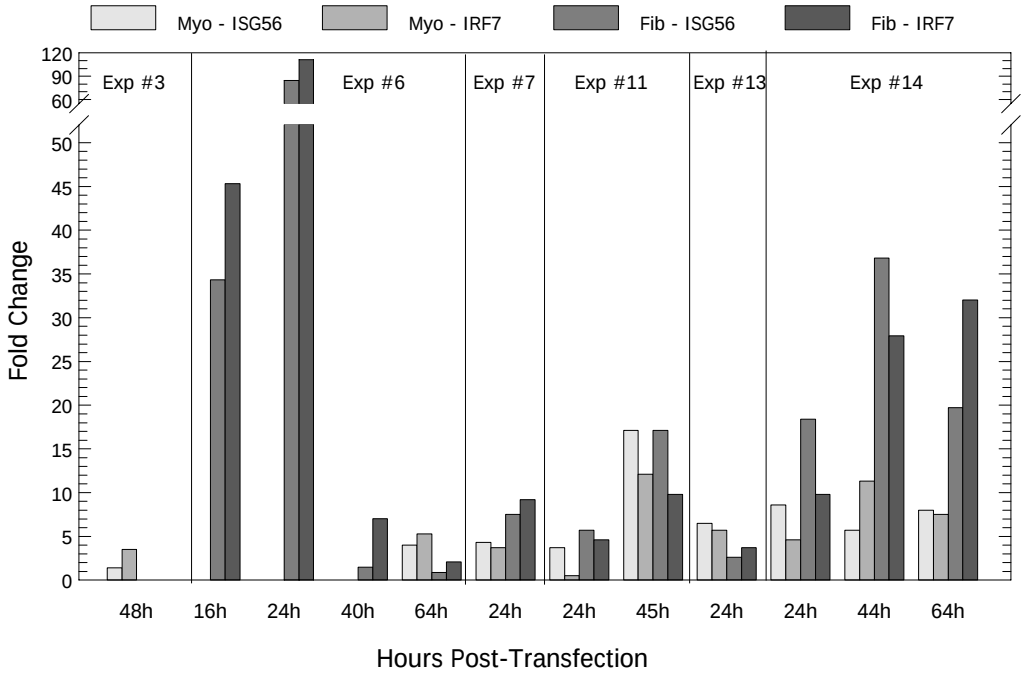
Myo - ISG56
Myo - IRF7
Fib - ISG56
Fib - IRF7
Exp #3
Exp #6
Exp #7
Exp #11
Exp #13
Exp #14
Fold Change
48h
16h
24h
40h
64h
24h
24h
45h
24h
24h
44h
64h
Hours Post-Transfection

8B:

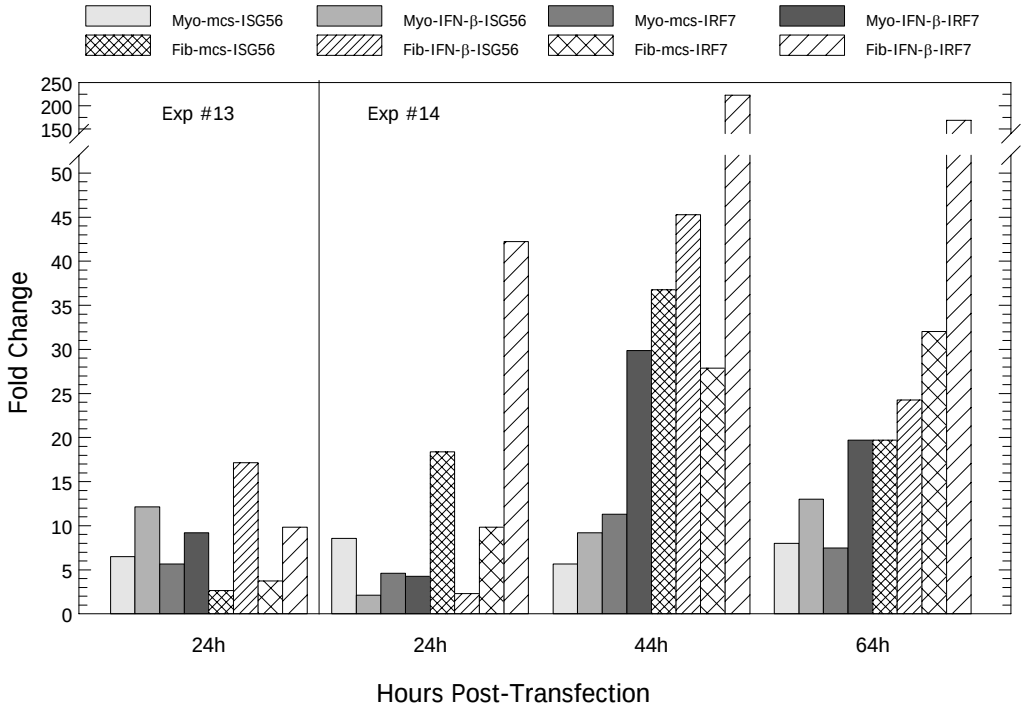
Myo-mcs-ISG56
Myo-IFN-β-ISG56
Myo-mcs-IRF7
Myo-IFN-β-IRF7
Fib-mcs-ISG56
Fib-IFN-β-ISG56
Fib-mcs-IRF7
Fib-IFN-β-IRF7
Exp #13
Exp #14
Fold Change
24h
24h
44h
64h
Hours Post-Transfection

APPENDIX 2

Proteomic Study of T3D-Infected Primary Cardiac Myocyte Cultures at Different Time Points by Two Dimensional Difference Gel Electrophoresis (2D-DIGE)

In collaboration with Drs. James Stephenson and Joel Sevinsky at Research Triangle Institute, RTP, NC.

INTRODUCTION

RNA viruses, like reovirus, stimulate pattern recognition receptors (PRRs), such as retinoic acid-inducible gene-I (RIG-I) and melanoma differentiation-associated gene 5 (Mda 5) (2, 4) to activate the IPS-1/MAVS/VISA/Cardif-mediated pathway for phosphorylation of TANK-binding kinase 1 (TBK1) and IκK ε, which then activate transcription factors IRF-3 and NF-κB to induce IFN-β transcription. Secreted IFN-β binds to the IFN-α/β-receptor on the cell surface, activates tyrosine kinases Tyk2 and Jak1, and induces hundreds of interferon stimulated genes (ISGs). Reovirus induction of and sensitivity to IFN-β in cardiac myocytes determines virus strain-specific differences in viral myocarditis and cardiac myocyte cytopathic effect (7). In order to identify new proteins or protein post-translational modifications which might be involved in the IFN pathway or other protective pathways in cardiac myocytes, we used the proteomics tools 2D-DIGE and MALDI-TOF-TOF to investigate proteome changes after reovirus infection of primary cardiac myocyte cultures.

Since reovirus T3D is stronger than other reovirus strains in inducing IFN-β in cardiac myocyte cultures, we did a time course study of T3D infection to identify a single time point for future studies comparing different reovirus strains.

MATERIALS AND METHODS

All of the materials and methods for this section are the same as those described in Chapter 3, except that: 1) instead of using a reovirus panel, the only virus used here was T3D; 2) instead of harvesting protein at 12 hr post-infection, protein from T3D infected samples was harvested at 8, 12, and 18 hr post-infection; 3) instead of triplicate samples for each virus infection, each time point contained quadruplicate samples.

RESULTS

2D-DIGE Gel set up. Eight Gels were run as shown in Table App.2.1. Every time-point included samples labeled with Cy3 and samples labeled with Cy5, to avoid bias caused by CyDye labeling.

Gel image analysis. The annotated preparative gel ("pick gel") image with master numbering is shown in Figure App.2.1. Gel images were analyzed by DeCyder 2D version 6.5 software and the DeCyder Extended Data Analysis (EDA) module Version 1.0. By combing the analysis results from the Biological Variation Analysis (BVA) module and EDA module, 243 differentially expressed protein spots (Students *t*-test with $P<0.05$) were picked for protein identification by MALDI-TOF-TOF.

BVA analysis. Differentially expressed protein spots between mock-infected and T3D-infected samples at different time-points and between different time-points within T3D-infected samples, identified as $P<0.05$ by a paired Students *t*-test, are summarized in Figure App.2.2. Results demonstrated the following. First, the fewest differences between mock and T3D-infected cultures occurred at 12 hours post-infection. However, since mock-infected cultures were harvested only at 12 hours, this comparison may be the most accurate, while the other groups may also include more general variations in cultures over time. Second, as expected, when comparing T3D-infected cultures to each other, there were fewest proteins in common (only 28) between the earliest comparison (8 hr *vs* 12 hr) and the latest comparison (12 hr *vs* 18 hr). Proteins in common between all three groups (61) likely increased or decreased dramatically over time.

Principle component analysis (PCA). In the EDA module, PCA analysis was carried out to analyze reproducibility. PCA is a statistical analysis to reduce the complexity of the data by eliminating variables that provide little additional information. This analysis was based on 118 differentially expressed proteins ($P <=0.01$ by one-way ANOVA, and the protein presents in >=80% of spot maps). Each spot represents the 118 proteins from the same gel. PCA results (Figure App.2.3) showed that quadruplicate samples were tightly clustered as expected, indicating the high reducibility of the 2D-DIGE technique. The 12 hour infection was *not* more similar to mock-infected cultures than the 8 hour or 18 hour infections were, perhaps because the stringency of the ANOVA test ($P <= 0.01$) provides a more powerful segregation of the data.

Hierarchical clustering of spot maps. The EDA module provides a pattern analysis to group protein spots of similar expression patterns. Hierarchical clustering algorithms were applied here, which can combine or split the data pair-wise and thereby generates a treelike structure called a dendrogram. In this analysis, data is re-arranged and set into a better ordered data set, which can provides an easy overview of the data. Here the Hierarchical clustering analysis was based on the same set of protein spots as those in the PCA analysis. Changes in protein expression are relative to mock. Results (Figure App.2.4) demonstrated that protein expression profiles differ over time following infection, and display minimal variation between quadruplicates. Thus, protein expression profiling in primary cardiac myocyte cultures by 2D-DIGE is reproducible and quantitative.

Identification of proteins. Sixty-eight protein spots were identified with a Total Protein Score higher than 60 by IPI database search (specific for mouse) and higher than 64 by SwissSprot database search (all organisms). Identified proteins are listed in Table App.2.2 using results from SwissProt as an example. Proteins identified were found in many pathways. Among those proteins, Cryptdin 4 was selected as an interesting protein, because of its known role in protecting against infectious pathogens in the intestine.

Quantitation and identification of Cryptdin 4. Cryptdin 4 is an α-defensin from the antimicrobial peptide defensin family. It is abundant in cells and tissues involved in host defenses against microbial infections, and functions by permeabilizing the bacterial membrane (1, 3, 5, 6). Defensins were reported to have antiviral effects against several enveloped viruses as well, but has never been found to be associated with non-enveloped viruses, like reovirus which was used here. Cryptdin 4 has the highest antimicrobial activity

of the known mouse α-defensins in *in vitro* assays, and is found predominantly in the intestine. Importantly, no defensins have ever been associated with protection in the heart. Cryptdin 4 is synthesized as a pre-pro-protein, and then is cleaved by MMP-7 (8, 9) to release the mature 32-amino acid cryptdin 4 peptide. Quantitation demonstrated that cryptdin 4 protein increased over the time (Figure App.2.5). Peptide information from MALDI-TOF-TOF indicated that the identification was of high quality (Figure App.2.6), and provided the basis for its relatively strong score (Table App.2.2, 92.9).

Confirmation of cryptdin 4 expression in primary cardiac myocyte cultures. To investigate cryptdin 4 mRNA expression, total RNA was harvested from T3D-infected cardiac myocyte and cardiac fibroblast cultures, and subjected to reverse transcription and Real Time PCR. Three pairs of primers were designed for different purpose. Primers unique for cryptdin 4, were forward (563): 5'-GGACCAGGCTGTGTCTATCT-3' and reverse (556): 5' - CGTATTCCACAAGTCCCACG - 3'. Primers for all cryptdins but not cryptdin 4, were forward (567): 5'-GACCAGGCTGTGTCTGTCT-3' and reverse (568): 5' - CCCTTTCTGCAGGTCCCATT - 3'. Primers for all cryptdins, but not 20 and 26, were forward (569): 5'- TCCTCCTCTCTGCCCT-3' and reverse (570): 5'- TCTTCCCCTGGCTGCT -3'. While these primers were sensitive and specific when used on L cell genomic DNA, Cr:NIH(S) mouse brain genomic DNA and cDNA from intestine, the primers did not generate signals using cDNA from primary cardiac myocyte and fibroblast cultures (data not shown).

DISCUSSION

This T3D time-course studies indicated that over the 8, 12 and 18 hours post-T3D infection of primary cardiac myocyte cultures, some proteins were differentially expressed early, some in the middle and some late. Some were differentially expressed at multiple time-points as well. In order to maximize the chances of identifying proteins differentially expressed at either early or late times post-infection, we selected 12 hours post-infection as the time for comparing the proteomes of multiple reovirus strains (Chapter 3).

While identification of T3D induction of cryptdin 4 was exciting, it was most likely a mis-identification, for the following reasons. First, the gel spot was not at the correct position for the molecular weight (MW) of the cryptdin 4 precursor (10 kD) or the mature cryptdin 4 protein (3 kD), and instead was in the upper part of the gel, where the MW should be around 100 kD. Second, although the database scores were high, there were no ionization data (i.e. sequence-specific MS data) for any of the putative cryptdin 4 peptides, and therefore identification was based solely on mass:charge data (the first MS in tandem MS). While this can provide accurate protein identification, it is not as conclusive as sequence-specific data. Third, cryptdin 4 mRNA was undetectable, despite controls indicating that the Real-Time PCR was both sensitive and specific. And fourth, cryptdin 4 should be secreted and found outside of cells, although its detection in our cardiac myocyte lysates could have indicated a new mechanism / pathway for cryptdin 4 function. In sum, the data suggest that the cryptdin 4 identification was an error, and it was not pursued further.

REFERENCES

1. **Cummings, J. E., and T. K. Vanderlick.** 2007. Kinetics of cryptdin-4 translocation coupled with peptide-induced vesicle leakage. Biochemistry **46:**11882-91.

2. **Loo, Y. M., J. Fornek, N. Crochet, G. Bajwa, O. Perwitasari, L. Martinez-Sobrido, S. Akira, M. A. Gill, A. Garcia-Sastre, M. G. Katze, and M. Gale, Jr.** 2008. Distinct RIG-I and MDA5 signaling by RNA viruses in innate immunity. J Virol **82:**335-45.

3. **Maemoto, A., X. Qu, K. J. Rosengren, H. Tanabe, A. Henschen-Edman, D. J. Craik, and A. J. Ouellette.** 2004. Functional analysis of the alpha-defensin disulfide array in mouse cryptdin-4. J Biol Chem **279:**44188-96.

4. **Saito, T., and M. Gale, Jr.** 2008. Differential recognition of double-stranded RNA by RIG-I-like receptors in antiviral immunity. J Exp Med **205:**1523-7.

5. **Selsted, M. E., S. I. Miller, A. H. Henschen, and A. J. Ouellette.** 1992. Enteric defensins: antibiotic peptide components of intestinal host defense. J Cell Biol **118:**929-36.

6. **Selsted, M. E., and A. J. Ouellette.** 2005. Mammalian defensins in the antimicrobial immune response. Nat Immunol **6:**551-7.

7. **Sherry, B., J. Torres, and M. A. Blum.** 1998. Reovirus induction of and sensitivity to beta interferon in cardiac myocyte cultures correlate with induction of myocarditis and are determined by viral core proteins. J Virol **72:**1314-23.

8. **Shirafuji, Y., H. Tanabe, D. P. Satchell, A. Henschen-Edman, C. L. Wilson, and A. J. Ouellette.** 2003. Structural determinants of procryptdin recognition and cleavage by matrix metalloproteinase-7. J Biol Chem **278:**7910-9.

9. **Weeks, C. S., H. Tanabe, J. E. Cummings, S. P. Crampton, T. Sheynis, R. Jelinek, T. K. Vanderlick, M. J. Cocco, and A. J. Ouellette.** 2006. Matrix metalloproteinase-7 activation of mouse paneth cell pro-alpha-defensins: SER43 down arrow ILE44 proteolysis enables membrane-disruptive activity. J Biol Chem **281:**28932-42.

Table App.2.1. Gel set-up for T3D time-course comparison

Gel number	Cy3	Cy5
25098	Mock_12hr	T3D_8hr
25099	T3D_8hr	T3D_12hr
25100	T3D_18hr	Mock_12hr
25101	T3D_12hr	T3D_8hr
25102	Mock_12hr	T3D_12hr
25103	T3D_12hr	T3D_18hr
25105	T3D_8hr	Mock_12hr
25106	T3D_18hr	T3D_12hr

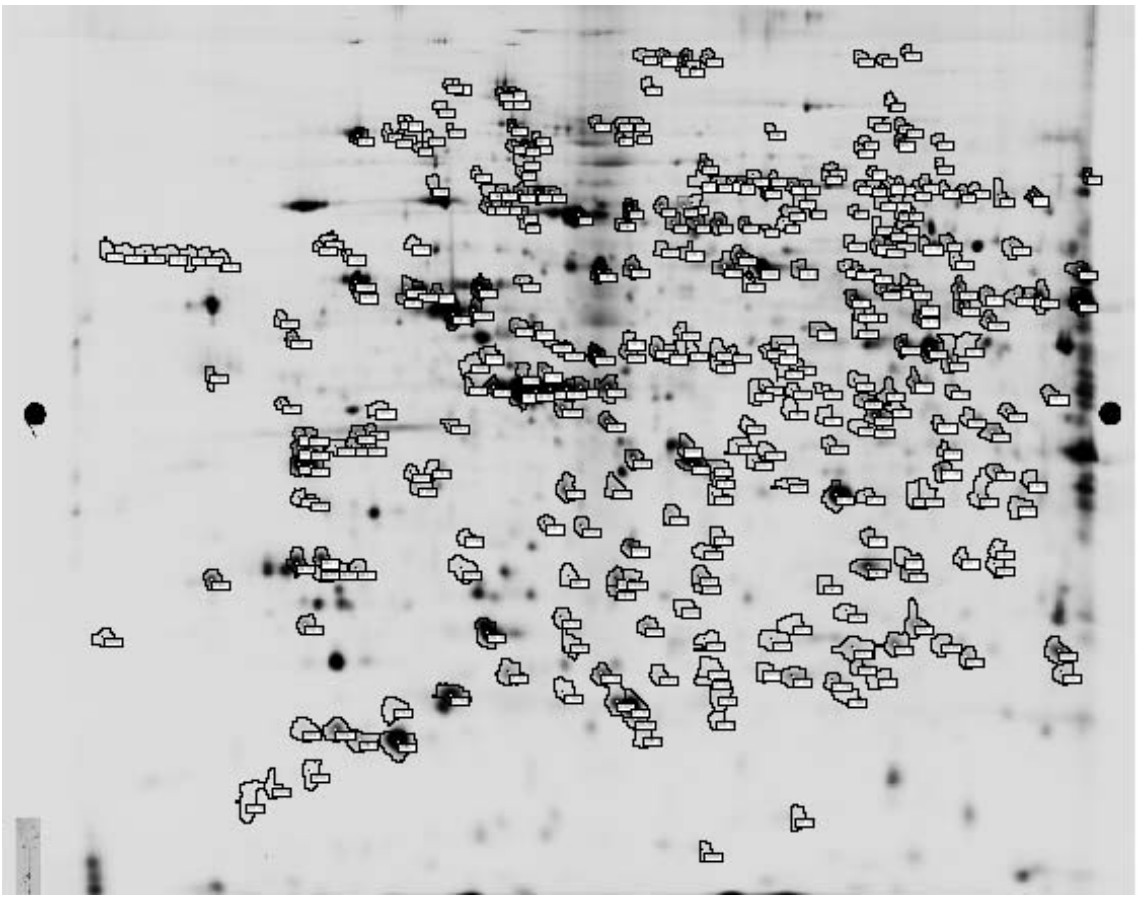

Figure App.2.1. Annotated preparative gel ("pick gel") image for T3D time-point comparison.

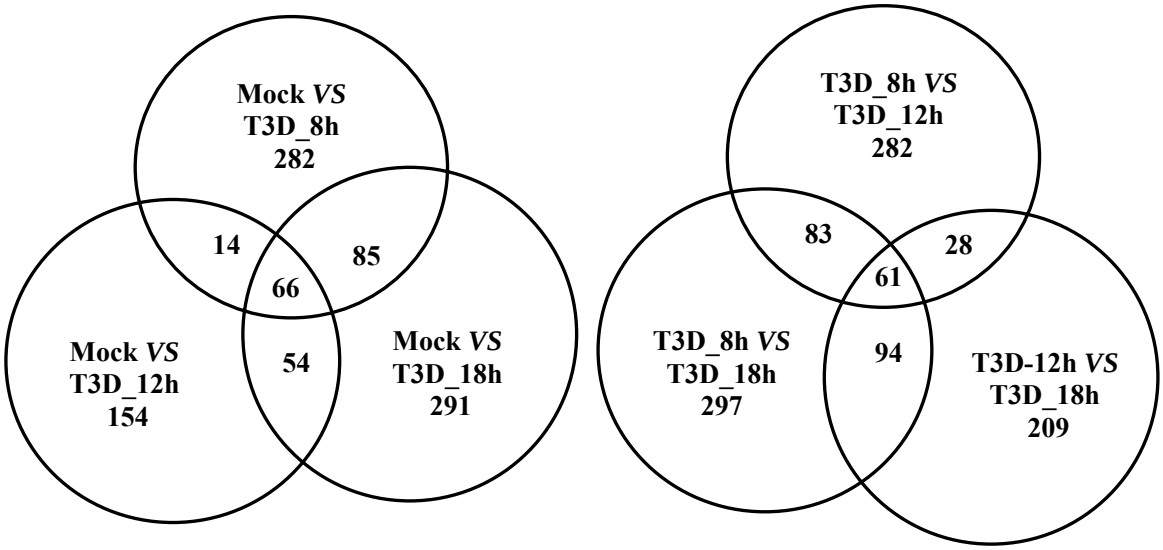

Figure App.2.2. Differentially expressed proteins at different times following reovirus T3D infection of primary cardiac myocyte cultures. Average ratio for each protein spot from quadruplicate samples (quadruplicate gels) was analyzed by Student *t* test (statistical significance at $P < 0.05$). Because of limited cell cultures, mock-infected cultures were harvested only at 12 hours.

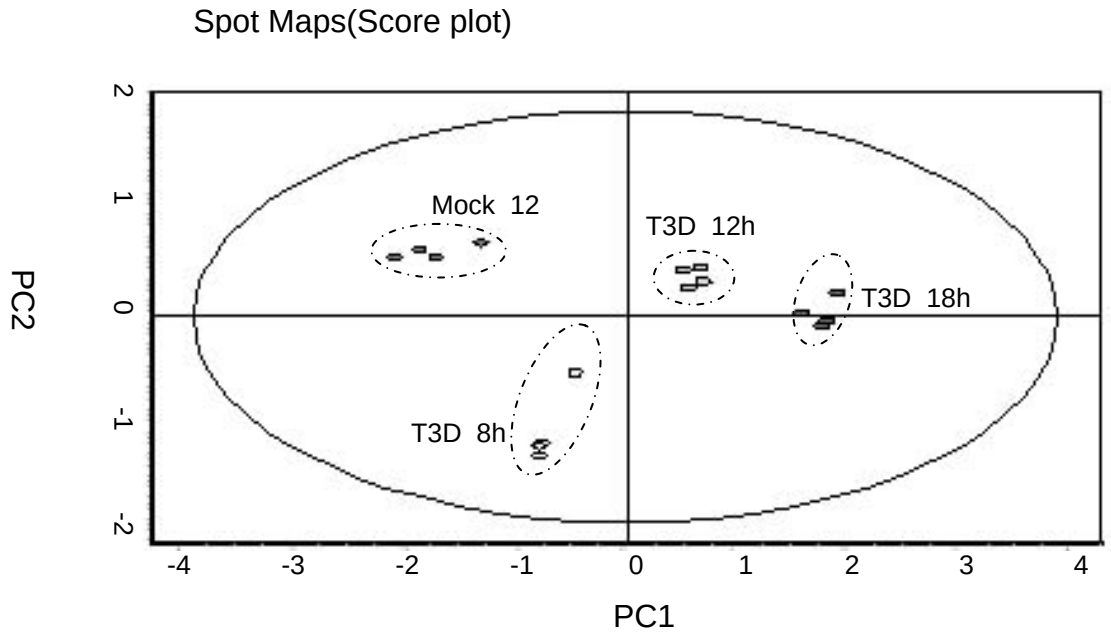

Figure App.2.3. Principle Component Analysis (PCA) of mock- or T3D-infected primary cardiac myocyte cultures. PC1 comprises 72.8% of the variance and PC2 comprises 16.9% of the variance.

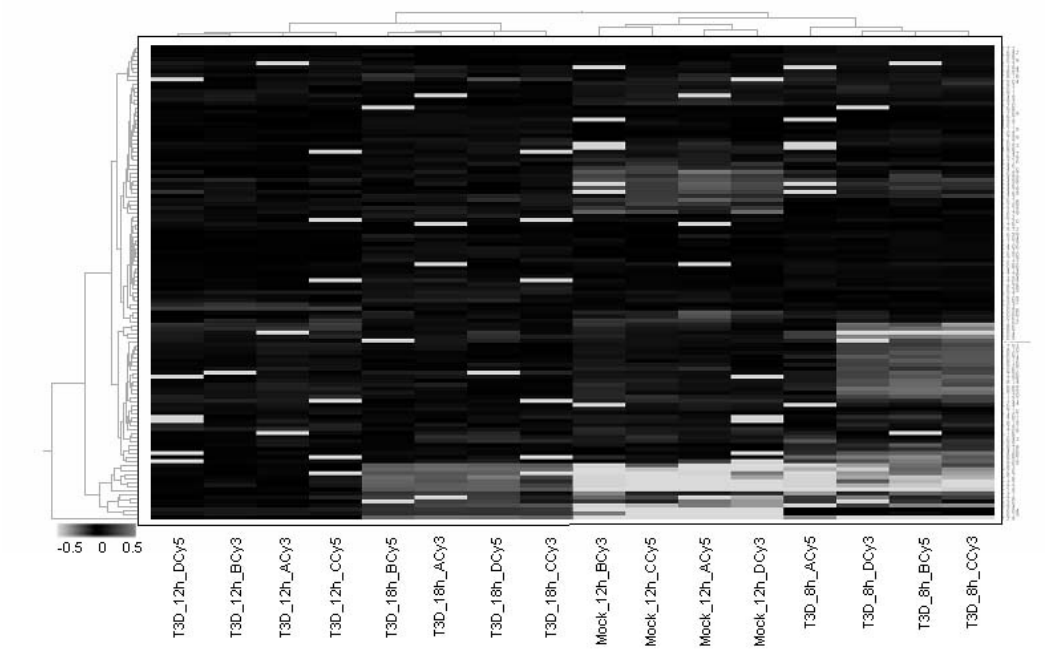

Figure App.2.4. Hierarchical clustering of spot maps. Changes in protein expression are relative to mock. Red: Increase. Green: Decrease. Black: No change. White: no protein spot was detected on that gel.

Table App.2.2. Proteins identified from SwissProt database search of the T3D time-course comparison

Spot No.	Total Protein Score	Description
1816	335	(P91754) Actin (Fragment)
2120	316	(P58771) Tropomyosin 1 alpha chain (Alpha-tropomyosin)
2592	259	(Q9DCT2) NADH-ubiquinone oxidoreductase 30 kDa subunit, mitochondrial precursor (EC 1.6.5.3) (EC 1.
1801	255	(P50138) Actin
1272	231	(P05216) Tubulin alpha-6 chain (Alpha-tubulin 6)
2280	224	(P48036) Annexin A5 (Annexin V) (Lipocortin V) (Endonexin II) (Calphobindin I) (CBP-I) (Placental a
2494	201	(Q99PT1) Rho GDP-dissociation inhibitor 1 (Rho GDI 1) (Rho-GDI alpha) (GDI-1)
1642	183	(Q9CZ13) Ubiquinol-cytochrome C reductase complex core protein I, mitochondrial precursor (EC 1.10.
2543	178	(P35215) 14-3-3 protein zeta/delta (Protein kinase C inhibitor protein-1) (KCIP-1) (Mitochondrial i
1810	176	(Q98972) Actin, muscle-type (OlMA1) [Actin, alpha cardiac muscle 1]
2119	168	(P42123) L-lactate dehydrogenase B chain (EC 1.1.1.27) (LDH-B) (LDH heart subunit) (LDH-H)
949	155	(P02769) Serum albumin precursor (Allergen Bos d 6)
1520	150	(P00514) cAMP-dependent protein kinase type I-alpha regulatory chain
1164	147	(P27773) Protein disulfide isomerase A3 precursor (EC 5.3.4.1) (Disulfide isomerase ER-60) (ERp60)
1305	141	(P09244) Tubulin beta-7 chain (Tubulin beta 4') [Tubulin beta-5 chain]
2354	141	(P24142) Prohibitin (B-cell receptor associated protein 32) (BAP 32)
1717	128	(Q04447) Creatine kinase, B chain (EC 2.7.3.2) (B-CK)
2162	125	(P14869) 60S acidic ribosomal protein P0 (L10E)
1247	124	(P00829) ATP synthase beta chain, mitochondrial precursor (EC 3.6.3.14)
2685	124	(P14701) Translationally controlled tumor protein (TCTP) (p23) (21 kDa polypeptide) (p21) (Lens epi
661	123	(P12419) Major nonstructural protein mu-NS
2857	120	(P08733) Myosin regulatory light chain 2, ventricular/cardiac muscle isoform (MLC-2) (MLC-2v)
1909	119	(P08865) 40S ribosomal protein SA (P40) (34/67 kDa laminin receptor) (Colon carcinoma laminin-bindi
1302	118	(P05218) Tubulin beta-5 chain
1051	117	(P31948) Stress-induced-phosphoprotein 1 (STI1) (Hsp70/Hsp90-organizing protein) (Transformation-se
850	112	(P38646) Stress-70 protein, mitochondrial precursor (75 kDa glucose regulated protein) (GRP 75) (Pe
1372	111	(P30837) Aldehyde dehydrogenase X, mitochondrial precursor (EC 1.2.1.3) (ALDH class 2)
1635	111	(Q9CZ13) Ubiquinol-cytochrome C reductase complex core protein I, mitochondrial precursor (EC 1.10.

Table App.2.2. Continued

2753	110	(P17209) Myosin light chain 1, atrial isoform
2308	109	(P97429) Annexin A4 (Annexin IV)
2555	108	(O08709) Peroxiredoxin 6 (EC 1.11.1.-) (Antioxidant protein 2) (1-Cys peroxiredoxin) (1-Cys PRX) (A
523	107	(P55072) Transitional endoplasmic reticulum ATPase (TER ATPase) (15S Mg(2+)-ATPase p97 subunit) (Va
915	103	(P19378) Heat shock cognate 71 kDa protein
2638	101	(O08709) Peroxiredoxin 6 (EC 1.11.1.-) (Antioxidant protein 2) (1-Cys peroxiredoxin) (1-Cys PRX) (A
1326	99.7	(Q9TU23) Hypothetical protein KIAA0373
1750	97.3	(Q9QYR9) Acyl coenzyme A thioester hydrolase, mitochondrial precursor (EC 3.1.2.2) (Very-long-chain
1590	97	(P17182) Alpha enolase (EC 4.2.1.11) (2-phospho-D-glycerate hydro-lyase) (Non-neural enolase) (NNE)
2455	95.2	(Q9Y696) Chloride intracellular channel protein 4 (Intracellular chloride ion channel protein p64H1
1233	94.8	(P05216) Tubulin alpha-6 chain (Alpha-tubulin 6)
1185	93.8	(P42932) T-complex protein 1, theta subunit (TCP-1-theta) (CCT-theta)
854	92.9	(P28311) Cryptdin-4 precursor
1794	90.2	(Q9Z2I9) Succinyl-CoA ligase [ADP-forming] beta-chain, mitochondrial precursor (EC 6.2.1.5) (Succin
696	88	(P58252) Elongation factor 2 (EF-2)
1058	86.4	(P00949) Phosphoglucomutase (EC 5.4.2.2) (Glucose phosphomutase) (PGM)
940	84.7	(Q8TYS1) 50S ribosomal protein L37e [Meiosis-specific nuclear structural protein 1]
793	84.4	(Q9Z1E9) Golgi apparatus protein 1 precursor (Golgi sialoglycoprotein MG-160) (E-selectin ligand 1)
205	83.6	(Q8TYS1) 50S ribosomal protein L37e
772	83.2	(P12419) Major nonstructural protein mu-NS [Insulin-like growth factor-binding protein 5 precursor]
2520	82.9	(P25788) Proteasome subunit alpha type 3 (EC 3.4.25.1) (Proteasome component C8) (Macropain subunit
729	82.8	(P12419) Major nonstructural protein mu-NS [Insulin-like growth factor-binding protein 5 precursor]
2901	82.5	(P18760) Cofilin, non-muscle isoform
1248	82.3	(P09103) Protein disulfide isomerase precursor (EC 5.3.4.1) (PDI) (Prolyl 4-hydroxylase beta subuni
551	80.2	(P25886) 60S ribosomal protein L29 (P23)
1613	77.6	(P29758) Ornithine aminotransferase, mitochondrial precursor (EC 2.6.1.13) (Ornithine--oxo-acid ami
2769	77.5	(Q43292) 60S ribosomal protein L37
286	77.4	(P13533) Myosin heavy chain, cardiac muscle alpha isoform (MyHC-alpha)
289	77.2	(Q63617) 150 kDa oxygen-regulated protein precursor (Orp150) (Hypoxia up-regulated 1)
2415	76.8	(Q02193) Brain-derived neurotrophic factor precursor (BDNF)
438	75.1	(P40644) High mobility group protein 1 homolog

Table App.2.2. Continued

2681	73.8	(Q9R1P1) Proteasome subunit beta type 3 (EC 3.4.25.1) (Proteasome theta chain) (Proteasome chain 13
1209	73.1	(Q9HIS1) 30S ribosomal protein S14P
2847	73.1	(Q9QVP4) Myosin regulatory light chain 2, atrial isoform (Myosin light chain 2a) (MLC-2a) (MLC2a) (
2216	70.9	(P35308) Sperm protamine P1 (Cysteine-rich protamine)
2115	69.7	(Q9N1Q5) Nuclear autoantigen Sp-100 (Speckled 100 kDa) (Nuclear dot-associated Sp100 protein) (Frag [Peroxiredoxin 6]
2479	69.2	(O29387) 50S ribosomal protein L37e [Sperm tail associated protein]
495	68.9	(P12883) Myosin heavy chain, cardiac muscle beta isoform (MyHC-beta)
719	67.5	(O74015) 50S ribosomal protein L37e
2198	66.5	(Q9TU23) Hypothetical protein KIAA0373 [eukaryotic translation elongation factor 1 delta isoform b]
2044	66.4	(Q9TU23) Hypothetical protein KIAA0373
950	66.2	(P02769) Serum albumin precursor (Allergen Bos d 6)
1194	64.5	(P19226) 60 kDa heat shock protein, mitochondrial precursor (Hsp60) (60 kDa chaperonin) (CPN60) (He
2109	64.2	(P75556) Hypothetical protein MG075 homolog (G07_orf1030)

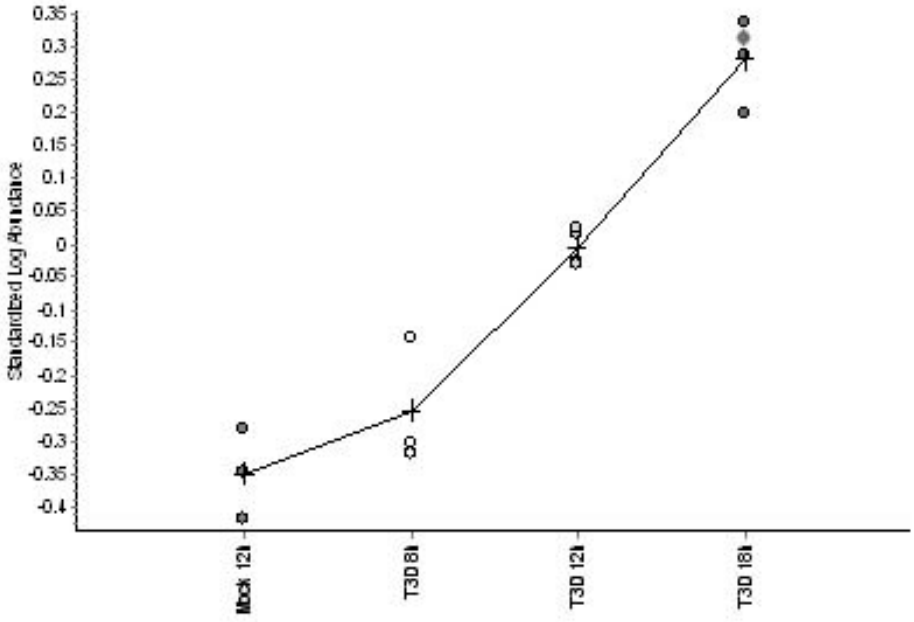

Figure App.2.5. Cryptdin 4 protein (spot 854) at different times post-T3D infection of primary cardiac myocyte cultures.

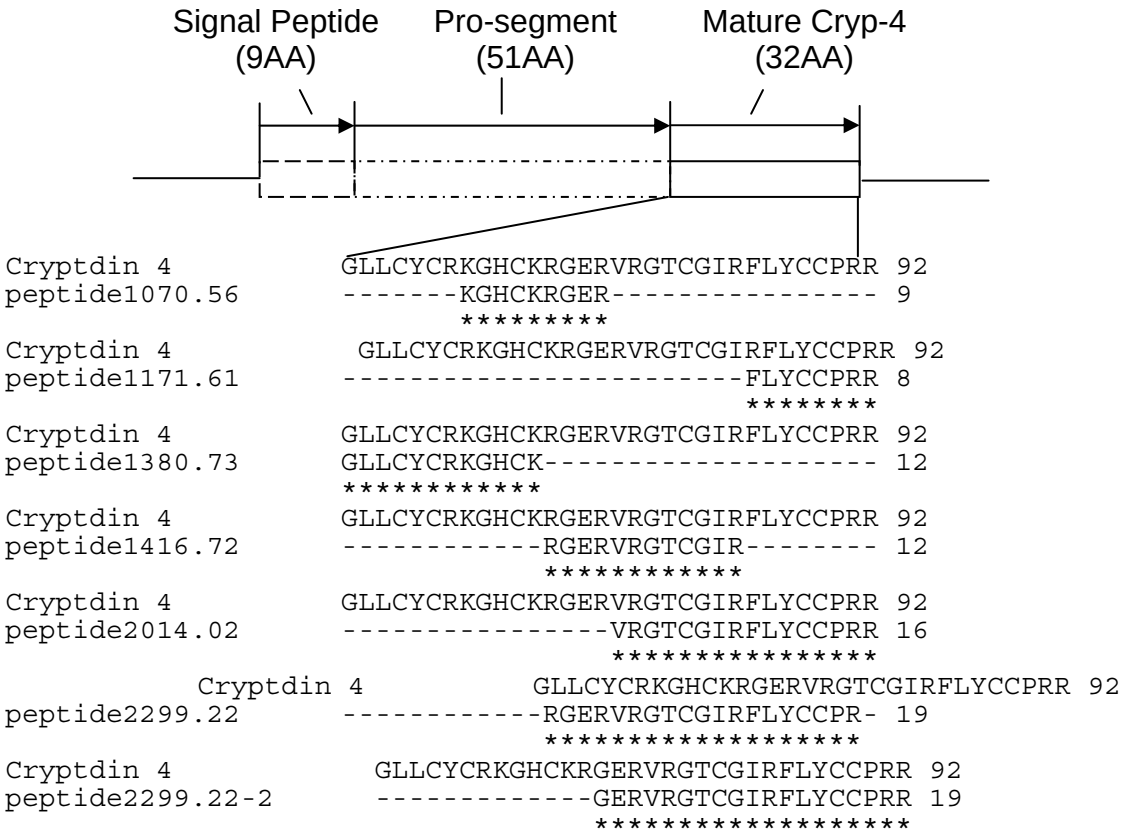

Figure App.2.6. Peptide information for cryptdin 4 and sequence alignment to the cryptdin 4 RefSeq from GenBank. The schematic figure is the structure of the pre-pro-cryptdin 4 precursor. In each line, the top sequence is from GenBank and the bottom sequence is based on the MALDI-TOF-TOF data for the indicated peptide.

APPENDIX 3

Proteomic Study of T3D-Infected Primary Cardiac Myocyte Cultures at 18 Hours Post-Infection by LC-MS/MS

In collaboration with Drs. Kevin Blackburn and Michael Goshe in the Department of Molecular and Structural Biochemistry, NC State University

INTRODUCTION

From the T3D time-course study, cryptdin 4 was identified as an exciting protein induced by T3D infection of cardiac myocytes. However, Real-Time PCR did not detect cryptdin 4 mRNA, and other concerns suggested the original identification might be in error (see Appendix II). Therefore, new infected lysates were subjected to a 1-dimensional gel followed by LC-MS/MS to determine whether cryptdin 4 protein could be identified again. Since the 2D-DIGE experiment suggested that cryptdin 4 increased over time, lysates were harvested at18 hours post-infection for this experiment.

MATERIALS AND METHODS

Whole cell protein extracts from T3D infected primary cardiac myocyte cultures were harvested 18 hours post-infection in TNE buffer.

1D gel electrophoresis. Approximately 25 μg of total protein extract from T3D- or mock-infected samples were loaded onto Invitrogen NuPAGE 4-12% Bis-Tris gels (1.0mm x 10 well). Detailed steps are as follows:

1. Sample was prepared according to Table App.3.1;
2. Samples were boiled for 5 minutes, followed by pause spin down
3. Samples were loaded onto the gel
4. Gel was electrophoresed at 90V for 5 minutes, then 200V for approximately 30 minutes in MES SDS Running Buffer
5. Gel was rinsed with ddH_2O
6. Gel was fixed in 50% Methanol, 10% Acetic acid, 40% ddH2O for 10 minutes at room temperature with gentle shaking
7. Gel was rinsed with ddH_2O
8. Gel was stained with Coomassie (Invitrogen, catalog # IM-6025) for at least 4 hours(>=3 hours, but <=16 hours) and then de-stained in ddH2O with gentle shaking at room temperature for >=7 hours.
9. The entire lane for each sample lane was cut into 10 pieces and put into methanol-treated 0.65ml eppendorf tubes (Figure App.3.1).

In Gel Lys-c Digestion. A detailed description of the in-gel digestion protocol is provided in Wilm et al (1). Briefly, gel slices were washed twice with acetonitrile and 100 mM Tris pH 8.0 at 1:1 ratio in a volume sufficient to cover the slice for 30 minutes with gentle shaking. The washed gel pieces were shrunk with neat acetonitrile sufficient for immersion. Then proteins in the gel slice were reduced for 30 minutes in 10 mM

dithiothreitol (DTT, Sigma, catalog # D5545) in 100 mM Tris pH8.0 at 37ºC and alkylated with 55 mM iodoacetamide (IAA, Sigma, catalog # I1149) for 20 minutes at room temperature. After washing with 50 mM ammonium bicarbonate twice, gel slices were shrunk in neat acetonitrile and swollen in 50 mM ammonium bicarbonate twice more. Following the third shrink, they were swollen in 50 mM Tris pH8.0 containing 10 ng/µl Lys-c (Wako Lysle Endopeptidase, mass spectrometry Grade, catalog # 121-05063, Lot # PEN 6311). Digestion proceeded overnight for 16 – 18 hours at 37ºC.

Protein extraction following in-gel digestion. A 1% formic acid / 2% acetonitrile extraction solution was added to the in-gel digestion tubes, the mixtures were sonicated in a bath for 5 minutes, and then they were incubated for 30 minutes at room temperature with occasional vortexing. Finally, the supernatant containing digested protein was harvested.

LC-MS/MS. Samples were filtered through home-made Porex filters by a pump into autosampler vials, and 2 µl of the internal standard, Rabbit Phosphorylase B, was added to each vial for quantitation. For loading on the LC-MS-MS spectrophotometer, the ejection volume for each vial was set to 20 µl. The ejection sequence was from high molecular weight to low molecular weight, and from T3D virus-infected to mock-infected. There was a blank sample between the virus-infected and mock-infected.

Protein identification. Peptide information from LC-MS/MS was matched against the full mouse protein database (NCBI RefSeq) and a mouse cryptdin database for protein identification.

RESULTS

Differentially expressed proteins between virus- and mock-infected samples in primary cardiac myocyte cultures. Identified proteins which were differentially expressed between T3D- and mock-infected samples with a change greater than two-fold are summarized in Table App.3.2. Proteins unique to T3D-infection or which were found in a band unique to T3D-infection are summarized in Table App.3.3. Proteins unique to Mock-infection or which were found in a band unique to mock- infection are summarized in Table App.3.4. T3D infection up-regulated some proteins (shown as a positive ratio), and down-regulated some proteins (shown as a negative ratio). T3D stimulated opposite effects for different forms of some proteins. For instance, T3D infection decreased expression of a high molecular weight pyruvate kinase (Gel slice 1), but increased expression of lower molecular weight forms (Gel slices 4 and 5).

Changes in heat shock protein (HSP) expression in primary cardiac myocyte cultures following T3D infection. Seventeen HSPs with different GenBank accession number were identified from database searches (Table App.3.5). Again, T3D either up- or down-regulated them, and induced opposite effects for different molecular weight forms.

DISCUSSION

We did not identify cryptdin 4 expression in this proteomic study, providing further evidence that the previous identification (Appendix II) was in error. We identified many

HSPs in both T3D- and mock-infected primary cardiac myocyte cultures, including the one we are most interested in, Hsp25. However, compared to other HSPs, Hsp25 expression was not as abundant as others, and we did not detect Hsp25 expression in T3D-infected samples. The absence of Hsp25 in T3D-infected samples could reflect differences in sensitivity of the two proteomic approaches, given the much greater protein complexity in the MS/MS analysis from LC compared to 2D-DIGE.

REFERENCES

1. **Wilm, M., A. Shevchenko, T. Houthaeve, S. Breit, L. Schweigerer, T. Fotsis, and M. Mann.** 1996. Femtomole sequencing of proteins from polyacrylamide gels by nano-electrospray mass spectrometry. Nature **379:**466-9.

Table App.3.1. Sample preparation for 1D gel electrophoresis (µl)

	T3D	Mock
Sample	19.5	19.5
NuPage LDS sample buffer(4x)	7.5	7.5
NuPage reducing agent(10x)	3	3
Total	30	30

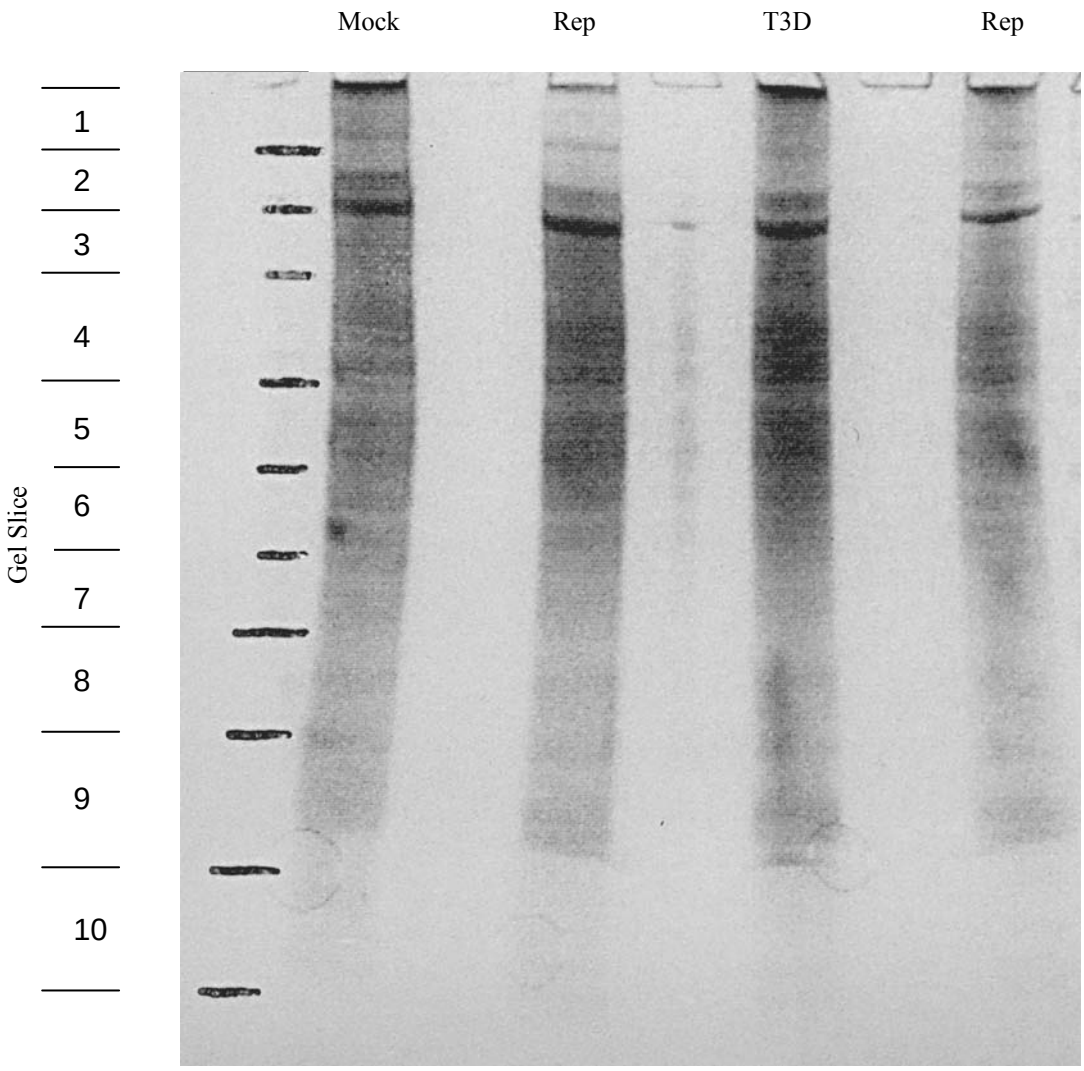

Figure App.3.1. Gel slice distribution on 1D-gel image.

Table App.3.2. Proteins differentially expressed between T3D-and mock-infected primary cardiac myocyte cultures

Protein Key [1]	Protein.Name	Fold change (T3D/Mock)	Gel Slice	Protein Ave Mass
35114	gi|31982178|NP_032644.2| malate dehydrogenase 1	-28.53	1	36468
19325	gi|13195690|NP_077239.1| ribosomal protein S27a [Mus musculus]	-27.76	9	17950
15990	gi|157671923|NP_062613.3| ubiquitin C [Mus musculus]	-27.76	9	82550
19423	gi|6755919|NP_035794.1| ubiquitin B [Mus musculus]	-27.76	9	34368
31117	gi|76443694|NP_001029037.1| ribosomal protein S27a [Mus musculus]	-27.76	9	17950
17363	gi|28316746|NP_783583.1| histone cluster 4	-20.62	9	11367
4466	gi|30061359|NP_835583.1| histone cluster 1	-20.62	9	11367
20133	gi|33859482|NP_031933.1| eukaryotic translation elongation factor 2 [Mus musculus]	-17.88	1	95314
25056	gi|6755040|NP_035202.1| profilin 1 [Mus musculus]	-17.56	1	14957
16155	gi|21450277|NP_659149.1| Na+/K+ -ATPase alpha 1 subunit [Mus musculus]	-15.67	1	112982
20115	gi|6678768|NP_032564.1| myristoylated alanine rich protein kinase C substrate [Mus musculus]	-14.64	4	29661
32417	gi|33859624|NP_035441.1| S100 calcium binding protein A4 [Mus musculus]	-14.05	9	11721
34454	gi|6678413|NP_033441.1| triosephosphate isomerase 1 [Mus musculus]	-13.66	9	26712
8453	gi|22267442|NP_080175.1| ubiquinol cytochrome c reductase core protein 2 [Mus musculus]	-11.59	1	48234
1626	gi|13626040|NP_112462.1| A kinase (PRKA) anchor protein (gravin) 12 [Mus musculus]	-11.40	1	180695
21251	gi|40254577|NP_035425.2| ribosomal protein S12 [Mus musculus]	-10.88	9	14515
32806	gi|31982520|NP_031407.2| acyl-Coenzyme A dehydrogenase	-10.76	1	47897
29414	gi|162463438|NP_001104805.1| similar to ATP synthase	-10.67	9	11509
12781	gi|163965357|NP_001106670.1| nascent polypeptide-associated complex alpha subunit isoform a [Mus musculus]	-10.52	1	220499
25056	gi|6755040|NP_035202.1| profilin 1 [Mus musculus]	-10.38	9	14957
14442	gi|145966915|NP_598841.1| filamin B	-10.24	1	276599
4580	gi|31981562|NP_035229.2| pyruvate kinase	-10.23	1	57845
19199	gi|153791853|NP_034991.3| myosin	-9.97	9	18864
16178	gi|133778978|NP_034645.2| insulin-like growth factor 2 receptor [Mus musculus]	-9.89	1	273816
30749	gi|125347376|NP_034357.2| filamin	-9.63	1	280501
3861	gi|145864471|NP_001078847.1| RIKEN cDNA 0610038P03 [Mus musculus]	-9.45	1	221497

Table App.3.2. Continued

151	gi|115496850|NP_001070022.1| spectrin alpha 2 [Mus musculus]	-9.35	1	285345
16833	gi|31980744|NP_038823.2| ATP synthase	-9.20	9	11424
3283	gi|6671507|NP_031418.1| actin	-9.13	1	42009
5920	gi|18859641|NP_542766.1| myosin	-8.58	1	222879
8243	gi|134031947|NP_032679.2| myosin binding protein C	-8.52	1	141395
8959	gi|117938332|NP_787030.2| spectrin beta 2 isoform 1 [Mus musculus]	-8.47	1	274223
11757	gi|117938334|NP_033286.2| spectrin beta 2 isoform 2 [Mus musculus]	-8.47	1	251156
26289	gi|31543330|NP_032736.2| nicotinamide nucleotide transhydrogenase [Mus musculus]	-8.45	1	113882
6278	gi|6806903|NP_033852.1| ATPase	-8.36	1	109753
34439	gi|153792649|NP_001093105.1| muscle embryonic myosin heavy chain 3 [Mus musculus]	-8.32	1	223791
7406	gi|158635979|NP_001103610.1| ATPase	-8.24	1	114858
5495	gi|31542159|NP_058025.2| ATPase	-8.23	1	113638
9784	gi|88196776|NP_001034634.1| myosin	-8.02	1	219738
2921	gi|124486959|NP_001074719.1| myosin	-7.99	1	223561
8943	gi|51491845|NP_001003908.1| clathrin	-7.74	1	191557
26254	gi|47059073|NP_035710.2| thrombospondin 1 [Mus musculus]	-7.51	1	129690
3594	gi|31981600|NP_035015.2| NADH dehydrogenase (ubiquinone) 1 alpha subcomplex	-7.22	9	10915
11483	gi|6754524|NP_034829.1| lactate dehydrogenase A [Mus musculus]	-7.20	1	36498
519	gi|124487139|NP_001074654.1| filamin C	-7.13	1	291119
28487	gi|6679439|NP_032933.1| peptidylprolyl isomerase A [Mus musculus]	-7.01	8	17971
33856	gi|134288917|NP_084514.2| dynein	-6.78	1	532046
31850	gi|61743961|NP_033773.1| AHNAK nucleoprotein isoform 1 [Mus musculus]	-6.65	1	604254
15880	gi|41322921|NP_958788.1| plectin 1 isoform 3 [Mus musculus]	-6.11	1	514887
10888	gi|163310736|NP_001074711.2| talin 2 [Mus musculus]	-6.08	1	271667
11209	gi|31560653|NP_032852.2| phosphofructokinase	-5.63	1	85360
28106	gi|18859597|NP_077182.1| NADH dehydrogenase (ubiquinone) 1	-5.51	9	14163
17524	gi|31712036|NP_853613.1| eukaryotic translation initiation factor 5A [Mus musculus]	-5.42	9	16832
9513	gi|6753810|NP_034304.1| fatty acid binding protein 3	-5.38	9	14818
35070	gi|13385268|NP_080073.1| cytochrome b-5 [Mus musculus]	-5.12	8	15241
24959	gi|6755809|NP_035732.1| talin 1 [Mus musculus]	-5.05	1	269833

Table App.3.2. Continued

19325	gi|13195690|NP_077239.1| ribosomal protein S27a [Mus musculus]	-4.76	1	17950
15990	gi|157671923|NP_062613.3| ubiquitin C [Mus musculus]	-4.76	1	82550
19423	gi|6755919|NP_035794.1| ubiquitin B [Mus musculus]	-4.76	1	34368
13897	gi|124486606|NP_001074488.1| histone H3-like [Mus musculus]	-4.62	8	15241
18758	gi|21489953|NP_473386.1| histone cluster 2	-4.62	8	15388
4542	gi|30061345|NP_835514.1| histone cluster 1	-4.62	8	15404
27897	gi|6680161|NP_032237.1| H3 histone	-4.62	8	15327
16349	gi|6681137|NP_031856.1| diazepam binding inhibitor isoform 2 [Mus musculus]	-4.54	9	10000
11445	gi|83921595|NP_001033088.1| diazepam binding inhibitor isoform 1 [Mus musculus]	-4.54	9	15228
8786	gi|6753498|NP_034071.1| cytochrome c oxidase subunit IV isoform 1 [Mus musculus]	-4.45	8	19530
35160	gi|167716841|YP_001686702.1| ATP synthase F0 subunit 8 [Mus musculus musculus]	-4.44	9	7784
20950	gi|34538602|NP_904332.1| ATP synthase F0 subunit 8 [Mus musculus]	-4.44	9	7766
9491	gi|27369581|NP_766024.1| solute carrier family 25 (mitochondrial carrier	-4.38	3	74569
26213	gi|12963571|NP_075691.1| NADH dehydrogenase (ubiquinone) 1 alpha subcomplex	-4.17	8	12575
1217	gi|7305121|NP_038783.1| glycogenin 1 [Mus musculus]	-4.02	1	37402
20556	gi|22165347|NP_035638.1| eukaryotic translation initiation factor 1 [Mus musculus]	-4.00	9	12746
26589	gi|146219830|NP_001078919.1| catenin	-3.85	3	104925
17369	gi|146231979|NP_001078922.1| catenin	-3.85	3	101744
28605	gi|83745122|NP_031641.2| catenin	-3.85	3	104925
11456	gi|148747424|NP_031476.3| solute carrier family 25 (mitochondrial carrier	-3.70	1	32904
29820	gi|19882225|NP_080212.1| arginyl-tRNA synthetase [Mus musculus]	-3.68	3	75721
31307	gi|13385322|NP_080119.1| NADH dehydrogenase (ubiquinone) 1 beta subcomplex	-3.64	8	16330
26697	gi|21728370|NP_080178.1| CDGSH iron sulfur domain 2 [Mus musculus]	-3.48	9	15242
10792	gi|21314826|NP_080886.1| NADH dehydrogenase 1 beta subcomplex 4 [Mus musculus]	-3.46	8	15081
13178	gi|113680348|NP_032010.2| fascin homolog 1	-3.45	4	54508
14475	gi|6756085|NP_035907.1| zyxin [Mus musculus]	-3.30	3	60546
27823	gi|13384700|NP_079610.1| endoplasmic reticulum protein ERp19 [Mus musculus]	-3.27	8	19048
19179	gi|6671762|NP_031736.1| creatine kinase	-3.09	5	43045

Table App.3.2. Continued

15418	gi|6681095|NP_031834.1| cytochrome c	-3.06	8	11605
6293	gi|157951643|NP_150371.4| actinin alpha 2 [Mus musculus]	-2.89	3	103833
23590	gi|13385726|NP_080495.1| ubiquinol-cytochrome c reductase binding protein [Mus musculus]	-2.84	9	13561
24809	gi|6677783|NP_033109.1| ribosomal protein L30 [Mus musculus]	-2.79	8	12784
12259	gi|20982845|NP_631888.1| pigpen [Mus musculus]	-2.71	4	52673
1767	gi|83745120|NP_080296.3| ribosomal protein	-2.68	9	11650
15418	gi|6681095|NP_031834.1| cytochrome c	-2.67	9	11605
3461	gi|124301206|NP_766340.3| sorbin and SH3 domain containing 2 [Mus musculus]	-2.67	3	142428
27945	gi|6677775|NP_033105.1| ribosomal protein L22 [Mus musculus]	-2.66	8	14758
3862	gi|23956096|NP_062363.1| USO1 homolog	-2.64	3	106983
11452	gi|162287370|NP_001002011.2| lamin A isoform A [Mus musculus]	-2.54	3	74237
7264	gi|6754450|NP_034764.1| fatty acid binding protein 5	-2.52	8	15137
9243	gi|21312159|NP_081168.1| eukaryotic translation initiation factor 1B [Mus musculus]	-2.45	9	12823
19199	gi|153791853|NP_034991.3| myosin	-2.43	7	18864
34280	gi|16716343|NP_444301.1| cytochrome c oxidase	-2.36	9	8469
33205	gi|160415213|NP_031510.2| ras homolog gene family	-2.36	8	22006
7347	gi|31542143|NP_058082.2| ras homolog gene family	-2.36	8	21782
28148	gi|45597447|NP_035564.1| superoxide dismutase 1	-2.29	8	15942
13197	gi|9790219|NP_062745.1| destrin [Mus musculus]	-2.25	8	18521
18785	gi|6679567|NP_033012.1| polymerase I and transcript release factor [Mus musculus]	-2.01	4	43953
16469	gi|33563260|NP_034602.1| HIV-1 Rev binding protein [Mus musculus]	-1.96	4	57914
28469	gi|31560313|NP_067497.2| ubiquitin specific protease 14 isoform 1 [Mus musculus]	-1.83	4	56002
32542	gi|7657357|NP_056596.1| nucleosome assembly protein 1-like 1 [Mus musculus]	-1.76	4	45345
6592	gi|6678481|NP_033482.1| ubiquitin-conjugating enzyme E2L 3 [Mus musculus]	1.81	8	17861
16686	gi|27754144|NP_079592.2| NADH dehydrogenase (ubiquinone) 1 beta subcomplex	1.90	8	21710
3283	gi|6671507|NP_031418.1| actin	1.90	5	42009
16488	gi|7106387|NP_036097.1| proteasome (prosome	1.97	7	26411
28456	gi|9256624|NP_061358.1| phosphoglycerate mutase 2 [Mus musculus]	1.99	7	28827
17627	gi|6671509|NP_031419.1| actin	2.00	5	41736
11470	gi|7110703|NP_032976.1| protease (prosome	2.00	5	45626
31618	gi|7305143|NP_038848.1| hexokinase 2 [Mus musculus]	2.04	3	102535

Table App.3.2. Continued

30658	gi|161353502|NP_033955.2| serine (or cysteine) proteinase inhibitor	2.15	4	46533
26113	gi|161353504|NP_001104513.1| serine (or cysteine) proteinase inhibitor	2.15	4	46533
7406	gi|158635979|NP_001103610.1| ATPase	2.16	2	114858
11741	gi|19072792|NP_083848.1| thioredoxin domain containing 4 [Mus musculus]	2.16	5	46853
34347	gi|6753530|NP_034094.1| crystallin	2.19	7	20068
17225	gi|6756039|NP_035869.1| tyrosine 3-monooxygenase/tryptophan 5-monooxygenase activation protein	2.20	7	27778
26529	gi|70778976|NP_032854.2| phosphoglycerate kinase 1 [Mus musculus]	2.23	4	44550
25984	gi|51093840|NP_660121.2| eukaryotic translation initiation factor 3 subunit 6 interacting protein [Mus musculus]	2.24	4	66613
12788	gi|114326546|NP_075907.2| phosphoglycerate mutase 1 [Mus musculus]	2.26	7	28832
4580	gi|31981562|NP_035229.2| pyruvate kinase	2.26	4	57845
6278	gi|6806903|NP_033852.1| ATPase	2.27	2	109753
5592	gi|21313476|NP_079811.1| SAR1a gene homolog 2 [Mus musculus]	2.28	7	22381
27489	gi|124430537|NP_001074443.1| sorcin isoform 1 [Mus musculus]	2.28	7	21627
23409	gi|7106289|NP_034179.1| dihydrofolate reductase [Mus musculus]	2.30	7	21606
34454	gi|6678413|NP_033441.1| triosephosphate isomerase 1 [Mus musculus]	2.30	7	26712
10194	gi|21312260|NP_082546.1| aldehyde dehydrogenase 1 family	2.31	4	57553
6577	gi|21312012|NP_080979.1| NADH dehydrogenase (ubiquinone) 1 alpha subcomplex	2.32	7	19992
20460	gi|31980762|NP_038699.2| superoxide dismutase 2	2.32	7	24602
21908	gi|6671539|NP_031464.1| aldolase 1	2.33	5	39356
11735	gi|6678393|NP_033432.1| troponin I	2.33	7	24258
30658	gi|161353502|NP_033955.2| serine (or cysteine) proteinase inhibitor	2.35	5	46533
26113	gi|161353504|NP_001104513.1| serine (or cysteine) proteinase inhibitor	2.35	5	46533
3437	gi|161353506|NP_001104514.1| serine (or cysteine) proteinase inhibitor	2.35	5	46533
8453	gi|22267442|NP_080175.1| ubiquinol cytochrome c reductase core protein 2 [Mus musculus]	2.36	5	48234
14404	gi|160298209|NP_034454.2| glutamate oxaloacetate transaminase 1	2.37	5	46247
22990	gi|7657067|NP_056589.1| ERO1-like [Mus musculus]	2.38	4	54084

Table App.3.2. Continued

16809	gi|20070412|NP_613063.1| ATP synthase	2.40	8	23363
25585	gi|13195646|NP_077185.1| LIM only protein HLP [Mus musculus]	2.41	7	22727
24603	gi|28893017|NP_796066.1| methionine-R-sulfoxide reductase B3 [Mus musculus]	2.42	7	20224
30088	gi|176865892|NP_038534.2| eukaryotic translation initiation factor 4A2 isoform a [Mus musculus]	2.46	5	46402
30655	gi|176866061|NP_001116510.1| eukaryotic translation initiation factor 4A2 isoform c [Mus musculus]	2.46	5	41290
7982	gi|31981605|NP_034988.2| myosin	2.47	7	21189
10047	gi|31981382|NP_035960.2| inosine 5'-phosphate dehydrogenase 2 [Mus musculus]	2.48	4	55815
14730	gi|30519911|NP_848713.1| transgelin 2 [Mus musculus]	2.48	7	22395
11863	gi|31980648|NP_058054.2| ATP synthase	2.49	5	56300
19152	gi|6679805|NP_032046.1| FK506 binding protein 2 [Mus musculus]	2.52	9	15343
31814	gi|161484662|NP_001002239.2| ribosomal protein L17 [Mus musculus]	2.56	7	21397
10674	gi|33859753|NP_077777.1| RAS related protein 1b [Mus musculus]	2.58	7	20824
29003	gi|29126205|NP_803421.1| acetyl-Coenzyme A acyltransferase 2 (mitochondrial 3-oxoacyl-Coenzyme A thiolase) [Mus musculus]	2.60	5	41829
23040	gi|45504394|NP_034708.1| integrin beta 1 (fibronectin receptor beta) [Mus musculus]	2.61	2	88231
15149	gi|6755965|NP_035825.1| voltage-dependent anion channel 2 [Mus musculus]	2.64	7	31732
14325	gi|27370516|NP_766599.1| isocitrate dehydrogenase 2 (NADP+)	2.65	5	50934
23693	gi|157951700|NP_033944.2| calsequestrin 2 [Mus musculus]	2.68	5	48176
34717	gi|6753912|NP_034369.1| ferritin heavy chain 1 [Mus musculus]	2.70	7	21066
19325	gi|13195690|NP_077239.1| ribosomal protein S27a [Mus musculus]	2.71	3	17950
15990	gi|157671923|NP_062613.3| ubiquitin C [Mus musculus]	2.71	3	82550
19423	gi|6755919|NP_035794.1| ubiquitin B [Mus musculus]	2.71	3	34368
31117	gi|76443694|NP_001029037.1| ribosomal protein S27a [Mus musculus]	2.71	3	17950
16690	gi|6754036|NP_034455.1| glutamate oxaloacetate transaminase 2	2.73	5	47411
34130	gi|112181167|NP_031599.2| complement component 1	2.73	7	31024

Table App.3.2. Continued

2632	gi|84871986|NP_032186.2| glutathione peroxidase 1 [Mus musculus]	2.75	7	22179
6447	gi|6755714|NP_035656.1| transgelin [Mus musculus]	2.78	7	22575
1382	gi|7304987|NP_038836.1| cysteine and glycine-rich protein 3 [Mus musculus]	2.82	7	20894
3946	gi|33563264|NP_034989.1| myosin	2.83	7	22421
4266	gi|6680231|NP_032279.1| high mobility group box 3 [Mus musculus]	2.84	7	23010
28225	gi|84781781|NP_001028485.1| PDGFA associated protein 1 [Mus musculus]	2.84	7	20604
29380	gi|19526463|NP_080405.1| endoplasmic reticulum protein ERp29 precursor [Mus musculus]	2.91	7	28823
10595	gi|84794552|NP_061346.2| phosphatidylethanolamine binding protein 1 [Mus musculus]	2.91	7	20830
542	gi|13385408|NP_080195.1| ribosomal protein L11 [Mus musculus]	2.92	7	20252
25431	gi|148747410|NP_666097.3| archain 1 [Mus musculus]	2.93	4	57229
2321	gi|46430508|NP_997406.1| ribosomal protein L23a [Mus musculus]	2.94	7	17695
8526	gi|10946936|NP_067490.1| adenylate kinase 1 [Mus musculus]	2.95	7	23116
9358	gi|18250296|NP_077180.1| ribosomal protein L24 [Mus musculus]	2.97	7	17778
19325	gi|13195690|NP_077239.1| ribosomal protein S27a [Mus musculus]	2.98	10	17950
15990	gi|157671923|NP_062613.3| ubiquitin C [Mus musculus]	2.98	10	82550
19423	gi|6755919|NP_035794.1| ubiquitin B [Mus musculus]	2.98	10	34368
31117	gi|76443694|NP_001029037.1| ribosomal protein S27a [Mus musculus]	2.98	10	17950
14542	gi|21312062|NP_081051.1| transmembrane emp24 domain-containing protein 10 [Mus musculus]	2.98	7	24910
19684	gi|30089710|NP_783593.1| histone cluster 2	3.01	8	13988
17243	gi|113679874|NP_080948.2| glutathione S-transferase	3.07	7	25709
25043	gi|162417994|NP_001104783.1| ribosomal protein L21-like [Mus musculus]	3.07	7	18626
31639	gi|6753556|NP_034113.1| cathepsin D [Mus musculus]	3.07	5	44953
32917	gi|31982186|NP_032643.2| malate dehydrogenase 2	3.09	7	35611
6679	gi|21450129|NP_659033.1| acetyl-Coenzyme A acetyltransferase 1 precursor [Mus musculus]	3.09	5	44816
24067	gi|30794476|NP_068680.1| protein kinase	3.10	5	43185
23402	gi|19526814|NP_598427.1| NADH dehydrogenase (ubiquinone) flavoprotein 1 [Mus musculus]	3.13	5	50834

Table App.3.2. Continued

8991	gi|58037267|NP_082235.1| protein disulfide isomerase-associated 6 [Mus musculus]	3.14	5	48689
21497	gi|6679501|NP_032973.1| protease (prosome	3.14	4	49184
26864	gi|6755963|NP_035824.1| voltage-dependent anion channel 1 [Mus musculus]	3.17	7	30755
2916	gi|31560385|NP_062621.2| ribosomal protein L21 [Mus musculus]	3.21	7	18578
5027	gi|125988403|NP_083977.1| signal peptidase complex subunit 3 [Mus musculus]	3.22	7	20313
30612	gi|6680690|NP_031478.1| peroxiredoxin 3 [Mus musculus]	3.23	7	28127
16809	gi|20070412|NP_613063.1| ATP synthase	3.25	7	23363
11720	gi|96975138|NP_038584.2| hypoxanthine guanine phosphoribosyl transferase 1 [Mus musculus]	3.25	7	24570
15852	gi|6754724|NP_034947.1| proteasome (prosome	3.27	5	36539
8240	gi|13277394|NP_077798.1| GrpE-like 1	3.28	7	24307
3003	gi|6680121|NP_032209.1| glutathione S-transferase	3.29	7	25716
13636	gi|6754084|NP_034488.1| glutathione S-transferase	3.29	7	25970
15435	gi|21313679|NP_082138.1| ATP synthase	3.29	7	18749
5368	gi|28076911|NP_081040.1| glutathione S-transferase	3.34	7	25519
4643	gi|6754976|NP_035164.1| peroxiredoxin 1 [Mus musculus]	3.35	7	22176
18616	gi|31981945|NP_033464.2| ribosomal protein L13a [Mus musculus]	3.38	7	23464
17228	gi|6754090|NP_034492.1| glutathione S-transferase omega 1 [Mus musculus]	3.40	7	27497
1136	gi|6677813|NP_033124.1| ribosomal protein S8 [Mus musculus]	3.41	7	24205
30329	gi|76677915|NP_084367.1| GTP-binding protein PTD004 isoform b [Mus musculus]	3.41	5	30376
20036	gi|58037117|NP_080964.1| NADH dehydrogenase (ubiquinone) Fe-S protein 3 [Mus musculus]	3.41	7	30149
24822	gi|83921612|NP_663342.3| thioredoxin domain containing 5 [Mus musculus]	3.42	5	46415
1168	gi|6677777|NP_033106.1| ribosomal protein L26 [Mus musculus]	3.43	7	17258
5073	gi|6677819|NP_033127.1| Harvey rat sarcoma oncogene	3.45	7	23763
32806	gi|31982520|NP_031407.2| acyl-Coenzyme A dehydrogenase	3.48	5	47897
28472	gi|6678365|NP_033417.1| RAN	3.48	7	24423
27815	gi|34328471|NP_062364.3| ras related v-ral simian leukemia viral oncogene homolog A [Mus musculus]	3.50	7	23552
13502	gi|6755198|NP_036098.1| proteasome (prosome	3.50	7	27372
31466	gi|7242197|NP_035315.1| proteasome (prosome	3.53	7	26372
12511	gi|6755843|NP_035749.1| troponin T2	3.53	5	34219

Table App.3.2. Continued

8147	gi|6679261|NP_032836.1| pyruvate dehydrogenase E1 alpha 1 [Mus musculus]	3.57	5	43231
19689	gi|6681273|NP_031932.1| eukaryotic translation elongation factor 1 alpha 2 [Mus musculus]	3.57	5	50454
23088	gi|10092608|NP_038569.1| glutathione S-transferase	3.57	7	23609
21524	gi|21450157|NP_659048.1| LIM and cysteine-rich domains 1 [Mus musculus]	3.58	5	40996
25848	gi|30841008|NP_851415.1| RAB18	3.59	7	23035
18935	gi|6755258|NP_035355.1| RAB18	3.59	7	23035
6424	gi|31982030|NP_598557.3| Rho GDP dissociation inhibitor (GDI) alpha [Mus musculus]	3.61	7	23407
10771	gi|11612509|NP_071722.1| v-ral simian leukemia viral oncogene homolog B (ras related) [Mus musculus]	3.61	7	23349
5771	gi|6678097|NP_033280.1| serine (or cysteine) proteinase inhibitor	3.63	5	42599
7737	gi|7304963|NP_038913.1| chloride intracellular channel 4 (mitochondrial) [Mus musculus]	3.63	7	28729
32536	gi|124487362|NP_001074562.1| ADP-ribosylation factor interacting protein 1 [Mus musculus]	3.65	5	41518
23266	gi|13654249|NP_112467.1| phosphoglycerate kinase 2 [Mus musculus]	3.66	5	44883
9387	gi|6679441|NP_032934.1| peptidylprolyl isomerase C [Mus musculus]	3.69	7	22794
26800	gi|51511741|NP_001003933.1| reticulon 3 isoform 2 [Mus musculus]	3.71	7	101919
31854	gi|54607016|NP_001003934.1| reticulon 3 isoform 1 [Mus musculus]	3.71	7	103878
3155	gi|34740335|NP_035784.1| tubulin	3.73	5	50151
21023	gi|160298217|NP_034487.2| glutathione S-transferase	3.78	7	25563
774	gi|21450625|NP_659207.1| eukaryotic translation initiation factor 4A1 [Mus musculus]	4	5	46154
33922	gi|31980840|NP_059078.2| RAB11a	3.81	7	24393
34327	gi|6679583|NP_033023.1| RAB11B	3.81	7	24489
18906	gi|6755350|NP_035417.1| ribosomal protein L10A [Mus musculus]	3.82	7	24916
30355	gi|6679651|NP_031959.1| enolase 3	3.84	5	47024
9862	gi|6671549|NP_031479.1| peroxiredoxin 6 [Mus musculus]	3.84	7	24826
11863	gi|31980648|NP_058054.2| ATP synthase	3.87	4	56300
8930	gi|16716353|NP_444306.1| reticulon 3 isoform 4 [Mus musculus]	3.90	7	25427
15999	gi|83699424|NP_033103.2| ribosomal protein L18 [Mus musculus]	3.95	7	21644
14706	gi|6680836|NP_031617.1| calreticulin [Mus musculus]	3.97	4	47994
3727	gi|32401425|NP_861461.1| glutathione S-transferase	3.98	7	23537

Table App.3.2. Continued

22455	gi|6753036|NP_033786.1| aldehyde dehydrogenase 2	4.02	4	56537
33577	gi|28916703|NP_796230.1| peroxiredoxin 5 related sequence 1 protein [Mus musculus]	4.02	7	24995
23262	gi|71774133|NP_035279.2| peptidylprolyl isomerase B [Mus musculus]	4.04	7	23713
30359	gi|176865998|NP_001116509.1| eukaryotic translation initiation factor 4A2 isoform b [Mus musculus]	4.13	5	36166
5580	gi|21313144|NP_080218.1| GTP-binding protein PTD004 isoform a [Mus musculus]	4.18	5	44729
14998	gi|6755100|NP_035249.1| ErbB3-binding protein 1 [Mus musculus]	4.21	5	43698
23491	gi|21704100|NP_663533.1| mitochondrial trifunctional protein	4.25	5	51386
2941	gi|6681069|NP_031817.1| cysteine and glycine-rich protein 1 [Mus musculus]	4.27	7	20583
26783	gi|6755376|NP_035430.1| ribosomal protein S7 [Mus musculus]	4.28	7	22126
29782	gi|33186863|NP_058018.2| ribosomal protein L13 [Mus musculus]	4.28	7	24305
5865	gi|20070420|NP_613067.1| es1 protein [Mus musculus]	4.33	7	28090
26529	gi|70778976|NP_032854.2| phosphoglycerate kinase 1 [Mus musculus]	4.39	5	44550
24632	gi|148747526|NP_033031.2| RAB7	4.40	7	23489
3155	gi|34740335|NP_035784.1| tubulin	4.44	4	50151
8383	gi|124486895|NP_001074743.1| phosphogluconate dehydrogenase [Mus musculus]	4.45	5	53247
1060	gi|46849708|NP_035636.1| succinate-Coenzyme A ligase	4	5	50114
15153	gi|33859554|NP_034339.1| fumarate hydratase 1 [Mus musculus]	4.48	5	54370
6996	gi|31981939|NP_033477.2| tubulin	4.49	5	49585
31422	gi|33504483|NP_084043.1| ribosomal protein S9-like [Mus musculus]	4.57	7	22591
34006	gi|31982526|NP_065631.3| parvin	4.58	5	42329
31759	gi|8393784|NP_059076.1| septin 9 isoform c [Mus musculus]	4.59	4	38599
8154	gi|22165384|NP_666228.1| tubulin	4.84	5	49831
27488	gi|33859662|NP_036167.1| vesicle amine transport protein 1 homolog (T californica) [Mus musculus]	4.85	5	43096
11292	gi|6754816|NP_035021.1| septin 2 [Mus musculus]	4.90	5	41525
20408	gi|78214312|NP_033855.2| ATP synthase	4.90	7	28948
16829	gi|113866024|NP_077776.2| RAB5C	4.94	7	23412
18218	gi|13385374|NP_080163.1| RAB5A	4.95	7	23598
4580	gi|31981562|NP_035229.2| pyruvate kinase	4.96	5	57845

Table App.3.2. Continued

24536	gi|21313162|NP_083852.1| RAB1B	4.96	7	22187
22200	gi|6679587|NP_033022.1| RAB1	4.97	7	22677
3977	gi|28916687|NP_803130.1| RAB5B	5.05	7	23706
31286	gi|6755262|NP_035359.1| RAB5B	5.05	7	23706
1363	gi|21746161|NP_076205.1| tubulin	5.21	5	49953
15891	gi|28173550|NP_033989.2| cell division cycle 10 homolog [Mus musculus]	5.26	5	50649
5086	gi|27734154|NP_775589.1| RAB8B	5.40	7	23603
19735	gi|38372905|NP_075615.2| cell line NK14 derived transforming oncogene [Mus musculus]	5.40	7	23668
22578	gi|21313536|NP_084501.1| dihydrolipoamide S-succinyltransferase (E2 component of 2-oxo-glutarate complex) [Mus musculus]	5.44	5	48994
5239	gi|7710086|NP_057885.1| RAB10	5.50	7	22540
27592	gi|21311975|NP_080953.1| RAS-associated protein RAB13 [Mus musculus]	5.69	7	22770
20432	gi|58037109|NP_080960.1| NADH dehydrogenase (ubiquinone) 1 beta subcomplex	5.76	7	21023
3452	gi|38198665|NP_938085.1| p47 protein [Mus musculus]	5.76	5	40953
1363	gi|21746161|NP_076205.1| tubulin	5.87	4	49953
8154	gi|22165384|NP_666228.1| tubulin	5.87	4	49831
18082	gi|116089273|NP_032138.3| guanosine diphosphate (GDP) dissociation inhibitor 2 [Mus musculus]	5.99	5	50537
31587	gi|6755202|NP_036101.1| proteasome beta 3 subunit [Mus musculus]	6.04	7	22965
15035	gi|22267440|NP_059071.1| osteoclast stimulating factor 1 [Mus musculus]	6.54	7	23782
24832	gi|10946940|NP_067493.1| RAB2A	6.72	7	23547
35160	gi|167716841|YP_001686702.1| ATP synthase F0 subunit 8 [Mus musculus musculus]	6.75	10	7784
20950	gi|34538602|NP_904332.1| ATP synthase F0 subunit 8 [Mus musculus]	6.75	10	7766
3196	gi|148747558|NP_035693.3| peroxiredoxin 2 [Mus musculus]	6.76	7	21778
27032	gi|31982856|NP_031887.2| dihydrolipoamide dehydrogenase [Mus musculus]	7.15	4	54272
13051	gi|61888838|NP_058043.3| hydroxyacyl-Coenzyme A dehydrogenase type II [Mus musculus]	7.74	7	27273
16005	gi|21312564|NP_082320.1| calponin 3	8.03	5	36428
12266	gi|30519997|NP_848760.1| bleomycin hydrolase [Mus musculus]	8.18	5	52511
16513	gi|34328206|NP_035840.2| tryptophanyl-tRNA synthetase [Mus musculus]	9.35	4	54325
34425	gi|6754994|NP_035995.1| poly(rC) binding protein 1 [Mus musculus]	11.52	5	37497

Table App.3.2. Continued

8735	gi|133922588|NP_001001892.2| histocompatibility 2	13.00	5	41301
29867	gi|6996913|NP_031611.1| annexin A2 [Mus musculus]	29.12	5	38676

[1] Identification number for LC-MS/MS

Table App.3.3. Proteins unique to T3D infection in primary cardiac myocyte cultures

Protein Key [1]	Protein.Name	Gel Slice	protein.fmolOnColumn [2]
16512	gi|104294890|NP_001035785.1| signaling molecule ATTP [Mus musculus]	9	22
15164	gi|10946948|NP_067499.1| nicotinamide phosphoribosyltransferase [Mus musculus]	4	48
5514	gi|110625979|NP_080283.3| eukaryotic translation elongation factor 1 gamma [Mus musculus]	4	45
20442	gi|110626104|NP_032357.2| interferon-induced protein with tetratricopeptide repeats 1 [Mus musculus]	4	25
20442	gi|110626104|NP_032357.2| interferon-induced protein with tetratricopeptide repeats 1 [Mus musculus]	5	99
30942	gi|112807186|NP_766307.2| GCN1 general control of amino-acid synthesis 1-like 1 [Mus musculus]	1	3
30942	gi|112807186|NP_766307.2| GCN1 general control of amino-acid synthesis 1-like 1 [Mus musculus]	4	58
15978	gi|114326482|NP_033309.3| signal transducer and activator of transcription 1 [Mus musculus]	3	62
14987	gi|117956381|NP_598774.2| proteasome (prosome	5	238
946	gi|118601013|NP_033828.2| adenine phosphoribosyl transferase [Mus musculus]	8	47
26519	gi|124430543|NP_079894.2| sorcin isoform 2 [Mus musculus]	7	41
519	gi|124487139|NP_001074654.1| filamin C	2	11
9223	gi|124517663|NP_034860.2| annexin A1 [Mus musculus]	5	214
13723	gi|13195624|NP_077159.1| NADH dehydrogenase (ubiquinone) 1 alpha subcomplex 10 [Mus musculus]	5	153
19325	gi|13195690|NP_077239.1| ribosomal protein S27a [Mus musculus]	7	163
6546	gi|133778955|NP_034510.3| histocompatibility 2	4	34
6546	gi|133778955|NP_034510.3| histocompatibility 2	5	435
30782	gi|13385290|NP_080097.1| calcium-regulated heat-stable protein (24kD) [Mus musculus]	7	35
34858	gi|146229342|NP_067624.2| myosin light chain 2	8	208
28722	gi|146260276|NP_001005858.2| similar to interferon-induced protein with tetratricopeptide repeats 3 [Mus musculus]	5	156
15475	gi|148222065|NP_035019.1| nebulin [Mus musculus]	8	44
11456	gi|148747424|NP_031476.3| solute carrier family 25 (mitochondrial carrier	3	19
11456	gi|148747424|NP_031476.3| solute carrier family 25 (mitochondrial carrier	2	49
16794	gi|153945886|NP_766277.3| DEAD/H box polypeptide RIG-I [Mus musculus]	3	13
15990	gi|157671923|NP_062613.3| ubiquitin C [Mus musculus]	2	80
15990	gi|157671923|NP_062613.3| ubiquitin C [Mus musculus]	4	91

Table App.3.3. Continued

15990	gi|157671923|NP_062613.3| ubiquitin C [Mus musculus]	7	163
33169	gi|158635992|NP_058557.2| carboxyl terminal LIM domain protein 1 [Mus musculus]	5	232
12826	gi|160333390|NP_034520.2| histocompatibility 2	5	324
24771	gi|160333553|NP_033102.2| ribosomal protein L12 [Mus musculus]	8	198
2347	gi|160420310|NP_001091448.2| H2b histone family	8	509
33886	gi|165377065|NP_079923.3| UMP-CMP kinase [Mus musculus]	7	45
3571	gi|16716381|NP_444322.1| lysyl-tRNA synthetase [Mus musculus]	3	15
20181	gi|170295823|NP_035823.3| vascular cell adhesion molecule 1 [Mus musculus]	3	37
18974	gi|170650724|NP_032846.2| peptidase D [Mus musculus]	4	32
24342	gi|188528613|NP_071306.2| glia maturation factor	8	40
34702	gi|19527228|NP_598768.1| CDGSH iron sulfur domain 1 [Mus musculus]	9	44
32935	gi|19527306|NP_598840.1| adenosine kinase [Mus musculus]	5	127
1454	gi|21312570|NP_081676.1| lectin	4	141
32663	gi|21553309|NP_659146.1| apolipoprotein A-I binding protein [Mus musculus]	7	74
3980	gi|22094075|NP_031477.1| solute carrier family 25	3	19
3980	gi|22094075|NP_031477.1| solute carrier family 25	2	46
32266	gi|23956082|NP_058676.1| ribosomal protein L5 [Mus musculus]	1	23
2463	gi|27229082|NP_081239.1| leucine zipper and CTNNBIP1 domain containing [Mus musculus]	7	30
34428	gi|27369748|NP_766120.1| aldhehyde dehydrogenase family 5	4	123
26269	gi|29244126|NP_808356.1| H2A histone family	8	429
16164	gi|29788764|NP_033764.2| adenylosuccinate lyase [Mus musculus]	4	44
9234	gi|30061379|NP_783592.1| histone cluster 1	8	429
4891	gi|30089706|NP_835501.1| histone cluster 1	8	509
21797	gi|31543946|NP_067359.2| radical S-adenosyl methionine domain containing 2 [Mus musculus]	5	68
28732	gi|31560560|NP_035159.2| ribosomal protein SA [Mus musculus]	5	257
3555	gi|31980821|NP_058586.2| dynactin 3 [Mus musculus]	8	86
3054	gi|31981458|NP_444338.2| glutaredoxin [Mus musculus]	9	23
4580	gi|31981562|NP_035229.2| pyruvate kinase	2	14
7950	gi|31982522|NP_031409.2| acyl-Coenzyme A dehydrogenase	5	244
16536	gi|33469123|NP_036185.1| asparagine synthetase [Mus musculus]	4	54
15153	gi|33859554|NP_034339.1| fumarate hydratase 1 [Mus musculus]	4	36
19435	gi|34878892|NP_035027.1| neurofibromin [Mus musculus]	8	51
33942	gi|45592934|NP_033033.1| RAS-related C3 botulinum substrate 1 [Mus musculus]	8	60
4826	gi|46275816|NP_996893.1| MAM domain containing glycosylphosphatidylinositol anchor 2 [Mus musculus]	8	172
12707	gi|46559412|NP_848142.1| protein kinase C and casein kinase substrate in neurons 1 [Mus musculus]	5	147

Table App.3.3. Continued

26029	gi|54292132|NP_803155.1| phosphoserine aminotransferase 1 [Mus musculus]	5	88
21520	gi|56606023|NP_001008419.1| aldehyde oxidase 3-like 1 [Mus musculus]	7	35
14438	gi|6677977|NP_033213.1| cytochrome c oxidase subunit VIIa polypeptide 2-like [Mus musculus]	9	74
7863	gi|6679299|NP_032857.1| prohibitin [Mus musculus]	7	22
17102	gi|6679421|NP_032924.1| cytochrome P450 reductase [Mus musculus]	3	27
18188	gi|6679961|NP_032124.1| myotrophin [Mus musculus]	9	56
10627	gi|6680359|NP_032356.1| interferon gamma inducible protein 47 [Mus musculus]	5	73
672	gi|6680363|NP_032358.1| interferon-induced protein with tetratricopeptide repeats 2 [Mus musculus]	4	78
8482	gi|66955877|NP_034524.2| histocompatibility 2	5	324
3408	gi|6753098|NP_033824.1| apolipoprotein B editing complex 2 [Mus musculus]	7	101
10093	gi|6753178|NP_035923.1| barrier to autointegration factor 1 [Mus musculus]	9	30
1930	gi|6753364|NP_033991.1| cell division cycle 42 [Mus musculus]	7	37
7543	gi|6753950|NP_034390.1| guanylate nucleotide binding protein 2 [Mus musculus]	4	103
17078	gi|6754132|NP_034521.1| histocompatibility 2	5	324
31140	gi|6754288|NP_034631.1| interferon-induced protein with tetratricopeptide repeats 3 [Mus musculus]	5	208
122	gi|6755076|NP_035230.1| protein kinase	5	162
8541	gi|6755206|NP_035317.1| proteasome (prosome	7	69
17641	gi|7106331|NP_034566.1| H2A histone family	8	309
14498	gi|7110693|NP_032880.1| protein kinase	5	162
6994	gi|7305443|NP_038749.1| ribosomal protein L7a [Mus musculus]	1	8
4812	gi|75677414|NP_031829.2| cortactin [Mus musculus]	3	19
2695	gi|77736537|NP_958927.2| mitogen-activated protein kinase kinase kinase kinase 5 [Mus musculus]	2	6
2695	gi|77736537|NP_958927.2| mitogen-activated protein kinase kinase kinase kinase 5 [Mus musculus]	3	38
31278	gi|82617575|NP_084011.1| glutamyl-prolyl-tRNA synthetase [Mus musculus]	2	24
3140	gi|84042521|NP_001033320.1| barrier to autointegration factor 1 [Mus musculus]	9	30
30889	gi|84781779|NP_001028477.1| NADH dehydrogenase (ubiquinone) 1 beta subcomplex	8	25
33787	gi|85861164|NP_035086.2| oxoglutarate dehydrogenase (lipoamide) [Mus musculus]	3	47
23183	gi|90093349|NP_033758.2| activity-dependent neuroprotective protein [Mus musculus]	4	33

[1] Identification number for LC-MS/MS;

[2] Concentration calculated based on molecular weight of the indicated protein, relative to the internal standard

Table App.3.4. Proteins unique to Mock infection in primary cardiac myocyte cultures

Protein Key [1]	Protein Name	Gel Slice	protein.fmolOnColumn [2]
6736	gi|100818462|NP_663519.2| RAP1	4	17
4241	gi|109150433|NP_062757.2| leprecan 1 isoform 2 [Mus musculus]	3	15
29911	gi|10946574|NP_067248.1| creatine kinase	5	150
31743	gi|10946796|NP_067405.1| Rab interacting lysosomal protein-like 1 [Mus musculus]	9	28
16419	gi|10946862|NP_067442.1| troponin I	7	17
24621	gi|110225360|NP_001035992.1| Bloom syndrome protein homolog [Mus musculus]	4	62
26426	gi|110227377|NP_001035999.1| gelsolin-like capping protein [Mus musculus]	5	53
15276	gi|110227379|NP_031625.2| gelsolin-like capping protein [Mus musculus]	5	53
5514	gi|110625979|NP_080283.3| eukaryotic translation elongation factor 1 gamma [Mus musculus]	1	23
5514	gi|110625979|NP_080283.3| eukaryotic translation elongation factor 1 gamma [Mus musculus]	5	87
2449	gi|110626031|NP_035447.3| KH domain containing	4	56
1746	gi|112181182|NP_031773.2| cytochrome c oxidase	9	1216
8394	gi|113205059|NP_035862.2| nuclease sensitive element binding protein 1 [Mus musculus]	5	134
1742	gi|114326499|NP_075017.2| myosin	7	19
1742	gi|114326499|NP_075017.2| myosin	9	105
7838	gi|115270960|NP_038891.4| Bcl2-associated athanogene 3 [Mus musculus]	3	16
17572	gi|116014342|NP_001070652.1| basigin isoform 2 [Mus musculus]	4	43
17572	gi|116014342|NP_001070652.1| basigin isoform 2 [Mus musculus]	5	63
8460	gi|116256512|NP_001070733.1| heterogeneous nuclear ribonucleoprotein D isoform a [Mus musculus]	5	86
8876	gi|116256516|NP_001070735.1| heterogeneous nuclear ribonucleoprotein D isoform d [Mus musculus]	5	86
9938	gi|117606316|NP_076362.2| centrosomal protein 70 [Mus musculus]	4	109
13322	gi|117676367|NP_035055.2| novel nuclear protein 1 [Mus musculus]	9	2841
32651	gi|117956377|NP_058571.2| Y box protein 2 [Mus musculus]	5	78
11353	gi|124248577|NP_036004.2| proteasome 26S ATPase subunit 4 [Mus musculus]	5	78
6065	gi|124517693|NP_001074906.1| fibulin 2 isoform b [Mus musculus]	2	18
35110	gi|125490378|NP_058057.3| nuclear autoantigenic sperm protein isoform 2 [Mus musculus]	4	30
6341	gi|125628659|NP_075553.2| aspartyl beta-hydroxylase isoform 1 [Mus musculus]	3	24
26004	gi|126090505|NP_001074944.1| nuclear autoantigenic sperm protein isoform 1 [Mus musculus]	4	30
4913	gi|12963653|NP_075860.1| protein (peptidyl-prolyl cis/trans isomerase) NIMA-interacting 1 [Mus musculus]	8	22

Table App.3.4. Continued

490	gi|13195626|NP_077160.1| glutathione peroxidase 7 [Mus musculus]	7	11
9283	gi|13195648|NP_077188.1| reticulon 4 isoform C [Mus musculus]	5	36
12793	gi|13384998|NP_079838.1| tetratricopeptide repeat domain 11 [Mus musculus]	8	37
18251	gi|13385036|NP_079862.1| ribosomal protein L15 [Mus musculus]	7	22
28645	gi|13385090|NP_079904.1| cytochrome c oxidase	9	556
2649	gi|13385168|NP_079986.1| ubiquinol-cytochrome c reductase	7	139
30027	gi|13385260|NP_080066.1| thioesterase superfamily member 2 [Mus musculus]	8	65
19816	gi|13385296|NP_080100.1| basic leucine zipper and W2 domains 1 [Mus musculus]	5	94
28757	gi|13385434|NP_080215.1| phosphoribosylaminoimidazole carboxylase	5	30
17219	gi|13385492|NP_080263.1| NADH dehydrogenase (ubiquinone) 1 alpha subcomplex	8	168
25605	gi|13385558|NP_080337.1| NADH dehydrogenase (ubiquinone) 1 beta subcomplex 8 [Mus musculus]	8	302
14566	gi|13385854|NP_080628.1| peptidylprolyl isomerase D [Mus musculus]	5	56
25696	gi|13385872|NP_080650.1| interleukin enhancer binding factor 2 [Mus musculus]	5	23
20669	gi|13385942|NP_080720.1| citrate synthase [Mus musculus]	5	328
29809	gi|13386060|NP_080835.1| thioredoxin domain containing 17 [Mus musculus]	9	82
23281	gi|13386100|NP_080890.1| NADH dehydrogenase (ubiquinone) 1 alpha subcomplex	9	135
12018	gi|13386122|NP_080908.1| replication protein A3 [Mus musculus]	9	38
24124	gi|13386230|NP_081692.1| calmodulin-like 3 [Mus musculus]	8	63
8486	gi|13386272|NP_082221.1| citrate synthase-like protein [Mus musculus]	5	71
21734	gi|13399310|NP_080239.1| ribosomal protein S10 [Mus musculus]	7	82
22885	gi|134031976|NP_082509.2| leucine-rich PPR motif-containing protein [Mus musculus]	2	25
1626	gi|13626040|NP_112462.1| A kinase (PRKA) anchor protein (gravin) 12 [Mus musculus]	2	15
26556	gi|145279206|NP_035213.2| phosphatidylinositol 3-kinase	1	41
17704	gi|146260280|NP_001041526.1| heterogeneous nuclear ribonucleoprotein A/B isoform 1 [Mus musculus]	5	36
15990	gi|157671923|NP_062613.3| ubiquitin C [Mus musculus]	5	54
26919	gi|157909799|NP_033057.3| retinoblastoma binding protein 7 [Mus musculus]	5	31
9229	gi|15826844|NP_035584.1| serine (or cysteine) proteinase inhibitor	5	29
7799	gi|158517832|NP_035473.2| SEC61	9	112
31338	gi|158631225|NP_034250.3| eukaryotic translation initiation factor 1A [Mus musculus]	8	64
21485	gi|158966670|NP_001103681.1| annexin A6 isoform b [Mus musculus]	4	252
18474	gi|160333923|NP_058085.2| heterogeneous nuclear ribonucleoprotein U [Mus musculus]	3	38

Table App.3.4. Continued

4804	gi|160707896|NP_035629.2| serine/threonine kinase receptor associated protein [Mus musculus]	5	37
11221	gi|161016826|NP_031900.3| receptor accessory protein 5 [Mus musculus]	8	69
1014	gi|162417975|NP_034627.3| isocitrate dehydrogenase 1 (NADP+)	5	33
29663	gi|162417977|NP_001104790.1| isocitrate dehydrogenase 1 (NADP+)	5	33
11983	gi|164698479|NP_001106958.1| septin 9 isoform a [Mus musculus]	5	7
11983	gi|164698479|NP_001106958.1| septin 9 isoform a [Mus musculus]	4	35
9238	gi|164698481|NP_001106959.1| septin 9 isoform b [Mus musculus]	5	7
9238	gi|164698481|NP_001106959.1| septin 9 isoform b [Mus musculus]	4	35
15383	gi|164698483|NP_001106960.1| septin 9 isoform c [Mus musculus]	5	7
15383	gi|164698483|NP_001106960.1| septin 9 isoform c [Mus musculus]	4	33
3571	gi|16716381|NP_444322.1| lysyl-tRNA synthetase [Mus musculus]	4	61
2427	gi|167234372|NP_663600.2| eukaryotic translation initiation factor 4B [Mus musculus]	3	27
25495	gi|169808394|NP_081925.2| spermatogenesis associated	9	202
5472	gi|170295840|NP_035718.2| tripartite motif protein 28 [Mus musculus]	3	21
17680	gi|171906578|NP_033037.2| RAD23b homolog [Mus musculus]	4	58
7128	gi|18390323|NP_080973.1| RAB14	7	29
25222	gi|183980004|NP_796275.3| heterogeneous nuclear ribonucleoprotein L [Mus musculus]	4	91
4765	gi|18700004|NP_570934.1| acetyl-Coenzyme A acyltransferase 1 [Mus musculus]	5	38
13540	gi|188219614|NP_035800.2| ubiquitin carboxy-terminal hydrolase L1 [Mus musculus]	7	63
32216	gi|19705424|NP_033465.1| proteasome 26S non-ATPase subunit 3 [Mus musculus]	4	49
7040	gi|19882201|NP_598862.1| proteasome 26S non-ATPase subunit 2 [Mus musculus]	3	13
32510	gi|20806532|NP_035863.1| cold shock domain protein A short isoform [Mus musculus]	5	78
16550	gi|21312298|NP_082506.1| serine hydroxymethyltransferase 2 (mitochondrial) [Mus musculus]	5	59
7870	gi|21312968|NP_080431.1| signal sequence receptor	8	33
34687	gi|21313140|NP_083840.1| Tax1 (human T-cell leukemia virus type I) binding protein 3 [Mus musculus]	9	144
32008	gi|21703726|NP_663335.1| isopentenyl-diphosphate delta isomerase isoform 1 [Mus musculus]	1	26
4958	gi|21704066|NP_663516.1| RAS-related protein-1a [Mus musculus]	7	31
2018	gi|21886811|NP_058020.1| S100 calcium binding protein A11 (calizzarin) [Mus musculus]	9	1140
3980	gi|22094075|NP_031477.1| solute carrier family 25	8	8
24816	gi|22122795|NP_666341.1| dynein cytoplasmic 1 light intermediate chain 1 [Mus musculus]	4	58
17778	gi|22122797|NP_666342.1| acetyl-Coenzyme A acyltransferase 1B [Mus musculus]	5	38
3586	gi|25742730|NP_742083.1| ribosomal protein L32 [Mus musculus]	8	55

Table App.3.4. Continued

6766	gi|27754103|NP_080235.2| proteasome 26S ATPase subunit 6 [Mus musculus]	5	77
22764	gi|28076915|NP_081148.1| ubiquitin-associated protein 2 [Mus musculus]	9	32
22866	gi|28076935|NP_081427.1| dynactin 2 [Mus musculus]	5	35
25225	gi|28974984|NP_803228.1| aspartyl-tRNA synthetase [Mus musculus]	4	26
12636	gi|29789191|NP_081626.1| asparaginyl-tRNA synthetase [Mus musculus]	4	68
8396	gi|30089708|NP_783588.1| histone cluster 1	10	38
22598	gi|30424876|NP_780445.1| Fe-containing alcohol dehydrogenase 1 [Mus musculus]	1	15
22598	gi|30424876|NP_780445.1| Fe-containing alcohol dehydrogenase 1 [Mus musculus]	9	24
11634	gi|30794412|NP_081703.1| TAF15 RNA polymerase II	4	131
4247	gi|31542070|NP_067305.2| acid phosphatase 1	8	32
5495	gi|31542159|NP_058025.2| ATPase	2	24
21139	gi|31543940|NP_062780.2| vesicle-associated membrane protein	7	33
23918	gi|31543974|NP_061223.2| tyrosine 3-monooxygenase/tryptophan 5-monooxygenase activation protein	7	66
32532	gi|31560267|NP_075627.2| mitogen activated protein kinase kinase 2 [Mus musculus]	5	52
5620	gi|31560517|NP_036105.2| ribosomal protein L27a [Mus musculus]	7	61
19476	gi|31980808|NP_058572.2| eukaryotic translation initiation factor 3	5	53
31975	gi|31981147|NP_077754.2| leucine aminopeptidase 3 [Mus musculus]	4	36
20527	gi|31981273|NP_075638.2| CNDP dipeptidase 2 [Mus musculus]	5	40
30927	gi|31981302|NP_038500.2| annexin A6 isoform a [Mus musculus]	4	252
10938	gi|31981748|NP_660117.2| ribonuclease/angiogenin inhibitor 1 [Mus musculus]	5	87
929	gi|31981892|NP_666236.2| Rho GTPase activating protein 1 [Mus musculus]	5	45
28065	gi|32567788|NP_666306.2| phosphatidylinositol-binding clathrin assembly protein [Mus musculus]	4	50
24931	gi|32880197|NP_872591.1| heterogeneous nuclear ribonucleoprotein A2/B1 isoform 2 [Mus musculus]	7	24
5035	gi|33620739|NP_034990.1| myosin	9	357
21963	gi|33859604|NP_035318.1| proteasome (prosome	5	31
4145	gi|33859811|NP_849209.1| mitochondrial trifunctional protein	1	46
12944	gi|34328185|NP_035309.2| prosaposin [Mus musculus]	9	280
22085	gi|34419622|NP_570951.2| poly(A) binding protein	4	27
22085	gi|34419622|NP_570951.2| poly(A) binding protein	3	33
20948	gi|34538600|NP_904330.1| cytochrome c oxidase subunit I [Mus musculus]	1	45
8554	gi|34610207|NP_666329.2| alanyl-tRNA synthetase [Mus musculus]	3	21
16322	gi|34915988|NP_033898.1| basigin isoform 1 [Mus musculus]	4	43
16322	gi|34915988|NP_033898.1| basigin isoform 1 [Mus musculus]	5	63
28072	gi|39930477|NP_149156.1| septin 8 [Mus musculus]	5	29
3844	gi|41282022|NP_908942.1| calumenin isoform 2 [Mus musculus]	5	145

Table App.3.4. Continued

6049	gi|45476573|NP_032414.1| eukaryotic translation initiation factor 3	5	30
7193	gi|47458804|NP_998824.1| signal transducer and activator of transcription 3 isoform 1 [Mus musculus]	3	10
34958	gi|50363232|NP_057910.3| nestin [Mus musculus]	1	92
5423	gi|55926127|NP_067262.1| spectrin beta 3 [Mus musculus]	1	44
26423	gi|56605979|NP_663430.2| basic transcription factor 3 [Mus musculus]	7	47
28693	gi|58037145|NP_081219.1| small nuclear ribonucleoprotein D2 [Mus musculus]	8	87
5797	gi|58037481|NP_084101.1| sec1 family domain containing 1 [Mus musculus]	4	27
2077	gi|59797056|NP_032751.1| natriuretic peptide precursor type A [Mus musculus]	8	147
35171	gi|62184371|YP_220565.1| cytochrome c oxidase subunit I [Mus musculus molossinus]	1	45
3283	gi|6671507|NP_031418.1| actin	4	48
7532	gi|66773165|NP_062774.2| acid phosphatase 6	5	17
19294	gi|6677779|NP_033107.1| ribosomal protein L28 [Mus musculus]	8	89
25356	gi|6677801|NP_033118.1| ribosomal protein S17 [Mus musculus]	9	238
30543	gi|6678077|NP_033268.1| secreted acidic cysteine rich glycoprotein [Mus musculus]	5	62
14025	gi|6678369|NP_033419.1| troponin C	8	73
31719	gi|6678437|NP_033455.1| tumor protein	7	68
25182	gi|6678551|NP_033523.1| vesicle-associated membrane protein 2 [Mus musculus]	9	143
10223	gi|6678682|NP_032521.1| lectin	10	18
10223	gi|6678682|NP_032521.1| lectin	9	126
23135	gi|6678794|NP_032953.1| mitogen-activated protein kinase kinase 1 [Mus musculus]	5	59
2144	gi|6679012|NP_032698.1| nucleosome assembly protein 1-like 4 [Mus musculus]	5	56
33598	gi|6679158|NP_032775.1| nucleobindin 1 [Mus musculus]	4	41
6074	gi|6679465|NP_032951.1| protein kinase C substrate 80K-H [Mus musculus]	4	98
29655	gi|6680229|NP_032278.1| high mobility group box 2 [Mus musculus]	7	23
31431	gi|6680297|NP_032324.1| DnaJ (Hsp40) homolog	5	21
6283	gi|6680618|NP_031408.1| acyl-Coenzyme A dehydrogenase	5	103
17952	gi|6680720|NP_031505.1| ADP-ribosylation factor 4 [Mus musculus]	8	28
3132	gi|6680832|NP_031615.1| calmodulin 2 [Mus musculus]	8	63
22680	gi|6680834|NP_031616.1| calmodulin 3 [Mus musculus]	8	63
14706	gi|6680836|NP_031617.1| calreticulin [Mus musculus]	5	457
22455	gi|6753036|NP_033786.1| aldehyde dehydrogenase 2	5	36
15308	gi|6753060|NP_033803.1| annexin A5 [Mus musculus]	7	28
17801	gi|6753138|NP_033851.1| Na+/K+ -ATPase beta 1 subunit [Mus musculus]	5	64
2011	gi|6753244|NP_033920.1| calmodulin 1 [Mus musculus]	8	63
8786	gi|6753498|NP_034071.1| cytochrome c oxidase subunit IV isoform 1 [Mus musculus]	9	111

Table App.3.4. Continued

7177	gi|6754206|NP_034568.1| hexokinase 1 [Mus musculus]	3	48
16397	gi|6754208|NP_034569.1| high mobility group box 1 [Mus musculus]	7	32
18004	gi|6754222|NP_034578.1| heterogeneous nuclear ribonucleoprotein A/B isoform 2 [Mus musculus]	5	36
7264	gi|6754450|NP_034764.1| fatty acid binding protein 5	9	70
23854	gi|6754696|NP_034928.1| macrophage migration inhibitory factor [Mus musculus]	9	221
24217	gi|6754910|NP_035078.1| nuclear distribution gene C homolog [Mus musculus]	5	65
26563	gi|6754970|NP_035161.1| procollagen-proline	4	86
32638	gi|6754974|NP_035991.1| protein kinase C and casein kinase substrate in neurons 1 [Mus musculus]	5	147
4406	gi|6755106|NP_035252.1| procollagen-lysine	3	29
33188	gi|6755300|NP_035384.1| retinol binding protein 1	8	67
18390	gi|6755372|NP_036182.1| ribosomal protein S3 [Mus musculus]	1	45
14408	gi|6755967|NP_035826.1| voltage-dependent anion channel 3 [Mus musculus]	1	62
1439	gi|6755995|NP_035845.1| WD repeat domain 1 [Mus musculus]	1	47
27977	gi|7106303|NP_034249.1| EH-domain containing 1 [Mus musculus]	4	87
27960	gi|7106381|NP_035992.1| protein kinase C and casein kinase substrate in neurons 2 [Mus musculus]	4	42
9543	gi|72004262|NP_001025445.1| NADH dehydrogenase (ubiquinone) Fe-S protein 5 [Mus musculus]	8	32
8524	gi|7305305|NP_038892.1| N-myc downstream regulated gene 2 [Mus musculus]	5	195
2451	gi|7305441|NP_038790.1| ribosomal protein L3 [Mus musculus]	5	37
8662	gi|74315975|NP_081633.1| proteasome 26S non-ATPase subunit 1 [Mus musculus]	3	14
9795	gi|7549799|NP_035795.1| ubiquitin-conjugating enzyme E2I [Mus musculus]	8	60
28103	gi|75677420|NP_031762.2| collagen	1	203
4899	gi|78711834|NP_001030609.1| A kinase (PRKA) anchor protein 2 isoform 2 [Mus musculus]	2	20
5593	gi|7949005|NP_058035.1| ATP synthase	9	129
1767	gi|83745120|NP_080296.3| ribosomal protein	8	78
3950	gi|83816893|NP_031866.2| DEAD (Asp-Glu-Ala-Asp) box polypeptide 5 [Mus musculus]	4	153
22615	gi|8392847|NP_058556.1| ARP1 actin-related protein 1 homolog A [Mus musculus]	5	49
971	gi|8393627|NP_058545.1| interferon regulatory factor 3 [Mus musculus]	5	7
13577	gi|8393866|NP_058674.1| ornithine aminotransferase [Mus musculus]	5	107
13040	gi|84662730|NP_476513.2| far upstream element (FUSE) binding protein 1 [Mus musculus]	3	34
29892	gi|84662736|NP_035420.2| ribosomal protein L6 [Mus musculus]	1	58
7169	gi|88853578|NP_031480.2| adaptor protein complex AP-1	3	20

Table App.3.4. Continued

7544	gi|91064878|NP_081506.3| protein kinase C binding protein 1 [Mus musculus]	4	142
2907	gi|9256519|NP_061341.1| ribosomal protein	9	624
7447	gi|93587673|NP_001035277.1| DEAD box polypeptide 17 isoform 4 [Mus musculus]	4	62
6454	gi|94158994|NP_031492.2| apoptosis inhibitor 5 [Mus musculus]	4	24
1222	gi|9506767|NP_062342.1| histone cluster 2	7	31
12919	gi|9506843|NP_062263.1| lamin A isoform C2 [Mus musculus]	3	18
12919	gi|9506843|NP_062263.1| lamin A isoform C2 [Mus musculus]	4	60
5319	gi|9790261|NP_062652.1| Trk-fused [Mus musculus]	4	70
24483	gi|9910452|NP_064304.1| mitogen-activated protein kinase kinase 1 interacting protein 1 [Mus musculus]	9	126

[1] Identification number for LC-MS/MS;
[2] Concentration calculated based on molecular weight of the indicated protein, relative to the internal standard

Table App. 3.5. Heat shock proteins identified by LC-MS/MS in T3D- and Mock-infected primary cardiac myocyte cultures

Protein Key [1]	GenBank accession number	Official Name	Official Symbol	Also known as	Sample	Gel Slice	protein Fmol On Column [2]	Fold change (T3D/ mock)
9939	NP_038588.2	heat shock protein 1	Hspb1	27kDa; Hsp25; Hspb1	Mock	7	26	
25564	NP_032329.1	heat shock protein 1 (chaperonin 10)	Hspe1	10kDa; mt-cpn10; MGC117526; Hspe1	T3D	9	144	-3.48
					Mock	9	503	
25692	NP_034607.3	heat shock protein 1 (chaperonin)	Hspd1	60kDa; Hsp60; Hspd1	T3D	4	1172	1.74
					Mock	4	674	
2685	NP_038586.2	heat shock protein 1-like	Hspa1l	Msh5; Hsc70t; MGC150263; MGC150264; Hspa1l	T3D	3	223	
					Mock	4	111	
					Mock	5	53	
16358	NP_034609.2	heat shock protein 1A	Hspa1a	Hsp72; hsp68; Hsp70-3; Hsp70.3; hsp70A1; MGC189852; Hspa1a	T3D	3	227	
					Mock	4	119	
					Mock	5	53	
16965	NP_034608.2	heat shock protein 1B	Hspa1b	Hsp70; hsp68; Hsp70-1; Hsp70.1; Hspa1b	T3D	3	227	
					Mock	4	119	
					Mock	5	53	
1916	NP_001002012.1	heat shock protein 2	Hspa2	70kDa; HSP70.2; HSP70A2; Hsp70-2; MGC7795; MGC58299; Hspa2	T3D	3	427	3.78
					Mock	3	113	
					T3D	4	157	-2.44
					Mock	4	382	
					Mock	5	53	
31320	NP_032326.3	heat shock protein 4	Hspa4	70kDa; APG-2; Hsp110; Hsp70RY; AI317151; KIAA4025; mKIAA4025; Hspa4	T3D	3	41	1.24
					Mock	3	34	
29256	NP_071705.2	heat shock protein 5	Hspa5	Bip; Sez7; mBiP; 78kDa; Grp78; SEZ-7; Hsce70; AL022860; AU019543; D2Wsu17e; D2Wsu141e; Hspa5	T3D	3	744	1.78
					Mock	3	419	
					Mock	4	801	
21081	NP_038896.2	heat shock protein family, member 7 (cardiovascular)	Hspb7	27kDa; cvHsp; Hsp25-2; MGC107591; Hspb7	Mock	7	8	

Table App.3.5. Continued

9525	NP_112442.2	heat shock protein 8	Hspa8	Hsc70; Hsc71; Hsc73; Hsp73; Hspa10; MGC102007; MGC106514; MGC118485; 2410008N15Rik; Hspa8	T3D	3	1055	1.93
					Mock	3	547	
					T3D	4	265	-5.21
					Mock	4	1382	
					Mock	5	99	
368	NP_034611.2	heat shock protein9	Hspa9	Csa; Mot2; 74kDa; Grp75; Hsc74; Hsp74; Mot-2; Pbp74; Hsp74a; Hspa9a; Mthsp70; Mortalin; Hspa9	T3D	3	253	1.88
					Mock	3	134	
					T3D	4	36	-11.31
					Mock	4	413	
18068	NP_080676.3	DnaJ (Hsp40) homolog, subfamily B, member 11	Dnajb11	Dj9; ABBP-2; AL024055; 1810031F23Rik; Dnajb11	T3D	5	103	1.64
					Mock	5	63	
238	NP_032328.2	heat shock protein 90 alpha (cytosolic), class B member 1	Hsp90ab1	90kDa; Hsp84; Hsp90; Hspcb; C81438; Hsp84-1; AL022974; MGC115780; Hsp90ab1	T3D	1	22	-12.54
					Mock	1	274	
					T3D	2	40	3.23
					Mock	2	13	
					T3D	3	738	-1.19
					Mock	3	878	
					T3D	4	95	2.81
					Mock	4	34	
11985	NP_034610.1	heat shock protein 90, alpha (cytosolic), class A member 1	Hsp90aa1	hsp4; 86kDa; 89kDa; Hsp89; Hsp90; Hspca; Hsp86-1; AL024080; AL024147; Hsp90aa1	T3D	1	21	-5.24
					Mock	1	111	
					T3D	2	40	3.23
					Mock	2	13	
					T3D	3	735	-1.10
					Mock	3	808	
1755	NP_035761.1	heat shock protein 90, beta (Grp94), member 1	Hsp90b1	TA-3; Tra1; gp96; ERp99; GRP94; Targ2; Tra-1; Hsp90b1	Mock	1	82	
					T3D	3	356	-1.38
					Mock	3	489	
					T3D	4	59	4.26
					Mock	4	14	
14897	NP_038587.2	heat shock 105kDa/110kDa protein 1	Hsph1	105kDa; Hsp105; Hsp110; hsp-E7I; AI790491; Hsph1	Mock	3	9	

[1] Identification number for LC-MS/MS;
[2] Concentration calculated based on molecular weight of the indicated protein, relative to the internal standard

APPENDIX 4

Ingenuity Pathway Analysis (IPA) of Differentially Expressed Proteins 12 Hours Post-Reovirus Infection of Primary Cardiac Myocyte Cultures

INTRODUCTION

Reovirus infection can activate many pathways, including the Ras/RalGEF/p38 (7), P53 (5), and JAK-STAT pathways (4). In order to identify additional pathways that may be activated by reovirus infection of cardiac myocytes, and novel proteins that might be involved in known pathways, we used Ingenuity Pathways Analysis (IPA) software (http://www.ingenuity.com/) to analyze the MALDI-TOF-TOF proteomics data obtained from reovirus-infected primary cardiac myocyte cultures (Chapter 3). IPA software is applied to proteomic data to analyze pathways and protein-protein interactions. It can construct networks of directly interacting proteins and build dynamic pathway models based on information in the Ingenuity Pathway Knowledge Base. It is currently widely used in diverse research fields, such as bioinformatics (6), oncology (3), infectious diseases (1), and genetics (2).

MATERIALS AND METHODS

Differentially expressed proteins identified from MALDI-TOF-TOF in Chapter 3 were analyzed by free trial IPA software using the Compare Analysis in the Core module.

RESULTS

Differentially expressed proteins among primary cardiac myocyte cultures infected with different reovirus strains. Comparison of differentially expressed proteins among the four different reovirus infections is summarized in Table App.4.1. Differentially expressed proteins unique to T3D or 8B infection are summarized in Tables App.4.2 and 4.3, respectively. Comparison of differentially expressed proteins that are unique to T3D and 8B infection are summarized in Table App.4.4. Since there were almost no uniquely differentially expressed proteins in T1L and DB93A infections, no summaries were prepared for those infections. For that reason, the following IPA analysis was also focused on only T3D and 8B infections.

Biological function analysis. Differentially expressed proteins unique to either T3D or 8B infection, or unique to both of them, or common to all four virus infections were imported for IPA analysis. Proteins with the same biological function were grouped together, and groups were then further organized by virus strain-specific effects (see Supp. Table 3.2 in Chapter 3).

Canonical pathways analysis. The same set of proteins used for the biological function analysis was used for the canonical pathways analysis. Proteins that belong to the same pathway were grouped together, and groups were then further organized by virus strain-specific effects (Table App.4.5).

Network analysis. The same set of proteins used above was used for the network analysis. A total of seven networks were constructed from identified proteins (3 for T3D

infection, and 4 for 8B infection). Molecular information for all of the 7 networks is summarized in Table App.4.6, Legends in the networks were summarized in Figure App.4.1, which are copied from Ingenuity Systems IPA 7 Feature Manual, and direct interactions between molecules in each network are shown in Figures App.4.2-4.8.

Post translational modification (PTM) analysis. A detailed description for PTM analysis was provided in the Materials and Methods of Chapter 3. One interesting PTM identified here was phosphorylation of reovirus μNS. From the MS/MS information, one peptide with a mass of 1058.6 from spot 772 with peptide sequence of (R)MTLRSLMK(N) was predicted to be phosphorylated at the Serine amino acid. In addition, there were a total of 29 proteins which were identified from more than 1 spot each, indicating PTMs. They are summarized in Table App.4.7.

DISCUSSION

The IPA analysis provided a visualization of possible protein-protein interactions and constructed protein networks among the pathways. This analysis suggested that the most myocarditic reovirus, 8B, triggered more pathways than the non-myocarditic reovirus, T3D, which might reflect its greater cytopathic effect. While these analyses are only speculative, they are "hypothesis generating" and provide suggestions for future studies.

REFERENCES

1. **Bernardino, A. L., D. Kaushal, and M. T. Philipp.** 2009. The antibiotics doxycycline and minocycline inhibit the inflammatory responses to the Lyme disease spirochete Borrelia burgdorferi. J Infect Dis **199:**1379-88.

2. **Burgner, D., S. Davila, W. B. Breunis, S. B. Ng, Y. Li, C. Bonnard, L. Ling, V. J. Wright, A. Thalamuthu, M. Odam, C. Shimizu, J. C. Burns, M. Levin, T. W. Kuijpers, and M. L. Hibberd.** 2009. A genome-wide association study identifies novel and functionally related susceptibility Loci for Kawasaki disease. PLoS Genet **5:**e1000319.

3. **Dumesic, P. A., F. A. Scholl, D. I. Barragan, and P. A. Khavari.** 2009. Erk1/2 MAP kinases are required for epidermal G2/M progression. J Cell Biol **185:**409-22.

4. **Goody, R. J., J. D. Beckham, K. Rubtsova, and K. L. Tyler.** 2007. JAK-STAT signaling pathways are activated in the brain following reovirus infection. J Neurovirol **13:**373-83.

5. **Huang, S., L. K. Qu, and A. E. Koromilas.** 2004. Induction of p53-dependent apoptosis in HCT116 tumor cells by RNA viruses and possible implications in virus-mediated oncolysis. Cell Cycle **3:**1043-5.

6. **Kadegowda, A. K., M. Bionaz, B. Thering, L. S. Piperova, R. A. Erdman, and J. J. Loor.** 2009. Identification of internal control genes for quantitative polymerase chain reaction in mammary tissue of lactating cows receiving lipid supplements. J Dairy Sci **92:**2007-19.

7. **Norman, K. L., K. Hirasawa, A. D. Yang, M. A. Shields, and P. W. Lee.** 2004. Reovirus oncolysis: the Ras/RalGEF/p38 pathway dictates host cell permissiveness to reovirus infection. Proc Natl Acad Sci U S A **101:**11099-104.

Table App.4.1. Comparison of differentially expressed proteins among the four different reovirus infections in primary cardiac myocyte cultures 12 hours post-infection

Spot #	Accession#	Avg Ratio T3D [1]	Avg Ratio 8B [1]	Avg Ratio DB93 A [1]	Avg Ratio T1L [1]	Function	Description
1854	P35601		13.32	7.06		transcription regulator	replication factor C (activator 1) 1, 145kDa
804	IPI00461436	1.11	1.58	1.15	1.24	other	chromosome 18 open reading frame 55
791	Q9CWW7	1.22	1.91	1.21	2.2	transcription regulator	CXXC finger 1 (PHD domain)
2550	IPI00468068	-1.77	-2.54	-1.41	-1.44	other	(P14602) Heat shock 27 kDa protein (HSP 27)
2552	IPI00468068	1.45	1.24	1.38	1.24	other	(P14602) Heat shock 27 kDa protein (HSP 27)
747	IPI00169804		3.86		2.86	kinase	adenosine kinase
880	Q04750		-1.36		-1.1	enzyme	topoisomerase (DNA) I
864	Q99MN1		2.26		1.47	enzyme	lysyl-tRNA synthetase
490	IPI00283327	1.26		1.14		other	asp (abnormal spindle) homolog, microcephaly associated (Drosophila)
809	IPI00775950	-1.08		-1.12		other	caldesmon 1
1379	IPI00756691	-1.12	-1.22	-1.1		other	golgi reassembly stacking protein 2, 55kDa
1563	Q64345	6.42	2.23	1.83		other	interferon-induced protein with tetratricopeptide repeats 3
1564	Q64345	5.99	2.09	1.85		other	interferon-induced protein with tetratricopeptide repeats 3
1968	Q61937	1.12	1.23	1.2		transcription regulator	nucleophosmin 1

[1] Average expression of triplicate samples for indicated virus infection, relative to triplicate samples for mock-infected cultures. A positive value indicates greater protein expression in the viral infection; a negative number means less protein expression in the viral infection.

Table App.4.2. Differentially expressed proteins unique to T3D infection in primary cardiac myocyte cultures

Spot #	Brief name in IPA	Accession #	Avg Ratio T3D/ Mock [1]	Function	Description
901	IMMT	IPI00381413	-1.47	other	inner membrane protein, mitochondrial (mitofilin)
763	CCDC49	IPI00119661	-1.36	other	coiled-coil domain containing 49
67	GOLGA4	Q91VW5	-1.23	other	golgi autoantigen, golgin subfamily a, 4
1757	DNAJB11	Q99KV1	-1.2	other	DnaJ (Hsp40) homolog, subfamily B, member 11
1858	SUGT1	Q9CX34	-1.09	other	SGT1, suppressor of G2 allele of SKP1 (S. cerevisiae)
558	PDD6IP	Q9WU78	-1.08	other	programmed cell death 6 interacting protein
2097	EEF1D	P57776	-1.08	translation regulator	eukaryotic translation elongation factor 1 delta (guanine nucleotide exchange protein)
918	LMNB1	P14733	1.1	other	lamin B1
1025	PGM1	Q9D0F9	1.1	enzyme	phosphoglucomutase 1
1712	ACTB	IPI00110850	1.11	other	actin, beta
2400	PSME1	P97371	1.13	other	proteasome (prosome, macropain) activator subunit 1 (PA28 alpha)
2121	PPA1	IPI00110684	1.19	enzyme	pyrophosphatase (inorganic) 1
2022	TPM1	IPI00123316	1.22	other	tropomyosin 1 (alpha)
1784	TNNT2	P50752	1.23	other	troponin T type 2 (cardiac)
326	POLR3E	Q9CZT4	1.37	transcriptio n regulator	polymerase (RNA) III (DNA directed) polypeptide E (80kD)
530	IMMT	IPI00395113	1.38	other	inner membrane protein, mitochondrial (mitofilin)
325	ZFP62	IPI00410892	1.41	other	zinc finger protein 62 homolog (mouse)
2103	C13ORF24	IPI00317622	1.49	other	chromosome 13 open reading frame 24
532	ZFP422-RS1	IPI00347645	1.68	other	zinc finger protein 422, related sequence 1
585	EG328825	IPI00340036	1.9	other	predicted gene, EG328825

[1] As for Table 1.

Table App.4.3. Differentially expressed proteins unique to 8B infection in primary cardiac myocyte cultures

Spot #	Brief name in IPA	Accession #	Avg Ratio 8B/ Mock [1]	Function	Description
119	LAMB1	P02469	1.13	other	laminin, beta 1
139	RFC1	P35601	-1.23	transcription regulator	replication factor C (activator 1) 1, 145kDa
166	ASPM	IPI00283327	1.14	other	asp (abnormal spindle) homolog, microcephaly associated (Drosophila)
199	COL1A1	P11087	1.25	other	collagen, type I, alpha 1
200	COL1A1	P11087	1.16	other	collagen, type I, alpha 1
210	COL1A1	P11087	1.2	other	collagen, type I, alpha 1
337	MYH6	Q02566	-1.32	enzyme	myosin, heavy chain 6, cardiac muscle, alpha (cardiomyopathy, hypertrophic 1)
340	ZFP758	IPI00457523	-1.13	other	zinc finger protein 758
342	MYH6	Q02566	-1.38	enzyme	myosin, heavy chain 6, cardiac muscle, alpha (cardiomyopathy, hypertrophic 1)
416	UTP11L	Q9CZJ1	-1.19	other	UTP11-like, U3 small nucleolar ribonucleoprotein, (yeast)
444	UBE1	Q02053	-1.09	enzyme	ubiquitin-activating enzyme E1
470	HSPA4	Q61316	-1.08	other	heat shock 70kDa protein 4
497	UBE1	Q02053	-1.13	enzyme	ubiquitin-activating enzyme E1
520	STRN	O55106	-1.17	other	striatin, calmodulin binding protein
521	VCP	Q01853	-1.14	enzyme	valosin-containing protein
541	HSPA4L	P48722	-1.17	other	heat shock 70kDa protein 4-like
605	PLOD2	Q9R0B9	1.04	enzyme	procollagen-lysine, 2-oxoglutarate 5-dioxygenase 2
606	PRKCSH	IPI00115680	1.13	enzyme	protein kinase C substrate 80K-H
609	GFM1	Q8K0D5	1.11	translation regulator	G elongation factor, mitochondrial 1
618	GLG1	Q61543	1.27	other	golgi apparatus protein 1
624	VCP	Q01853	-1.05	enzyme	valosin-containing protein
666	GSN	P13020	-1.25	other	gelsolin (amyloidosis, Finnish type)
677	PLOD3	Q9R0E1	1.12	enzyme	procollagen-lysine, 2-oxoglutarate 5-dioxygenase 3
710	GSPT1	IPI00230355	-1.17	translation regulator	G1 to S phase transition 1
719	GFM1	Q8K0D5	-1.18	translation regulator	G elongation factor, mitochondrial 1
735	GOLGA4	Q91VW5	1.14	other	golgi autoantigen, golgin subfamily a, 4
754	6430526 N21RIK	IPI00623614	3.53	other	RIKEN cDNA 6430526N21 gene
761	ASPM	IPI00283327	1.82	other	asp (abnormal spindle) homolog, microcephaly associated (Drosophila)
787	CALD1	IPI00775950	1.24	other	caldesmon 1
797	DYNC1I2	O88487	1.15	other	dynein, cytoplasmic 1, intermediate chain 2

Table App.4.3. Continued

801	NDUFS1	IPI00308882	1.18	enzyme	NADH dehydrogenase (ubiquinone) Fe-S protein 1, 75kDa (NADH-coenzyme Q reductase)
852	HSPA5	P20029	1.17	other	heat shock 70kDa protein 5 (glucose-regulated protein, 78kDa)
869	HSPA9	P38647	1.39	other	heat shock 70kDa protein 9 (mortalin)
870	ZNF791	IPI00350919	1.26	other	zinc finger protein 791
874	PDIA4	P08003	1.19	enzyme	protein disulfide isomerase family A, member 4
951	SDHA	IPI00230351	1.15	enzyme	succinate dehydrogenase complex, subunit A, flavoprotein (Fp)
952	PLS3	IPI00776023	1.12	other	plastin 3 (T isoform)
954	HSPA1B	P17879	1.2	other	heat shock 70kDa protein 1B
973	LCP1	Q61233	1.09	other	lymphocyte cytosolic protein 1 (L-plastin)
1082	P4HA1	Q60715	1.23	enzyme	procollagen-proline, 2-oxoglutarate 4-dioxygenase (proline 4-hydroxylase), alpha polypeptide I
1092	P4HA1	Q60715	1.24	enzyme	procollagen-proline, 2-oxoglutarate 4-dioxygenase (proline 4-hydroxylase), alpha polypeptide I
1153	PDIA3	P27773	1.22	peptidase	protein disulfide isomerase family A, member 3
1166	PDIA3	P27773	1.14	peptidase	protein disulfide isomerase family A, member 3
1188	CAP2	Q9CYT6	-1.35	other	CAP, adenylate cyclase-associated protein, 2 (yeast)
1219	P4HB	P09103	1.12	enzyme	procollagen-proline, 2-oxoglutarate 4-dioxygenase (proline 4-hydroxylase), beta polypeptide
1234	P4HB	P09103	1.05	enzyme	procollagen-proline, 2-oxoglutarate 4-dioxygenase (proline 4-hydroxylase), beta polypeptide
1280	FSCN1	Q61553	1.14	other	fascin homolog 1, actin-bundling protein (Strongylocentrotus purpuratus)
1283	DLD	O08749	1.15	enzyme	dihydrolipoamide dehydrogenase
1290	RAD23B	P54728	-1.09	other	RAD23 homolog B (S. cerevisiae)
1392	ATP5B	P56480	1.09	transporter	ATP synthase, H+ transporting, mitochondrial F1 complex, beta polypeptide
1416	SEPT11	IPI00454143	1.16	other	septin 11
1464	DCTN2	IPI00116112	-1.08	other	dynactin 2 (p50)
1474	PRKAR1A	IPI00762049	-1.17	kinase	protein kinase, cAMP-dependent, regulatory, type I, alpha (tissue specific extinguisher 1)
1511	PDIA6	IPI00222496	1.08	enzyme	protein disulfide isomerase family A, member 6
1514	ENO1	P17182	1.3	transcription regulator	enolase 1, (alpha)
1515	ENO1	P17182	-1.15	transcription regulator	enolase 1, (alpha)
1554	ENO3	P21550	-1.37	enzyme	enolase 3 (beta, muscle)
1581	UQCRC1	Q9CZ13	1.17	enzyme	ubiquinol-cytochrome c reductase core protein I
1584	PDHA1	P35486	-1.2	enzyme	pyruvate dehydrogenase (lipoamide) alpha 1
1680	ACOT2	Q9QYR9	1.12	enzyme	acyl-CoA thioesterase 2
1812	NDUFA10	Q99LC3	1.14	enzyme	NADH dehydrogenase (ubiquinone) 1 alpha subcomplex, 10, 42kDa
1964	PPP1CB	IPI00311873	-1.16	phosphatase	protein phosphatase 1, catalytic subunit, beta isoform
2017	LDHB	P16125	-1.2	enzyme	lactate dehydrogenase B

Table App.4.3. Continued

2024	LASP1	Q61792	1.14	transporter	LIM and SH3 protein 1
2068	PDHB	IPI00132042	-1.15	enzyme	pyruvate dehydrogenase (lipoamide) beta
2114	MDH1	P14152	-1.24	enzyme	malate dehydrogenase 1, NAD (soluble)
2124	MDH1	P14152	-1.25	enzyme	malate dehydrogenase 1, NAD (soluble)
2246	ECH1	O35459	1.15	enzyme	enoyl Coenzyme A hydratase 1, peroxisomal
2325	TPM4	IPI00421223	1.09	other	tropomyosin 4
2356	APOBEC2	Q9WV35	-1.41	enzyme	apolipoprotein B mRNA editing enzyme, catalytic polypeptide-like 2
2470	ERP29	P57759	1.1	transporter	endoplasmic reticulum protein 29

[1] As for Table 1.

Table App.4.4. Comparison of differentially expressed proteins unique to both T3D and 8B infections in primary cardiac myocyte cultures

Spot #	Accession#	Avg Ratio T3D/ Mock [1]	Avg Ratio 8B/ Mock [1]	Function	Description
273	IPI00283327	1.12	-1.83	other	asp (abnormal spindle) homolog, microcephaly associated (Drosophila)
341	Q02566	1.33	-1.32	enzyme	myosin, heavy chain 6, cardiac muscle, alpha (cardiomyopathy, hypertrophic 1)
344	Q02566	1.3	-1.31	enzyme	myosin, heavy chain 6, cardiac muscle, alpha (cardiomyopathy, hypertrophic 1)
535	P56399	1.27	-1.25	peptidase	ubiquitin specific peptidase 5 (isopeptidase T)
723	Q8BUK6	-1.18	-1.19	other	hook homolog 3 (Drosophila)
600	Q01853	-1.12	-1.13	enzyme	valosin-containing protein
1355	IPI00113073	1.07	-1.12	enzyme	aldehyde dehydrogenase 1 family, member B1
350	Q91VW5	-1.19	-1.11	other	golgi autoantigen, golgin subfamily a, 4
1135	IPI00462482	-1.08	-1.09	other	UDP-N-acteylglucosamine pyrophosphorylase 1-like 1
1486	IPI00313296	-1.12	-1.09	other	ribonuclease/angiogenin inhibitor 1
1592	IPI00138084	-1.08	-1.08	kinase	adenosine kinase
462	Q01853	-1.06	-1.07	enzyme	valosin-containing protein
1286	Q61553	1.09	1.14	other	fascin homolog 1, actin-bundling protein (Strongylocentrotus purpuratus)
502	P08113	1.51	1.15	other	heat shock protein 90kDa beta (Grp94), member 1
619	P23116	1.22	1.17	translation regulator	eukaryotic translation initiation factor 3, subunit A
1614	Q07076	1.19	1.2	ion channel	annexin A7
178	P46735	1.22	1.29	other	myosin IB
871	IPI00406652	1.28	1.61	other	chromosome 14 open reading frame 50

[1] As for Table 1.

Table App.4.5. Canonical pathway analysis for differentially expressed proteins in T3D- and 8B-infected primary cardiac myocyte cultures

Canonical Pathways	Group	-Log(P-value)	Ratio	Molecules
Unique for T3D				
Mechanisms of Viral Exit from Host Cells	T3D	4.01E00	6.82E-02	ACTB, PDCD6IP, LMNB1
Caveolar-mediated Endocytosis	T3D	8.12E-01	1.22E-02	ACTB
VEGF Signaling	T3D	7.45E-01	1.03E-02	ACTB
Virus Entry via Endocytic Pathways	T3D	7.35E-01	1.04E-02	ACTB
Fcγ Receptor-mediated Phagocytosis in Macrophages and Monocytes	T3D	7.13E-01	9.62E-03	ACTB
Clathrin-mediated Endocytosis	T3D	5.25E-01	5.99E-03	ACTB
Leukocyte Extravasation Signaling	T3D	4.73E-01	5.13E-03	ACTB
LPS/IL-1 Mediated Inhibition of RXR Function	T3D	4.33E-01	4.88E-03	ALDH1B1
Xenobiotic Metabolism Signaling	T3D	3.48E-01	3.52E-03	ALDH1B1
Cardiac Hypertrophy Signaling	T3D	4.01E-01	4.29E-03	HSPB1
For both T3D and 8B				
Purine Metabolism	T3D	2.38E00	9.09E-03	MYH6, POLR3E, VCP, ADK (includes EG:132)
	8B	1.22E00	9.09E-03	MYH6, ATP5B, VCP, ADK (includes EG:132)
Calcium Signaling	T3D	2.13E00	1.46E-02	TPM1, MYH6, TNNT2
	8B	1.22E00	1.46E-02	MYH6, TPM4, PRKAR1A
NRF2-mediated Oxidative Stress Response	T3D	2.1E00	1.62E-02	ACTB, DNAJB11, VCP
	8B	6.36E-01	1.08E-02	ERP29, VCP
Glycolysis/Gluconeogenesis	T3D	1.79E00	1.39E-02	ALDH1B1, PGM1
	8B	6.63E00	4.86E-02	PDHA1 (includes EG:5160), ALDH1B1, ENO1, ENO3, DLD, PDHB (includes EG:5162), LDHB
Cellular Effects of Sildenafil (Viagra)	T3D	1.44E00	1.32E-02	MYH6, ACTB
	8B	2.36E00	2.65E-02	MYH6, PDIA3, PPP1CB, PRKAR1A
Aryl Hydrocarbon Receptor Signaling	T3D	1.38E00	1.27E-02	ALDH1B1, HSPB1
	8B	7.89E-01	1.27E-02	ALDH1B1, HSPB1
Tight Junction Signaling	T3D	1.35E00	1.22E-02	MYH6, ACTB
	8B	7.7E-01	1.22E-02	MYH6, PRKAR1A
Protein Ubiquitination Pathway	T3D	1.29E00	1.49E-02	PSME1, USP5, SUGT1
	8B	7.15E-01	1.49E-02	USP5, UBA1, HSPA5

Table App.4.5. Continued

Ascorbate and Aldarate Metabolism	T3D	1.27E00	1.16E-02	ALDH1B1
	8B	9.41E-01	1.16E-02	ALDH1B1
Interferon Signaling	T3D	1.17E00	3.45E-02	IFIT3
	8B	8.47E-01	3.45E-02	IFIT3
Pentose Phosphate Pathway	T3D	1.16E00	1.1E-02	PGM1
	8B	8.34E-01	1.1E-02	PDHB (includes EG:5162)
Actin Cytoskeleton Signaling	T3D	1.09E00	8.44E-03	MYH6, ACTB
	8B	1.05E00	1.27E-02	MYH6, PPP1CB, GSN
Galactose Metabolism	T3D	1.03E00	8.62E-03	PGM1
	8B	7.1E-01	8.62E-03	PRKCSH
Histidine Metabolism	T3D	1.01E00	8.33E-03	ALDH1B1
	8B	6.92E-01	8.33E-03	ALDH1B1
Bile Acid Biosynthesis	T3D	9.83E-01	1E-02	ALDH1B1
	8B	6.66E-01	1E-02	ALDH1B1
β-alanine Metabolism	T3D	9.25E-01	1.02E-02	ALDH1B1
	8B	1.5E00	2.04E-02	ALDH1B1, ECH1
Death Receptor Signaling	T3D	8.81E-01	1.54E-02	HSPB1
	8B	5.72E-01	1.54E-02	HSPB1
Propanoate Metabolism	T3D	8.81E-01	7.69E-03	ALDH1B1
	8B	2.43E00	2.31E-02	ALDH1B1, ECH1, LDHB
Butanoate Metabolism	T3D	8.75E-01	7.52E-03	ALDH1B1
	8B	4.81E00	3.76E-02	SDHA (includes EG:6389), PDHA1 (includes EG:5160), ALDH1B1, ECH1, PDHB (includes EG:5162)
Pyruvate Metabolism	T3D	8.55E-01	6.71E-03	ALDH1B1
	8B	6.03E00	4.03E-02	PDHA1 (includes EG:5160), ALDH1B1, DLD, MDH1, PDHB (includes EG:5162), LDHB
Valine, Leucine and Isoleucine Degradation	T3D	8.3E-01	9.01E-03	ALDH1B1
	8B	1.31E00	1.8E-02	ALDH1B1, ECH1
Agrin Interactions at Neuromuscular Junction	T3D	8.12E-01	1.39E-02	ACTB
	8B	5.09E-01	1.39E-02	LAMB1
Arginine and Proline Metabolism	T3D	8.12E-01	5.46E-03	ALDH1B1
	8B	2.23E00	1.64E-02	ALDH1B1, P4HA1, P4HB
Regulation of Actin-based Motility by Rho	T3D	7.64E-01	1.08E-02	ACTB
	8B	1.19E00	2.15E-02	PPP1CB, GSN
Starch and Sucrose Metabolism	T3D	7.45E-01	5.05E-03	PGM1
	8B	4.49E-01	5.05E-03	PRKCSH
Glycerolipid Metabolism	T3D	7.26E-01	6.41E-03	ALDH1B1
	8B	4.33E-01	6.41E-03	ALDH1B1

Table App.4.5. Continued

IL-6 Signaling	T3D	7.13E-01	1.04E-02	HSPB1
	8B	1.09E00	2.08E-02	COL1A1, HSPB1
p38 MAPK Signaling	T3D	7.05E-01	1.05E-02	HSPB1
	8B	4.14E-01	1.05E-02	HSPB1
14-3-3-mediated Signaling	T3D	6.46E-01	8.77E-03	PDCD6IP
	8B	3.64E-01	8.77E-03	PDIA3
Hepatic Fibrosis / Hepatic Stellate Cell Activation	T3D	5.87E-01	7.41E-03	MYH6
	8B	8.52E-01	1.48E-02	COL1A1, MYH6
Fatty Acid Metabolism	T3D	5.76E-01	5.21E-03	ALDH1B1
	8B	8.3E-01	1.04E-02	ALDH1B1, ECH1
Tryptophan Metabolism	T3D	5.7E-01	3.92E-03	ALDH1B1
	8B	1.5E00	1.18E-02	ALDH1B1, ECH1, PLOD3
Pyrimidine Metabolism	T3D	5.64E-01	4.31E-03	POLR3E
	8B	2.96E-01	4.31E-03	APOBEC2
Oxidative Phosphorylation	T3D	5.56E-01	6.02E-03	PPA1
	8B	3.13E00	3.01E-02	SDHA (includes EG:6389), NDUFS1, NDUFA10 (includes EG:4705), ATP5B, UQCRC1
Germ Cell-Sertoli Cell Junction Signaling	T3D	5.53E-01	6.62E-03	ACTB
	8B	2.87E-01	6.62E-03	GSN
Lysine Degradation	T3D	5.48E-01	4.27E-03	ALDH1B1
	8B	2.21E00	1.71E-02	ALDH1B1, PLOD2, ECH1, PLOD3
Dendritic Cell Maturation	T3D	5.3E-01	6.06E-03	FSCN1
	8B	7.46E-01	1.21E-02	COL1A1, FSCN1
ERK/MAPK Signaling	T3D	4.67E-01	5.21E-03	HSPB1
	8B	1.19E00	1.56E-02	PPP1CB, HSPB1, PRKAR1A
Integrin Signaling	T3D	4.44E-01	4.93E-03	ACTB
	8B	2.02E-01	4.93E-03	PPP1CB
Unique for 8B				
Cardiac Hypertrophy Signaling	8B	1E00	1.29E-02	PDIA3, HSPB1, PRKAR1A
Glycerophospholipid Metabolism	8B	3.32E-01	5.15E-03	PDIA3
Glyoxylate and Dicarboxylate Metabolism	8B	1.07E00	8.47E-03	MDH1
Glucocorticoid Receptor Signaling	8B	1.4E00	1.42E-02	HSPA4, HSPA1B, HSPA9, HSPA5
Lysine Biosynthesis	8B	1.29E00	1.52E-02	KARS
Arachidonic Acid Metabolism	8B	3.07E-01	4.42E-03	PLOD3
Synaptic Long Term Potentiation	8B	9.76E-01	1.74E-02	PPP1CB, PRKAR1A
Fatty Acid Elongation in Mitochondria	8B	1.09E00	2.22E-02	ECH1

Table App.4.5. Continued

Huntington's Disease Signaling	8B	4.03E00	2.97E-02	SDHA (includes EG:6389), HSPA4, DYNC1I2, HSPA1B, ATP5B, HSPA9, HSPA5
PPARα/RXRα Activation	8B	6.47E-01	1.08E-02	PDIA3, PRKAR1A
Hepatic Cholestasis	8B	2.98E-01	6.02E-03	PRKAR1A
Mitochondrial Dysfunction	8B	4.21E00	3.49E-02	SDHA (includes EG:6389), PDHA1 (includes EG:5160), NDUFS1, NDUFA10 (includes EG:4705), ATP5B, UQCRC1
PXR/RXR Activation	8B	5.2E-01	1.16E-02	PRKAR1A
TR/RXR Activation	8B	4.49E-01	1.06E-02	ENO1
Role of BRCA1 in DNA Damage Response	8B	6.34E-01	1.89E-02	RFC1
RAR Activation	8B	2.44E-01	5.59E-03	PRKAR1A
α-Adrenergic Signaling	8B	4.21E-01	9.43E-03	PRKAR1A
CCR3 Signaling in Eosinophils	8B	3.55E-01	8.26E-03	PPP1CB
HIF1α Signaling	8B	4.06E-01	9.52E-03	LDHB
Melatonin Signaling	8B	1.26E00	2.56E-02	PDIA3, PRKAR1A
Neuropathic Pain Signaling In Dorsal Horn Neurons	8B	1.03E00	1.92E-02	PDIA3, PRKAR1A
Endothelin-1 Signaling	8B	2.39E-01	5.35E-03	PDIA3
Relaxin Signaling	8B	3.17E-01	6.8E-03	PRKAR1A
Renin-Angiotensin Signaling	8B	3.7E-01	8.33E-03	PRKAR1A
Thrombin Signaling	8B	2.06E-01	4.93E-03	PDIA3
CDK5 Signaling	8B	1.95E00	3.19E-02	LAMB1, PPP1CB, PRKAR1A
Lipid Antigen Presentation by CD1	8B	1.04E00	5E-02	PDIA3
Corticotropin Releasing Hormone Signaling	8B	3.49E-01	7.35E-03	PRKAR1A
Role of CHK Proteins in Cell Cycle Checkpoint Control	8B	7.96E-01	2.94E-02	RFC1
GNRH Signaling	8B	3.46E-01	7.52E-03	PRKAR1A
Melanocyte Development and Pigmentation Signaling	8B	4.45E-01	1.12E-02	PRKAR1A
Androgen Signaling	8B	9.23E-01	1.41E-02	HSPA4, PRKAR1A
Aldosterone Signaling in Epithelial Cells	8B	1.19E00	2.04E-02	PDIA3, HSPA5
CREB Signaling in Neurons	8B	6.7E-01	1.05E-02	PDIA3, PRKAR1A
Nucleotide Excision Repair Pathway	8B	7.84E-01	2.86E-02	RAD23B
Nitric Oxide Signaling in the Cardiovascular System	8B	4.99E-01	1.09E-02	PRKAR1A

Table App.4.5. Continued

Cardiac β-adrenergic Signaling	8B	9.11E-01	1.45E-02	PPP1CB, PRKAR1A
Amyloid Processing	8B	6.34E-01	1.79E-02	PRKAR1A
Endoplasmic Reticulum Stress Pathway	8B	1.04E00	5.56E-02	HSPA5
Insulin Receptor Signaling	8B	8.58E-01	1.45E-02	PPP1CB, PRKAR1A
Phototransduction Pathway	8B	6.26E-01	1.59E-02	PRKAR1A
Chemokine Signaling	8B	4.94E-01	1.3E-02	PPP1CB
Sonic Hedgehog Signaling	8B	8.62E-01	3.23E-02	PRKAR1A
IGF-1 Signaling	8B	4.29E-01	1.02E-02	PRKAR1A
Dopamine Receptor Signaling	8B	1.26E00	2.2E-02	PPP1CB, PRKAR1A
cAMP-mediated Signaling	8B	2.51E-01	6.1E-03	PRKAR1A
Hypoxia Signaling in the Cardiovascular System	8B	5.47E-01	1.41E-02	P4HB
BMP signaling pathway	8B	4.89E-01	1.25E-02	PRKAR1A
Citrate Cycle	8B	3.43E00	5.08E-02	SDHA (includes EG:6389), DLD, MDH1
Methane Metabolism	8B	1.12E00	1.52E-02	PDIA6
Glycine, Serine and Threonine Metabolism	8B	1.36E00	1.33E-02	PDIA3, DLD
Alanine and Aspartate Metabolism	8B	4.39E00	4.55E-02	PDHA1 (includes EG:5160), DLD, KARS, PDHB (includes EG:5162)
Valine, Leucine and Isoleucine Biosynthesis	8B	3.02E00	4.55E-02	PDHA1 (includes EG:5160), PDHB (includes EG:5162)
Phenylalanine, Tyrosine and Tryptophan Biosynthesis	8B	2.5E00	2.99E-02	ENO1, ENO3
Cysteine Metabolism	8B	7.01E-01	1.11E-02	LDHB
Ubiquinone Biosynthesis	8B	1.4E00	1.68E-02	NDUFS1, NDUFA10 (includes EG:4705)
Phospholipid Degradation	8B	4.71E-01	9.35E-03	PDIA3
Inositol Phosphate Metabolism	8B	3.07E-01	5.68E-03	PDIA3
Pentose and Glucuronate Interconversions	8B	6.57E-01	6.58E-03	PDIA6
Aminoacyl-tRNA Biosynthesis	8B	9.6E-01	1.2E-02	KARS

Table App.4.6. Network analysis comparing differentially expressed proteins from T3D- and 8B-infected primary cardiac myocyte cultures [1]

Network	Analysis	Molecules in Network	Score	Focus Molecules	Top Functions
1	8B	ACSM3, **ADK (includes EG:132)**, **ALDH1B1**, **ASPM**, beta-estradiol, Ck2, **EIF3A, ENO1**, EPO, FSH, **GORASP2, HSPA4L, IFIT3, LCP1**, LOC284230, MAMLD1, Mapk, MYC, **NPM1** (includes EG:18148), **PDIA6**, Pka**, PLOD2, PLOD3, PLS3, PPP1CB, PRKAR1A, PRKCSH, RFC1, RNH1**, RPL21 (includes EG:79449), **SEPT11**, TGFB1, **TOP1**, TRAF6, **UBA1**	49	22	Cell Cycle, Cancer, Drug Metabolism
1	T3D	**ACTB**, Actin, **CALD1**, Calmodulin, Caspase, Ck2, ERMN, ESPN, F Actin, Fascin, **FSCN1**, FSCN3, Hsp90, **HSP90B1, HSPB1, IMMT**, IPP, **LMNB1**, MAEA (includes EG:10296), MAP6**, MYH6**, MYH13, MYH16, MYH7B (includes EG:668940), **MYO1B**, Myosin, NLRP4A, NTP, **PDCD6IP, PPA1, SUGT1, TNNT2, TPM1**, Tropomyosin, **VCP**	35	15	Cardiovascular System Development and Function, Skeletal and Muscular System Development and Function, Tissue Development
2	8B	Actin, **ATP5B**, ATPase, **CALD1**, Calmodulin, **CAP2**, Caspase, **COL1A1,** Collagen(s), ERK, F Actin, Fascin, **FSCN1, GSN, GSPT1**, Hsp70, Hsp90, **HSP90B1, HSPA4, HSPA5, HSPA9, HSPA1B, HSPB1, LAMB1,** MHC Class I (complex), **MYH6, MYO1B, P4HA1, P4HB, PDIA3, PDIA4, TPM4,** Tropomyosin, Ubiquitin, **VCP**	48	22	Cellular Function and Maintenance, Amino Acid Metabolism, Post-Translational Modification
2	T3D	ACSM3**, ASPM**, beta-estradiol, BUD31 (includes EG:8896), C11ORF10, **C18ORF55**, C9ORF5, **CCDC49**, CDC123, CHCHD8, CPA2, **CXXC1**, DSCR3**, EEF1D**, **EIF3A**, GINS3, **GOLGA4**, HNF4A, **HOOK3, IFIT3**, IFT122, IL10, KDELR3, PCDH21, **PGM1, PIBF1, POLR3E, RNH1,** SLC35A1, SLC35A5, TGFB1, TTC22, **USP5**, USP30, USP36	32	14	Cell-mediated Immune Response, Immunological Disease, Drug Metabolism

Table App.4.6. Continued

3	8B	AMT (includes EG:275**), C18ORF55, CXXC1, DLD, GFM1, GLG1, GOLGA4**, HNF4A, **HOOK3**, IL12 (complex), **KARS, LYRM4, MDH1**, NDUFA3, NDUFA4, NDUFA5, NDUFA7, NDUFB1, NDUFB3, NDUFB5, **NDUFS1**, NDUFV1, PAN2 (includes EG:9924), PDHA2, PDHA1 (includes EG:29554), **PDHA1** (includes EG:5160), PDHB (includes EG:5162), PDHX, **RAD23B**, TDO2, **USP5**, USP30, USP36, USP46, **UTP11L** (includes EG:51118)	32	16	Lipid Metabolism, Small Molecule Biochemistry, Nucleic Acid Metabolism
3	T3D	**ADK** (includes EG:132), ALDH18A1, ALDH1A3, **ALDH1B1, ANXA7**, BAG5, Ca2+, CASP14, CCL6, CIAPIN1, CIDEC, DLEU1, DNAJB6**, DNAJB11**, DNAJC13, DNASE1L3, FBN2 (includes EG:689008), GM2A, **GORASP2**, HCG 2015956, HIVEP2, HNRNPA0, Hsp70, KITLG, LTB4R2, MYC, MYO9B, NPM3, **NPM1** (includes EG:18148), NQO2, PRL2C3, **PSME1**, TNF, TPP2, UBR2	14	7	Gene Expression, Cellular Assembly and Organization, Drug Metabolism
4	8B	**ACOT2, ANXA7, APOBEC2**, C11ORF82, CREB1, **DCTN2, DYNC1I2, ECH1**, EGFR, **ENO3, ERP29**, Hap1-Hd, HTT, IFI203, JPH2, KBTBD10**, LASP1**, LDHAL6A, **LDHB, NDUFA10** (includes EG:4705), NDUFA9 (includes EG:362440), PDGF BB, PDRG1, PLD3, polyglutamic acid, PRRX2, SCAMP3, SDH**, SDHA** (includes EG:6389), SFXN3, SLC2A4**, STRN**, TNF, TP53, **UQCRC1**	26	14	Neurological Disease, Cell Death, Hematological Disease

[1] Bold indicates proteins identified from SwissProt database searching using data from MALDI-TOF-TOF in the experiment.

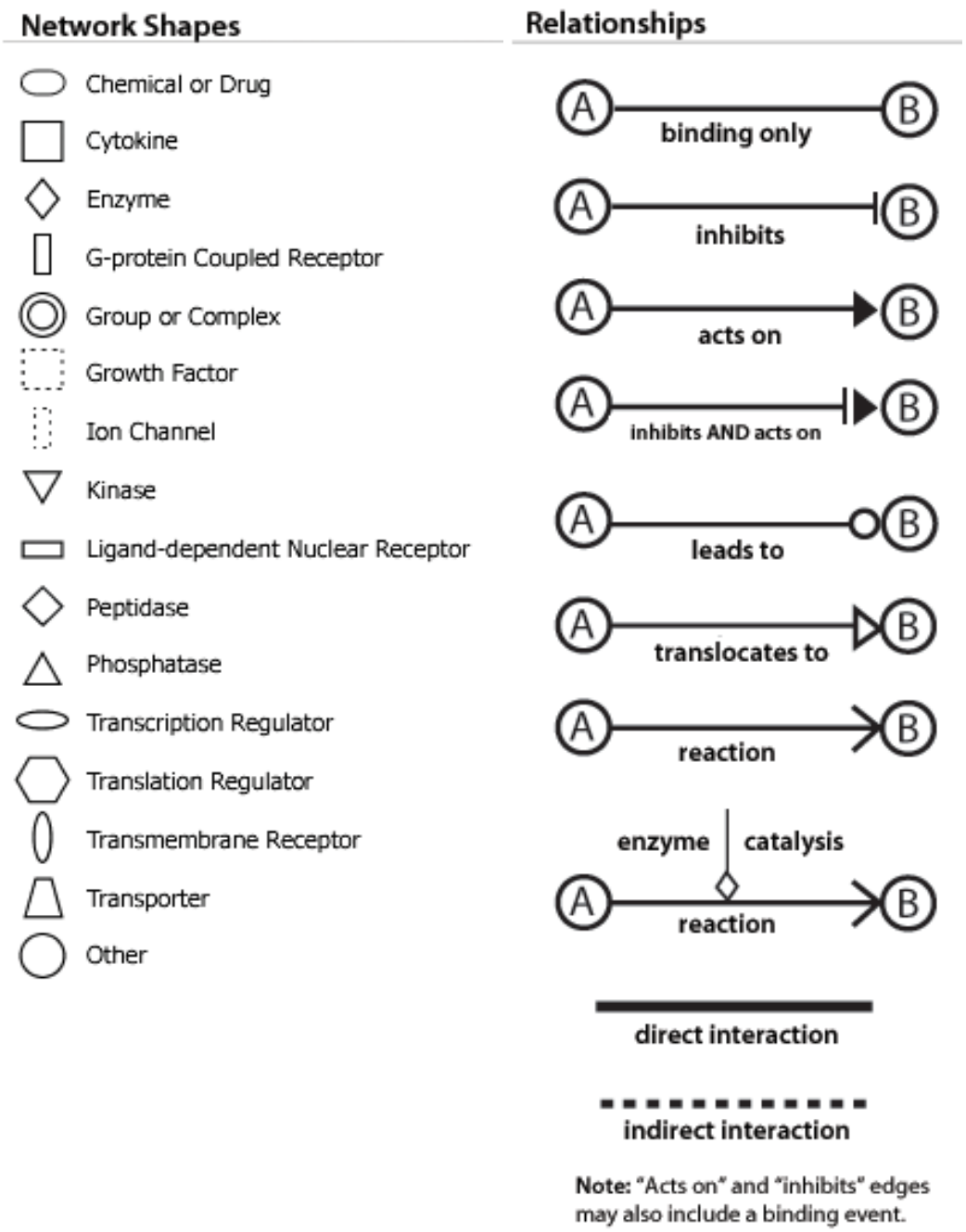

Figure App.4.1. IPA symbols. Copied from Ingenuity Systems IPA 7 Feature Manual, Updated 11/2008; Copyright © Ingenuity Systems 2000 - 2009 All Rights Reserved.

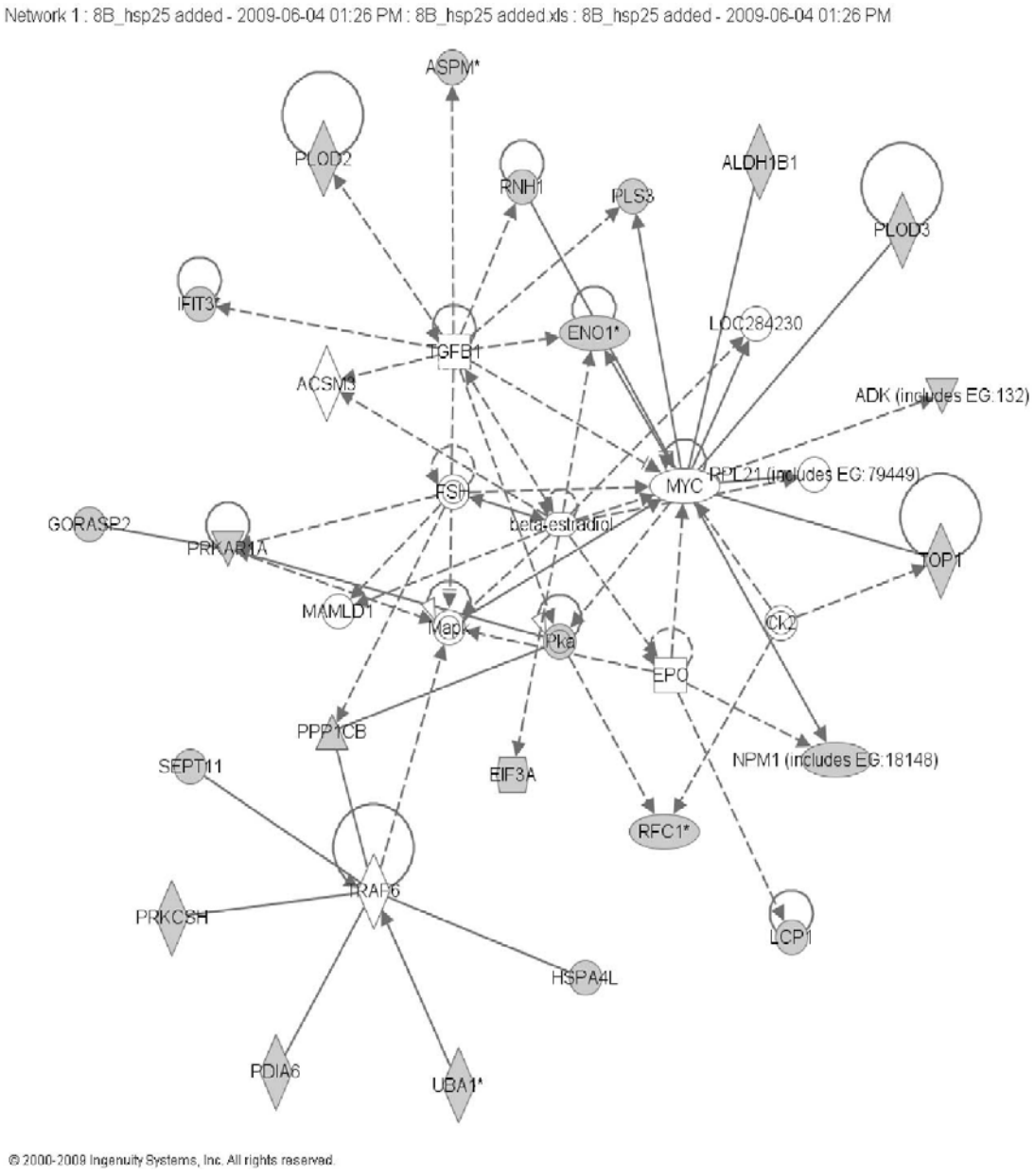

Figure App.4.2. Network of differentially expressed proteins involved in cell cycle, cancer, and drug metabolism in 8B-infected primary cardiac myocyte cultures. Shaded proteins indicate the ones identified as differentially expressed in 2D-DIGE and MALDI-TOF-TOF.

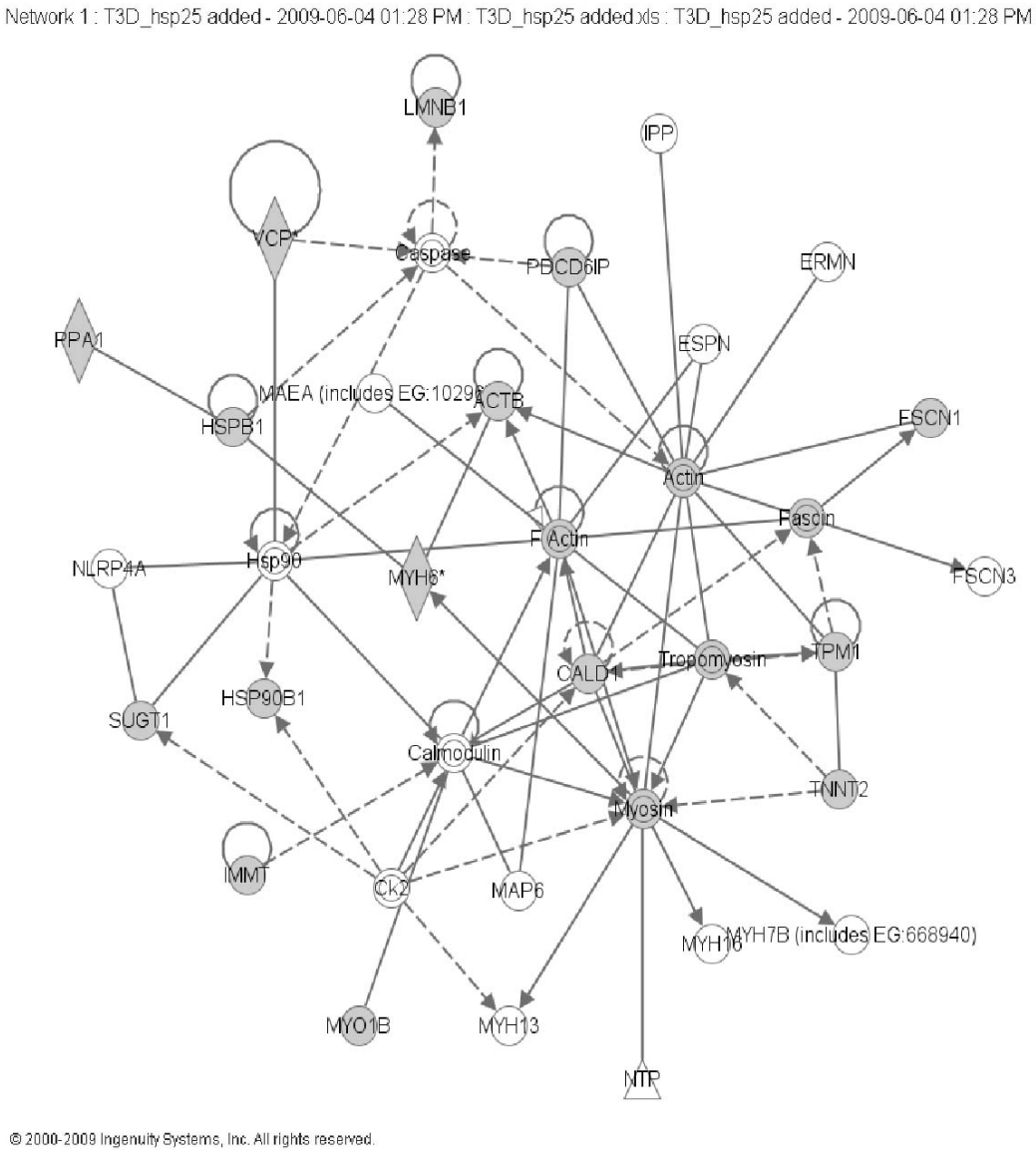

Figure App.4.3. Network of differentially expressed proteins involved in cardiovascular system development and function, skeletal and muscular system development and function, and tissue development in T3D-infected primary cardiac myocyte cultures. Legend is as for Figure 1.

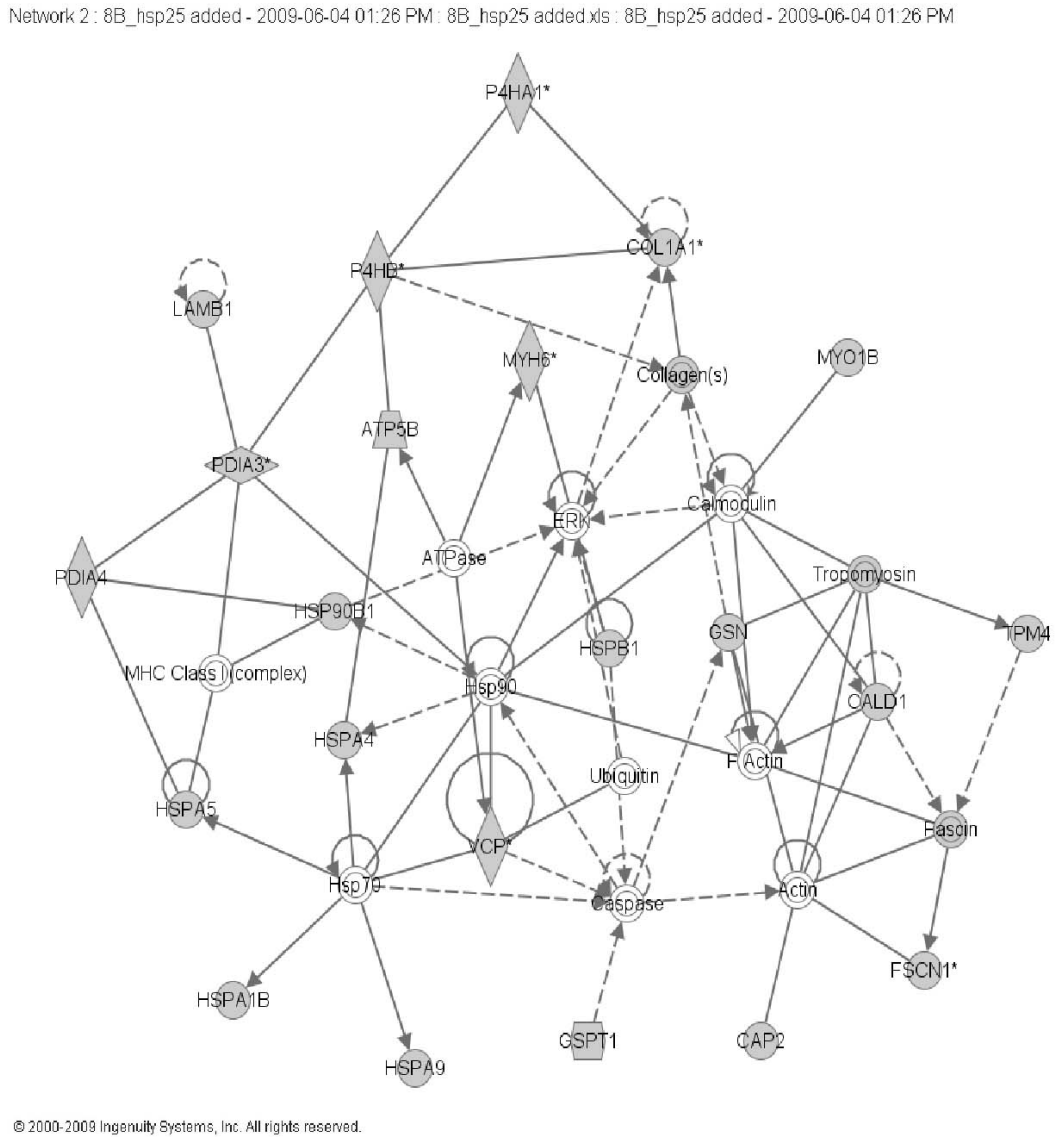

Figure App.4.4. Network of differentially expressed proteins involved in cellular function and maintenance, amino acid metabolism, and post-translational modification in 8B-infected primary cardiac myocyte cultures. Legend is as for Figure 1.

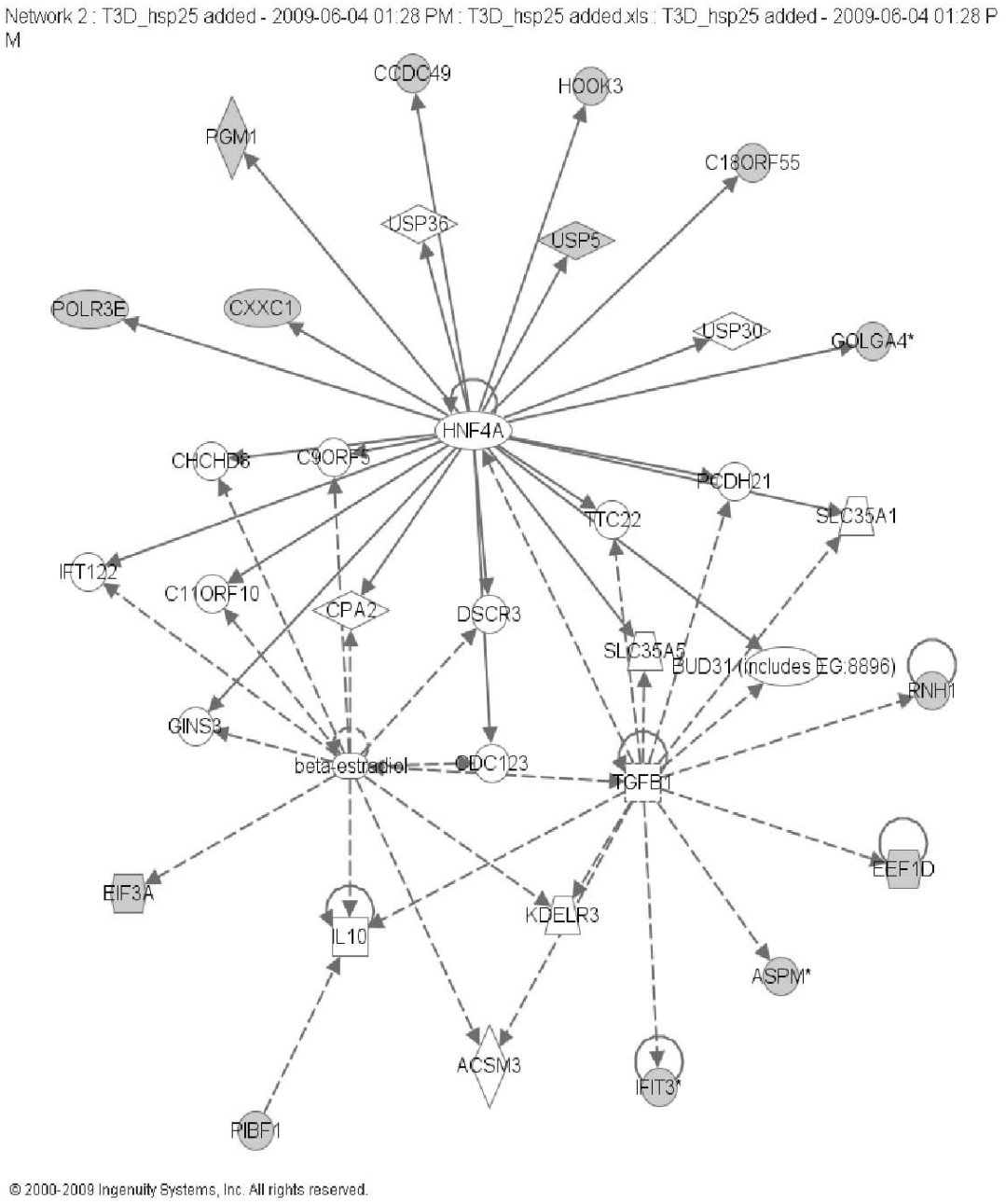

Figure App.4.5. Network of differentially expressed proteins involved in cell-mediated immune responses, immunological disease, and drug metabolism in T3D-infected primary cardiac myocyte cultures. Legend is as for Figure 1.

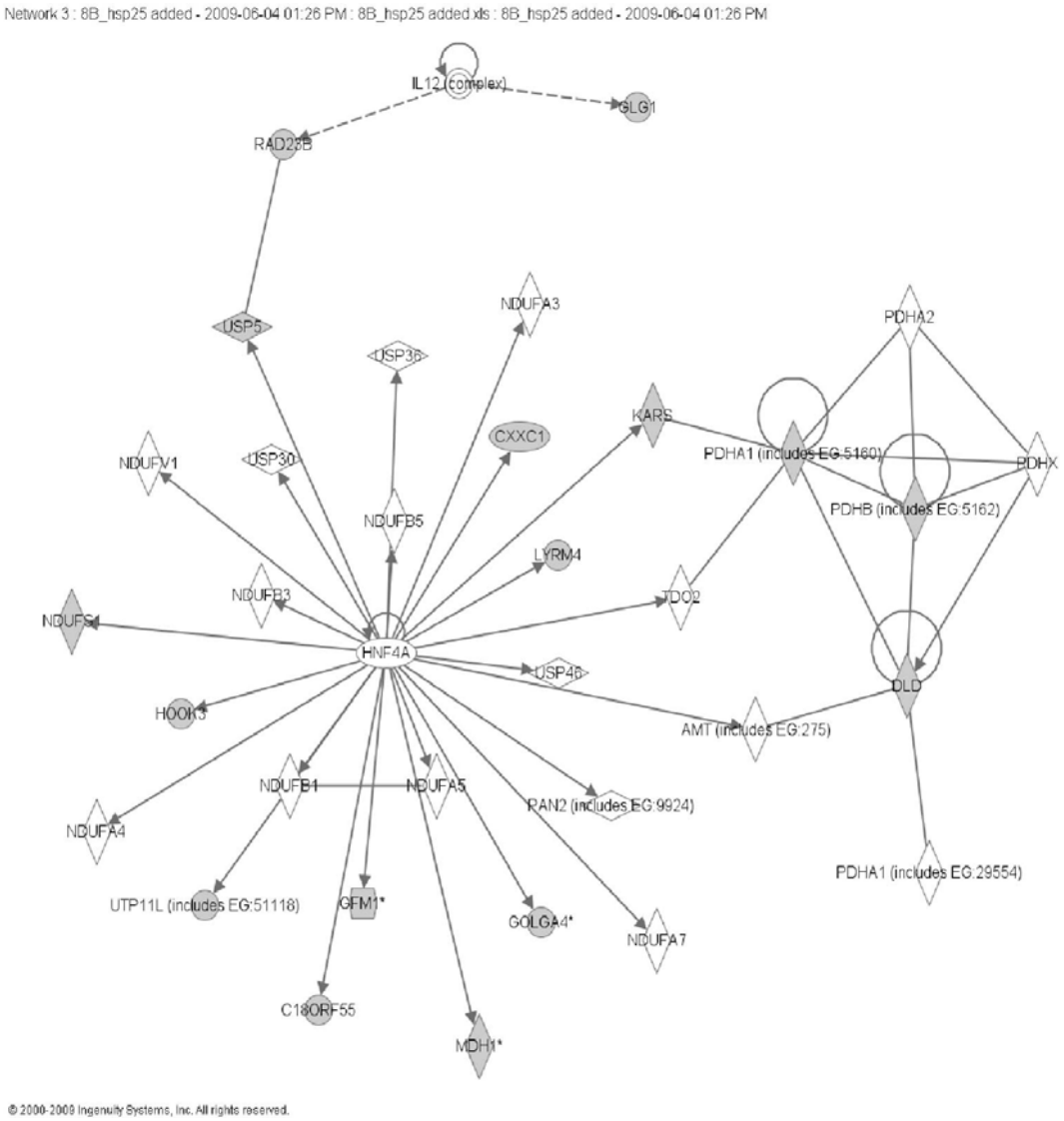

Figure App.4.6. Network of differentially expressed proteins involved in lipid metabolism, small molecule biochemistry, and nucleic acid metabolism in 8B-infected primary cardiac myocyte cultures. Legend is as for Figure 1.

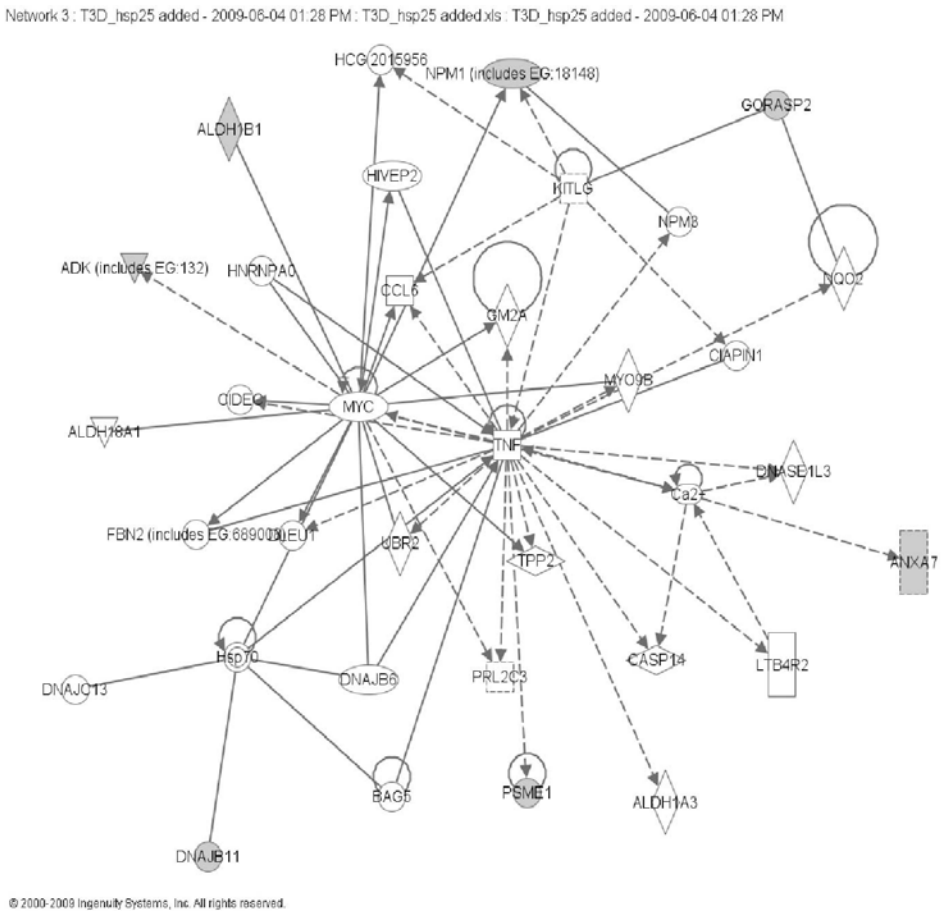

Figure App.4.7. Network of differentially expressed proteins involved in gene expression, cellular assembly and organization, and drug metabolism in T3D-infected primary cardiac myocyte cultures. Legend is as for Figure 1.

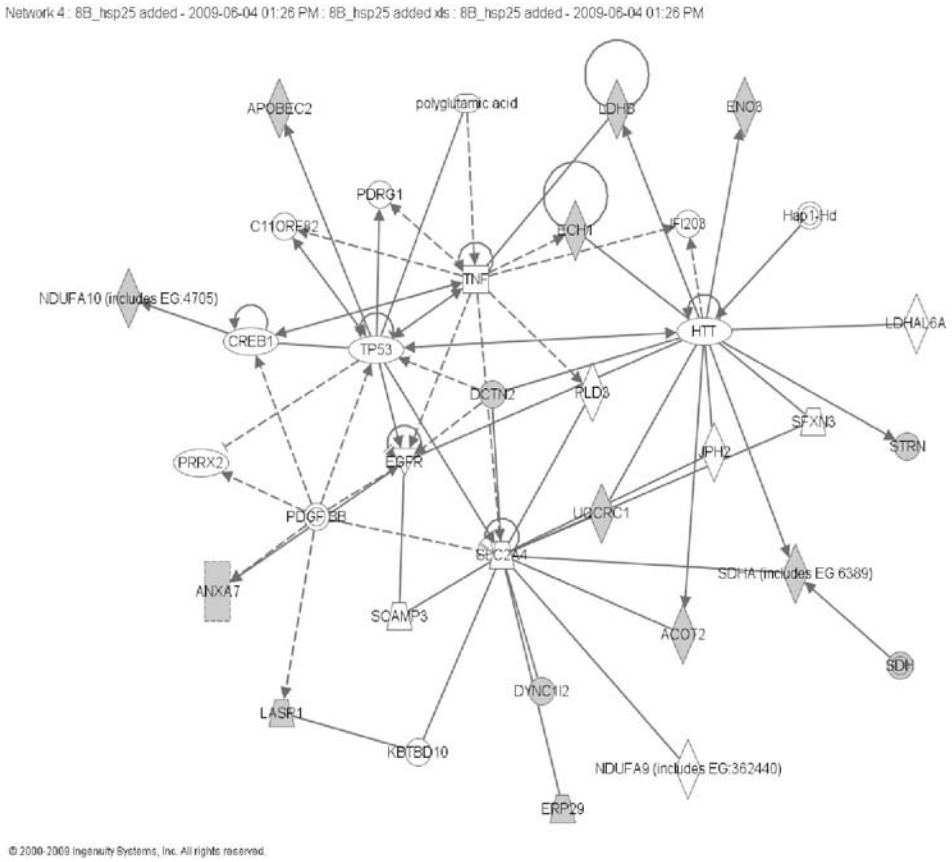

Figure App.4.8. Network of differentially expressed proteins involved in neurological disease, cell death, and hematological disease in 8B-infected primary cardiac myocyte cultures. Legend is as for Figure 1.

Table App.4.7. Differentially expressed proteins with putative PTMs

Spot #	ProMW	ProPI	AccessNum	ProName
1526, 2121	30926	11.4	SFR5_MOUSE	(O35326) Splicing factor; arginine/serine-rich 5
1219, 1234	57108	4.79	PDI_MOUSE	(P09103) Protein disulfide isomerase precursor
199, 200, 210	137859	5.84	CA11_MOUSE	(P11087) Collagen alpha 1(I) chain precursor
759, 765, 766, 772, 806, 875	79910	5.66	VM3_REOVD	(P12419) Major nonstructural protein mu-NS
2114, 2124	36323	6.16	MDHC_MOUSE	(P14152) Malate dehydrogenase; cytoplasmic
2550, 2552, 2558	23000	6.12	HS27_MOUSE	(P14602) Heat shock 27 kDa protein (HSP 27)
1514, 1515	46980	6.36	ENOA_MOUSE	(P17182) Alpha enolase (EC 4.2.1.11)
193, 619, 901, 2068	161852	6.38	IF3A_MOUSE	(P23116) Eukaryotic translation initiation factor 3
1144, 1153, 1166	56586	5.98	PDA3_MOUSE	(P27773) Protein disulfide isomerase A3 precursor
1118, 1411	64193	10.3	RT03_MAIZE	(P27928) Mitochondrial ribosomal protein S3
139, 1854, 1966	125907	9.38	RFC1_MOUSE	(P35601) Activator 1 140 kDa subunit
1396, 1405	56502	7.53	DHAM_MOUSE	(P47738) Aldehyde dehydrogenase; mitochondrial
535, 581	95772	4.89	UBP5_MOUSE	(P56399) Ubiquitin carboxyl-terminal hydrolase 5
2448, 2470	28805	5.9	ER29_MOUSE	(P57759) Endoplasmic reticulum protein ERp29
462, 521, 600, 624	89252	5.14	TERA_MOUSE	(Q01853) Transitional endoplasmic reticulum ATPase
743, 761	80660	9.76	XE7_HUMAN	(Q02040) B-lymphocyte antigen precursor
441, 444, 497	117734	5.43	UBA1_MOUSE	(Q02053) Ubiquitin-activating enzyme E1 1
337, 341, 342, 344	223427	5.57	MYH6_MOUSE	(Q02566) Myosin heavy chain; cardiac muscle alpha
1082, 1092	60872	5.62	P4H1_MOUSE	(Q60715) Prolyl 4-hydroxylase alpha-1 subunit
952, 973	70105	5.2	PLSL_MOUSE	(Q61233) L-plastin (Lymphocyte cytosolic protein 1)
606, 618, 870, 1359, 1416	133646	6.45	GLG1_MOUSE	(Q61543) Golgi apparatus protein 1 precursor
1280, 1286	54240	6.21	FSC1_MOUSE	(Q61553) Fascin (Singed-like protein)
1968, 1974	32540	4.62	NPM_MOUSE	(Q61937) Nucleophosmin (NPM) (Nucleolar
787, 809, 1654	115891	5.69	SCP1_MOUSE	(Q62209) Synaptonemal complex protein 1 (SCP-1)
1563, 1564	47192	5.51	IFT3_MOUSE	(Q64345) Interferon-induced protein with
609, 719	83497	6.48	EFG1_MOUSE	(Q8K0D5) Elongation factor G 1; mitochondrial
325, 1748, 1856	37000	9.86	XERC_SYNP7	(Q8KUV2) Tyrosine recombinase xerC
605, 677	84473	6.34	PLO2_MOUSE	(Q9R0B9) Procollagen-lysine;2-oxoglutarate
185, 515, 530, 585, 804, 871, 1773, 2103, 2130	13633	11	RS13_RALSO	(Q8XV35) 30S ribosomal protein S13
67, 166, 350, 433, 735, 1864, 1892	257406	5.3	GOA4_MOUSE	(Q91VW5) Golgi autoantigen; golgin subfamily A

APPENDIX 5

Over-Expression of Hsp27D and Hsp25 by Transfection of Primary Cardiac Fibroblast Cultures

INTRODUCTION

Western blot analysis and indirect immunofluorescent microscopy demonstrated that mouse cardiac fibroblasts do not express detectable Hsp25 (Chapter 3). Therefore we wished to over-express Hsp25 in this cell type to determine whether Hsp25 expresses anti-viral effects against reovirus infection.

Dr. Wolfgang Dillmann at the University of California, San Diego generated constructs to over-express wild type Hsp27, and also mutated Hsp27 (Hsp27A, with an alanine instead of serine at amino acids 15, 78 and 82 and therefore providing HSP27 that cannot be phosphorylated; and Hsp27D, with an aspartic acid at those same locations, and therefore providing a "phosphomimetic" form of HSP27) (1). While we use mouse cells in our studies and Hsp27 is the human form, their studies and others have shown that over-expressed Hsp27 functions in mouse cardiac cells. They kindly provided their wild type and mutated Hsp27 plasmids for us to use in our experiments. However, DNA sequencing demonstrated that all 3 plasmids for Hsp27 were the same, and were all Hsp27D. Therefore, experiments were carried out using only the phosphomimetic Hsp27 (Hsp27D; subcloned into pCAGGs). Mouse Hsp25 was cloned into the pCAGGs for over-expression as well.

MATERIALS AND METHODS

Hsp27D over-expression. Briefly, Hsp27D was PCR-amplified from Dr. Dillmann's plasmid pSRHSP27D using primers that included restriction digestion sites and a Kozak site. The forward primer was #776: 5'-CTCGAGGCCACCATGACCGAGCGCCGCGTC-3' and the reverse was #777: 5'-CCCGGGTTACTTGGCGGCAGTCTCATCG-3'. High fidelity Phusion DNA polymerase and a gradient PCR with Tm of 70, 73, and 76ºC in Dr. Matthew Breen's lab were used. The amplified Hsp27D sequence was subcloned into the pCAGGs vector (sequence shown in Figure App.5.1). Cardiac fibroblasts were transfected as described in Appendix I, resulting in approximately 50% of cells transfected. Plaque assays were as described in Chapter 2.

Hsp25 over-expression. Full length cDNA of Hsp25 was amplified using gradient PCR from cDNA reverse transcribed from untreated mouse cardiac myocyte total cell RNA. PCR conditions were the same as those used for amplifying Hsp27D. Primers for Hsp25, Hsp25A (to change amino acids 15 and 86 from serine to alanine) and Hsp25D (to change amino acids 15 and 86 from serine to aspartic acid), are listed in Table App.5.1. QuikChange® Site-Directed Mutagenesis Kit (Stratagene, La Jolla, CA, Catlog # 200518) was used to generate mutations. Unfortunately, no colonies were isolated with the desired mutations, and therefore these constructs were not pursued further. Cardiac fibroblasts were transfected and analyzed as for Hsp27D.

Detection of reovirus replication by Western blot. Primary cardiac fibroblasts from Cr:NIH(S) and IFN-α/β-receptor-null (ABRKO) mice were transfected with either

Hsp27D or Hsp25 using an Amaxa kit (detailed description provided in Appendix I). Forty-eight hours post transfection, cells were infected with T3D or 8B at an moi of 3 pfu per cell. Whole cell lysates were harvested using TNE buffer (50 mM Tris HCl pH 7.6, 150 mM NaCl, 2 mM EDTA pH 8.0, 1% (v/v) NP-40 containing a cocktail of protease and phosphatase inhibitors) at 16 and 24 hours post-infection. Rabbit anti-reovirus polyclonal antisera (Sherry laboratory preparation) was used to probe for T3D and 8B viral proteins at a 1:5000 dilution. Hsp25 and Hsp27 polyclonal antibodies from assay designs (catalog # SPA-801 and # SPA-803, respectively) were applied at 1:1000 dilution to detect over-expressed Hsp25 and Hsp27D.

RESULTS

Transfected Hsp25 and Hsp27D do not inhibit virus replication in cardiac fibroblast cultures. Transfected Hsp27D did not inhibit reovirus replication in cardiac fibroblasts from either wild type or IFN-α/β receptor null mice (Figure App.5.2). Western Blot results were consistent with plaque assay results, in that neither over-expressed Hsp25 nor Hsp27D repressed viral protein expression. Of interest, viral protein expression in both of pCAGGs empty vector-tansfected or Hsp25/Hsp27D-transfected samples was much lower than that in mock-transfected samples (Figure App.5.3).

DISCUSSION

Transfected Hsp25 and Hsp27D did not inhibit reovirus replication. Several reasons may be responsible for this. First, the transfection rate for primary cardiac fibroblast cultures using the Amaxa kit is not high enough to transfect most of cells. Our flow cytometry results indicated that only about 50% of cells were transfected using a GFP-expressing plasmid. Therefore, even if Hsp25/Hsp27D inhibited reovirus replication two-fold, that would only decrease replication 25% in the cultures, and that would be difficult to detect by Western Blot or plaque assay. Second, cardiac fibroblasts do not express Hsp25, so they may not express the necessary proteins that coordinate with Hsp25 for Hsp25 to play its normal biological role. Finally, we found that the Amaxa transfection process sometimes induced antiviral genes in both cardiac myocytes and fibroblasts even when empty vector was used (Appendix I). Western Blot results here showed that virus replicated less in pCAGGs-transfected than in mock-transfected cardiac fibroblasts, suggesting that the transfection process may have induced antiviral effects here as well. This makes it difficult to interpret Hsp25/27D transfection results.

REFERENCES

1. **Hollander, J. M., J. L. Martin, D. D. Belke, B. T. Scott, E. Swanson, V. Krishnamoorthy, and W. H. Dillmann.** 2004. Overexpression of wild-type heat shock protein 27 and a nonphosphorylatable heat shock protein 27 mutant protects against ischemia/reperfusion injury in a transgenic mouse model. Circulation **110:**3544-52.

……
TGCTAACCATGTTCATGCCTTCTTCTTTTTCCTACAGCTCCTGGGCAACGTGCTGGTTaTTGTGCTGT
CTCATCATTTTGGCAAAGAATTCctcgagGCCACC***ATGACCGAGCGCCGCGTCCCCTTCTCGCTCCTGC***
GGGGCCCCGACTGGGACCCCTTCCGCGACTGGTACCCGCATAGCCGCCTCTTCGACCAGGCCTTCG
GGCTGCCCCGGCTGCCGGAGGAGTGGTCGCAGTGGTTAGGCGGCAGCAGCTGGCCAGGCTACGTG
CGCCCCCTGCCCCCCGCCGCCATCGAGAGCCCCGCAGTGGCCGCGCCCGCCTACAGCCGCGCGCTC
GACCGGCAACTCGACAGCGGGGTCTCGGAGATCCGGCACACTGCGGACCGCTGGCGCGTGTCCCTG
GATGTCAACCACTTCGCCCCGGACGAGCTGACGGTCAAGACCAAGGATGGCGTGGTGGAGATCACC
GGCAAGCACGAGGAGCGGCAGGACGAGCATGGCTACATCTCCCGGTGCTTCACGCGGAAATACACG
CTGCCCCCCGGTGTGGACCCCACCCAAGTTTCCTCCTCCCTGTCCCCTGAGGGCACACTGACCGTGG
AGGCCCCCATGCCCAAGCTAGCCACGCAGTCCAACGAGATCACCATCCCAGTCACCTTCGAGTCGCG
GGCCCAGCTTGGGGGCCCAGAAGCTGCAAAATCCGATGAGACTGCCGCCAAGTAAcccgggcaccaccacca
ccaccactgagatatctgagctcaaTTCACTCCTCAGGTGCAGGCTGCCTATCAGAAGGTGGTGGCTGGTGTGGC
CAATGCCCTGGCTCACAAATACCACTGAGATCGATCTTTTTCCCTCTGCCAAAAATTATGGGGACA
TCATGAAGCCC……

Figure App.5.1. Full length cDNA sequence of Hsp27D with part of pCAGGs sequence. Bold italic capital letters indicate cDNA sequence for Hsp27D, shaded letters indicate mutated bases, underlined lower case letters indicate restriction enzyme sites, and underlined capital letters indicate the Kozak site.

Table App.5.1. Primers for amplifying wild type and mutated Hsp25 [1]

Gene name	Primers	Sequences
Hsp25	Forward (#789)	5'-CTCGAGGCCACCATGACCGAGCGCCGCGTG-3'
	Reverse (#790)	5'-CCCGGGCTACTTGGCTCCAGACTGTTCAGAC-3'
HSP25D(Ser15)	Forward (#813)	5'-CTGCGGAGCCCG**GA**CTGGGAACCATTC-3'
	Reverse (#814)	5'-GAATGGTTCCCAG**TC**CGGGCTCCGCAG-3'
HSP25A(Ser15)	Forward (#815)	5'-CTGCGGAGCCCG**GC**CTGGGAACCATTC-3'
	Reverse (#816)	5'-GAATGGTTCCCAG**GC**CGGGCTCCGCAG-3'
HSP25D(Ser86)	Forward (#817)	5'-TCAACCGACAGCTC**GA**CAGCGGGGTCTCGGA-3'
	Reverse (#818)	5'-TCCGAGACCCCGCTG**TC**GAGCTGTCGGTTGA-3'
HSP25A(Ser86)	Forward (#819)	5'-TCAACCGACAGCTC**GC**CAGCGGGGTCTCGGA-3'
	Reverse (#820)	5'-TCCGAGACCCCGCTG**GC**GAGCTGTCGGTTGA-3'

[1] Bold indicates the mutated nucleotides.

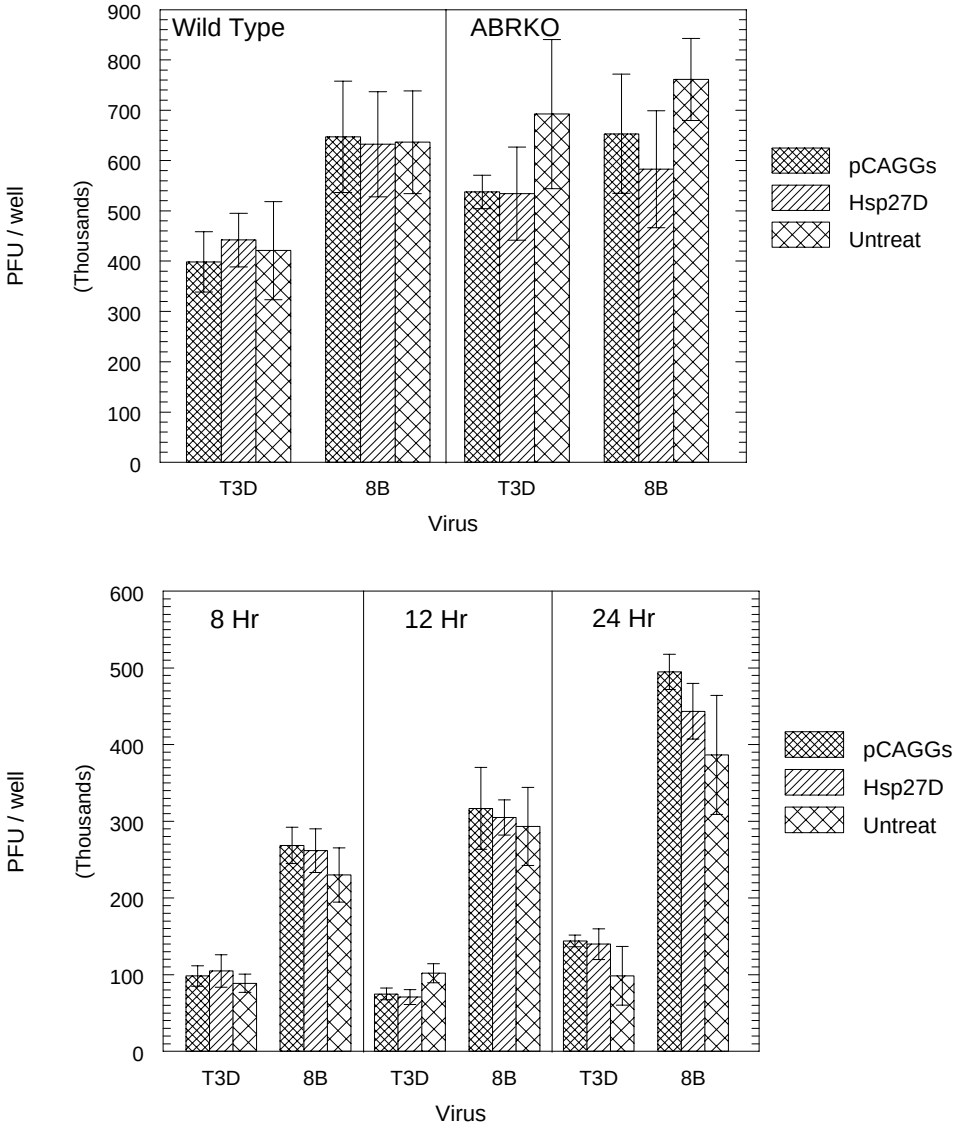

Figure App.5.2. Transfected Hsp27D / Hsp25 does not affect reovirus replication. Triplicate wells of primary cardiac fibroblast cultures were transfected with the indicated plasmid, and were infected with the indicated virus 24 hours later. A) Infections in cells generated from wild type or IFN-α/β-receptor-null (ABRKO) mice at an moi of 10 pfu per cell, harvested at 52 hours post-infection. B) Infections in cells generated from wild type mice at an moi of 3 pfu per cell, harvested at the indicated time post-infection. Bars represent the average ± standard deviation.

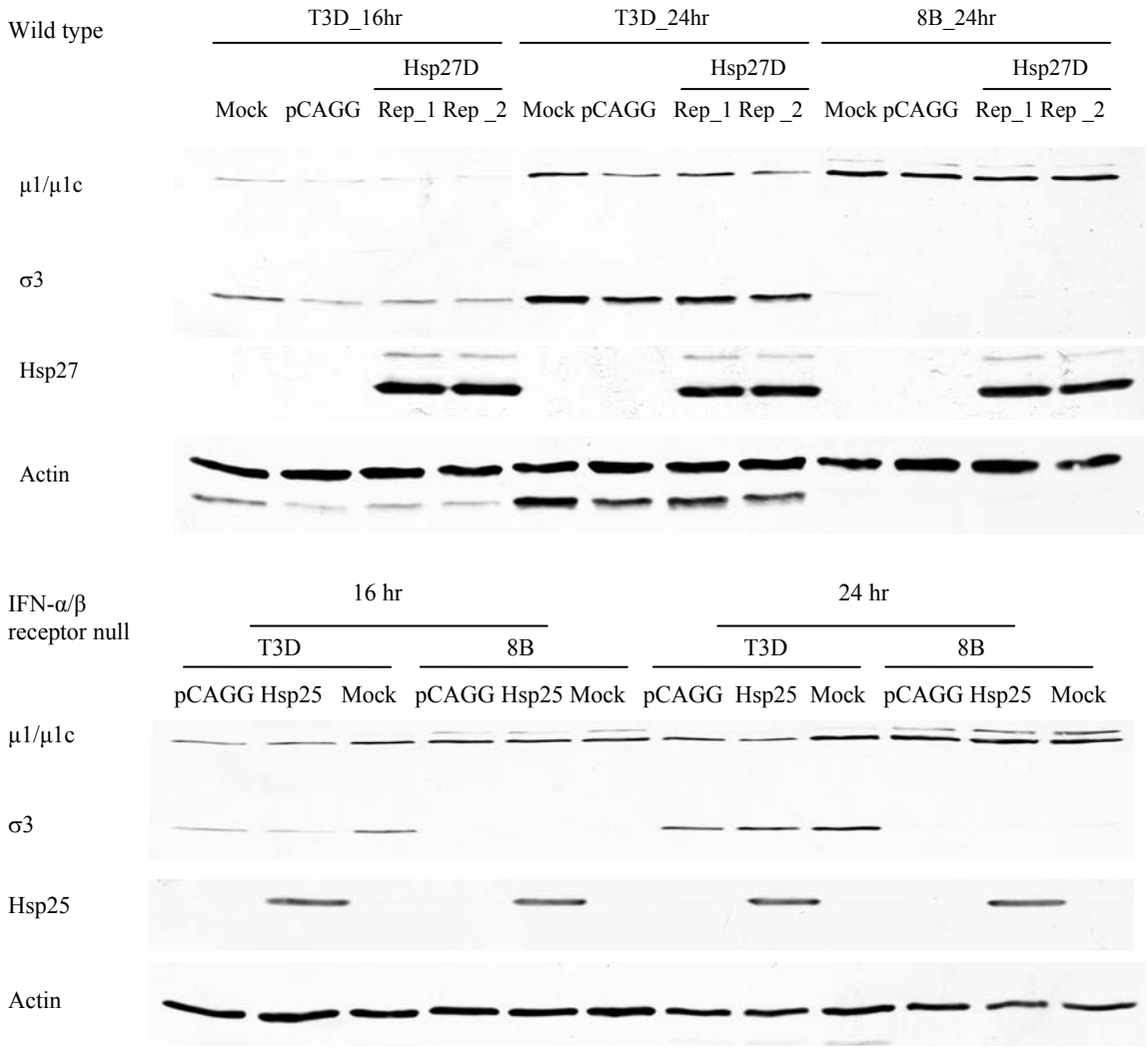

Figure App.5.3. Effects of transfected Hsp25 / Hsp27D on reovirus protein expression in wild type and ABRKO primary cardiac fibroblast cultures

SUMMARY

Since myocarditis is so common in humans, and viruses are such important pathogens causing myocarditis, it is critical to elucidate the mechanisms for the host immune system's antiviral effects in defense against virus infection. Type I IFN (IFN-α/β) plays an essential role in innate immunity. Reovirus induction of and sensitivity to IFN-β has been demonstrated to determine myocarditis *in vivo* in a mouse model and *in vitro* in primary murine cardiac myocyte and cardiac fibroblast cultures. However, the antiviral effects of IFN-α, which uses the same receptor as IFN-β, and in particular the antiviral roles of individual IFN-α subtypes, have not been clearly investigated yet. The major reason for this is the high homology among IFN-α subtypes, which makes distinguishing between IFN-α subtypes very difficult. Here we developed a 3'-base mismatch method to design primers for Real-Time PCR to quantify reovirus T3D induction of 14 individual IFN-α subtypes in primary murine cardiac myocyte and cardiac fibroblast cultures. Primers were demonstrated to amplify individual IFN-α subtypes with extreme specificity, and IFN-α1, -α2, -α4, -α5 and –α8/6 were induced significantly by T3D infection in both cell types. Comparison of IFN-α subtype induction between cardiac myocytes and cardiac fibroblasts revealed that reovirus induction of IFN-α is both subtype- and cell type-specific. The levels of IFN-α expression were both higher and spanned a greater range in cardiac myocytes than in fibroblasts. Viral induction of IFN-α1, -α2, -α5, and -α8/6 required IFN-α/β signaling in both cell types, while induction of IFN-β and -α4 was more dependent on IFN signaling in myocytes than fibroblasts. Since IFN expresses its antiviral effects through induction of IFN stimulated

genes (ISGs), IFN-α induction of ISG56, a well-characterized antiviral protein, and IRF7, an IFN-induced transcription regulator was determined by treating cardiac myocytes and cardiac fibroblasts with purified murine IFN-α1, -α2, -α4, or -α5 from PBL. This was a fortunate collaboration, because these preparations are not yet commercially available. Results identified that treatment with the IFN-α subtypes induced IRF7 and ISG56 in both cardiac cell types, however induction was always greater in cardiac fibroblasts than in cardiac myocytes consistent with our previous reports for IFN-β. Finally, the antiviral effects of each IFN-α subtype was determined. Results showed that all of the IFN-α subtypes tested exhibited antiviral effects and inhibited reovirus T3D replication in both cell types. The IFN-α antiviral effects were subtype-specific, and suggested that IFN-α4 and –α5 were stronger than IFN-α1 and –α2. This first investigation of viral induction of IFN-α in cardiac cells for any virus demonstrates that IFN-α is induced in cardiac cells, that it is both subtype- and cell type-specific, and that it is likely important in the antiviral cardiac response. In the future, it would be of interest to investigate several areas. First, why does reovirus infection of cardiac cells induce only certain IFN-α subtypes? While transcription factors regulating expression of some IFN-α subtypes have been identified, it is not clear whether their roles are cell type-specific. For example, IRF-3 is required for viral induction of IFN-β in early passage MEFs but not late passage MEFs, because late passage MEFs express high basal levels of IRF-7 (3). It is also not clear whether reovirus would activate those transcription factors equally well in different cell types. Second, are these IFN-α subtypes antiviral against other myocarditic viruses in cardiac cells? The different Type I IFNs bind the same receptor but stimulate

different responses (4). Viruses subvert IFN signaling by different mechanisms (5), so it is possible this repression would be both IFN-α subtype- and virus-specific. Finally, do individual IFN-α subtypes play an antiviral role *in vivo*? While there have been two studies where different IFN-α subtypes were injected into mice to determine their effects protecting against myocarditis, those studies used viruses that induced immune-mediated pathology (2, 8), so it is not clear how IFN-α subtypes would affect direct virus-induced cardiac pathology. Mice could be injected as in those studies and tested for reovirus, or mice could be deleted for individual IFN-α genes. However, it would probably be difficult to detect the effect of deleting single IFN-α genes while all other Type I IFN genes were intact.

In addition, a proteomics tool, 2D-DIGE, coupled with MALDI-TOF-TOF, was applied to identify novel antiviral proteins and post-translational modifications in reovirus-infected primary murine cardiac myocyte cultures. First, a time course study using T3D only, which was chosen for its ability to induce IFN well, was carried out to determine a good time point for the subsequent virus panel experiment. Results demonstrated that 12 hours post-infection would likely identify differentially expressed proteins occurring at both early (8 hour) and late (18 hour) times post-infection. The next experiment was designed to compare proteome changes induced by reoviruses with different potentials for causing myocarditis and inducing IFN-β. A small panel of viruses, which included T3D, 8B, DB93A and T1L, provided both typical cases (T3D inducing IFN well and being non-myocarditic) and atypical cases (DB93A inducing IFN poorly but still being non-myocarditic). One hundred and twenty-four differentially expressed proteins were identified, and their expression patterns correlated with virus infection, the potential to induce IFN-β or the potential to cause

myocarditis. Most of the identified proteins were unique for T3D or 8B or for both T3D and 8B. So the subsequent IPA pathway analysis excluded DB93A and T1L and compared T3D and 8B only. IPA analysis revealed that 8B affected more molecules with various biological functions and diverse pathways than T3D, which may be correlated with its potent myocarditic phenotype. Moreover, PTM analysis identified that modification of a small heat shock protein, Hsp25, is virus strain-specific. While all four reoviruses up-regulated Hsp25 diphosphorylation through a p38-MAPK-dependent and IFN-independent pathway, 8B infection decreased total Hsp25 protein. This is the first evidence that a virus can modulate Hsp25 by decreasing its abundance. Our preliminary data showed that inhibition of Hsp25 phosphorylation by a p38-MAPK inhibitor increased cytopathic effect (CPE) induced by T3D in IFN-α/β-null cardiac myocyte cultures and induced by 8B in wild type cultures. However, transfection of a phosphorylation mimic mutated Hsp27 (Hsp27D) and wild type Hsp25 into cardiac fibroblasts did not decrease CPE or viral replication, may be due to the inefficiency of the Amaxa transfection method. Therefore, further investigations of the potential antiviral functions of Hsp25 and its phosphorylated form in the heart need a better approach, such as using Hsp25 transgenic mice. If over-expressed Hsp25 is antiviral, what is the mechanism? Many mechanisms have been proposed for Hsp25 cardioprotective and anti-apoptotic functions; are they also involved in antiviral effects? Another interesting direction is to study how the potently myocarditic reovirus 8B can decrease total Hsp25. Is it by degrading Hsp25 protein or mRNA, or by affecting synthesis by some post-transcriptional mechanism? And which reovirus gene(s) is responsible for this effect? Finally, is Hsp25 antiviral for other viruses, does it use similar mechanisms, and do those viruses subvert

Hsp25 function? There are many questions, because an antiviral role for Hsp25 is a new field.

Results here demonstrate that reovirus infection can induce IFN-α secretion and phosphorylation of Hsp25. Could there be underyling mechanistic links between these two processes? It has been reported that IFN-β treatment can moderately up-regulate phosphorylation of Hsp27 in primary astrocyte cultures from human fetal brain (6). In addition, IFN-α was found to increase Hsp27 expression and activate p38-MAPK phosphorylation in human oropharyngeal epidermoid carcinoma KB cells (1). Although those studies emphasized the capacity of IFN-α to induce apoptosis, and Hsp27 was merely one representative factor indicative of a stress response, the results indicate that IFN-α can modulate Hsp27. In our studies, reovirus infection induced IFN-α in primary cardiac myocyte and cardiac fibroblast cultures, and IFN-α played an antiviral role against reovirus infection. We hypothesize that Hsp25 is also antiviral since the potently myocarditic reovirus 8B degrades Hsp25, Hsp25 degradation has never been observed as a general stress response, and viruses often degrade cell proteins involved in the innate antiviral response. One possible consequence of viral infection could be that secreted IFN-α/β, in addition to inducing synthesis of well-characterized antiviral effector proteins, also up-regulates synthesis of Hsp25 and activates p38-MAPK to phosphorylate pre-existing and new Hsp25. In this way, IFN-α/β and Hsp25 could synergize for antiviral effects. Our studies demonstrated that reovirus stimulates Hsp25 phosphorylation in cardiac myocytes, and that it is p38-MAPK-dependent. While our studies demonstrated that reovirus stimulates Hsp25 phosphorylation in cardiac myocytes even in the absence of IFN-α/β function, i.e. phosphorylation can occur

independent of IFN, they did not address the converse question, i.e. can reovirus-induced IFN-α/β stimulate Hsp25 phosphorylation? Therefore, synergy between reovirus induction of IFN-α/β and IFN-α/β activation of p38-MAPK remains a possibility in cardiac myocytes. In our studies, despite reovirus induction of IFN-α/β expression, reovirus failed to up-regulate Hsp25 mRNA or protein accumulation in cardiac myocytes. This suggests that IFN-α/β does not up-regulate Hsp25 expression in cardiac myocytes. However since previous studies in human oropharyngeal epidermoid carcinoma KB cells measured only Hsp27 protein (1), it remains possible that IFN-α effects there were post-transcriptional, and that reovirus also induces Hsp25 protein expression post-transcriptionally in cardiac myocytes, but that reovirus simultaneously induces its degradation for a net neutral effect. This can be investigated by measuring effects of IFN-α/β treatment of cardiac myocytes on Hsp25 protein expression.

Protein distribution across tissues and localization within cells has evolved for optimal biological function. In mice, Hsp25 mRNA is expressed at high levels in most tissues that have contact with the external environment, including the esophagus, skin, eye, stomach, lung and urinary bladder, and at moderate levels in the heart, skeletal muscle, testis, uterus, and large intestine (7). This distribution of Hsp25 is consistent with a protective role in innate immunity. However, since Hsp25 remains localized inside cells, it can provide only "autocrine" protective function, i.e. protecting only the infected cell. Of course, if it prevents synthesis or release of virus release from that cell, it also provides indirect protection to the entire tissue. In contrast, IFN-α and IFN-β are secreted cytokines which bind other cells to up-regulate hundreds of antiviral ISGs, and therefore their main protective function is

"paracrine". It is possible that the IFNs and Hsp25 have evolved as complementary strengths in the innate immune response to viral infection.

REFERENCES

1. **Caraglia, M., A. Abbruzzese, A. Leardi, S. Pepe, A. Budillon, G. Baldassare, C. Selleri, S. D. Lorenzo, A. Fabbrocini, G. Giuberti, G. Vitale, G. Lupoli, A. R. Bianco, and P. Tagliaferri.** 1999. Interferon-alpha induces apoptosis in human KB cells through a stress-dependent mitogen activated protein kinase pathway that is antagonized by epidermal growth factor. Cell Death Differ **6:**773-80.

2. **Cull, V. S., E. J. Bartlett, and C. M. James.** 2002. Type I interferon gene therapy protects against cytomegalovirus-induced myocarditis. Immunology **106:**428-37.

3. **Hata, N., M. Sato, A. Takaoka, M. Asagiri, N. Tanaka, and T. Taniguchi.** 2001. Constitutive IFN-alpha/beta signal for efficient IFN-alpha/beta gene induction by virus. Biochem Biophys Res Commun **285:**518-25.

4. **Jaks, E., M. Gavutis, G. Uze, J. Martal, and J. Piehler.** 2007. Differential receptor subunit affinities of type I interferons govern differential signal activation. J Mol Biol **366:**525-39.

5. **Randall, R. E., and S. Goodbourn.** 2008. Interferons and viruses: an interplay between induction, signalling, antiviral responses and virus countermeasures. J Gen Virol **89:**1-47.

6. **Satoh, J., and S. U. Kim.** 1995. Cytokines and growth factors induce HSP27 phosphorylation in human astrocytes. J Neuropathol Exp Neurol **54:**504-12.

7. **Wakayama, T., and S. Iseki.** 1998. Expression and cellular localization of the mRNA for the 25-kDa heat-shock protein in the mouse. Cell Biol Int **22:**295-304.

8. **Wang, Y. X., V. da Cunha, J. Vincelette, K. White, S. Velichko, Y. Xu, C. Gross, R. M. Fitch, M. Halks-Miller, B. R. Larsen, T. Yajima, K. U. Knowlton, R. Vergona, M. E. Sullivan, and E. Croze.** 2007. Antiviral and myocyte protective effects of murine interferon-beta and -{alpha}2 in coxsackievirus B3-induced myocarditis and epicarditis in Balb/c mice. Am J Physiol Heart Circ Physiol **293:**H69-76.